Elucidating the role of mycobacterial Resuscitation-promoting factors in stress response and metal acquisition

Mariam Mohamed Nur

Thesis submitted for the degree of

Doctor of Philosophy at

The University of Leicester

Department of Respiratory Sciences

University of Leicester

December 2022

Abstract

Tuberculosis (TB) is an infectious disease caused by members of the *Mycobacterium tuberculosis* complex. TB remains a global health threat. It has been estimated that one-fourth of the world's population is infected with *Mycobacterium tuberculosis*. The bacteria's ability to enter a dormant state makes it an exceptionally successful human pathogen, and results in latent infection. Resuscitation-promoting factors (Rpfs) are cell wall cleaving enzymes that have been postulated to reactivate dormant bacteria via peptidoglycan remodelling; however, the precise molecular mechanism of resuscitation remains unknown. This project was focused on investigation of the roles of Rpfs in *Mycobacterium marinum* during growth in normal and stressful conditions. While all Rpfs were dispensable for growth of *M. marinum* in optimal conditions, *rpfA* had a specific role in the osmotic stress response and showed impaired growth in media containg 550mM NaCl, with a pronounced growth defect on 7H10 agar. Moreover, the mutant had impaired survival in 2 M NaCl. A series of Δ*rpfA* strains complemented with *M. tuberculosis rpfA* were generated to investigate the role of the *ydaO* riboswitch in osmotic tolerance of *M. marinum*. The *M. marinum* mutant with the mutated *ydaO* riboswitch which could not bind the ligand (cyclic di-AMP) had a profound growth defect on 7H10 agar and impaired survival in 2 M NaCl. RpfA was detected in culture supernatant of *M. marinum* using western blot and mass-spectrometry approaches.

Several double and one triple *rpf* deletion mutants were generated and their growth was investigated. Finding of this project suggest that a double *rpfAB* deletion mutant had a growth defect in Sauton's medium which was ameliorated by addition of haemin and $ZnSO_4$. Genetic complementation of this growth defect was achieved with

either *rpfA* (from *M. tuberculosis* or *M. marinum*) or *rpfB* from *M. marinum*, suggesting functional redundancy.

Generation of *M. marinum* Δ*rpfAEB* was only possible when selection of mutant was done in media supplemented with haemin and $ZnSO_4$. The mutant showed delayed colony formation on agar, impaired growth in Sauton's medium and the inability to reach high optical densities compared to wild type *M. marinum*. We were able to both genetically and metabolically complement the growth defect of Δ*rpfAEB* using *rpfB*, haemin, $ZnSO_4$ and culture supernatant. The need for both haemin and $ZnSO_4$ for generation and complementation of the triple mutant suggests a possible role for Rpfs in metal acquisition. Thus, findings within this project confirmed the distinct roles of *M. marinum* Rpfs in osmotic tolerance and growth in suboptimal conditions.

Scientific contributions

The following publication is based on *M. marinum rpf* mutants featured in this thesis: COMMANDEUR S., IAKOBACHVILI N., SPARRIUS M., **NUR MM.**, MUKAMOLOVA G.V., BITTER W. Zebrafish Embryo Model for Assessment of Drug Efficacy on Mycobacterial Persisters. *Antimicrob Agents Chemother*. 2020; 64(10): e00801-20. doi: 10.1128/AAC.00801-20.

Oral presentation: Nur M.M. The role of Resuscitation-promoting factors in function and assembly of mycobacterial secretion systems. The Summer Acid Fast Club meeting. 7 July 2017. Leicester.

Acknowledgements

Firstly, I would like to thank God, for everything.

I would like to thank my primary supervisor Prof. Galina Mukamolova, for her endless support, reassurance and for having faith in me… in spite of myself. I would also like to thank my second supervisor Prof. Primrose Freestone, for her scientific expertise and understanding nature. This doctoral work has been a rollercoaster of emotions and wonderful experimental findings that would have been impossible to see through without the support of such amazing scientists and human beings. I would also like to give my upmost thanks, to the members of Prof. Mukamolova's research group, present and past. To Baleegh Kadhim, Ohoud Al-humaidan, Kawther Al-Qaseer and Josh Auty, you made my experiences in the lab so much more enjoyable, a comradery I will forever cherish. I would like to give special thanks to Dr. Obolbek Turapov, for all his help throughout this PhD and for providing some of the funniest moments.

I am grateful to Dr. Sarah Glenn, for welcoming me into the lab when I first began, teaching me all about cloning, generating and providing me with the *ΔrpfA* complemented strains.

A thank you to Oliver Sampson, for furthering the investigations into the phenotypes of *ΔrpfAEB.*

Last but never least, I want to give a shout out to my big and wonderful family. First and foremost to my mother, may your love and support never end. I want to thank my siblings and my cousins for their craziness, their laughter and for believing in me.

This is dedicated to my late grandmother, may you rest in peace.

Table of Contents

List of abbreviations

ADC	Albumin Dextrose Catalse supplement
BCG	Bacille Calmette-Guerin
Cyclic-di-AMP	Cyclic di-Adenosine Monophosphate
CFU	Colony Forming Unit
CRP	cAMP receptor protein
cSN	Culture Supernatant
DMSO	Dimethyl Sulfoxide
DNA	Deoxyribonucleic Acid
DosR	Dormancy Survival Regulator
DT	Doubling time
EDTA	Ethylenediaminetetraacetic acid
ESAT-6	Early Secretory Antigenic Target 6
HIV	Human Immunodeficiency
IPTG	Isopropyl β-D-1-thiogalactopyroside
LA	Lysogeny Agar
LB	Lysogeny Broth
Lsr2	Nucleoid-associated protein Lsr2
Mtb	*Mycobacterium tuberculosis*
OD	Optical Density
PAGE	Polyacrylamide Gel Electrophoresis
RD1	Region Of Difference 1
RNA	Ribonucleic Acid
Rpf	Resuscitation-Promoting Factor
SD	Standard deviation
SDS	Sodium Dodecyl Sulfate
SEM	Standard error of mean
TB	Tuberculosis
WHO	World Health organisation
WT	Wild type
X- gal	5-bromo-4-chloro-3-indolyl β-D-galactopyranoside

List of figures

List of tables

Chapter 1

Introduction

1.1 Tuberculosis - a historical overview and modern situation

Tuberculosis (TB) is an infectious, air-borne disease caused by *Mycobacterium tuberculosis* (Mtb). It is an ancient disease that has been known for over 70,000 years as judged from the revelation of 2400 BC skeletal Egyptian mummies who exhibited abnormal characteristic of TB (Nerlich *et al.,* 1997; Crubėzy *et al.,* 1998, Morse *et al.,* 1964, Salo *et al.,*1994*)*. It has been hypothesised that the genus *Mycobacterium* originated more than 150 million years ago (Hayman, 1984), and evolved into an obligate pathogen adapted to the human host. The high mortality rates in the past as well as the present has placed TB infection as one of the top causes of death by a single infectious agent (WHO, 2020).

Historically, TB has been referred to by a number of different names coined by various cultures: *phthisis* (Greek), *yaksma* (India), *chaky oncay* (Incan), and *consumptione* (Latin) (Meachen, 1936). Interestingly, all of the terms adopted by the different cultures alludes to the “consuming effect” caused by the disease such as the evident symptoms including, weight loss, fatigue and weakness (Major, 1945). Similarly, within Europe, the disease was referred to as “consumption” along with the Greek name “*phthisis*, up until the mid-19th century, after which it was labelled as “tuberculosis” by Johann Lukas Schönlein (1839). Similarly, in the novel “The life and death of Mr. Badman”, the author, John Bunyan describes TB as "Captain of All These Men of Death" because of its epidemic proportions in Europe and North America, determining one in four deaths (Bunyan, 1808).

During the 19th century, TB was at the forefront of scientific debate in regard to the different hypotheses surrounding the etiopathological origin of the disease and whether or not TB was contagious. Notably, it had been considered as both a

hereditary disease and as a cancer by Southern and Northern Europe, respectively (Frith, 2014). The division of such ideologies can also be attributed to the names given to the disease by researchers from different parts of Europe. For instance, Johann Lukas Schönlein separated the different families of “hematic diseases”, by terming them ‘scrofula’, ‘phthisis’ and ‘tuberculosis’, depending on disease localization (Daniel, 2000; Dubos & Dubos, 1952). Scrofula, is a disease affecting the lymph nodes in the neck (Major, 1932), and was described as a new clinical form of TB in the middle ages. The illness was known in England and France as "king's evil", and it was widely believed that persons affected could heal with a royal touch (Maulitz & Maulitz, 1973). The use of the term *‘phthisis’*, became synonymous with pulmonary TB and was not to be interchangeably used with extra pulmonary TB, as was concurred by the German pathologist Rudolf Virchow (Virchow, 1863). It is an interesting differentiation to make due to TB being an infection which begins in the lungs but can spread throughout the body. Therefore, the discussion of these being distinct disease entities or manifestations of the same illness is a noteworthy one. The notion of progression within the field of TB research has been highlighted as one stemming from speculation and observation to one of actual visualization of the infectious bacterium.

The first ever isolation of the “tubercle bacillus” was done by Robert Koch in 1882 and both Europe and North America reached the heights of its TB epidemic in the 18th and 19th centuries (Krause, 1928; Grigg, 1958). This discovery led to a better understanding of TB disease and infection.

Presently, Mtb has latently infected one-quarter of the world’s population and has resulted in an estimated 9 million new TB cases each year, causing nearly two million deaths (Houben & Dodd, 2016; WHO TB report, 2019). More than 80% of all TB patients live in Sub-Saharan Africa and Asia, with India having the greatest annual

cases in the world (WHO TB report, 2020). Latent TB is associated with dormant Mtb bacteria that persist in the host for decades after the intial infection before reactivating to cause active disease (Stewart et al., 2003). Mtb infection is further complicated by the co-infection with human immunodeficiency virus (HIV) and development of acquired immune deficiency syndrome (AIDS) (Figure1) (Pawlowski et al., 2012). HIV/AIDS has been identified as the main risk factor predisposing individuals to Mtb infection and increased reactivation of latent TB (by 20%). The World Health Organization (WHO) (WHO, 2020) has estimated that 2.6 million new cases of HIV infection and 1.8 million AIDS-related deaths occur per year. Individuals who are infected with HIV-1 are 26-31 time more likely to develop TB than HIV-uninfected people living in the same country (WHO, 2020). In 2019, 208, 000 TB deaths occurred in HIV positive individuals (WHO, 2020). TB and HIV co infections both pose a profound effect on the immune system. HIV positive individuals with latent TB infection are more likely to develop TB disease, resulting in higher probabilities of mortality as well as the acqusition of new TB infection (Bell and Noursadeghi, 2018; ArunMohan et al., 2016; Scriba et al., 2017).

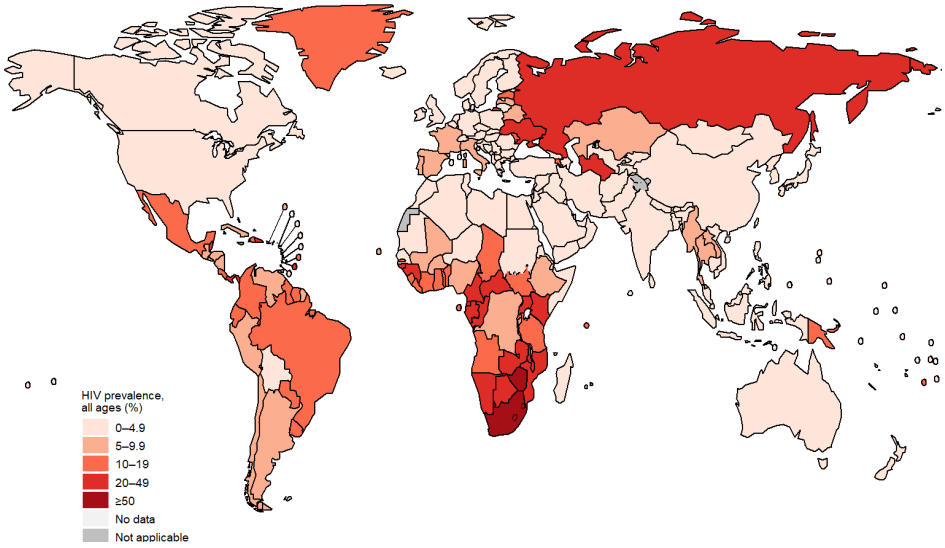

Figure 1: Estimated HIV prevalence in new and relapse TB cases, 2021 (Global tuberculosis report, 2022).

The mechanisms by which this process occurs, remain largely unknown. However, analyses of the known HIV mediated pathways which promote Mtb proliferation may give insights into how disease exacerbation is attained. This can be derived from experimental data on $CD4^+$ T cells. The likelihood of a more rapid rate of disease progression and less survival rates is greater in HIV-1 patients with active TB and controlled $CD4^+$ T cells counts than in patients without active TB (Ezeamama et al., 2015). Furthermore, one reason for the higher case fatality rates in HIV/TB co-infected individuals, stems from delayed diagnosis and treatment due to atypical presentation of TB disease and lower rates of sputum smear positivity (Whitehorn et al., 2010).

Both HIV-1 and Mtb infect macrophages and HIV-1 replication is facilitated by Mtb stimulated macrophages at the site of infection (Hoshino et al., 2002*;* Hoshino et al., 2007). There is a reduction in apoptosis in response to Mtb, stemming from reduced secretion of TNF-α by HIV-infected macrophages (Kumawat et al., 2010; Patel et al.,

2007). Furthermore, Mtb specific $CD4^+$ T cells, can be infected and depleted by HIV-1, resulting in decreased population of cells producing IFN-γ, TNF-α and other cytokines required in controlling both pathogens.

1.2 TB pathogenesis

The initial Mtb infection involves the entry of aerosolised droplets of Mtb into the alveolar passages of the lung from infected humans. It has also been postulated that Mtb is engulfed by alveolar epithelial type II pneumocytes (Harriff et al., 2014). The postulation arises from the notion that the type II pneumocytes are present in larger numbers and experimental data have illustrated the ability of these cells to support the growth of Mtb following infection (Sato, 2002). Mtb infection is often localised in the lungs, however, extra pulmonary TB can occur when the bacteria disseminates to other parts of the body (Behr and Waters, 2014). Interestingly, Mtb infrequently leads to symptomatic disease. An estimated 5-10% of immune-sensitised individuals develop TB (Young et al., 2009). Therefore, the onset of infection pertains to an intricate interaction between host and bacterial factors and is ultimately a reflection of the complex nature of disease. As previously mentioned Mtb/HIV co-infections promote not only the progression of infection but increase the risk of disseminated TB in individuals who are immunocompromised (Dziusmikeyeva & Gorenok, 2012).

The site of multiplication of Mtb is within the membrane-bound phagosome inside the macrophage. Mtb is able to evade macrophage defences by directly inhibiting the phagosomal maturation, fusion of phagosomes and lysosomes, as well as organelle acidification (Ehrt and Schnappinger, 2009). Often, individuals are able to elicit an immune response that is sufficient to eliminate Mtb in spite of harbouring the bacteria; this is thought to account for approximately 90–95% of people. The containment of TB

infection relies on elicit immune responses that successfully control Mtb replication. Even though these people continue to harbor the TB-causing bacteria somewhere in their bodies, usually in their lungs, they do not become sick and are said to be latently infected (Dutta and Karakousis, 2014). This phenomenon of disease progression is largely centred on the evolutionary strategy of Mtb as a pathogen. The transmission of the pathogen depends on its ability to not kill its host, but rather replicate to high enough levels within the host and find a new host (Balloux et al., 2017). This balancing act is of upmost importance to ensure proliferation of pathogen progeny transmission.

1.3 TB treatment and transmission

Attempts to treat TB prior to the discovery of antimicrobials and antibiotics in the 1930's was largely based on futile efforts using herbal remedies (Bramwell, 1851), phototherapy (Aitken, 1937) along with extreme interventions involving bleeding and purging. The treatment of TB involves combination drug therapy, this is due to the complexity of cellular structure of Mtb coupled with it its unique metabolism and ability to persist without replication.

There are many potent drugs for treating TB, with "first line" anti-mycobacterial drugs such as Isoniazid, ethambutol, pyrazinamide and rifampicin routinely used against active TB disease. However, re-emergence of TB has been attributed to development of multiple drug resistance (Dalton et al., 2012). There was an estimated 0.5 million cases of multi-drug resistant TB (MDR-TB) in 2007 (WHO, 2020). For MDR TB, WHO recommends to have six months of TB drug treatment, consisting of a two-month intensive treatment phase, using second-line drugs in the following manner, Isoniazid with rifampicin, pyrazinamide and ethambutol. Once complete, this is followed by a four month continuation phase, using a combination of Isoniazid

with rifampicin. Multiple TB drugs are required to be taken together to prevent TB drug resistance.

Both bacterial and host factors contribute towards latent TB infection and reactivation of latent TB has been of continuous interest (Salgame et al., 2015). Latent tuberculosis infection (LTBI) is defined by proof of immune sensitisation to mycobacterial antigens with the absence of clinical and radiological signs of disease (Barry et al., 2009). However, the state of bacilli found in individuals with LBTI are heterogeneous in nature and as the prevailing view would have LBTI is rather a range of infection states, such as those bacteria eradicated by the host immune response and those persisting at subclinical active infection levels and could reactivate (Esmail et al., 2014).

It has long been postulated that dormant bacteria are associated with LTBI. Individuals latently infected with Mtb retain dormant bacilli in old lesions throughout their lifetime and these can reactivate and cause active tuberculosis (Kell & Young, 2000).

1.4 Mycobacterial cell wall

Mycobacteria include both pathogenic and free-living non-pathogenic saprophytes. Non-pathogenic mycobacteria include the very well-studied *Mycobacterium smegmatis*. The pathogenic Mtb is the causative agent of TB and good model organisms for investigation of this disease include *Mycobacterium bovis BCG* and *Mycobacterium marinum*; the latter of which the work in this thesis is based on.

A hallmark of mycobacteria is their intricate cell wall. The main components of the mycobacterial cell wall are the peptidoglycan (PG) layer (also known as murein), mycolic acid (MA) and arabinogalactan (AG) (Jankute et al., 2015). The presence of this waxy coating contributes to Mtb's successful ability as a pathogen as it facilitates

drug resistance. Conversely, the mycobacterial cell wall is of significant interest as it acts as a target for mycobacteria-specific drugs (Jankute et al., 2015). Moreover, in mycobacteria, the PG plays a vital role in the cell's growth, cellular signalling and inter-bacterial communication, as well as in the initiation of the host immune response (Brooks et al., 2011; Dziadek et al., 2016).

The PG is essential for survival in almost all bacteria and its basic core structure remains universal to all bacteria: a glycan backbone and short cross-linked peptide side chains (Rogers et al., 1980). This macromolecule provides shape, rigidity, and osmotic stability to both Gram-negative and Gram-positive bacteria (Schleifer and Kandler, 1972). The backbone of PG is made up of glycan chains with a repeating disaccharide motif of N-acetylglucosamine β-1,4 N-acetylmuramic acid (GlcNAc-MurNAc) (Figure 2) (Weidel and Pelzer, 1964; Vollmer et al., 2008). However, mycobacterial PGs possess several notable structural modifications. Mur*N*Ac is oxidized to N-glycolylmuramic acid (Mur*N*Glyc), both MurNAc and Mur*N*Glyc are found in mycobacterial PG (Kotani et al., 1970; Essers & Schoop, 1978). The presence of Mur*N*Glyc increases the resistance of *M. smegmatis* PG to lysozyme (Raymond et al., 2005); however, deletion of *namH* in Mtb had no notable effect on morphology, antibiotic resistance replication of bacteria *in vivo* and slightly improved of survival of mice (Jesse et al., 2014). Further modification such as the amidation of the α-carboxylic group of d-isoglutamate (d-iGlu) and the ε-carboxylic group of the mDAP residues in mycobacteria (Kotani et al., 1970; Mahapatra et al., 2008) helps protect against antimicrobial factors such as lysozyme, antimicrobial peptides and cell wall acting drugs (Girardin et al., 2003; Roychowdhury et al., 2005). This is achieved by lowering the net negative charge of the cell wall. Furthermore, the mycobacterial lipid content is higher than those in Gram positive and Gram negative bacteria, and

accounts for approximately 40% of the total cell mass (Brennan, 2003). This may explain the increased discovery of highly hydrophobic new antimicrobials targeting the cell wall, as the permeability and sensitivity to hydrophobic antibiotics is influenced by MA's (Jankute et al., 2015). However, there are several FDA-approved drugs, PG precursor inhibitors and commercial antibiotics which could be used in TB therapy. For instance, 4-Aminoquinazolines target GlmU by inhibit PG precursor biosynthesis and have been tested in vitro against Mtb MurB homologue (Patel et al., 2020). Due to the similarities in structure of MurC and MurD/MurE and MurF, researchers have hypothesised the possibility of designing inhibitors which may simultaneously inhibit the Mur enzymes (Kouidmi et al., 2014). Thiadiazolidinones and D-cycloserine (Kim et al., 2003) also inhibits PG precursor biosynthesis, by targeting alanine racemase (Alr), which catalyses the conversion of L-alanine to D-alanine, required to synthesize the peptide component of Lipid II (De Chiara et al., 2020)

Due to the essentiality of the PG a fine balance must be sought between bacteria withstanding their own internal turgor pressure and the cell's ability to cleave the cell wall to support growth, division, and the assembly of trans-envelope structures such as bacterial secretion systems (Vollmer et al., 2008). Thus, PG cleavage is a highly regulated event. PG cleaving enzymes promote the growth process of the bacteria though the incorporation of newly synthesised murein peptide in the cell wall. Research in *E. coli* has suggested a vast number of PG hydrolases and other cleaving enzymes for almost each covalent bond in the *E. coli* murein (van Heijienoort., 2011). This diversity mirrors the various functions that these enzymes fulfil. Similarly, a comparative study of PG-active enzymes in mycobacteria, highlighted the presence of enzymes capable of degrading all major covalent bonds of mycobacterial PG (Machowski et al., 2014). Although there are significant differences between

mycobacterial species, the enzymes are encoded in all mycobacterial genomes, including *Mycobacterium leprae*, which has a considerably reduced genome (Machowski et al., 2014). The conservation of these genes emphasises the importance of PG remodelling for growth and repair from damage induced by the host immune responses such as lysozyme attack and osmotic stress.

Gram-positive and Gram-negative bacteria can both release muropeptides from the cell wall via cell wall cleaving enzymes. The former usually uses lysozyme-like hydrolytic enzymes such as amidases/muramidases. The latter uses lytic transglycosylases (LTG) to generate 1,6-anhydroMurNAc products (Reith and Mayer, 2011; Johnson *et al.,* 2013). LTG's are lysozyme-like enzymes that cleave the β-1,4 glycosidic bond between GlcNAc and MurNAc. Interestingly, unlike lysozyme, there is no transfer of the glycosyl moiety onto water but rather onto the C-6 hydroxyl group of the muramic acid, resulting in an intramolecular glycosyl transferase reaction (Thunnissen et al., 1995).

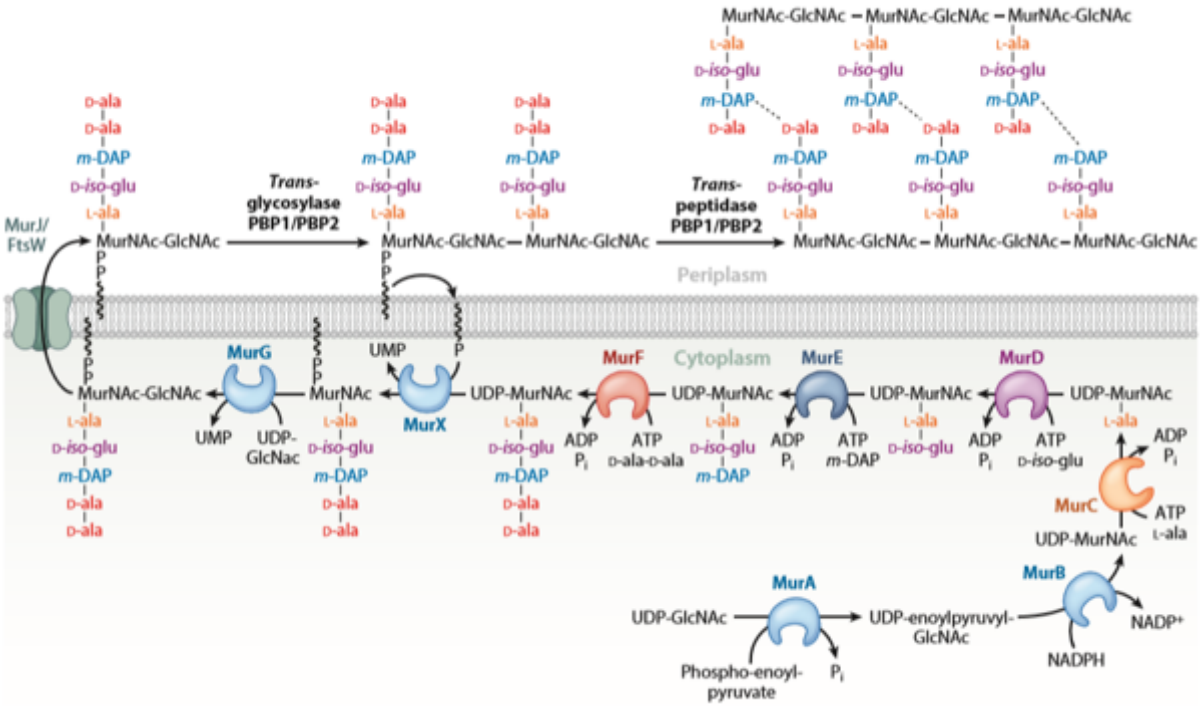

Figure 2: Biosynthesis pathway of peptidoglycan in Mtb (Jankute et al., 2015). PG precursors are synthesised in cells by Mur enzymes and transported on cell surface by the proposed flippases (MurJ or FtsW). PG precursors are incorporated into the existing PG by PBP1 and PBP2.

The mycobacterial genomes encode many lytic enzymes and Mtb has a number of PG endopeptidases (Anantharaman and Aravind, 2003), amidases (Boutte et al., 2016; Wu et al., 2019) and notably, five annotated resuscitation-promoting factors (Rpfs) (Mukamolova et al., 2002; Ravagnani et al., 2005).

The ground-breaking discovered of Rpfs in *Micrococcus luteus* by Mukamolova and colleagues (Mukamolova et al., 1998b; Mukamolova et al., 1999; Mukamolova et al., 2002), showed that Rpfs can resuscitate dormant bacteria and stimulate growth in suboptimal conditions. Moreover, *Micrococcus luteus* Rpf is able to degrade PG and to bind to, and cleave, a synthetic tri-*N*-acetylglucosamine (NAG) cell wall mimetic (Mukamolova et al., 2006; Telkov et al., 2006). Mutation of predicted catalytic residues eliminated muralytic activity and abolished resuscitation and growth stimulatory effects. The importance and potential specific roles of Rpf's in cell wall remodelling will be discussed in more depth in upcoming chapters (see section 3.1.1).

The significance of PG remodelling by cell wall cleavage in the active and continuous sense of growth has indicated the need to create space for the insertion of peptides in the cell wall. Mycobacterial dormancy and reactivation from this state, also involves the use of cell wall cleaving enzymes to intiate the growth process of mycobacteria from non-replicating phase.

1.5 Mtb dormancy

Following exposure to Mtb, 40% of individuals develop primary infection and active disease and 60% of individuals enter asymptomatic, non-infectious latent phase (Parrish et al., 1998). The latent infection can reactivate to clinically symptomatic disease from the clinically non-symptomatic state.

The ability of Mtb to exist in both active and dormant states has been associated

with its ability to cause persistent disease. The specific mechanism through which Mtb transitions out of dormancy remains elusive. However, the remodelling of the PG, by proteins such as Rpf's in the cell wall of Mtb is an essential process for pathogenesis, reactivation, and drug tolerance.

Latency is defined as the observation of infection without symptoms of disease (Salgame et al., 2015). Dormancy is a microbiological term referring to a reversible, physiological state of bacteria with reduced metabolic activity, in which cells can persist for extended period of time without division (Kaprelyants and Kell, 1993). Dormant bacteria may exist in a "non-culturable" or differentially culturable state (Mukamolova et al., 2003; Dhillon et al., 2014; Turapov et al., 2016). This relates to the inability of recovering colony-forming units when bacteria are plated on standard media yet retaining the ability to produce viable bacteria as judged by vital staining and having the capacity to resuscitate (Kaprelyants & Kell, 1993). Fluorescent marked reporter strains in the lungs of chronically infected mice, showed presence of a sub-population of non-dividing cells that were metabolically active (Manina et al., 2015). Although, Mtb bacilli can collectively be labelled as dormant, not all dormant bacilli will have the same phenotype (Shleeva et al., 2011). Furthermore, approximately 90% of sputum containing Mtb bacilli from treatment-naïve patients might not grow on agar and can only grow in the presence of growth factor supplementation, such as culture supernatant containing Rpfs and other components (Mukamolova et al., 2010; Chengalroyen et al., 2016; Gordhan et al., 2021; Honeyborne et al., 2016; Turapov et al., 2016). The differentially culturable bacteria also exhibit higher drug tolerance to first-line treatment drugs such as isoniazid and rifampicin (Mukamolova et al., 2010; Turapov et al., 2016). This subset of phenotypically drug tolerant Mtb cells known as persisters, do not grow in the presence of antibiotics and are therefore thought to

contribute to MDRTB. Jin Lee and colleagues (2019) successfully generated Mtb persister-like bacilli, derived from a biofilm culture and demonstrated trehalose metabolism remodelling, similar to that seen in Mtb following antibiotic-treatment.

It was previously thought that mycobacterial bacilli in latently infected individuals solely resided in granulomas and mature tubercle lesions, it has however been found that bacteria can be present outside granulomas; in endothelial cells, fibroblasts and adipose tissue (Hernández-Pando et al., 2000; Neyrolles et al., 2006), each of which will exert different environmental condition on Mtb.

1.6 Models of dormancy and latency

The transition of metabolically active Mtb into dormancy can be mimicked *in vitro.* These *in vitro* models have been used to model dormancy and explore conditions in which Mtb is naturally subjected to during the course of infection. The models also can be used to investigate the adaptive processes involved in this non-culturable state. This can be achieved by growing the bacteria in nutrient-limiting environments, which include essential conditions such as; starvation of essential nutrients, including carbon, nitrogen and phosphorus, as well as the depletion of oxygen, which prevents aerobic respiration by Mtb (Wayne & Sohaskey, 2001).

The most extensively studied condition is hypoxia, whereby the importance of oxygen tension *in vitro* was first shown (Wayne & Sohaskey, 2001). This model theoretically emulates aspects of *in vivo* latency conditions. Although Mtb is an obligate aerobe that grows most successfully in tissues with high oxygen content, such as the lungs, the bacilli are capable of surviving periods of extended anaerobiosis such as when subjected to hypoxic environments in the mature avascular calcified granulomas, with low oxygen levels (Grosset, 2003; Imboden & Schoolnik 1998; Tsai

et al., 2006). Moreover, adipose tissue has also been associated with hypoxia (Neyrolles et al., 2006).

The characterization of Mtb growth under these conditions was termed non-replicating persistence (NRP). The Wayne model is conducted by adding a low-inoculum Mtb culture to a continuously stirred and sealed tube, thus establishing a hypoxic environment with a consequential shift in Mtb physiology. The model relies on the slow depletion of oxygen to mimic this anaerobic environment. As oxygen is consumed, the culture optical density stops increasing and thus growth ceases (Wayne & Lin, 1982).

Growth under hypoxic conditions generates two distinct NRP states (NRP1 and NRP2); the initial state, NRP1 is a microaerophilic state. This stage is achieved when oxygen levels reach 1% saturation and is associated with the induction of glycine dehydrogenase activity. The second stage is an anaerobic state and occurs when oxygen levels reach 0.06% saturation, and cells display no further increase in optical density. It is characterized by the halt in cell enlargment, a decline in glycine dehydrogenase activity, susceptibility to metronidazole and antibiotic resistance. Furthermore, the NRP cells in the Wayne model were shown to be responsive to heat and were culturable when reintroduced to oxygen with division occurring in a synchronous fashion (Wayne & Hayes, 1996).

Environments that induce a more rapidly reversible growth arrest have been extensively characterized and there are a number of studies that have modified Wayne's hypoxic model (Honaker et al., 2009; Leistikow et al., 2010). These models use a faster anaerobic dormancy model and differs from the Wayne model in the larger size of stir bars and more rapid rate of stirring leading to a more homogeneous population of bacilli, as well as a more even oxygen distribution throughout the culture.

Compared to the Wayne model these modifications allow the available oxygen to be consumed more rapidly and thus reaching anaerobiosis quicker.

Transcription expression profiling using microarrays have indicated that non-replicating Mtb cells in the Wayne model undergo transcriptional reprogramming during hypoxia and that many metabolic genes are down-regulated whilst other gene sets involved are up-regulated (Muttucumaru et al., 2004). Creating an *in vitro* hypoxic environment has enabled the identification of genes and proteins induced in Mtb and *M. bovis* BCG during oxygen deprivation (Boon et al., 2001).The inhibition of respiration is a feature in microenvironments of hypoxia, treatment with NO or CO. The dormancy survival regulon (DosR regulon) consists of approximately 50 coregulated genes, which are induced during these conditions. This regulon contains genes required for energy acquisition from alternative carbon sources including the glyoxylate shunt, fatty acid metabolism, and nitrate reductase genes (Voskuil et al., 2003; Wayne & Lin 1982; Kai et al., 2009; Daniel et al., 2004). The published literature has suggested that the DosR regulon is controlled by a three-component regulatory system composed of two sensor histidine kinases, DosS and DosT, as well as a response regulator, DosR (Rickman *et al.,* 2005). In spite of most DosR-regulated genes not yet being characterized, the timing of their induction coupled with the conditions under which they respond indicates that they may play a role in adaptation of Mtb to its host environment.

Beyond hypoxic conditions, there is evidence suggesting that dormant Mtb in lung lesions suffer nutrient limitation. A nutrient starvation model was designed by (Loebel, 1933a; 1933b) to investigate the effect of nutrient restriction predicted to be in a granuloma on the metabolism of Mtb. Cultures were transferred from nutrient-rich medium into phosphate-buffered saline (PBS) and the respiration rate measured using

a manometer. Nutrient starvation resulted in a gradual shutdown of respiration to minimal levels, but bacilli remained viable and were able to recover when returned to rich medium (Loebel, 1933a).

Undoubtedly, there are limitations when using single stress models such as nutrient starvation, hypoxia and NO exposure, which cannot completely reproduce the dormancy stimulating conditions Mtb is subjected to *in vivo*. Currently, there are few multi-stress models, which have been investigated.

1.7 Animal models of latency in TB infection

A number of animals are currently being used as *in vivo* models to reflect and investigate latent tuberculosis disease in humans. Understandably, the more genetically similar animals are to humans the more likely they are to mimic human disease. To date there is no animal model that perfectly resembles human TB. The animal models used include monkeys, mice (i.e. the Cornell model), guinea pigs, rabbits and notably zebra fish (Prouty et al., 2003; Ordas et al., 2015).

The most notable evidence for dormant Mtb generated during infection is perhaps the Cornell model (McCune et al., 1956; Mccune et al., 1966). This was demonstrated using a mouse model whereby the mice were infected with virulent Mtb and the infection was allowed to establish for 2 weeks, followed by treatment with a combination of isoniazid and pyrazinamide 3 months. Primarily no bacilli could be detected in the mouse spleen; however, one third of the mice relapsed with development of culture-positive TB upon 3-month discontinuation of anti-tuberculosis drug treatment (Mccune et al., 1956). Furthermore, subsequent relapses could be stimulated by immunosuppressive steroid administration (Mccune et al., 1966). Thus, being indicative of the presence of dormant bacilli, which are unresponsive to drug

treatment. The murine model is favourable, owing to a number of factors, such as low cost, availability of immunological reagents and genetic tractability. Conversely, the Cynomolgus monkey model is very expensive with few immune reagents due to the lack of inbred monkey models. However, this model does in fact appear to more closely resemble human infection- particularly latent tubercular disease. In relation to latent establishment of disease, the effectiveness of guinea pigs and rabbits as models are rather differing. Guniea pigs are more extremely sensitive to hosting Mtb compared to rabbits (Dharmadhikari & Nardell, 2008). Disease progression is rapid following low-dose aerosol infection and is thus unable to establish latency, whilst the latter appears to resemble human TB more readily (Lurie et al., 1952). The pathology in the lungs of both guinea pigs and rabbits is reminiscent of human pathology, including the formation of classic *M. tuberculosis* granulomas. However, only C3HeB/FeJ mice have been shown to produce granulomas with a hypoxic core whereas BALB/c mice do not have this (Harper et al., 2012). Therefore, C3HeB/FeJ mice appear to be the better *in vivo* model when studying TB infection, as it is more similar to human TB disease. However, there is a relative lack of immunologic reagents for these animals (Flynn et al., 2003). Lastly, the zebra fish model is one, which utilizes *M. marinum*, the natural etiological agent of TB for this host (Prouty et al., 2003).

Compared to the other mentioned model systems for the study of Mtb infection, the zebra fish model has become a well-established vertebrate model for developmental studies (Ordas et al., 2015) and low-dose infection of adult zebra fish with *M. marinum* leads to persistent infections resembling latency that can be reactivated when subjected to gamma irradiation resulting in immune-compromise (Parikka et al., 2012). There are a number of factors, which make zebra fish ideal for laboratory work; they are small, easy to maintain in large numbers, breed quickly and

require relatively little care.

1.8 *M. marinum* as an Mtb infection model

M. marinum is a pathogenic and environmental mycobacterium which infects skin and soft tissue (Ang et al., 2000), it is well known due to its association with fish, amphibians and water (Swaim, 2006). The bacteria take between 7 and 14 days to grow and it produces photochromogenic colonies. The optimal growth temperature is around 32°C.

There are several factors which make *M. marinum* a suitable organism to study mycobacterial pathogenesis (Ordas et al., 2015; Prouty et al., 2003). It shares important pathogenic characteristics with Mtb and forms granulomatous lesions during chronic infection and has also been used to study the function of M.tb genes involved in intracellular survival and replication within macrophages (Davis et al., 2002).

M. marinum causes a similar disease and infections in its hosts, including latency and granuloma formation, and is amenable to the laboratory setting as it is genetically tractable and a relatively fast growing mycobacterium. These reasons make *M. marinum* a good model organism for studying mycobacterial pathogenesis.

To date, work by Iakobachvili (2014) resulted in the successful generation of three single *rpf* mutants (*rpfA*, *rpfB, rpfE*) and one double *rpfAE* deletion mutant in *M. marinum.* These mutants have been used as background strains for multiple *rpf* gene deletions in this project and a further *rpfC* deletion mutant has been generated. The research of Iakobachvili (2014) investigated localisation and expression patterns of *M. marinum* Rpf homologues in macrophage infection. However, research into *rpf* gene regulation and subsequent involvement in TB infection during physiological stresses excreted on the mycobacterial cell has never been attempted previously. Therefore, this project is aimed at elucidating the underlying regulatory mechanisms involved in

rpf gene expression during stress and metal acquisition using *M. marinum* as a model organism.

1.9 Resuscitation and Rpfs

Rpfs were initially discovered in *M. luteus* (Mukamolova et al., 1998a). Rpfs are secreted proteins, which have autocrine, paracrine signaling functions and are required for the resuscitation of dormant cells (Mukamolova et al., 2002). Resuscitation of Mtb from dormancy occurs via a mechanism involving cleavage of the PG by Rpfs and partnering proteins (Mukamolova et al., 2006). The involvement of Rpfs in the resuscitation of Mtb from its non-culturable state has been demonstrated using bacteria with multiple *rpf* genes deletions (Kana et al., 2008). Genome sequencing has revealed similar genes in various high G and C gram-positive bacteria such as *Corynebacterium spp*. and *Streptomyces spp*. (Ravagnani et al., 2005).

Rpfs can stimulate growth of viable bacteria and can increase the viable cell count of dormant *M. luteus* cultures at least 100-fold aswell as restore cultivability from a dormant state (Mukamolova et al., 2002; Mukamolova et al., 1998a). Moreover, structural studies of Rpfs; including NMR (Cohen-Gonsaud et al., 2005) and X-ray diffraction (Ruggiero et al., 2009) experiments have indicated the presence of catalytic domains which exhibit a fold situated towards the C-terminus of the conserved 70 amino acids residue segment, known as the Rpf domain. The Rpf domain is similar to that of C-type lysosomes; however, Rpfs are functionally more similar to lytic transglycosylases (Ravagnani *et al.,* 2005). The Rpf domain of *M. luteus* Rpf is needed for biological activity, thus it corresponds to a functional protein domain, further signifying its importance (Mukamolova *et al.,* 2006).

Mtb produces five resuscitation-promoting factor (*rpf*)-like proteins with significant

homology to the one essential Rpf of *M. luteus* (Mukamolova *et al.,* 2002)*;* RpfA (Rv0867c), RpfB (Rv1009), RpfC (Rv1884c), RpfD (Rv2389c) and RpfE (Rv2450c). Moreover, homology searches have shown that several *Mycobacterium spp*. such as *M. smegmatis, M. bovis (BCG)* and *M.marinum* contain Rpf-like proteins (Ravagnani et al., 2005). Deletion of 5 *rpf* genes from Mtb genome was possible but the resultant mutant was inpaired in resuscitation from dormancy and could not replicate in mice (Kana et al., 2008). Furthermore, the deletion of *rpfs* has been shown to increase sensitivity to SDS (Kana *et al.,* 2008), vancomycin and rifampin (Kana et al., 2010), which may be due to cell wall permeability defects. This observation can help develop an *in vivo* latency model using zebra fish and *M. marinum* to mimic human TB infection. It may potentially allow for the screening of effective compounds against Rpf proteins as well as investigate the roles of the different *rpfs* in stress response and *M. tuberculosis* infection both *in vitro* and *in vivo.*

The *rpf*-like genes are dispersed throughout the *Mtb* genome and can be found in different contexts (Cole et al., 1998). The multiplicity of Rpf proteins in Mycobacteria, have undoubtedly created a number of challenges in identifying the distinct roles of the individual Rpf, not only in their implication as cell wall cleavage but, particularly, the mechanisms of regulation of their expression and activity. Interestingly, the highly dissimilar contexts in which the *rpf*-like genes can be found in the *M. tuberculosis* genome are more suggestive of distinct roles for the Rpf proteins as opposed to having one common biological function (Mukamolova et al., 2002).

Notably, *M. marinum,* which will be used as the model organisms in presented work contains 4 Rpf-like protein homologues of those found in Mtb, RpfA, RpfB, RpfC and RpfE*;* all of whose precise actions are unknown. Figure 3 illustrates a schematic diagram of these genes.

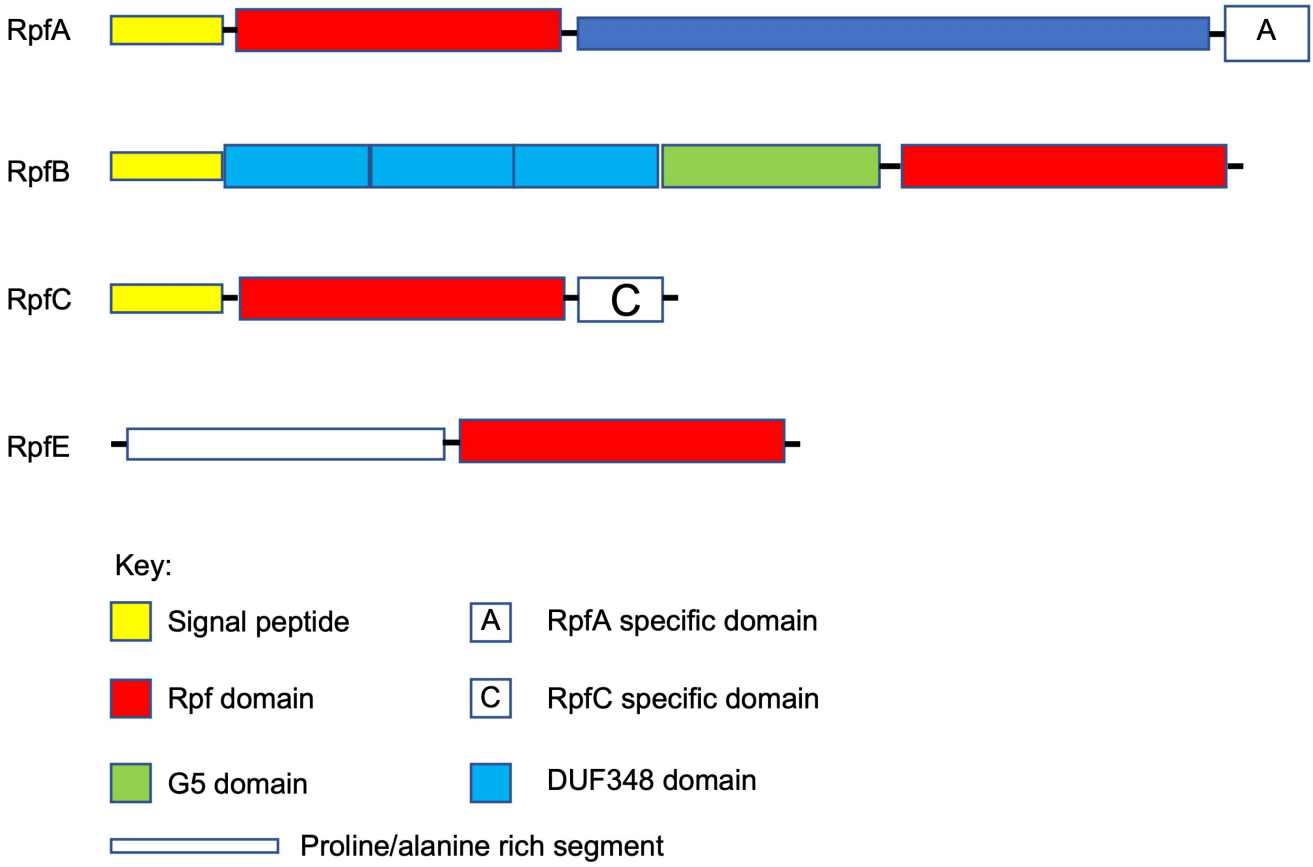

Figure 3: Domain structure of Rpf proteins in *M. marinum;* adapted from Ravagnani et al., 2005.

1.10 Rpf-dependent mycobacteria and their clinical importance

Non-replicating forms of mycobacteria have been associated with latent TB infection. It has been hypothesised that these forms of bacteria require specific cultivation conditions in order to grow (Chao & Rubin, 2010). Non-replicating viability pertains to a variety of different phenotypes that have been observed in bacteria such as *Vibrio species* and Mtb. Non-culturable bacteria, do not form colonies on agar and do not grow in liquid media, however, the bacteria can be visualised under microscopy by vital staining (Kaprelyants & Kell, 1993). These bacteria can be resuscitated i.e., transformed from their non-replicating state to an actively dividing state, only through the presence of recombinant Rpf or signalled by exogenous factors present in culture supernatant from actively dividing cultures (Kana & Mizrahi, 2010; Rosser et al., 2017). Thus, it is thought that a proportion of dormant bacteria are dependent of Rpf in order to actively start growing.

The molecular mechanisms underlying the formation of differentially culturable and Rpf-dependent bacteria are not well understood. *In vitro* differential culturability can be induced by a number of factors, these include multiple stresses within the host, prolonged stationary growth phase culture, and exposure to anti-tuberculous drugs (Deb et al., 2009; Loraine et al., 2016; Mukamolova et al., 2002; Shleeva et al., 2011). Rpf-dependent abd differentially culturable bacilli often make up the vast majority of the sample population (Mukamolova et al., 2010; Turapov et al., 2014; Turapov et al., 2016; Chengalroyen et al., 2016).

Rpf-dependent bacilli can be defined as a proportion of bacilli, which cannot be cultured in standard media and require Rpf to begin growth (Mukamolova et al., 2010). Growth of non-culturable bacteria can be achieved through the addition of exogenous Rpf obtained from culture supernatant of cells at exponential phase of growth but can

also be achieved with recombinant Rpf proteins (Mukamolova et al., 2010; Huang et al., 2014). Although, the recovered Rpf dependent bacilli has been shown to become culturable in the presence of varying form of Rpf supplementations (Turapov et al., 2016). Chengalroyen and colleagues (2016) showed that culture supernatant from an Mtb Rpf null strain, void of all Rpfs was able to resuscitate non-culturable bacteria. As previously discussed, Rpf are associated with other cell wall cleaving proteins, including RipA. It might be that the resuscitation that occurs in the absence of Rpfs is due to other factors that can regulate growth of non-replicating mycobacteria such as lipids (Zhang et al., 2001), muropeptides (Nikitushkin et al., 2013), cAMP (Shleeva et al., 2013) and possibly other compounds such as metals. It is also possible that various molecules can resuscitate dormant Mtb stimulating different branches of the same pathway.

Upon the discovery of Rpfs and their promising potential in TB therapy, it was postulated that the inhibition of Rpfs within the host could prevent reactivation of dormant cells and subsequent TB disease. Conversely, Seidi and Esfahlan (2013) hypothesised that Rpfs could be used to activate dormant bacilli, following the administration of a standard antibiotic regime for TB. It was theorised that the reactivation of TB using Rpfs would eradicate all TB reserves in the hosts and prevent latent TB in the treated subjects, ultimately, lowering the requirements for long-term expensive and toxic regimes in resistant forms. This notion is a rather simplistic take on how to eradicate TB as we do not yet fully understand the reactivation process itself let alone the potential harm deliberate resuscitation of dormant bacilli could cause to the human body.

Whilst the molecular mechanisms pertaining to rpf dependent reactivation of TB during latent infection remains largely unknown. There have been various theories surrounding potential means of rpf-dependent reactivation.

As previously mentioned Rpfs have cell was remodelling abilities and one way in which Rpf may reactivate dormant bacilli could potentially be by restricted cleavage of the modified PG in the dormant cells. Thus, promoting synthesis and growth of the cell wall and stimulating the beginning of division process in the dormant bacilli. Therefore, a restricted hydrolysis of PG can be critical for starting cell division.

This muralytic ability of Rpfs may also contribute to the dispersal of bacterial aggregation as it was shown that clumping of *M. luteus* cells (Nikitushkin et al., 2011) was needed for growth to begin during lag phase (Voloshin et al., 2005). Similarly, aggregation is important during the initial steps of reactivation of Mtb (Shleeva et al., 2003). It seems that Rpf proteins can participate in dispersion of these aggregates before the beginning of cell division. Lastly, it has been hypothesised that Rpfs remodel the mycobacterial peptidoglycan via the production of muropeptides which may act as bacterial signalling molecules (Keep et al., 2006). Muropeptides can be produced by cleaving the peptidoglycan through the combined action of Rpfs and other mycobacterial lytic enzymes, which in turn releases these low molecular weight molecules. These can be placed onto the cell and onto the neighbouring cells acting on a surface cellular receptor. Bacteria bind and respond to peptidoglycan through the action of eukaryotic-like serine/threonine protein kinases (STPKs) and associated serine/threonine protein phosphatase systems (Shah & Dworkin, 2010). STPKs are single, membrane-spanning polypeptides that have an external sensor domain and an internal cytoplasmic protein kinase domain that phosphorylates target proteins upon

detection of a cognate signal, resulting in a coordinated cellular response through a signal cascade.

Muropeptides interacted with a specific exogenous receptor – PASTA domain of the STPK PrkC. This binding results in activation and induces of other regulatory cellular protein. Literature has shown that muropeptides released during mutolysine induced hydrolysis of peptidoglycan by actively growing *B. subtilis* promote germination of *B. subtilis* spores. Interestingly, only meso-DAP-containing muropeptides can facilitate this growth released during the active growth of the bacteria promoted germination of *B. subtilis* spores (Shah et al., 2008). Both muramyl dipeptide and an Ala-D-γ-Glu-Dpm tripeptide from *B. subtilis* were unable to induce germination in this bacteria (Shah et al., 2008).

Mtb has a PrkC homolog known as protein kinase B, PknB (Kang et al., 2005). The PrkC gene controls the expression YocH, a supposed Rpf homolog in *B. subtilis,* which can also regulate the release of muropeptide (Atrih & Foster, 1999).

1.11 Regulation of Rpf expression

Genome-wide microarray techniques investigating transcriptional profiling in Mtb have provided further insights into both the transcription and regulation of *rpfs*. Experiments illustrating the deletion of individual *rpfs* in Mtb have caused some upregulation of the remaining genes (Downing et al., 2004), thus supporting the notion that the Rpf homologues in Mtb have specialized and slightly different functions.

Furthermore, these genes have not only been shown to be induced in a growth phase dependent manner both *in vitro* and *in vivo* (Tufariello et al., 2004; Mukamolova et al., 2002) but the exposure of Mtb to a number of stresses have resulted in the differential expression of *rpfs*. These included acid stress, nutrient starvation and low-oxygen (hypoxia), further emphasizing the potential individual roles of these proteins

(Gupta et al., 2010). Experimental data have shown that all Rpf proteins are expressed during early growth in mouse lungs (Tufariello et al., 2004).

Similarly, all *rpfs* are expressed in the early stages of resuscitation from non-culturability, however, *rpfC* was found to be more consistently highly expressed at all stages compared to other *rpfs* (Salina et al., 2019). The relative expression of both *rpfB* and *rpfE* was reduced in stationary phase, with *rpfC* being upregulated only during stationary and exponential growth phases. Thus, suggesting that *rpfB* and *rpfE* maybe required for growth in exponential phase, whereas *rpfC* and *rpfD* maybe needed in persistence and stationary phase (Gupta et al., 2010). Recent studies suggested that treatment of Mtb with a novel nitric oxide donor resulted in dramatic down-regulation of expression of *rpfA*, *rpfB* and *rpfE* and generation of Rpf-depdendent mycobacteria (Glenn et al., 2021).

In spite of the insights provided by these expression profiles the complicated nature of the regulatory mechanisms involved in *rpf* gene expression remain largely unknown. Recently, Uhía and colleagues (2018), generated mCherry fluorescent fusions constructs of *Mtb* Rpf proteins in order to investigate the specific function of Rpfs. Although the fusions were functional, the specific cellular localisation of Rpfs was not achievable (Uhia et al., 2018). Nevertheless, these annotations of the many suggested regulatory components that have been elucidated for *rpfs* over the years (Figure 4).

Figure 4: Schematic representation of regulatory components of *rpf* genes in *M. marinum.*

1.11.1. Transcriptional regulator MtrA

Mtb dormancy and reactivation is regulated by differential expression and functional activation of distinct sets of genes. The survival of Mtb in host macrophages largely depends on phagolysosome inhibition (Russell, 2003; Vergne et al., 2004). In order to adapt successfully, Mtb employs mechanisms that enable it to sense stress and remodel its transcriptome. This includes signal sensing and gene expression regulated by two-component systems (TCSs) (Bretl et al*.,* 2011). The Mtb genome contains 11 recognized pairs of genes encoding 2CR systems, along with other orphan kinases and regulators (Cole et al., 1998). MtrAB is a highly conserved two-component system implicated in the regulation of cell division in Actinobacteria and coordinates DNA replication with cell division. The histidine–aspartate two-component regulatory (2CR) signal transduction system was first revealed via Mtb genome sequence analysis and highlighted the presence of many regulator networks, believed to be essential for Mtb survival in both acute and chronic phases of human infection (Cole et al.,1998). MtrA has shown to have relatively high promoter activity in defined media and constant levels during intra-macrophage growth (Via et al., 1996; Zahrt & Deretic, 2000).

Furthermore, Deretic and colleagues' pioneer studies revealed *mtrA* as an essential gene in Mtb (Via et al., 1996; Zahrt & Deretic, 2000; Parish et al., 2003). MtrB phosphorylates MtrA and phosphorylated MtrA binds to the promoters of *oriA*, *fbpB*, *ripA* and *dnaA* (Fol et al., 2006; Rajagopalan et al., 2010). The MtrA regulon includes a number of cell division and cell wall metabolism genes, such as peptidoglycan hydrolase (*ripA*), mycolyltransferases (*fbpB, fbpC*) penicillin-binding protein involved in peptidoglycan biosynthesis (*ftsI, dacB1*), FtsZ-interacting protein (*sepF*), essential DivIVa family cell division protein (*wag31*) and resuscitation-promoting factors *rpf A-E*. Recent studies in *M. smegmatis* have shown that MtrB

associates with the septa in an FtsZ- and FtsI-dependent manner (Plocinska et al., 2012). Interaction of MtrB with FtsI is required for expression of the MtrA regulon.

Studies of the role of MtrAB two component system in using the faster growing and non-pathogenic *M. smegmatis* cells showed the MtrB sensor kinase to be non-essential in *M. smegmatis*, and *mtrB* disruption compromised MtrA-target expression and cell division (Plocinska et al., 2012; Al Zayer et al., 2011). The research indicated that the chromosomal copy of *mtrA* can only be disrupted by homologous recombination in the presence of an additional copy of *mtrA* on a conditionally replicating mycobacterial plasmid, which signifying that *mtrA* is essential (Sharma et al., 2015). It is the lipoprotein LpqB which modulates the activity of the MtrAB system in mycobacteria by interacting with the extra-cytoplasmic domain of MtrB to regulate drug resistance and cell wall homeostasis (Nguyen et al., 2010).

In other bacteria MtrA also links antibiotic production to sporulation *Streptomyces venezuelae* (Som et al., 2017). However, no work on the MtrAB system has been carried out in *M. marinum* to date.

Considering the importance of mycobacterial peptidoglycan cleaving enzymes, especially Rpfs, in cell wall remodelling and growth under stress, the further understanding of the transcriptional regulation of *rpfs* is of great importance as it may aid TB diagnoses and therapy. ChIP-seq and next-generation sequencing of macrophage studies using Mtb overexpressing His-MtrA, first revealed MtrA binding to the promoter regions of both *rpfA* and *rpfC* (Sharma et al., 2015; Chatterjee et al., 2018). It showed that *rpfA* and *rpfC* are likely regulated in an MtrA-dependent manner in Mtb grown in macrophages. This, along with previous studies using rpfB suggest that MtrA regulates at least three of the five rpf genes in Mtb. During intracellular growth MtrA targets such as *rpfA-E* are upregulated to facilitate cell wall processing

and septal divison upon Mtb reactivation and exit from the dormant and non-replicative persistent states (Mukamolova et al., 2002; Davies et al., 2008; Gupta et al., 2010; Kana & Mizrahi, 2010; Kondratieva et al., 2011). Conversely, MtrAB is downregulated during NO and envelope stress (Gorla et al., 2018).

MtrA protein appears to be a prominent antigen prior to the development of clinical TB. Pooled sera from TB patients, but not those from healthy controls, recognize MtrA, thus confirming its expression during active infection in humans (Singh et al., 2001). Most recently, phosphotransfer assays and FRET analysis has indicated that acetylated MtrA not only undergoes increased phosphorylation but that this results in greater interaction with MtrB as a result. Consequentially the acetylated MtrA, loses DNA-binding ability, leading to repression of oriC and rpf, who's binding MtrA would ordinarily be MtrA-phoshorylation dependent (Singh et al., 2021).

Whilst, the many MtrA promoter binding sites have been discovered, the MtrA regulon remains poorly understood. Determination of *mtrA* transcript levels by elective capture of transcribed sequences also con-firmed that *mtrA* is a constitutively expressed gene in Mtb.

1.11.2 Lsr2 regulation of Rpf expression

The mycobacterial Lsr2 protein is similar to the H-NS protein found in *E. coli* and is the first of its kind to be discovered in mycobacteria. H-NS works by mainly to repress gene transcription by binding to AT-rich sequences in a sequence independent way. H-NS has been implicated in virulence in *Shigella flexneri* and *Vibrio cholerae* (Dorman, 2007). Interestingly, H-NS is also able to activate gene expression, however, fewer examples of this exist and unlike H-NS Lsr2 can both activate and repress genes (Dorman, 2004). It had been postulated that Lsr2 exists in mycobacteria due to the

high GC content of the mycobacterial genome and that Lsr2 binds to silence horizontally acquired AT-rich sequences (Gordon et al., 2010) . However, research has shown that l*sr2* is upregulated during mycobacterial stress conditions such as nutrient starvation, prolonged hypoxia and antibiotic exposure, similar to that found during latent Mtb infection in humans (Colangeli et al., 2007; Rustad et al., 2008).

Lsr2 protein in both Mtb and *M. smegmatis* was shown to bind directly to DNA and protect against H_2O_2 and DNase I degradation *in vitro*. Moreover, a *M. smegmatis* Δ*lsr2* mutant was more susceptible to H_2O_2 stress (Colangeli et al., 2009). Changes in oxygen tension, during the course of *Mtb* infection include transitioning from high atmospheric oxygen levels during aerosol transmission to the micro-aerobic or anoxic environments within necrotic granulomas. The Lsr2 protein is a global transcriptional regulator important for allowing Mtb to respond to changes in oxygen levels that would be experienced during both transmission and infection (Bartek et al., 2014). Recent data has shown that the phosphorylation of Lsr2 by PknB is required to control Mtb growth and adaptation to non-permissive growth conditions (Al Qaseer et al., 2019).

The Mtb Δlsr2 strain was not susceptible to H_2O_2 growth under aerobic conditions, however, it showed severe growth impairment on solid media and defects in persistence and adaptation in altered oxygen levels (Bartek et al., 2014). The slowed growth was attributed to actual or perceived low-iron levels. Multiple genes (such as *Rv1067c, sigB, 3288c, Rv3424c, Rv3879c, and Rv3903c*) that were expressed more highly in the Δlsr2 strain also respond to cell envelope disruption through vancomycin addition (Provvedi et al., 2009). The conserved hypothetical proteins produced by the *Rv1501-Rv1507c* operon, that are involved in cell wall biosynthesis were upregulated in the Mtb Δ*lsr2* (Anthony et al., 2009). The differential regulation of genes responsible for cell wall biosynthesis seen in Mtb Δ*lsr2* could account for the cell envelope stress

experienced by this strain. This in turn would result in low internal iron levels in Mtb ∆lsr2 as a result of a potentially defective cell wall.

Interestingly, *rpfA* was found to be downregulated in the Mtb ∆lsr2 strain (Bartek et al., 2014). This suggests that Lsr2 regulates *rpf* gene expression. The ability of Lsr2 to both activate and repress genes, especially genes involved in cell wall remodelling and lipid biosynthesis makes it a global gene regulator. Furthermore, ChIP-chip and microarray analysis of Mtb ∆*lsr2* identified a higher proportion of genes that were upregulated than downregulated, suggesting a function for lsr2 in Mtb latency (Gordon et al., 2010).

11.1.3 Cyclic AMP Receptor Protein (CRP)

Cyclic AMP receptor proteins (CRP; Rv3676) belong to a superfamily of transcription factors that regulate a diversity of physiological processes in bacteria. These DNA-binding proteins primarily function as positive regulators except that a few from this family also act as negative regulator of transcription, depending upon the distance between the binding site and the transcription start-points (Barnard *et al.,* 2003). The best characterized member of this superfamily is the *E.coli* CRP, which controls the expression of numerous genes in response to changes in the intracellular concentration of cAMP as a result of starvation (Gosset et al., 2004). CRP distinguishing features include the presence of a nucleotide binding domain. The classical cAMP-binding domain (Schultz et al., 1991) is a versatile structure that has evolved to accommodate different functional specificities in response to a wide range of signals (Körner et al., 2003, Green et al., 2001). 3′,5′-Cyclic adenosine monophosphate (cAMP), one of the most widely used second messengers and a key modulator of bacterial physiology, regulates a variety of cellular process including virulence (Hofer & Lefkimmiatis, 2007). This second messenger is known to influence

several important aspects of the cellular response to infection. Upon binding cAMP, the cAMP:CRP complex binds to promoters containing DNA sequences related to the consensus TGTGANNNNNNT CACA (Berg & von Hippel, 1988). In the model organism *E.coli*, the level of cAMP is a key factor in osmoregulation via the cAMP receptor protein (CRP). Within macrophages, the cAMP concentration increases by 4-fold following Mtb infection and the intracellular cAMP levels increase by 50-fold in Mtb in host cells (Bai et al., 2009).

The mycobacterial genome contains a single CRP homologue encoded by ORF Rv3676 (Cole et al., 1998). Computational analysis provided insights into DNA and cAMP binding sites within the mycobacterial genome (Bai et al., 2005). We also reported the crystallization and preliminary X-ray diffraction data of this CRP/FNR regulator (Akif et al., 2006). Previously, while comparing the proteome profiles of Mtb and M. bovis BCG, Mattow and colleuagues (2001) observed differences in electrophoretic mobility of CRP proteins. Subsequently, such a mobility shift was attributed to point mutations in both the DNA and cAMP binding domains in CRP of *M. bovis* BCG. These mutations have been ascribed to the impaired DNA binding activity of *M. bovis* BCG-CRP in comparison to Mtb-CRP (Spreadbury et al., 2005). This might suggest these mutations to be one of the contributing factors in attenuation of the virulence of *M. bovis* BCG.

The mycobacterial life cycle includes the exposure to various conditions elicited by the host. One such condition that is of importance to the work featured in this thesis is the exposure to osmotic stress mediated by sodium chloride (NaCl). The regulation of genes involved in cell wall remodelling and reactivation during latency such as rpfs remains incomplete.

Hatzio (2013) and colleagues proposed that PknD, is involved in the osmosensory pathway of Mtb. Mtb's increased intracellular cAMP pool size in response to NaCl stress is partly mediated by PknD. However, the transcriptional regulator CRP orchestrates the overall process. Thus, the link between CRP and RpfA gene regulation is further suggestive of the specific role RpfA has in osmotic tolerance in mycobacteria.

The *rpfA* (Rv0867c) gene, along with several other genes were found to be Mtb CRP binding sites at the intergenic region of the Mtb H37Rv genome (Bai et al., 2005). Transcriptome analysis *in vitro* revealed significant transcriptional changes in the Rv3676 Mtb mutant compared to WT Mtb, including altered expression the *rpfA* gene (Rickman et al., 2005). Analysis showed that the upstream region of *rpfA* Mtb contained a similar site to the CRP binding site in *E.coli* that is required for Rv3676 mediated regulation of *rpfA* expression. This is evidence for *rpfA* gene expression being positively regulated by CRP. It may therefore also suggest that CRP is an important transcriptional regulator controlling Mtb reactivation during latency as *rpfs* are potentially implicated in cell wall remodelling, leading to reactivation from a dormant state. Importantly, ∆*rv3676* Mtb mutants revealed growth defects in laboratory cultures of bone marrow derived macrophages and in mouse models of tuberculosis (Rickman et al., 2005).

1.11.4 Riboswitches

The negative regulation by a homologue of the transcriptional regulator-cAMP receptor protein (CRP) for *rpfA* has been observed (Rickman et al., 2005). It is has been postulated that CRP binds to the promoter region of *rpfA* resulting in the repression of its expression. Moreover, in silico analysis of *rpfA* and its adjacent 5' untranslated region from *Streptomyces coelicolor* resulted in the characterization and identification

of a riboswitch assumed to be the *ydaO* element (Block et al., 2010). Similar to the hypothesized mode of action of CRP, the ydaO motif also has a role in the repression of genes, this has however been shown through experimental data indicating that the *ydaO* element binds to cyclic di-adenosine monophosphate (c-di-AMP), inducing conformational changes with subsequent repression of downstream genes. Riboswitches can control gene expression; they are complex folded RNA domains containing an aptamer and an expression platform. The former binds specific metabolites whilst the latter undergoes structural changes in response to the aptamers, which is responsible for regulating gene expression (Mandal & Breaker, 2004).

YdaO motif is largely found in gram-positive bacteria, including *Bacillus subtilis* and *Streptomyces coelicolor.* The motif is commonly associated with genes implicated in cell wall metabolism, osmotic stress and sporulation (Barrick et al., 2004). Therefore it has been suggested that the *ydaO* may serve as a mediator in critical cellular processes that result in complex rearrangements of cell walls, including germination and notably osmoadaptation.

In *S. coelicolor* the *rpfA* gene can be found downstream from the *ydaO* element (St-Onge et al., 2015). Recent characterization has shown that the cell wall hydrolases in *S. coelicolor* are expressed throughout active growth (Haiser et al., 2009). *In vitro* transcription assays using *S. coelicolor* have shown that the *rpfA* riboswitch promotes premature transcription termination in response to cyclic di-AMP (St-Onge & Elliot, 2017). The use of mutational analysis indicated that a decrease in *rpfA* transcription requires ligand binding. Changes in P1 stem sequence, affects *rpfA* riboswitch activity and the specific deletion of P4, P6, or P5 to P7 significantly increases read-through *in vivo* (St-Onge & Elliot, 2017). Distinctively, the *rpfA* riboswitch has an elongated p2

stem-loop, which is unlike the previously characterized *ydaO*-like riboswitches. Upon binding to cyclic di-AMP the P2-stemloop undergoes substantial restructuring. The use of a mutant riboswitch with a substituted P2 stem region, resulted in a dramatic increase in gene expression of *rpfA* (St-Onge & Elliot, 2017). Thus, *rpfA* expression is negatively regulate by the *ydaO* riboswitch and is positively affected by the antisense sRNA Scr3097.

Recently, the RpfB start codon was reannotated using translation start site mapping (Schwenk et al., 2018). A novel ribosome binding site thought to be targeted by a *rpfB* antisense RNA was identified and validated. Furthermore, the novel riboswitch identified has highlighted a possible co-regulation of resuscitation, cell wall synthesis and ribosome maturation, as *rpfB* is co-transcribed with both *ksgA* and *ispE* downstream (Schwenk et al., 2018). Thus, emphasising a controlled regulatory connection by a riboswitch.

Moreover, Hatzio and colleagues (2013) identified *rpfA* as one of many genes that was highly upregulated upon exposure of Mtb to sodium chloride, further highlighting the connection between the riboswitch in *rpfA* and its implication in response to osmotolerance. Furthermore, *rpfB* and *rpfE* have also been shown to have putative riboswitches (Schwenk, 2018), which may also have implications in mycobacterial stress responses.

The presence of riboswitches in three *rpf* genes coupled with Mtb's adaptability to changes in environmental osmolarity during transitions between airborne droplet nuclei, mucosal epithelia, alveolar macrophages, necrotic cells, and caseous granulomas (Price et al., 2008) has led to the questioning of whether Rpfs may be involved in remodeling the cell wall during changes in osmolarity. Not only is osmotic stress an environmental problem bacteria have to overcome during the course of

infection; but the presence of the *ydaO* motif in *rpfA* and its linked to osmoadaptation further suggests the potential cell wall remodeling role of *rpfs* during osmotic stress and the subsequent physiological adaptations associated with TB pathogenesis.

1.12 Aims and objectives

This project was aimed at elucidating the mechanistic details of Rpfs in mycobacterial stress response and their importance. As well as identifying specific roles for each of the Rpfs proteins.

Objectives:

1. Generate *rpfC* single deletion mutant, and multiple *rpf* double mutants as well as *rpf* triple mutant in *M. marinum*. To establish the importance of *rpfs* in mycobacterial growth using s7H9, Sauton's and solid mycobacterial media
2. To investigate the role of *rpfA* under osmotic stress, using various Δ*rpfA* complemented strains containing different *rpfA* regulatory components and riboswitch
3. To generate multiple deletion rpf mutans and establish their phenotypes
4. To establish whether *rpf* depletion results in impaired iron/metal acquisition

Chapter 2
Materials and Methods

2 .1 Materials

2.1.1 Reagents

All reagents were purchased from either Fischer Scientific Ltd or Sigma-Aldrich, unless otherwise stated.

2.1.2 Media

7H9 Middlebrook broth was prepared by suspending 4.7 g of 7H9 powder (Becton, Dickinson and Company) in 900ml nanopure water containing 2ml of 100% glycerol and autoclaved at 121ºC for 15 min. After cooling down 0.05% Tween 80 and 10% (v/v) ADC were added (these were always added to 7H9 medium and is referred to as 7H9 supplemented medium).

7H10 and 7H11 Middlebrook agar was prepared by suspending 19g of media powder (Becton, Dickinson and Company) in 900ml nanopure water and adding 2ml of 100% glycerol, and supplemented with 10% (v/v) ADC to a final volume of 1L.

Albumin-Dextrose-Complex (ADC) was prepared by dissolving 50g/L Bovine serum albumin, 20 g/L D-glucose and 8.5g/L sodium chloride in distilled water prior to filter sterilization.

Tween 80 10% (w/v) stock was prepared by dissolving 10 g tween in nanopure water (adjusted the final volume to 100 ml). Filter sterilised solution was kept at 4 ºC.

Sauton's medium was prepared as follows; 0.5g KH_2PO_4, 0.5g $MgSO_4$, 2.0 g citric acid, 0.05 g ferric ammonium citrate, 10ml glycerol and 4.0 g asparagine and made up in 1L deionised water. The pH was adjusted to 7.4 using NaOH before sterilisation at 121˚C. An addition of 0.05% Tween 80 was added before use to prevent clumping of *M. marinum* cells.

Luria-Bertani agar (LA) and Lysogeny broth (LB), were prepared by dissolving 10 g/L tryptone (Difco), 5g/L yeast extract (Difco), 5g/L sodium chloride (with 1.5% agar being added to LA) in distilled water.

2.1.3 Antibiotics

The below antibiotics were used at the mentioned concentrations: kanamycin at 50 µg/ml and ampicillin at 100 µg/ml. Stocks 100 mg/ml were prepared in water and filter-sterilised solutions were kept at -20 ºC.

2.2 Cultivation of bacterial strains

2.2.1 Frozen stocks

Frozen stocks of all mycobacterial strains were prepared by mixing 800 µl of mid-log phase bacteria with 400 µl 75 % (v/v) sterile glycerol in a 1.5 ml cryogenic tube (VWR) and stored at -80 °C. Similarly, for *E. coli* strains 800µl of overnight bacterial culture was mixed with 400µl of sterile 75% (v/v) glycerol in 1.5ml cryogenic tubes.

M. marinum starter cultures were prepared from frozen stocks by inoculating bacterial cells scraped from frozen glycerol stock into 7H9 supplemented medium and any appropriate antibiotics (section 2.1.3). *M. marinum* was grown at 32 °C in a shaking incubator (100 rpm) in supplemented 7H9 medium or Sauton's medium for 2 weeks. Bacteria were passaged and allowed to grow to OD_{600} ~0.5 from which a 1/10 dilution was made in 30ml flasks or sealed 10ml tubes. *E. coli* was grown from frozen stock, in 5ml LB, with appropriate antibiotic and grown overnight at 37°C in a shaking incubator (200 rpm). Growth of bacteria was monitored by measuring Optical Density at 600 nm (OD_{600}) using a spectrophotometer. Viability of bacteria were measured using the Miles and Misra method (Miles and Misra, 1938) to determine the number of colony forming units. The bacterial suspensions were serially diluted from 0 to 10^{-6} with 3 drops of 10 µl plated on 7H10 agar, unless otherwise stated.

2.3 Bacterial strains

Information about bacterial strains and their origins used in this work is summarised in Table 1.

Table 1: Table of strains used in this thesis and their sources		
Strains	**Description**	**Source**
E. coli DH5α	Plasmid propagation and cloning	Bioline
Wild type *M. marinum* M strain	*M. marinum* strain isolated from human	Originally provided by Dr. Lalita Ramakrishnan, University of Washington
Δ*rpfA M. marinum*	Unmarked in frame deletion of *rpfA*	Dr. Nino Iakobachvili (Iakobachvili, 2014)
Δ*rpfA::rpfA M. marinum M*	Δ*rpfA* complmented with *M. marinum rpfA* cloned into pmV306	Prof. Galina Mukamolova
Δ*rpfAB M. marinum M*	Unmarked in frame deletion of *rpfA* and *rpfB WT M. marinum M*	This work
Δ*rpfAB::rpfA M. marinum M*	*ΔrpfAB* complemented with *M. marinum rpfA* ligated into pmV306	This work
Δ*rpfAB::rpfB M. marinum M*	*ΔrpfAB* complemented with *M. marinum rpfB* ligated into pmV306	This work
Δ*rpfAEB::rpfA M. marinum M*	*ΔrpfAEB* complemented with *M. marinum rpfA* ligated into pmV306	This work
Δ*rpfAEB::rpfB M. marinum M*	*ΔrpfAEB* complemented with *M. marinum rpfB* ligated into pmV306	This work
Δ*rpfAC M. marinum M*	Unmarked in frame deletion of *rpfA* and *rpfC WT M. marinum M*	This work
Δ*rpfB M. marinum M*	Unmarked in frame deletion of *rpfB WT M. marinum M*	Dr. Nino Iakobachvili (Iakobachvili, 2014)
Δ*rpfBE M. marinum M*	Unmarked in frame deletion of *rpfB*and *rpfE WT M. marinum M*	This work
Δ*rpfC M. marinum M*	Unmarked in frame deletion of *rpfC WT M. marinum M*	This work
Δ*rpfCE M. marinum M*	Unmarked in frame deletion of *rpfC* and *rpfE WT M. marinum M*	This work
Δ*rpfE M. marinum M*	Unmarked in frame deletion of *rpfE WT M. marinum M*	Dr. Nino Iakobachvili (Iakobachvili, 2014)
Δ*rpfAEB M. marinum* M	*ΔrpfAEB* of *M. marinum*	This work

2.4 Gene cloning

2.4.1 Primers

100 μM custom made primers were purchased through Sigma-Aldrich and diluted in DNase/RNase free H_2O to working stock of 10μM.

A list of primers used in this study can be found in Table 2 below.

Table 2: Primer sequences and expected sizes for PCR products of *rpf* strains			
Constructs for flanking regions by appointed name	**Sequence (5'-3')**	**Amplicon size (kb)**	**Description**
MRpfApMV306F	attGGTACCGCCCTGTGAATTGCCT		Amplify the *M. marinum rpfA* and upstream region *(*complementation, pmV306 plasmid)
MRpfApMV306R	acgAAGCTTTCAGGCGAAGACGGTC		
MRpfBpMV306F	atcGGTACCGCCAACAGGCGATTCC CGGTTCG		Amplify the *M. marinum rpfB* and upstream region (complementation, pmV306 plasmid)
MRpfBpMV306R	catGAATTCGGTACGCCCGAGCAGC CGGATGG		
MRpfCFR1F	TACAAGCTTCCAGACGCCGCGCTG ACGGCGTC	1.2	Amplification of the *M. marinum rpfC* flanking regions upstream (FR1) and downstream (FR2) for generation of Δ*rpfC* construct
MRpfCFR1R	CAGGATCCTGTCATGTCCGACTTTT CGGCGGA		
MRpfCFR2F	TCAGGATCCCGTTAGGGGAATATC GTGGTTC	1.2	
MRpfCFR2R	ACAGCGGCCGCCGCCGCCATTCGG CGCTCAGC		
Deletion test primer name	**Sequence (5'-3')**	**Size fragments (kb)**	
MRpfCTESTF	TTGACCGCAACGAGGTCGTACTGC	0.3	
MRpfCTESTR	TCGTCCGGTATTGCGGATGTCGGC		
MRpfBTESTF	CGTCGTGGACGAAGTTCTGT	0.3	
MRpfBTESTR	GCTAGGCCAACAGGCGATTC		
MRpfETESTF MRpfETESTR	AGACCCCAAACAAGATGAGA	0.2	
	CAGCAATTCCTAACTGGACA		
MRpfATESTF	CTCACGTAACGGACGATAAC	0.1	
MRpfATESTR	TGGCTGCCGATCATCGCGAGG		
* Δ*rpfA*, Δ*rpfB,* Δ*rpfE* deletion constructions were provided as p2NIL plasmids and therefore flanking regions have not been included; restriction sites are underlined.			

2.4.2 Generation of complemented *MrpfA* mutant

Primers (see table below) were designed to amplify the *rpfA* gene sequence in *M. marinum* in order to complement back the gene into the *rpfA* mutant. The gene was amplified using PCR and WT *M. marinum* genomic DNA. Once the correct PCR product was visualized on 1% (w/v) agarose, the corresponding sized gene band was excised and purified from agar and primer contaminants. The *MrpfA* gene was then cloned into pmv306 after the plasmid was digested using the restriction sites KpnI and HindIII added to the *MrpfA* primers. Successful cloning of the gene was confirmed by both agarose gel and subsequent sequencing of the gene in the plasmid. The *MrpfA* gene in pmV306 was then electroporated into *M. marinum* ∆*rpfA.* The electroporated cells were spread on 7H10 agar containing 50 µg/ml kanamycin and incubated for 3-4 weeks until colonies were visible. 3 colonies were selected from the 7H10 agar plates and checked for presence of *MrpfA* gene via PCR amplification and agarose gel visualization using UV light.

2.4.*3* Polymerase Chain Reaction (PCR)

2.4.3.1. High fidelity Platinum Taq DNA PCR

DNA sequences were amplified by PCR with 1 x HiFi Buffer, 1.5 mM magnesium chloride, 0.25 µM forward primer, 0.25 µM reverse primer, 2mM dNTP, DMSO was used at 10 % v/v. DMSO (10% v/v) single colony DNA, 2 units per reaction Platinum *Taq* DNA polymerase and sterile, made upto 50µl RNAse and DNAse free water. Small amount of bacteria from single colonies were directly added to each reaction mixture. After an initial denaturation of 5 minutes at 95°C, the amplification profile was 30 cycles of denaturation (95°C for 30 seconds), annealing (55°C for 30 seconds) and extension (72°C for 1.5 minutes/kb); PCR was concluded with 1 cycle of 72°C for 7 minutes. Amplification products (10µl) were analysed on a 1% agarose gel containing 0.5µl/ml ethidium bromide.

2.4.3.2 Colony PCR

The DNA was amplified by PCR using the following reagents: 0.5µl of each forward and reverse primer (10µM), 0.1µl GoTaq DNA Polymerase (5U/µl), 1µl DMSO (10% v/v), 2µl 5x reaction buffer, 1µl dNTPS (2mM), made up to 10µl volumes in DNase/RNase free H_2O.

E. coli DNA was taken from colonies, scraped from LA agar, suspended in 50µl of PBS and heated to 95**°**C to release DNA before centrifugation at 13200rpm for 2 minutes to pellet cellular debris. *M. marinum* DNA template was obtained by resuspending colonies in 100µl DNAse/RNAse free water, heating samples to 95 °C for 20 min, centrifuging for 5 min and using 1µl of the resulting supernatant or adding a small, scraped amount of single colony from 7H10/7H11 agar directly to master mix in PCR tubes.

PCR protocol consisted of initial denaturation of 5 minutes at 95°C, the amplification profile was 30 cycles of denaturation (95°C for 30 seconds), annealing (55°C for 30 seconds) and extension (72°C for 1.5 minutes); PCR was concluded with 1 cycle of 72°C for 7 minutes. Amplification products (10µl) were analysed on a 1% agarose gel containing 0.5µl/ml ethidium bromide.

2.4.4 Isolation of plasmid DNA

Putative *E. coli cell* transformants were grown in 5ml LB overnight at 37°C, shaking at 200 rpm, with appropriate antibiotic. The cultures were centrifuged at 3000 × g for 12 minutes. Plasmid purification was performed on the bacterial pellets following the GenElute™ plasmid Miniprep kit. Ultimately, the plasmid was eluted using 60µl of DNase/ RNase free water.

E. coli transformants for plasmid extraction required 50ml cultures for larger scale plasmid purification using QIAfilter Plasmid Midi Kit (Qiagen). The procedure for culture growth is the same as above with extraction of plasmids being performed according to the Midi kit protocol.

2.4.5 DNA Gel Electrophoresis

To enable confirmation of the correct sized fragments the PCR reaction was subjected to gel electrophoresis; 1 % (w/v) agarose gel was prepared by dissolving 1% w/v agarose in Tris-aceate-EDTA (40mM Tris base, 20mM acetic acid, 1mM EDTA) buffer and 0.5 µg/ml ethidium bromide was added to visiualise DNA when exposed to UV light. DNA samples were combined with 6x loading dye and loaded onto the gel (5µl DNA: 1µl loading dye). Ultimately, the desired bands were excised using a blade and UView™ a UV transilluminator (Bio Rad). The extracted gel was purified according to the QIAquick® gel extraction kit protocol with DNA eluted in DNase/RNase free water.

Finally, the concentration of the eluted DNA was determined using a NanoDrop™ 2000c UV-Vis spectrophotometer.

2.4.6 Restriction digestion

DNA was digested using the following manufacturer's instructions; 10× cutsmart Buffer (New England Biolabs), DNA 1000ng/µl, restriction enzymes 10units/1000ng DNA and making the reaction mixture up to a final volume of 50 µl using DNase/ RNase free water for molecular cloning digestions. 1x NE Buffer, 10 units restriction enzyme, 1x BSA when needed, DNA and RNAse/DNAse free water to final volume. Digestions were incubated at 37 °C for 3 hours. Aliquots of digests were loaded onto a 1% (w/v) agarose gel containing 0.5µl/ml ethidium bromide to visualise the DNA by UV light exposure.

2.4.7 Ligation

DNA ligation used T4 DNA Ligase (Promega) as per the manufacturer's instructions. Reaction conditions were 100ng vector DNA, 150ng insert DNA, 1x Ligase buffer, 1 unit T4 DNA ligase and water to a final volume of 5µl, followed by overnight incubation at room temperature.

2.4.8 Transformation of E. coli competent cells

Alpha-select competent cells (Bioline) were used for the transformation of the ligated DNA insert and vector, according to manufacturer's protocol for all cloning procedures, with SOC medium being exchanged for LB with 25mM $MgSO_4$. Gene constructs in pGEM T-easy were plated on LA agar plates containing 100µg/ml ampicillin, 0.5mM IPTG and 80µg/ml X-gal and incubated at 37°C overnight. However, gene constructs in p2NIL plasmids were plated on LA agar plates containing 50 µg/ml kanamycin.

2.4.9 Preparation of competent mycobacteria and electroporation

A 200ml culture of WT *M. marinum* was grown in 7H9 supplemented media to a final OD_{600} = 0.6-0.8. The cells were harvested by centrifugation at 2000x g for 20 min. the supernatant was discarded and the mycobacterial pellet was washed in 10% (v/v) sterile glycerol 3 times at room temperature. The pellet was ultimately re-suspended in 1 ml 10% glycerol. Then, 3µl of purified and concentrated plasmid DNA was resuspended in 3µl DNase/RNase free water and added to 300 µl competent *M. marinum* cells. The DNA containing cells were transferred to a 2mm long electrode electroporation cuvette (Protech international) before being transformed at 2500, 1000Ω and 2500µF. Recovery of the electroporated cells was aided by the addition of 2ml 7H9 and overnight incubation at 32°C in a standing incubator. Following incubation 250µl of cells were plated onto 7H10 agar containing the appropriate antibiotic for selection and X-gal. Then, 200 µl of competent cells was electroporated with self-replicating plasmid DNA plated as a positive control, and 200 µl competent cells not electroporated with DNA were used as a negative control.

2.5 Protein Methods

2.5.1 Protein purification and expression

Large-scale recombinant RpfA (made by Iakobachvili, 2014) production was prepared by inoculating 500 ml LB containing 50µg/ml ampicillin with 2ml of overnight starter culture. Large-scale cultures were incubated at 37 °C until they reached an OD600 of 0.6-0.7 and expression was induced with 0.5mM IPTG.

After induction, cells were harvested at 8000 x g for 30 min at 4 °C (Beckman F10 rotor, Beckman Coulter Avanti J-30I centrifuge). 20 ml from loading buffer was used to resuspend the pellets; after sonication the the suspension 3 times for 30 sec with pausing for 3 min, centrifugation was then used at 20,000 x g for 35 minutes using

Beckman JA 25.5 rotor, Beckman Coulter Avanti J-30I centrifuge to obtain the soluble fraction.

Immobilized-metal affinity chromatography (IMAC) was prepared for 6xHistidine-tag protein, Before loading the clear lysate into Nickel column, loading buffer was used to wash the column and then washing with low concentration of imidazole (60mM). 250mM imidazole in loading buffer was used to elute the protein. Protein samples were concentrated by using (GeBAflex-Tube 1kDa MWCO) concentrators (Generon, UK). The tube was washed with distiller water and submerged with protein loading buffer prior to adding protein to prevent protein adherence. After incubation overnight in 4°C, the protein sample was centrifuged at a maximum speeds at 4°C for 30 minutes. The RpfA protein purification was obtained by gel filtration superdex 75 (ProSEC 16/60 3-70 HR SEC) column using ÄKTA™ Purifier system (GE Healthcare Life Sciences).

2.5.2 Western blots of Rpf proteins

SDS PAGE gel was transferred onto nitrocellulose membrane and a transfer was performed at 200 V for 1 hour. The membrane was removed and blocked in 5% w/v milk diluted in PBS for 30mins. PBS was used to wash the membrane and it was incubated overnight at 4 °C in primary sheep anti-Rpf antibody (as previously described by Mukamolova *et al.,* (2002).

This was followed by washing the membrane three times in PBS containing 0.1% Tween 20 (PBST) and incubating with secondary anti-sheep antibody conjugated o alkaline phosphatase at a 1:10000 dilution, in 2% (w/v) milk in PBS for 1 hour at room temperature using a rotator.

The membrane was further washed using PBST and 1 tablet of BCIP/NBT substrate (Sigma) dissolved in 10 ml nanopure water was added to the membrane, until dark visible bands could be seen, water was then used to stop the reaction.

2.6 Growth assays

2.6.1 Investigating the effects of NaCl on *M. marinum* growth on agar

To investigate the effects of NaCl on *M. marinum* growth a series of 7H10 agar plates with 10% ADC were made with different NaCL concentrations.

2.6.2 Investigating the effects of NaCl on *M. marinum* growth in liquid

To investigate the effects of NaCl on *M. marinum* growth in liquid 2x 7H9 medium. This medium then had a series of NaCl concentrations added to it, to make up the various NaCl concentrations to assess WT *M. marinum* growth. The 3 M NaCl solution was made by dissolving 175.32g of NaCl in 1 litre.

2.6.3 Assessment of *M. marinum* survival in 2 M NaCl solutions

M. marinum strains were grown from frozen stocks in universal tubes containing 5 ml supplemented 7H9 to an OD_{600} of 0.5.The cultures were then inoculated into glass flasks containing 30ml of supplemented 7H9 medium and grown to O.D 0.5. After bacterial cultures were centrifuged at 2000 x g for 20 minutes by transferring into 50ml falcon tubes. Following centrifugation the supernatant was carefully removed and the pellet was resuspended in 30ml of water, and recentrifuged as before and finally resuspended in 2M Sodium Chloride (NaCl) by diluting to an OD of 0.2. Culture samples were serially diluted from 10^{-1} to 10^{-7} and plated on 7H10 agar to attain CFU/ml counts. Weekly measurements were taken over 4 weeks. Survival in water experiments were set up alongside the starvation experiment as a control.

2.6.5 Generation of *rpfA* constructs for complementation studies

A number of Mtb and *M. marinum rpfA* complemented strains were generated by Dr. Sarah Glenn, with different lengths of the upstream regions of the *rpfA* gene, corresponding to the regulatory regions upstream of the *rpfA* gene, as depicted in the Table 3.

Table 3: *MrpfA* strains used for complementation experiments in osmotic tolerance assays

***M. marinum* Strain**	**Description**	**Source**
Δ*rpfA* C1	Δ*rpfA* strain containing pMV306 plasmid with Mtb *rpfA* and the internal predicted promoter (Mtb genome coordinates 965486-964315)	Dr.Sarah Glenn
Δ*rpfA* C2	Δ*rpfA* strain containing pMV306 plasmid with Mtb *rpfA* and the promoter upstream of the transcription start site (Mtb genome coordinates 965555-964315)	Dr.Sarah Glenn
Δ*rpfA* C3	Δ*rpfA* strain containing pMV306 plasmid with Mtb *rpfA* and the promoter upstream of the riboswitch start (Mtb genome coordinates 965832-964315)	Dr.Sarah Glenn
Δ*rpfA* C4	Δ*rpfA* strain containing pMV306 plasmid with Mtb *rpfA* and the entire upstream intragenic region of *rpfA* (Mtb genome coordinates 965985-964315)	Dr.Sarah Glenn
Δ*rpfA* pMV306:: *MrpfA*	Δ*rpfA* strain containing pMV306 plasmid containing *M. marinum rpfA* with the entire upstream region	Prof. Mukamolova
Δ*rpfA* SDM	Δ*rpfA* strain containing the mutated C4 contruct with double site-directed mutations in the riboswitch G168C/G169C	Dr. Laura Dixon/ Dr. Sarah Glenn

2.6.6 Preparation of culture supernatant for RpfA protein detection

WT *M. marinum,* Δ*rpfA* and Δ*rpfA* complemented strains were grown from frozen stock in 5ml of supplemented 7H9 and grown to exponential phase (OD 0.8). The cultures were then centrifuged at 2000 x g for 15mins. The strains were washed in 10% (v/v) glycerol three times in order to remove any traces of BSA that is present in ADC. The cells were then spun down and the supernatant was removed, the pellet was resuspended in Sauton's medium supplemented with 0.2% dextrose and 0.05% Tween 80, using a final volume of 10 ml and OD 0.3-0.4 for each of the strains. The strains were incubated overnight at 32˚C, shaking. OD's were measured, and once all the strains were at an OD 0.7-0.9, the cultures were placed on ice, spun down at 3,000 x g for 20 mins. The supernatant was then collected and filtered using a 10ml syringe and transferred to new falcon tubes. 20 µg/ml of tRNA (Sigma) was added to the culture supernatant, to act as a protein carrier. The proteins in the culture supernatant were precipitated using 10% (w/v) TCA as a final concentration. The TCA precipitated supernatant for each strain was incubated in ice for ~1 hour. The samples were then pelleted by centrifuging them at 2,000 x g for 30 mins at 4˚C. Once centrifuged, the supernatant was discarded and the pellet was washed in 500 µl of acetone and centrifuged at 20,000 x g, three times. The samples were transferred to 2ml tubes to accommodate the smaller use of volumes at this stage. The acetone was removed and the pellet allowed to dry at room temperature. 4x SDS solublisation buffer was added and the samples were boiled (92˚C for 4 mins) and the proteins were visualized on SDS page or stored at -20˚C for later use.

2.6.7 Growth of *M. marinum* strains in metal supplemented media, liquid and agar

M. marinum was grown at 32 °C in a standing incubator in supplemented 7H9 medium or Sauton's medium. Bacteria were passaged and allowed to grow to OD_{600} ~0.5 and diluted to 0.1 from which a 1/10 dilution was made for all *in vitro* growth studies. Growth of bacteria was measured at OD_{600} nm using a spectrophotometer. Viability of bacteria was measured using the Miles and Misra method (Miles and Misra, 1938) in order to determine the number of colony forming units. The bacterial suspensions were serially diluted from 0 to 10^{-5} and plated on 7H10 agar

The growth curves of WT *M. marinum* and *ΔrpfAB* strain in defined haemin, Zinc conditions were performed using Sauton's medium, 7H10 agar with 100 µM haemin and 100 µM ZnSO4.

The maximum growth rate was calcultated using the following equation: μ=2.303 (log10 *OD*2 – log10 *OD*1)/(*t*2 –*t*1), whereby μ represents specific growth rate; log10 OD2, as the log10 of the optical density measured at t2 and log10 OD1 as the initial optical density measured at t1 during the exponential growth phase. Time was measured in hours. Doubling time was calculated using excel and the following formula, t = Ln2/ μ.

2.6.8 Investigating the effect of culture supernatant in liquid

Freeze dried WT and Δ*rpfA M. marinum* culture supernatant was thawed on ice and rehydrated in 50% nanopure water and 50% Sauton's medium (as described in chapter 2). This was used directly as growth medium for WT, Δ*rpfAEB* and Δ*rpfAEB* complemented strains, alongside standard Sauton's control experiments. The strains were grown for 14 days, with daily OD_{600} nm readings.

2.6.9 Investigating cSN effects on solid medium

Freeze dried cSN from WT *M. marinum* was rehydrated in nanopure water and added to a final concentration of 10% (v/v) to 7H11 agar (Difco), with 10% (v/v) ADC. Exponentially grown *M. marinum* WT and Δ*rpfABE* strains were diluted to OD 0.5 and then serially diluted 10-fold and plated on 7H11 with cSN agar and 7H11 with 10% ADC alone. Images were taken on a 2-3 day interval for growth comparison and initial samples of cultures at OD 0.5 were plated on 7H10 with images being taken after 7 days.

2.7 Whole genome sequencing

Whole genome sequencing was carried out by Microbes NG (University of Birmingham). *M. marinum* Δ*rpfAEB* was streaked out on 7H10 agar and grown until confluent. The bacteria was scraped off the agar plate and sent in a tube with saline solution, provide by the company. The genome was analysed over a 10 week period and returned as a FASTA file. The genome was further analysed for missing *rpf* genes using BLAST and https://mycobrowser.epfl.ch/

2.8 Phase microscopy of *M. marinum* strains

WT *M. marinum* and Δ*rpfAEB* cultures were grown in s7H9 medium to an OD_{600} 0.7. The cultures were transferred onto slides and phase microscopy was carried out using Nikon Eclipse Ni-E microscope at a x1000 magnification to visualize any differences. The bacteria were observed across 10 fields of view, with the selected images being a representation of similar visualizations.

2.9 Statistical analyses

Microsoft excel was used to calculate, mean, standard deviation and standard error.

T-tests were used to compare WT with *rpfAEB*, when comparing only the two strains. The statistical analyses' comparing *ΔrpfAEB*, and *ΔrpfAEB*-complemented strains against WT, was achieved through a one way ANOVA test using Graphpad Prism.

Chapter 3

Resuscitation promoting factors are non-essential for growth in mycobacteria

3.1 Introduction

3.1.1 Rpf studies in other bacteria

Whilst the most extensively studied data pertaining to Rpfs can be found in Mycobacteria, Rpf homologues are widely spread in Actinobacteri*a.* Bioinformatics analysis has found homologs of Rpf only in the high G+C Gram positive bacterial phylum (Ravagnani et al., 2005), all of which have an Rpf domain. Eight subfamilies of Rpf in *Actinobacteria* have been proposed, along with two other families with distantly related proteins in Firmicutes have been putatively identified (Commichau & Halbedel, 2013; Ravagnani *et al.,* 2005). Rpf from *Mi. luteus* of the LysM subfamily is essential for growth (Mukamolova et al., 2002). Conversely, *Corynebacterium glutamicum* has two Rpfs encoding genes; Rpf2 from the RpfB subfamily, and *C. glutamicum* Rpf1 from the *Corynebacterium* subfamily. Contrary to *Mi. luteus*, *rpf* gene deletion experiments showed that *C. glutamicum* Rpfs are non-essential both individually and collectively. However, the *C. glutamicum* double *rpf* deletion strain exhibited slower growth and prolonged lag phase following transfer into fresh medium using long stored cells. Furthermore, this prolonged lag-phase phenotype could be restored in the single *C. glutamicum rpf* deletion strains, the double *rpf* strain and long stored WT, by reducing the lag-phase. However, the addition of purified Rpf1 or Rpf2 protein did not result in a lag-phase growth reduction (Hartmann et al., 2004).

S. coelicolor encodes five Rpf proteins (RpfA to RfpE) and collectively, the *S. coelicolor* Rpf's promote spore germination and are critical for growth under nutrient-limiting conditions (Sexton et al., 2015). These cells then undergo asynchronous round of chromosome segregation, cell division, and cell wall modification to yield chains of dormant exospores (Elliot & Flärdh, 2012). Rpf deletion studies in *S. coelicolor*,

highlighted a most pronounced germination defect in *ΔrpfA* compared to other single deletion strains and WT. Of the individual Rpfs, *ΔrpfA* mutants had the most severe germination defect, with *ΔrpfB* and *ΔrpfC* mutants behaving most like WT (Sexton et al., 2015). For the *ΔrpfB* mutant, this could be explained in part by the fact that RpfB reproducibly exhibited the lowest PG *in vitro* cleavage activity of all the Rpfs. The prevalence and number of Rpf homologues in Actinobacteria genomes suggest that Rpfs play an important role in these groups of bacteria. Due to many of these bacteria being non-spore-forming, and Rpf contributing to growth, resuscitation and possibly dormancy, their prevalence coincides with the need to perform roles such as sporulation in *Streptomyces*. However, the specific mechanisms surrounding resuscitation remain largely unknown.

Mtb has five Rpf homologues encoded throughout its genome by *rpfA*, *rpfB*, *rpfC*, *rpfD* and *rpfE*. However, single rpf genes are non-essential for Mtb growth in vitro and in mice (Tufariello et al., 2004). Kana and colleagues (2008) characterised single, double and multiple Rpf deletion strains in Mtb using allelic exchange mutagenesis resulting in unmarked in-frame *rpf* deletion strains. All the combinations of Mtb quadruple *rpf* gene deletion strains along with the Mtb quintuple Rpf deletion strain resulted in no growth defects and no loss of culturability. All strains displayed approximately the same doubling times during logarithmic growth and achieved similar cell densities in stationary phase. Although, no differences were seen in liquid growth for Mtb *rpf* deletion strains, progressive rpf-like gene loss differentially affects colony formation of Mtb on agar-solidified media, termed delayed colony-formation. The presence of *rpfE* and *rpfB* in two different Mtb quadruple mutants resulted in similar kinetics of colony formation on 7H11 agar compared to WT growth. The Mtb rpf null strain could be genetically complemented by introducing *rpfB* or *rpfE* but could not be

complemented with *rpfC* or *rpfD*. Similarly, the genetic complementation using *rpfE* in Mtb Δ*rpfACBE*, successfully completely reversed the delayed colony-forming phenotype. This may in turn signify functional superiority between the Rpfs in regard to growth on solid medium.

Due to Rpfs being cell-wall cleaving enzymes, their multiple deletions would result in cell wall defects and notably, Mtb *rpf* mutants lacking *rpfB* and *rpfE* were also hypersensitive to the cell wall damaging agent; sodium dodecylsulphate. Both, Δ*rpfACBD* and Δ*rpfACDE*, containing *rpfE* and *rpfB*, respectively, displayed similar phenotypes to that of the Mtb WT strain. Conversely, Mtb rpf deletion strains lacking both *rpfE* and *rpfB*, (Δ*rpfACBE* and Δ*rpfACBED*) displayed marked hypersensitivity to SDS.

Their findings indicated that Rpfs in Mtb were collectively dispensable for growth, however, the deletion of particular *rpfs*, such as the strains retaining *rpfD* or *rpfE* resulted in highly attenuated bacterial growth in mice, with rpfE containing Mtb mutants persisting better than *rpfD* containing Mtb mutant strains. This is suggestive of possible functional hierarchy within the mycobacterial Rpfs.

Ealand and colleagues (2018) investigated the role of Rpfs in *M. smegmatis*. The progressive deletion of *M. smegmatis* genes resulted in altered colony formation on solid medium. The *ΔrpfAB* double deletion mutant and rpf triple deletion mutants derived from the *ΔrpfAB* strain (*ΔrpfABE* and *ΔrpfABE2*) resulted in smooth colony formation on solid medium compared to WT and single deletions strains (Δ*rpfA*, Δ*rpfB*, Δ*rpfE* and Δ*rpfE2* (reannotated as being a homologue of MSMEG_4643, instead of what was previously a Mtb homologue of Rv1884c (Machowski et al., 2014). Colonies of this strain retained the typical rough and wrinkled morphology seen in *M. smegmatis* when grown on solid medium (Glickman & Jacobs, 2000). The defect could be

genetically complemented using Mtb *rpfA* (*Rv0867c*) and *rpfB* (*Rv1009*) genes together on a single integrating vector, pMVrpfAB and thereby restoring the cording phenotype of Δ*rpfAB* and Δ*rpfABEE2* mutants to WT. Thus, signifying the importance of Rpfs in cell morphology. Furthermore, the *M. smegmatis ΔrpfA* mutant derivatives; Δ*rpfAB*, Δ*rpfABE*, Δrpf*ABE2*, and Δrpf*ABEE2* mutant strains were defective in biofilm formation and more sensitive to rifampin compared to WT and single rpf deletion strains. These strains could also be genetically complemented with Mtb homologues *rpfA* and *rpfB.* This in turn highlights the requirement of RpfA and RpfB in *M. smegmatis* biofilm maturation and protection against cell-wall targeting agents.

Although, Rpfs have predominantly been studied in actinobacteria, *rpf* can also be found in firmicutes such as *Listeria monocytogenes*. Similar to the Rpfs found in Mtb the putative Rpfs of *L. monocytogenes* were found to be non-essential for growth in rich medium (BHI) as both single and double deletion strains were able to grow. However, the simultaneous deletion of *lmo252*2 and *lmo0816* in minimal medium with low starting cell density results in extended lag phase of the mutant (Pinto et al., 2013). *In vivo*, the deletion of *lmo2522* and *lmo0816*, either independently or in combination, does not affect the ability of *L. monocytogenes* mutants to replicate in mice spleens and livers infected with these strains (Witte et al., 2013).

The *L. monocytogenes* genome sequence analysis led by Ravagnani and colleagues (2005) proposed that the two proteins, Lmo0186 and Lmo2522, could promote resuscitation by a mechanism analogous to that described for Rpf proteins of Actinobacteria (Mukamolova et al., 2006; Telkov et al., 2006). Bioinformatics analysis predicted transglycosylase activity for both Rpf and Sps domains, whose activity has been confirmed in other Rpfs (Pinto et al., 2013). However, this remains to be confirmed.

The observed Mtb *rpfB* location, upstream from *ksgA* (coding for rRNA small subunit methyltransferase A) has also been witnessed in *L. monocytogenes*. Notably, Lmo0186 has the same domain structure as Mtb RpfB (Ravagnani et al., 2005), whereas Lmo2522 and the *Mi. luteus* Rpf share LysM domains, which mediate binding to bacterial cell wall peptidoglycan (Buist et al., 2008). The simultaneous deletion of the *rpf*-like *Lmo0186* and *Lmo2522* genes in *L. monocytogenes* resulted in an increased lag phase in minimal medium, but no obvious cell morphology alterations were observed in single or double deletions compared to the WT. However, the double mutant was able to reach similar growths of WT once it started to grow. Unlike, the *Mi. luteus* Rpf, both proteins were unable to stimulate growth of cells in a dose-dependent effect at 10 fM to 1 mM (Mukamolova et al., 2002; Pinto et al., 2013).

Interestingly, the possible link between bacterial dormancy and Rpfs has promoted the investigation into the presence of *rpf*-like genes in bacteria occupying various, diverse locations, including plant rhizosphere, contaminated soils, human microbiome and deep sea marine sediments (Bradley et al., 2019; Ye et al., 2020). Rpfs have been found in a unique, newly isolated Actinobacterium known as *Tomitella biformata.* This bacterium is a member of the suborder *Corynebacterineae*, isolated from an ice wedge in Fox Permafrost tunnel, Alaska (Katamaya et al., 2010). Furthermore, in environmental microbiology it has been postulated that a use for Rpfs lies in improving cultivation efficiency, a concept that has also been experimented with in clinical microbiology using Mtb sputum samples (Dusthackeer et al., 2019; Faraj *et al.,* 2020; Rosser et al., 2017).

Thus, the presence of Rpf homologues in numerous bacterial species highlights the importance of their further scientific investigation. Additionally, the multiplicity and

location of *rpf* genes across the genome of various species is suggestive of specific roles.

3.1.2 Generation of unmarked in frame deletion strategy for *rpf* mutant generation

In order to generate the *rpf* deletion strain a well-known gene deletion strategy developed by Parish & Stoker (2000) was utilized. This deletion strategy is the same as that used by Kana and colleagues (2008) to generate multiple *rpf* deletion strains in Mtb and therefore its use in this project, constructing further *rpf* deletion strains in *M. marinum* employs a pre-existing, successful method. Mutant generation involves a two-step process, whereby the chosen flanking regions of the mutant construct are first separately cloned the p2NIL manipulation vector (Figure 5a). This vector is a suicide plasmid containing kanamycin resistance gene and an origin of replication for *E. coli* (OriE) making it feasible to transform the construct into competent *E. coli* cells. However, once the plasmid has integrated into the genomic DNA following electroporation of the final construct into the mycobacterial cell the plasmid is incapable of replicating, owing to its lack of origin of replication for these bacteria.

Ultimately, a PacI cassette containing *lacZ, sacB* and *hygromycin* resistance marker genes is excised from a pGOAL19 vector and ligated into p2NIL plasmid. The final construct contains the flanking regions cloned into their respective restriction sites in p2NIL, which are separated by a small region of the cloning vector along with an OriE, kanamycin resistance gene and a PacI cassette (Figure 5b). The resulting mutant is left with no antimicrobial markers allowing for multiple gene deletions using the same mutant as a background strain without compromising the growth of strain due to the presence of multiple antibiotic markers.

Following transformation into *E. coli* competent cells, standard blue/ white colony screening is used and blue colonies are initially selected from LA/ kanamycin/ X-gal plates as putative single cross over transformants, and grown in LB medium with kanamycin. These single cross over mutants are grown without antibiotics to promote the loss of plasmid and facilitate double cross over events bacterial culture containing potential double crossover mutants are plated onto 7H10 agar plates containing 2% (w/v) sucrose and 50µl/ml x-gal. Double cross over can be screened for using colony PCR of white colonies as these are the sucrose resistant colonies.

This strategy was used to successfully generate a single and multiple double *M. marinum Δrpf* strains.

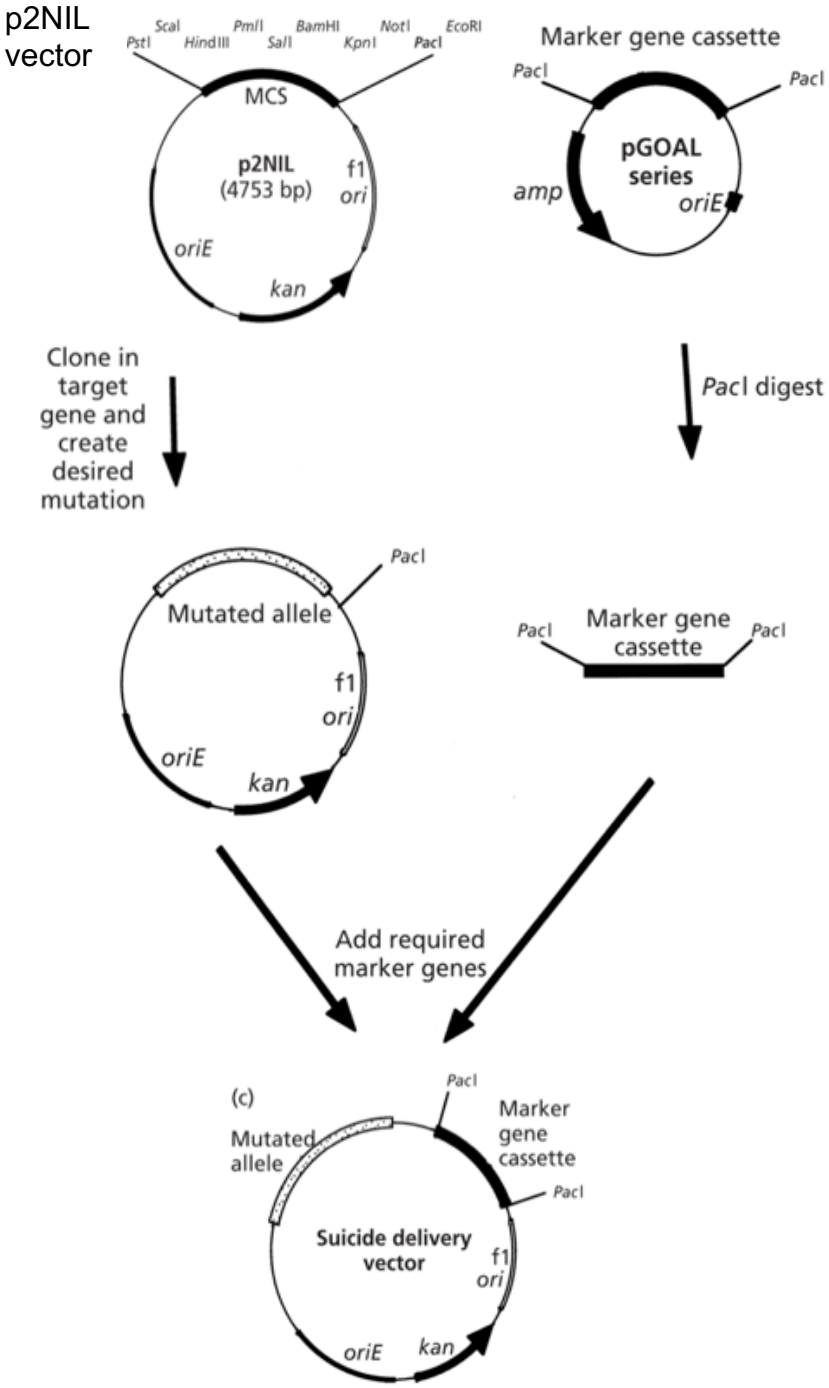

Figure 5: Schematic representation of the cloning strategy for generating suicide delivery vectors. **(A)** The target gene is cloned into the p2NIL vector creating the desired mutation (B) The PacI cassette containing *lacZ sacB* and hygromycin resistance genes is excised from pGOAL 19 vector and cloned into the PacI site of the p2NIL/mutated gene vector, creating the final suicide delivery vector. (c) The final vector contains oriE, the kanamycin resistance gene (kan) and PacI cassette.

3.2 Results

3.2.1 Generation of *M. marinum rpf* deletion strains

M. marinum has four *rpf* genes. Three single *rpf* deletion mutants (Δ*rpfA*, ΔrpfB and Δ*rpfE*) were previously generated in the laboratory (Iakbachvili, 2014), their individual deletion showed that *rpfs* were non-essential in *M. marinum* growth both in liquid and agar media. In this section, the aforementioned method of deleting genes in *M. marinum* resulted in the successful generation of the single *rpf* mutant; *ΔrpfC;* the double *rpf* deletion strains; *ΔrpfAB, ΔrpfBE, ΔrpfCE* and *ΔrpfAC.*

The *rpf* genes are located across the mycobacterial genome and possess numerous regulatory components indicative of possible specialised functions for each of the Rpfs, as previously described in Chapter 1. Therefore, these *Δrpf M. marinum* strains were created in order to assess their roles in mycobacterial growth and later osmotic stress (Chapter 4).

The generation of deletion strains involves the creation of double crossover mutants, which can result in either WT *M. marinum* or the deletion of the desired *rpf* gene. Potential candidates were selected from X-gal/sucrose 7H10 agar plates and amplified by PCR using specific *rpf* deletion primers.

In this project Δ*rpfC* was successfully generated from WT *M. marinum* using deletion constructs and approximately 1kb of DNA sequence both upstream and downstream of the *rpf*C gene to minimize possible polar effects on downstream genes. The fragments were amplified by PCR from *M. marinum* genomic DNA. The fragments were initially cloned into p-GEM T-easy vector followed by cloning into the manipulation vector p2NIL. The 5' fragments were cloned into the HindIII (upstream

fragment) and BamHI sites (downstream fragment); 3' fragments were cloned into the BamHI (upstream region) and NotI (downstream region) of the p2NIL vector.

3.2.2 Generation of Δ*rpfC* construct and Δ*rpfC* mutant

In order to generate the *rpfC* deletion mutant forward and reverse primers of the upstream and down stream flanking regions were designed in order to generate an unmarked, in-frame deletion of *rpfC* (Figure 6).

The nucleotide regions the primers were designed for were ascertained based on BLAST data showing the full *rpfC* gene sequence. The primers were used in a PCR reaction using WT *M. marinum* genomic DNA to amplify the two flanking regions, referred to as flanking region 1 (FR1) and flanking region 2 (FR2). Figure 6 shows the PCR product of FR1 and FR2 following PCR purification on 1% (w/v) agarose gel. This corresponds to the expected fragment size of FR1 (1.2 Kb) and FR2 (1.1 Kb), thus indicating the successful amplification of this region.

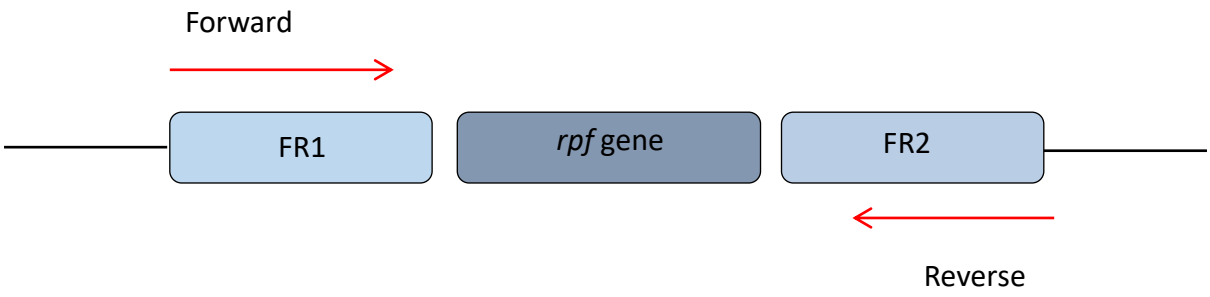

Figure 6: Schematic diagram of gene deletion strategy for diagnostic PCR in *M. marinum rpf* deletion strains. Flanking regions amplify the *rpf* gene of interest and adjacent areas. Successful deletion of *rpf* gene, generates smaller PCR product than WT DNA.

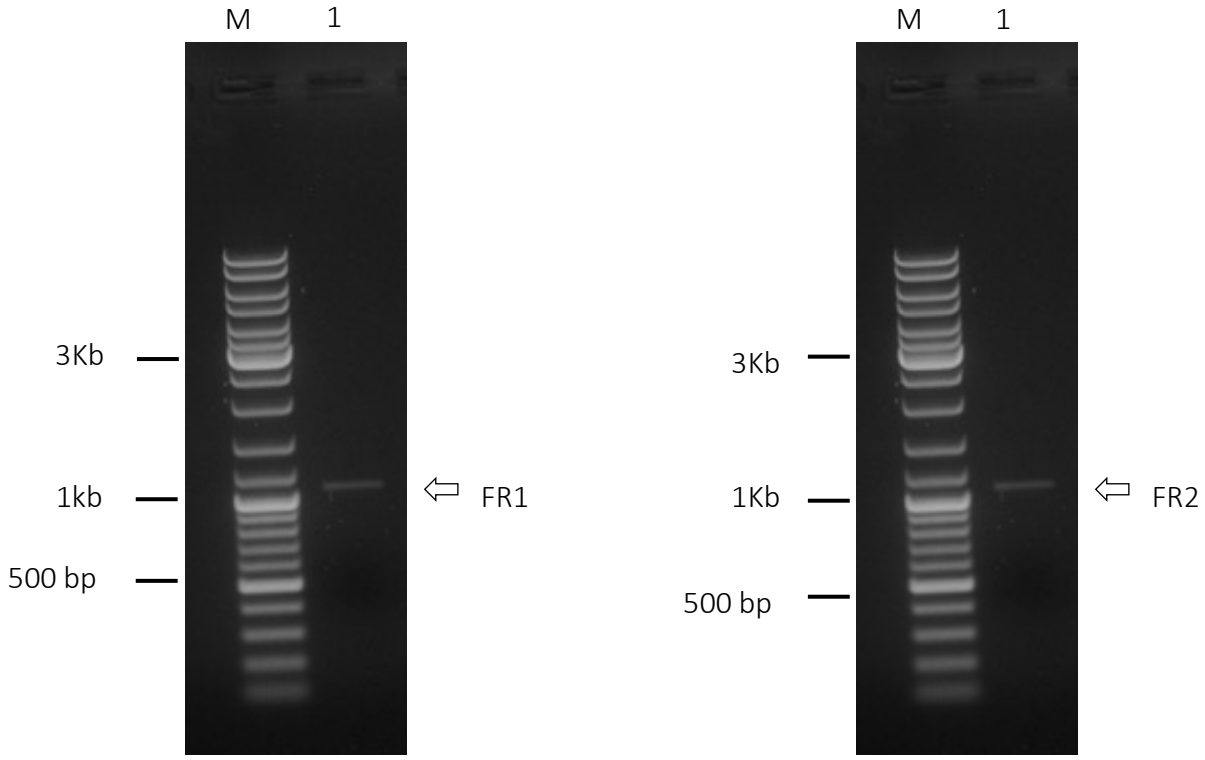

Figure 7: Generation of *M. marinum* Δ*rpfC* construct; left gel; FR1 PCR product following PCR purification: lane M, 1 Kb DNA ladder; lane 1, *rpfC* FR1, PCR product (1.2kb) **right gel:** FR2 PCR product following PCR purification: lane M; 1 Kb DNA ladder; lane 1; *rpfC* FR2, PCR product (1.1kb)

Following the visualization of both FR1 and FR2 on agarose gel, the bands were excised and ligated into pGEM T-easy vector and transformed into *E. coli* cells. Successful transformants were selected and the pGEM T-easy plasmids containing the fragments were extracted and digested using EcoR1 restriction enzymes to ensure that they were not empty plasmids. Figure 8 shows plasmid DNA obtained from 2 transformants that have been digested and have a band corresponding to the size of both the plasmid (~3 Kb) and FR1 (1.2 Kb). Those plasmids containing the correct insert were sent for sequencing to ensure there were no spontaneous mutations present.

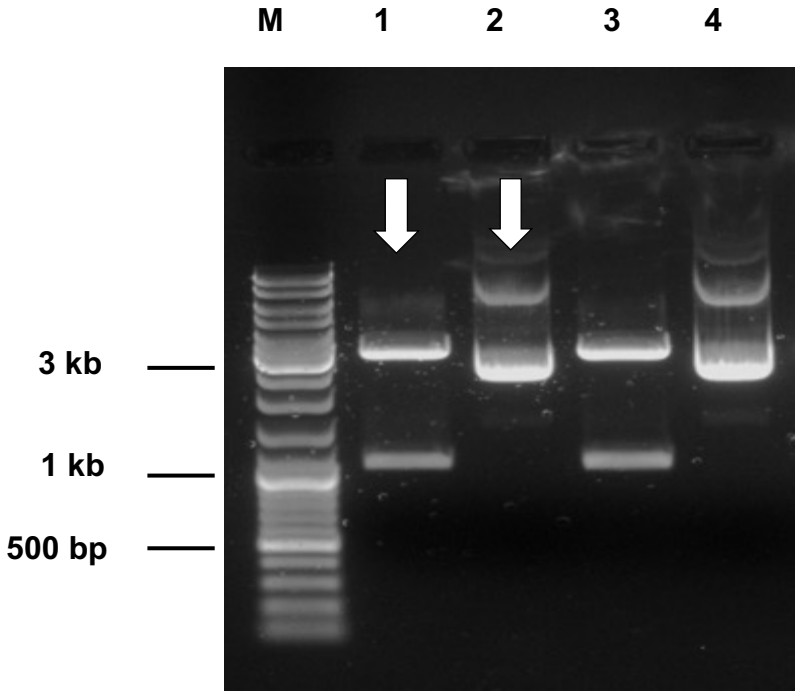

Figure 8: Digest of Fragment 1 (FR1) in pGem- T easy vector of Δ*rpfC* construct (~4kb) using EcoR1 restriction enzyme following isolation of 2 single colony transformants; lane M; 1 Kb DNA ladder; lanes 1 and 3; single digest FR1 (~1.2kb) in pGEM T-easy vector (~3 Kb) with EcoR1; 2 and 4; undigested FR1 in pGEM T-easy vector

Once the sequencing was confirmed for the *rpfC* flanking region constructs, the fragments were excised and ligated into a p2NIL vector and the vector was electroporated into WT *M. marinum* competent cells. The competent cells were then plated onto 7H10 agar containing kanamycin for which plasmid containing cells were selected against. The successful colonies were selected and underwent diagnostic PCR to confirm gene deletion. Figure 9, shows the successful deletion of ∆*rpfC.* lanes 1-12 show the presence of double cross overs with corresponding sizes to that of WT *rpfC* in *M. marinum.* Lane 13 shows the confirmation of *rpfC* deletion, with a gene deletion size of 300bp (Table 1).

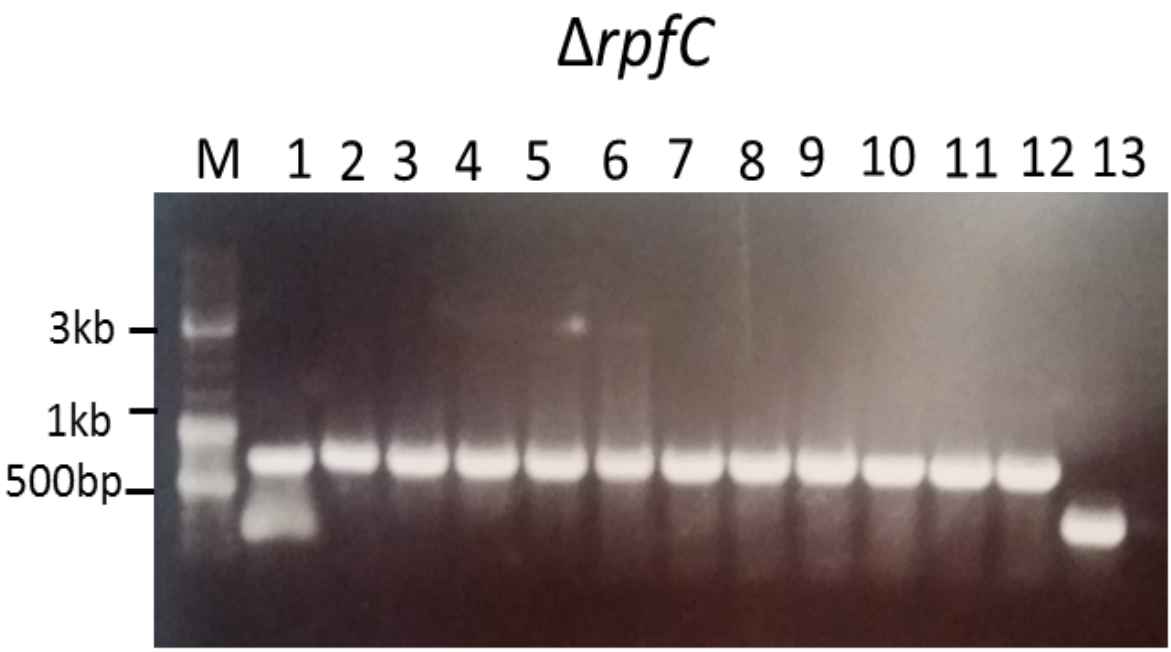

Figure 9: Diagnostic PCR of *M. marinum ΔrpfC* strain using *rpfC* specific primers. Lane 1-12 show *WT* size for *rpfC*, lane 12 shows deleted *rpfC* size

3.2.3 Generation and confirmation of *M. marinum* ∆*rpf* double deletion strains

M. marinum rpf double deletions strains (*ΔrpfAB, ΔrpfBE, ΔrpfCE* and *ΔrpfAC*) were generated using the same unmarked, in-frame deletion strategy as that described for the single *M. marinum rpf* strains (Parish & Stoker, 2000). Diagnostic primers (Iakobachvili, 2014) that adhere to the flanking regions lying outside of the *rpf* gene of interest were used to confirm that the double cross over event had occurred. The strains with the gene still present resulted in much larger amplicons compared to strains having resulted in the deletion of the *rpf* gene, producing a smaller sized amplicons on agarose gel. The agarose gel (Figure 10) indicates the expected gene sizes for all four *rpf* genes along with the expected deletion size for their respective deletion strains (see Table 4).

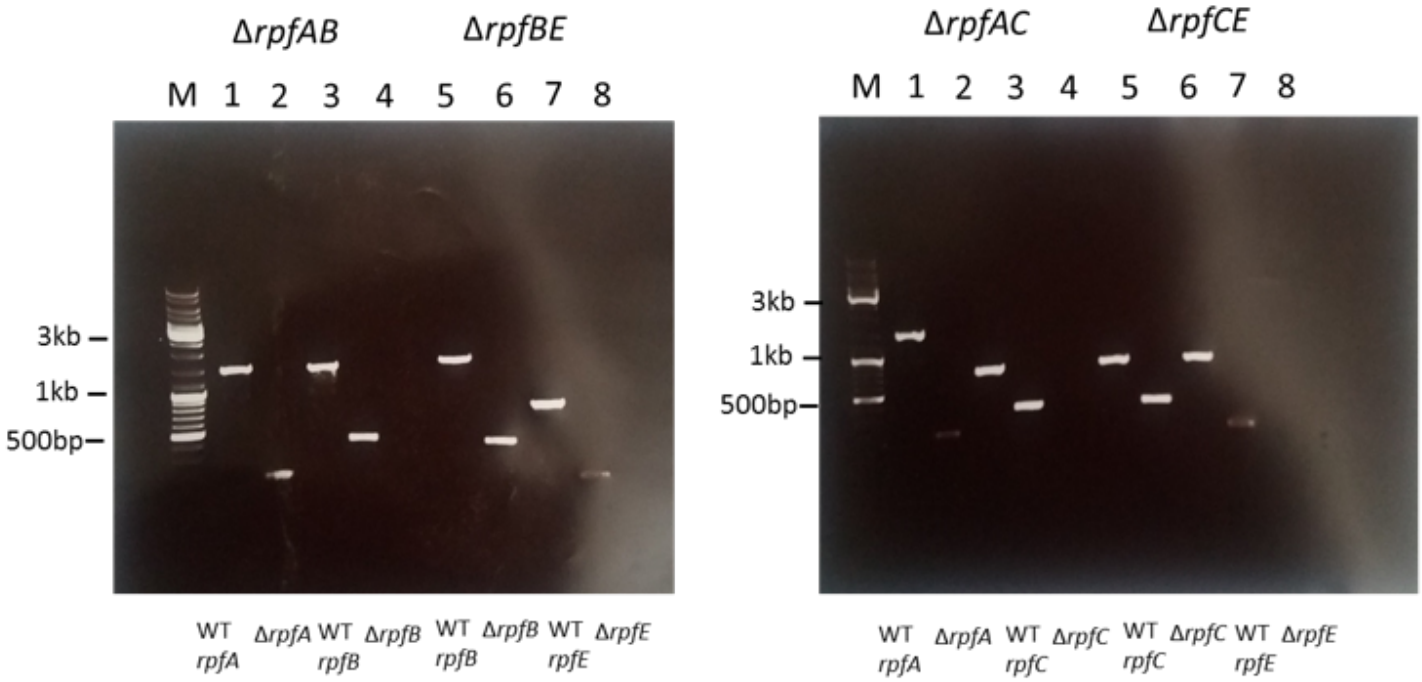

Figure 10: Gene deletion confirmation of *M. marinum Δrpf* mutants using diagnostic PCR on 1% agarose agar. *M. marinum rpf* deletion strains were confirmed using rpf gene specific primers for *rpfA*, *rpfB* and *rpfE*. **Left gel: *ΔrpfAB;*** lane 1 and 3 WT sizes for *rpfA* and *rpfB*; lanes 2 and 4, sizes for the deleted strains of *rpfA* and *rpfB*. ***ΔrpfBE;*** lanes 5 and 7, WT sizes for *rpfB* and *rpfE*; lanes 6 and 8, sizes for deleted strains of *rpfB* and *rpfE*.
Right Gel: *ΔrpfAC;* lanes 1 and 3, WT sizes for *rpfA* and *rpfC*; lanes 2 and 4, sizes for the deleted strains of *rpfA* and *rpfC*. ***ΔrpfCE;*** lanes 5 and 7, *WT* sizes for *rpfC* and *rpfE*; lanes 6 and 8, sized for the deleted strains of *rpfC* and *rpfE*

M. marinum strain with *rpfA* gene still present yields a product size of 1655 bp and the specific gene deletion primers generates a product of 100 bp; strains with *rpfB* gene still present produce a product of 1300 bp and the deleted gene gives a size of 300bp; product with intact *rpfC* gene is 1100 bp and the deleted gene size is 300 bp; the presence of *rpfE* gene amplifies a band size of 950 bp and in the absence of the gene a 250bp band is produced.

These correspond with the sizes that were found for each of the deleted *rpf* genes in the *M. marinum* double deletion mutants (Figure 10). Thus, the deletion of *rpf* genes and consequent *M. marinum rpf* mutant generation has successfully been confirmed using diagnostic PCR.

Table 4: Expected amplicon sizes diagnostic PCR

***M. marinum rpf* gene**	**WT size (bp)**	**Deleted *rpf* gene size (bp)**
rpfA	1655	100
rpfB	1300	300
rpfC	1100	300
rpfE	950	250

3.2.4 Rpf*s* are non-essential for *in vitro* mycobacterial growth

The growth characteristics of multiple *rpf* double deletion strains have been studied in Mtb, *M. smegmatis* and other actinobacteria (Ealand et al., 2018; Hartmann et al., 2004; Kana, 2008), however, this has not been previously investigated in *M. marinum*. In order to assess any differences in growth; the growth phenotypes in 7H9 media was first investigated. *M. marinum WT* and *rpf* deleted strains were initially grown from frozen and measured at regular intervals over a 14 day period. Previous literature has shown that the deletion of single mycobacterial *rpf* genes does not result in attenuated growth in both s7H9 medium (11A) (Iakobachvili, 2014; Kana et al., 2008) and Sauton's minimal medium (Figure 11B). Similarly, none of the double ∆*rpf* strains resulted in a statistically significance difference in growth rate when grown in s7H9 medium ($p>0.05$). Once, the growth characteristics in 7H9 medium had been established and confirmed for the *M. marinum rpf* deletions strains, the growth of the strains in Sauton's medium was investigated. WT *M. marinum* and *rpf* mutants were grown in Sauton's medium as previously described for 7H9 medium. Results indicated by means of optical density, identified no difference in growth between WT and *rpf* deletion strains apart from the growth of *ΔrpfAB* in Sauton's medium which resulted in a statistically significant growth defect, that was absent in both WT and the other *Δrpf* double mutants (Figure 11B). In addition to the attenuated growth of *ΔrpfAB,* this strain does not grow to reach the same optical density as WT *M. marinum* and the other mutant strains. The maximum OD reached by *WT M. marinum* in s7H9 and Sauton's medium is 3.57 and 0.76, respectively, whereas that of *ΔrpfAB* is 3.50 and 0.49. This is indicative of a degree of redundancy in the genes and that the deletion of pairs of *rpfs* still allow for the growth of the bacteria. In order to further assess difference in

growth, the doubling times for the strains was calculated using Microsoft Excel. The calculations generated similar doubling times of all strains in 7H9 medium, ranging from (19.92-24.67 hrs) (Table 5). The values produced indicated no statistically significant difference in doubling time between the strains and corresponds with the similarities seen in optical densities ($p>0.05$). However, a difference in optical density was measured for *ΔrpfAB* when grown in Sauton's medium compared to *M. marinum* WT and *rpf* deletion strains. Notably, the doubling time results for Sauton's medium experiments showed that *ΔrpfAB* (62.49 hrs) ($p<0.05$) grew significantly slower compared to WT and other *rpf* deleted strains (17.04-23.99 hrs).

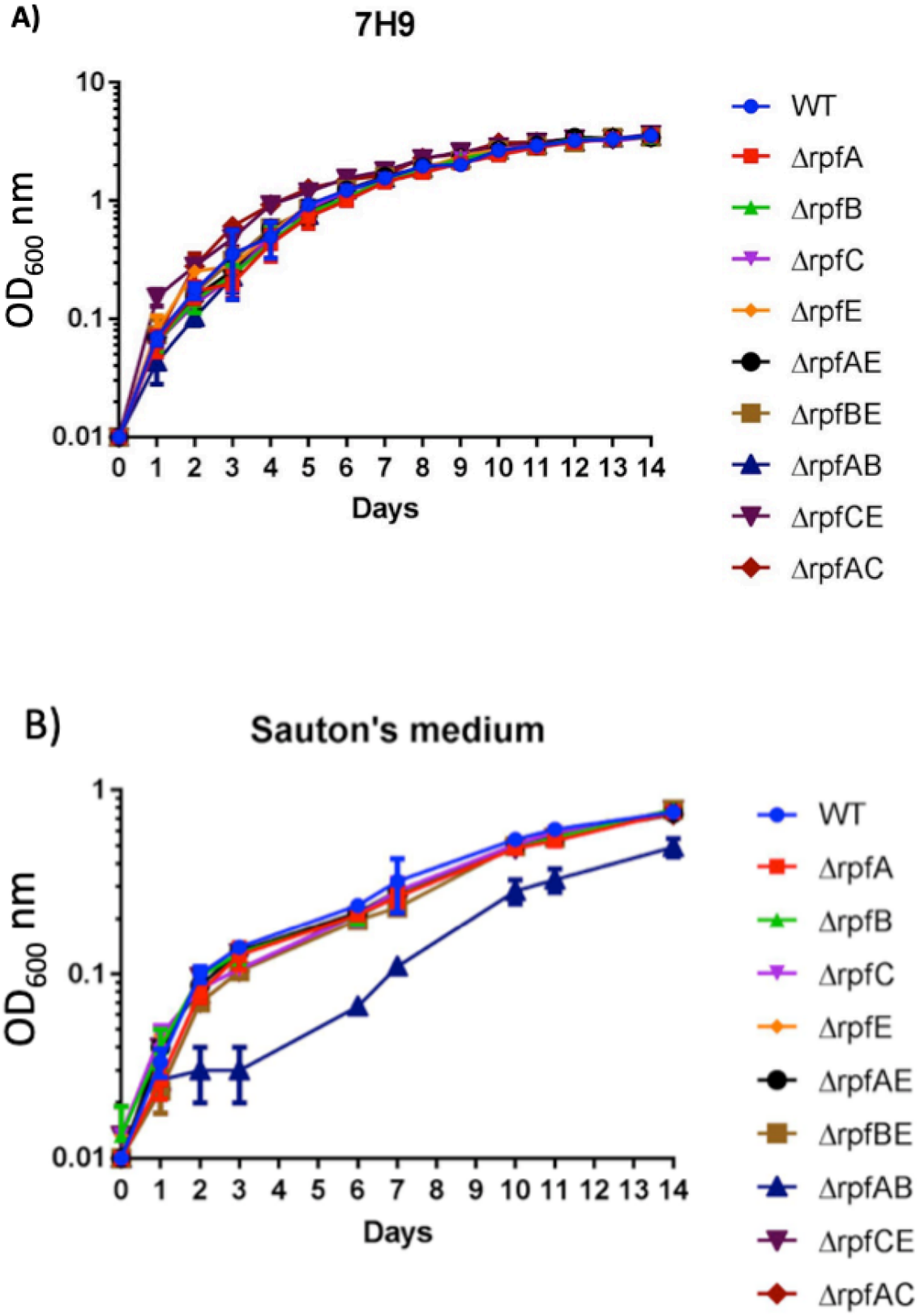

Figure 11: Characterising the growth of Δ*rpf* mutants in liquid medium (A) 7H9 supplemented medium **(B)** Sauton's medium; all single and double *M. marinum rpf* deletion strains have resulted in no significant difference in their growth in Sauton's medium apart from Δ*rpfAB* which has a growth defect (dark blue line). Data shown as mean±SEM (N=9), three experiments with 3 replicates in each experiment.

Table 5: Growth parameters of WT *M. marinum* and *Δrpf* mutants in 7H9 medium										
	WT	*ΔrpfA*	*ΔrpfB*	*ΔrpfC*	*ΔrpfE*	*ΔrpfAE*	*ΔrpfBE*	*ΔrpfAB*	*ΔrpfCE*	*ΔrpfAC*
Doubling time, hours (±S.D)	23.21 ±0.011	21.42 ±0.011	22.70 ±0.02	20.90 ±0.016	23.92 ±0.016	19.92 ±0.007	24.46 ±0.009	20.06 ±0.009	24.67 ±0.011	21.45 ±0.013
Max O.D	3.57	3.53	3.47	3.43	3.42	3.43	3.47	3.44	3.63	3.48

Table 6: Growth parameters of WT *M. marinum* and *rpf* mutants in Sauton's medium										
	WT	*ΔrpfA*	*ΔrpfB*	*ΔrpfC*	*ΔrpfE*	*Δrpf AE*	*Δrpf BE*	*Δrpf AB*	*ΔrpfCE*	*ΔrpfAC*
Doubling time, (hours) (± S.D)	17.14 ±0.003	17.04 ±0.003	17.41 ±0.003	23.99 ±0.002	24.45 ±0.002	22.63 ±0.002	15.75 ±0.002	62.49 ±0.002	19.72 ±0.003	17.85 ±0.002
Max O.D	0.76	0.76	0.78	0.75	0.75	0.75	0.78	0.49	0.78	0.74

Next, the growth of WT *M. marinum* and *rpf* deletion strains, were investigated on 7H10 agar (figure 13). Colony forming unit measurements were taken to assess viable bacteria counts of *rpf* mutant and WT strains (figure 12). Strains were grown to OD_{600} of 0.6-0.8 and diluted to OD_{600} nm 0.1, after which each of the strains were serially diluted in 7H9 supplemented medium to 10^{-6}. Any attenuation in growth for each of the strains was assessed based on the strains ability to increase in CFU counts over a 14-day period. The growth profiles of single and double *rpf* deletion as assessed using one-way ANOVA test (multiple comparison test) did not result in any significant differences in growth compared to WT and other *Δrpf* mutant strains on 7H10 agar strain (ranging between 10^6-10^7) ($p>0.05$). However, *ΔrpfAB* did exhibit a "delayed colony formation" on 7H10 agar, whereby it did not form colonies at higher dilutions (figure 13). This is a phenomenon, which has previously been seen in *rpf* deletion strains (Kana et al., 2008). As a result of this, the *ΔrpfAB*, does not show a pronounced increase in CFU over the 14-day period, when incubated for 7 days. Consequentially, the *M. marinum rpf* mutants, were again plated on 7H10 agar to assess whether the "delayed colony formation" was present in other *Δrpf* mutants. Yet, all single and double *Δrpf* strains formed colonies similar to WT on 7H10 agar (Figure 13), with the slight difference seen in *ΔrpfC* being attributed to lower bacterial counts as seen in the neat fraction compared to WT.

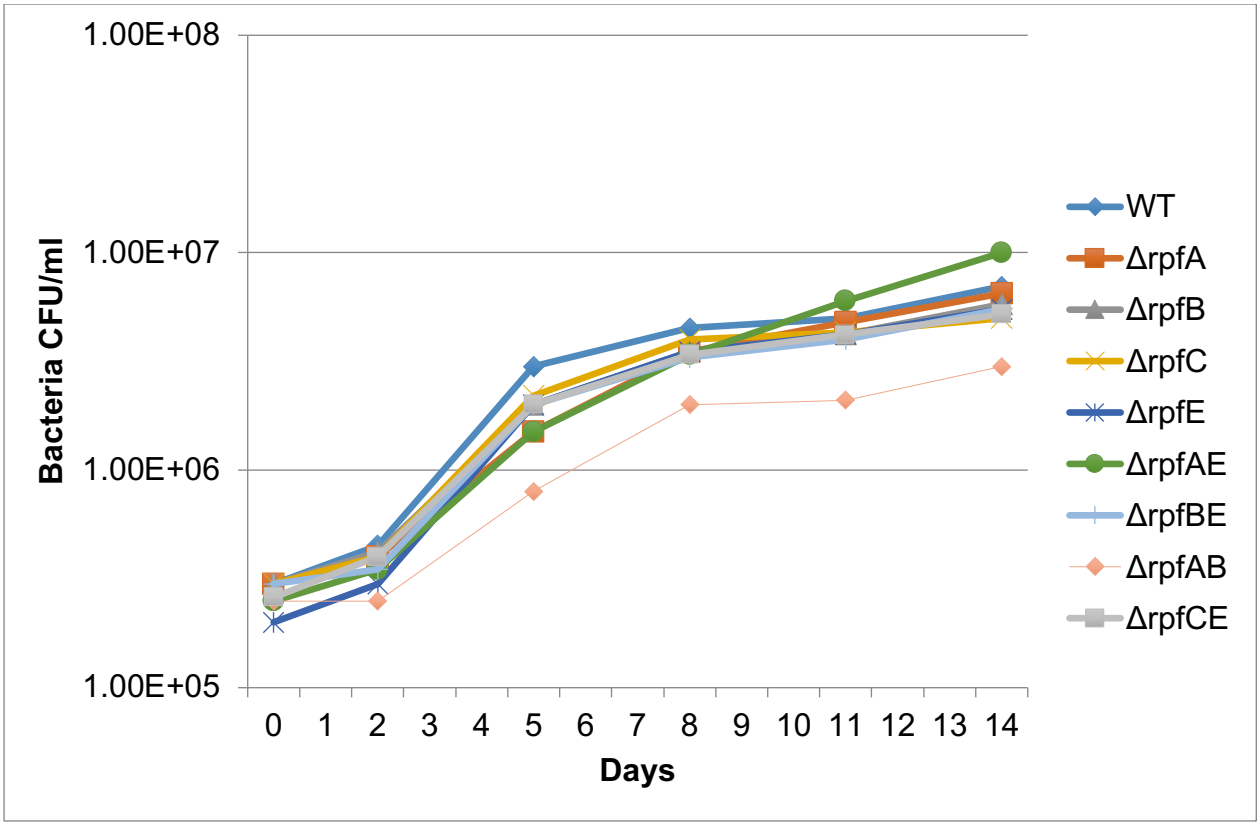

Figure 12: Growth of *M. marinum* strains on 7H10 agar. CFU/ml counts of *M. marinum WT* and *Δrpf* strains taken over 14 days following growth in s7H9 medium. Readings of agar plates were taken after 7 days incubation at 32 C°. Data is representative of 2 experiments; 3 technical replicates per experiment. Data shown as mean±SEM (N=6).

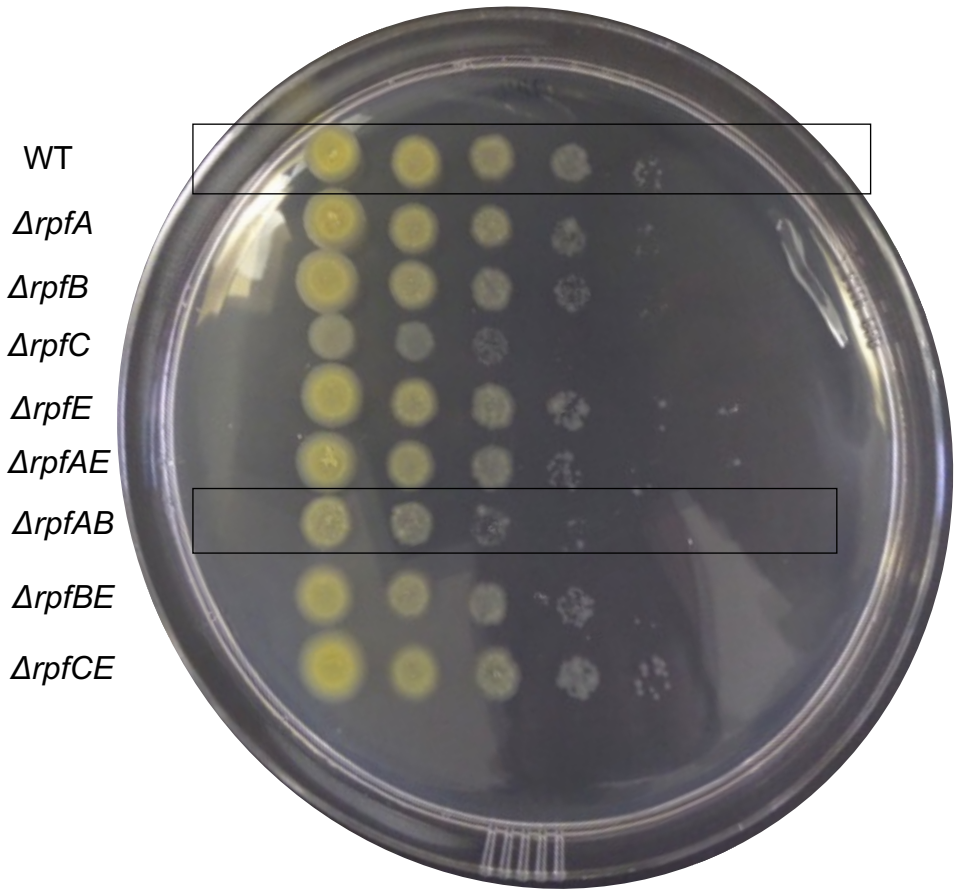

Figure 13: Characterising the growth of *M. marinum Δrpf* mutants on agar. Colony forming units of WT and *Δrpf M. marinum* strains grown in 7H9 supplemented medium and serially diluted down to 10^{-6}. Ten microliters of each dilution was then aliquoted onto 7H10 agar A representative image of 3 replicates

3.3 Discussion

This chapter has illustrated the successful generation of *M. marinum* ∆*rpfC*, the double deletion strains; ∆*rpfAB, ∆rpfBE, ΔrpfCE* and ∆*rpfAC* . Thus far, the growth of WT and *Δrpf* mutants resulted in no statistical significance in growth in both Sauton's and s7H9 media, except for Δ*rpfAB,* which exhibits a growth defect in Sauton's minimal medium and a "delayed colony formation" on agar compared to WT *M. marinum* and the other Δ*rpf* strains. Whilst *ΔrpfAB* has resulted in a distinct and reproducible phenotype on both 7H10 agar and in Sauton's medium, the fact that all strains are still able to grow in mycobacterial medium is indicative of their non-essentiality in mycobacterial growth, coinciding with previously published mycobacterial rpf deletion data. The growth defect seen in ∆*rpfAB* may however, be due to *rpfA* and *rpfB* carrying out a similar function in mycobacterial *in vitro* growth.

The lack of difference in *in vitro* growth that can be seen between WT and *rpf* mutants at both the lag phase and exponential phase in supplemented 7H9 medium agrees with that seen in previous *rpf* studies in other mycobacteria such as Mtb (Kana & Mizrahi, 2010). Therefore, these findings are not surprising. In Mtb Δ*rpfAB* exhibited altered colony morphology, had an impaired growth in primary mouse macrophages aswell as displaying a deficiency in reactivation induced in C57BL/6 mice following administration of nitric oxide synthase inhibitor or by $CD4^+$ T-cell depletion. Notably, these phenotypes were all absent in the single *ΔrpfA* and *ΔrpfB* mutants (Russell-Goldman et al., 2008). However, the single deletion of *ΔrpfB* in Mtb, has also been shown to display a deficiency in reactivation in mice, albeit to a lesser extent of that of *ΔrpfAB* (Tufariello et al., 2006).

Given the involvement of Rpfs in cell wall cleavage these phenotypes of cell wall composition and macrophage responses suggest that *M. tuberculosis* RpfA and RpfB

may influence the outcome of reactivation by possibly modulating innate immune responses resulting in compromised ability for persistence and reactivation. Conversely, the addition of Mtb derived RpfAB, aids in the detection of differentially culturable tubercle bacteria in clinical samples (Gordhan et al., 2021). Further highlighting the importance of both RpfA and RpfB in Mycobacterial reactivation.

The “delayed colony formation” seen in *M. marinum ΔrpfAB,* has previously been described and seen in Mtb *rpf* quadruple mutants retaining *rpfD* and its derived quintuple mutants (Kana et al., 2008). This phenotype in the quintuple mutant could be genetically complemented with *rpfB* or *rpfE* and ΔrpfACBE complemented with *rpfE* completely reversed the delay in colony formation. This would however suggest a functional superiority of RpfE in Mtb. The homology of RpfE in *M. marinum* to RpfE in Mtb is high; suggesting that a delay in colony formation may also have been present in double deletion *M. marinum* mutant lacking *rpfE*, such as *ΔrpfAE*, *ΔrpfBE* and *ΔrpfCE*. Yet, no difference in growth in both s7H9 or Sauton’s media was detected in these strains compared to WT, nor was there a delay in colony formation on solid agar. These findings suggest that the presence of RpfA and RpfB is required for normal growth in minimal medium and colony formation on agar in *M. marinum*.

Interestingly, the difference that can only be seen under minimal growth conditions and is that observed in Δ*rpfAB* in Sauton’s medium (Figure 11). Moreover, 7H9 medium is supplemented with albumin, dextrose and NaCl, which is a key difference between minimal mycobacterial medium and standard medium. The absence of these ingredients coupled with Δ*rpfAB* possible need for a richer medium may be the reason for its attenuated growth in Sauton’s medium. It does not however, undermine the notion of *rpfs* potentially performing distinct roles in mycobacterial stress response and growth.

Chapter 4

Role of RpfA in mycobacterial osmotic tolerance

4.1 Introduction

4.1.1 Osmotic stress and bacterial adaptation

The survival of bacteria is directly related to their ability to adapt to the challenges of environmental stresses and antibiotic pressures within the niches the bacteria inhabit. During the course of infection, bacteria encounter many environmental obstacles and osmotic stress is one of them. Under hyperosmotic conditions, compatible solutes accumulate in bacteria either through synthesis or through import. The changes, which bacteria undergo in response to extracellular osmolarity, have yet to be fully elucidated. Some of the best-studied bacteria for which osmotic tolerance has been investigated and characterized include *E. coli,* as well as the actinobacteria, *B. subtilis* and *C. glutamicum* (Fränzel et al., 2010; Hoffman & Bremer, 2016). The regulation of key cellular processes such as DNA replication, cell growth, metabolism and capsule biosynthesis (Costanzo et al., 2000; Kalivoda et al., 2013; Lin et al., 2013), and the modulation of bacterial physiology is mediated by 3′,5′-cyclic adenosine monophosphate (cAMP), a secondary messenger produced from ATP by the enzyme adenylate cyclase. Osmoadaptation in *E. coli* has implicated the level of cAMP as a key factor in osmoregulation via cAMP receptor (CRP), mediated by the glucose effect on the induction of catabolic enzymes in *E. coli* (Balsalobre et al., 2006). Primary studies showed that glucose could repress the transcription of the lac operon by lowering intracellular cAMP concentrations (Pastan & Perlman, 1970; Ishizuka et al., 1993). The mode of action of CRP is through forming a complex with cAMP. Thereby activating it allowing it to bind to DNA, resulting in the transcriptional activation or repression of many promoters, which in turn determines the expression of genes. Notably, in mycobacteria a homologue of CRP, positively regulates the expression of *rpfA* gene (Rickman et al., 2005), a gene implicated in osmotic tolerance. It has been postulated that CRP binds to the promoter region of *rpfA* resulting

in the activation of its expression. Moreover, in silico analysis of *rpfA* and its adjacent 5'-untranslated region in *S. coelicolor* resulted in the characterization and identification of a riboswitch assumed to be the *ydaO* element (Block et al., 2010). The hypothesized mode of action for *ydaO* riboswitch is the repression of genes, by binding to cyclic di-adenosine monophosphate (c-di-AMP), inducing conformational changes with subsequent repression of downstream genes such as *rpfA*. To date the regulatory mechanisms and effects of NaCl on *rpfA* expression have not been investigated.

During the mycobacterial life cycle, the bacteria experience a variety of sodium chloride concentrations (Tan et al., 2013). In mycobacteria, the theornine/serine kinase PknD is the primary protein involved in the osmosensory pathway and is the first sensor of NaCl stress that dictates the adaptive response via phosphorylation of the anti-sigma factor Rv0516c (Hatzio et al., 2013). Recent experiments by Rebollo-Ramirez and Larrouy-Maumus (2019) using a targeted metabolic analysis combined with stable isotope tracing illustrated that Mtb responds to NaCl stress through increased intracellular mediated cAMP level, however, the findings also showed that *M. marinum* and *M. smegmatis* did not and that the increase in cAMP levels in Mtb is dependent on CRP and partly on the theornine/serine kinase PknD. Rebollo-Ramirez and Larrouy-Maumus (2019) argued that the absence of increased intracellular levels of cAMP in *M. marinum* and *M. smegmatis* could be due to the lack of expression of the adenylate cyclases in these organisms compared to Mtb upon exposure of 250mM NaCl. As *M. marinum* is an environmental organism it may be that 250mM NaCl is not a sufficiently high concentration of salt to promote higher levels of adenylate cyclase expression. However, as *M. marinum* can naturally be found in environments of high salt concentrations (Aronson, 1926). This organism will serve as a good organism to further investigate the possible link between rpfA and osmotic tolerance in mycobacteria.

The sensor–regulator hybrid histidine kinase (OsaC), consisting of OsaA and OsaB in Streptomyces *spp* is required to return the response regulator OsaB and the sigma factor SigB's expression back to constitutive levels after osmotic stress. SigB has been implicated in the proper differentiation and osmoprotection of *S. coelicolor* cells (Cho et al., 2001). Osmostress protectants in *B. subtilis* are imported through five osmotically controlled transport systems (OpuA to OpuE) and B. subtilis is able to use 15 known, naturally occurring compatible solutes to resist osmotic stress (Hoffman & Bremer, 2017). An interesting mapped antisense RNA of *B. subtilis* (S1290), has been shown to be upregulated during osmotic stress. This sRNA is transcribed from a promoter located on the opposite strand of the *opuBD* gene and covers in essence the complete *opuB* operon. Notably, stress sigma factor SigB has been shown to be responsible for stress induction of the S1290 promoter, as strains lacking SigB, did not produce any S1290 RNA following salt stress (Rath et al., 2020).

It has been postulated that there is a time-delayed osmotic induction of *opuB* as a result of transcriptional interference of RNA-polymerase complexes driving synthesis of the converging *opuB* and S1290 mRNA. In addition to this, recent investigations by Warmbold and colleagues (2020) into the two-MarR type regulators, GbsR and OpcR, on *gbsAB*, *opuB*, and *opuC* expression of *B. subtilis* highlighted that transcription of the *gbsR* and *opcR* regulatory genes is up-regulated in response to salt stress, and is also affected through auto-regulatory processes. Mtb has 13 different sigma factors and the SigB homologue (known as SigF), can be found downstream from *rpfB* which may provide further insight to *rpfA* mediated osmoadaptation in Mycobacteria. Sigma factor F (SigF), the general stress response factor of Mtb, is implicated in persistence. PknD can induce the phosphorylation of SigF. Misra and colleagues (2019) showed that the predicted regulatory Rv1364c protein of SigF acts as an independent SigF regulator and

is sensitive to the osmosensory signal, mediating the cross talk of PknD with the SigF regulon. Furthermore, it was shown that PknD can induce the phosphorylation of both Rv1364c and SigF, through an independent mechanism, that mobilises SigF release from Rv1364c (Misra et al., 2019). Notably, a sigF deletion strain of Mtb stopped growing in the murine lungs after 8 weeks of infection, while WT continued growth through 20 weeks (Geiman et al., 2004).

However, not much is currently known about the stress tolerance of mycobacteria in relation to key, habitat-relevant stress parameters such as osmotic stress. Mycobacteria can resist chronic and acute stresses, induced by solutes commonly found in microbial habitats. NaCl is an important solute, as it can be found abundantly in the mycobacterial host. Santos and colleagues (2015) studied mycobacterial stress phenotypes, including osmotic stress. Microbial samples from thermal and glacial environments were collected. The data found indicated that approximately 90% and 52% of samples, respectively, yielded mycobacterium isolates. Thus, further emphasising the adaptive mechanisms exhibited by mycobacteria to combat environmental stressors. The high temperature growing *M. parascrofulaceum* and *M. smegmatis* were both capable of growth in upto 1882mM NaCl. Interestingly, the lag phase of *M. smegmatis* was at is minimal when grown at 1000 mM NaCl. Changes in the degree of saturation of the fatty acids (the ratio between saturated and unsaturated fatty acids) in *M. parascrofulaceum* and *M. smegmatis* were also observed. In *M. parascrofulaceum* cells there was a decrease in the degree of saturation of fatty acids at concentrations of up to 342 mM NaCl, whereas *M. smegmatis* showed an increase in NaCl concentrations of up to 299mM (Santos et al., 2015). However, observation of specific groups of fatty acids were small, suggesting the plasma membrane composition required little change to function. Studies of NaCl exposure in Mtb, showed that increased concentrations of 250mM NaCl affected viability

of Mtb cells as growth was slowed down. Moreover, the incubation of Mtb cells at 1000mM NaCl resulted in a biphasic rapid killing of cells (Larrouy-Maumus et al., 2016).

The hydration and integrity of the bacterial cell and its compartments are determined by their solute concentrations and the osmotic pressures of their environments (Altendorf et al., 2009). Changes in the external osmotic pressures such as a decrease will result in a water influx and subsequent swelling and possible lysis. Conversely, any increase in external osmotic pressures will cause water efflux and dehydration. In order to endure exposure to constantly high osmotic pressures bacteria have to also possess high cytoplasmic solute concentrations. The osmoadaptive mechanisms utilized by bacteria include the release of solute via mechanosensitive channels, altering the water fluxes. The release of “osmolytes” such as in organic ions allow for the bacteria to osmoregulate solute accumulations. The majority of osmoregulatory systems are transcriptionally regulated (Altendorf et al., 2009; Krämer, 2010). As mentioned previously with the asRNA in *B. subtilis*, another important means of regulation is that of small regulatory RNAs, these serve as important determinants of bacterial cell wall structure, which in turn may influence the levels of osmoregulatory systems. Therefore, a greater understanding of the genetic mechanisms underpinning their survival will allow for improved therapeutic methods in TB infection.

The complex regulatory components of rpfs have been discussed in the previous chapter. In this chapter, the hypothesised involvement of *rpfA* in mycobacterial osmotic tolerance has been investigated through the generation of constructs, each comprising of systematic amplification of regulatory regions of *rpfA*, and the deletion of a *rpfA* coding region. To illustrate the constructs, a simplified schematic diagram, representing rpfA and the upstream region, including the ydaO element has been created (figure 14).

The schematic representation illustrates the *rpfA*'s two promoter regions, one which can be found upstream from the gene, just before the transcriptional start site and another which is internal. Two further promoter regions are present upstream from the ydaO element. The *rpfA* constructs generated target the inclusion of specific regions. The shortest construct is the C1 construct and only includes the region starting at the intragenic *rpfA* promoter to the end of the gene (965486-964315). The C2 construct includes both the intergenic and the upstream promoter regions (965555-964315). Both the C3 and C4 constructs include the riboswitch. C3 is amplified from the promoter before the riboswitch the end of the gene (965985-964315), whilst the C4 construct amplifies the entire intragenic regions, from the first promoter (visible in the diagram) upstream from the riboswitch to the end of the rpfA gene. In addition to these constructs a site-directed mutant with a mutation in the ligand binding site of the *ydaO* motif was generated from the original C4 construct. These constructs were used to further understand the involvement of the *ydaO* motif on Δ*rpfA* growth and osmotic tolerance.

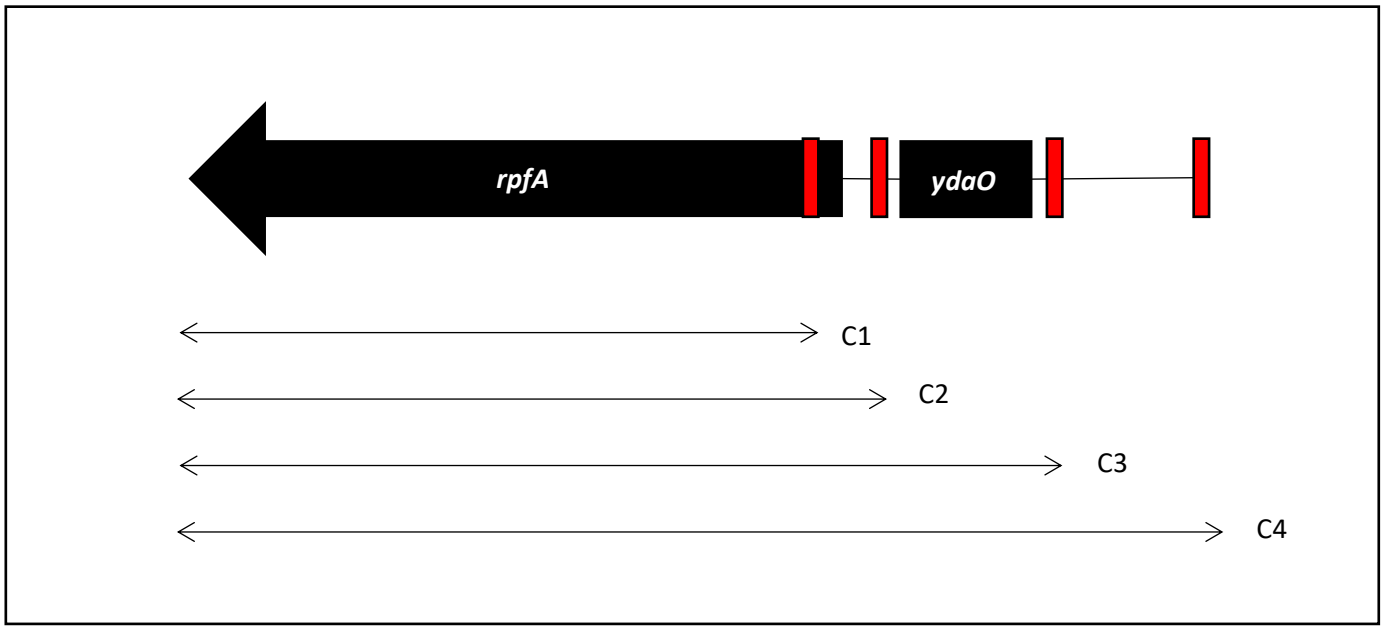

Figure 14: Schematic representation of *rpfA* and *ydaO* element. The promoter regions are shown in red boxes upstream and internal to *rpfA (*Mtb*).* C1; amplified the region from the intragenic promoter to the end of the gene (965486-964315); C2; amplified from the promoter region before the transcriptional start site (TSS) (965555-964315); C3; amplified from the promoter before the riboswitch (965832-964315); C4; amplified the entire intragenic region (965985-964315).The SDM mutant (not shown above) is C4 mutant with a mutation in the ligand binding site of the *ydaO* motif. In *ΔrpfA* has the coding region of *rpfA* was deleted.

4.1.2 Riboswitches

Riboswitches can normally be found in the 5' untranslated region of their mRNA targets (Serganov & Nudler, 2013). They can control gene expression and are complex folded RNA domains containing an aptamer and an expression platform. The former binds specific metabolites whilst the latter undergoes structural changes in response to the aptamers, which is responsible for regulating gene expression (Mandal & Breaker, 2004). The mode of action of riboswitches, mostly involves transcription elongation and translation initiation, but can also impact transcript processing and stability (Serganov & Nudler, 2013).

The *ydaO* riboswitch (Figure 15) is largely found in gram-positive bacteria, including *B. subtilis* and *S. coelicolor.* The *ydaO* motif is one of the most common riboswitches, with over 3,000 representatives in various bacterial species (Gardner et al, 2009). The motif is commonly associated with genes implicated in cell wall metabolism, osmotic stress and sporulation (Barrick et al., 2004). Initial research, highlighted ATP as the ligand for the *ydaO* element (Watson & Fedor, 2012), however, it has been shown to bind to the second messenger cyclic-di-AMP containing a pair of 3′,5′ linkages with subnanomolar affinity (Nelson et al., 2013).

In *B. subtilis*, *ydaO* riboswitch has been shown to prematurely terminate transcription in response to high levels of cyclic-di-AMP (Nelson et al., 2013). It has been suggested that the *ydaO* may serve as a mediator in critical cellular processes that result in complex rearrangements of cell walls, including germination and notably osmoadaptation.

In *S. coelicolor*, the *rpfA* gene can be found downstream from the *ydaO* element. Recent characterization has shown that the cell wall hydrolases in *S. coelicolor* are expressed throughout active growth. RpfA aids in exiting dormancy, through spore

germination (Haiser et al., 2009).

Cyclic-di-AMP is produced by diadenylate cyclase (DisA) (Witte et al., 2008). Investigations into *rpfA* transcript levels using a *S. venezuelae*, *disA* mutant incapable of producing cyclic-di-AMP, resulted in a fivefold increase in full-length *rpfA* transcript levels (St-Onge et al., 2015). Thus, suggesting, like its *B. subtilis* counterpart transcription regulation by a riboswitch.

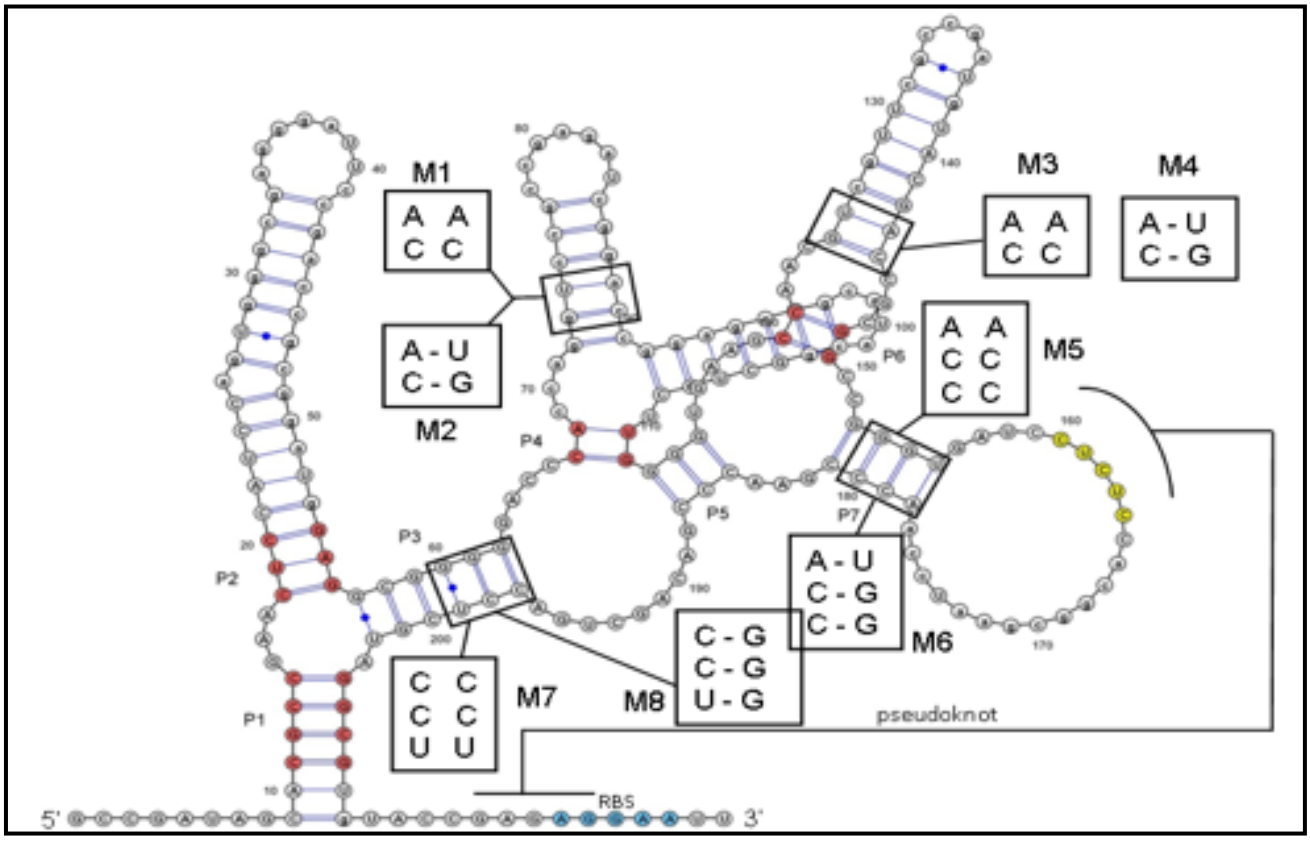

Figure 15: A schematic diagram of *ydaO* motif found upstream the *rpfA* gene in Mycobacteria. The image depicts the structure of the riboswitch and the pseudoknots present.

The presence of the *ydaO* motif in *rpfA* coupled with Mtb adaptability to changes in environmental osmolarity during transitions between airborne droplet nuclei, mucosal epithelia, alveolar macrophages, necrotic cells, and caseous granulomas (Price et al., 2008) has led to the questioning of whether *rpfA* may be involved in remodeling the cell wall during changes in osmolarity. Not only is osmotic stress an environmental problem, bacteria have to overcome during the course of infection; but the presence of the ydaO motif in *rpfA* and it's linked to osmoadaptation further suggests the potential cell wall remodeling role of *rpfs* during osmotic stress and the subsequent physiological adaptations associated with TB pathogenesis. Moreover, Hatzio and colleagues (2013) identified *rpfA* as one of many genes that was highly upregulated upon exposure of sodium chloride to Mtb. This suggest a connection between the regulation of *rpfA* gene expression via the *ydaO* element under osmotic conditions and thus osomotic adaptaion in mycobacteria.

Moreover, the global transcriptional regulator Lsr2, found upstream from *rpfA* is also important for allowing Mtb to respond to changes in oxygen levels is thought to also regulate expression of several *rpf* genes (Bartek et al., 2014). The phosphorylation of Lsr2 has been shown to influence its DNA binding ability to the upstream regions of *rpfA* and subsequently on the expression levels of *rpfA* compared to WT in Mtb (Al Qaseer et al., 2019). This protein functions in a similar way to H-NS from *E. coli*. H-NS works mainly to repress gene transcription by binding to AT-rich sequences in a sequence independent manner and has been implicated in virulence in *S. flexneri* and *V. cholerae* (Dorman, 2007). Although, H-NS is able to activate gene expression far fewer examples of this exist.

The work in this chapter aims to gain further insights into the involvement of *rpfA* in osmotic tolerance, survival under high NaCl conditions and investigating the roles of *ydaO* and other upstream regulatory components of *rpfA* under osmotic stress.

4.2 Results

4.2.1 M. marinum can grow in media with elevated salt concentrations

Previous studies have indicated several regulatory mechanisms involved in control of *rpf* gene expression (Pang et al., 2007; Barrick et al., 2004). Most notably, *rpfA* has been implicated in osmotic tolerance and has a riboswitch, which regulates gene expression. Further to this *rpfA* has been shown to be upregulated in the presence of NaCl (Hatzios et al., 2013). However, there have been no prior published experimental data in regard to the link between mycobacterial *rpfs* and osmotic tolerance.

In order to investigate the highest NaCl concentration at which WT *M. marinum* would exhibit a growth impairment, the growth of *WT M marinum* under elevated NaCl conditions in liquid media was investigated (figure 16). WT bacteria was grown in s7H9. The supplemented medium contains 10% ADC and 0.05% Tween 80. This is notable, as the ADC comprises of Albumin, dextrose and sodium chloride, as a result the salt concentration already present in sodium chloride has been accounted for when it comes to the final salt concentration present in the medium.

WT *M. marinum* was first grown in varying increments of NaCl (150-900mM NaCl). At the lower NaCl concentrations of 150-450mM, there was a decrease in doubling time (16.47-23.13 hrs) as well as an increase in bacterial yield (OD_{600}nm 6.25-9.5) as the maximum OD at these concentrations was substanitially higher compared to WT grown in standard 7H9 media. At a final NaCl concentration of 550 mM, an impaired growth of the WT *M. marinum* was observed. There was a significant increase in WT doubling time (49.12 hrs), which also results in a lower maximum OD (7.05) compared to WT grown at the lower NaCl concentrations. At the higher salt concentrations (650-900 mM NaCl), there is an increase in doubling at 650mM NaCl (43.16hrs), 750mM

NaCl (194.22 hrs), 900mM NaCl (35.39 hrs). The longest doubling time was observed at 750mM NaCl and this corresponds with the delay observed in optical density measurement. Growth of WT at this concentration was observed at day 6 of the experiment. Interestingly, the doubling time at 900mM NaCl seems to decrease compared to WT growth at 750mM NaCl. However, there is an extended lag phase at 900mM NaCl as an increase in optical density is only observed at day 13. These findings suggest that 550mM NaCl is the concentration to further investigate the role of the *rpfA ydaO* motif which as previously described is implicated in osmotic tolerance. Furthermore, the bacteria grow better at final salt concentrations of up to 450 mM NaCl (Figure 16) compared to the standard medium, which contains 150 mM salt. These findings may provide a better, faster growing alternative medium for the cultivation of the slow growing *M. marinum.* Such high salt concentrations have been documented to be unfavourable environments for bacteria to grow efficiently and successfully. However, the bacteria continued to grow up until final NaCl concentrations of 850 mM and do not cease to grow fully upon the addition of 900 mM NaCl.

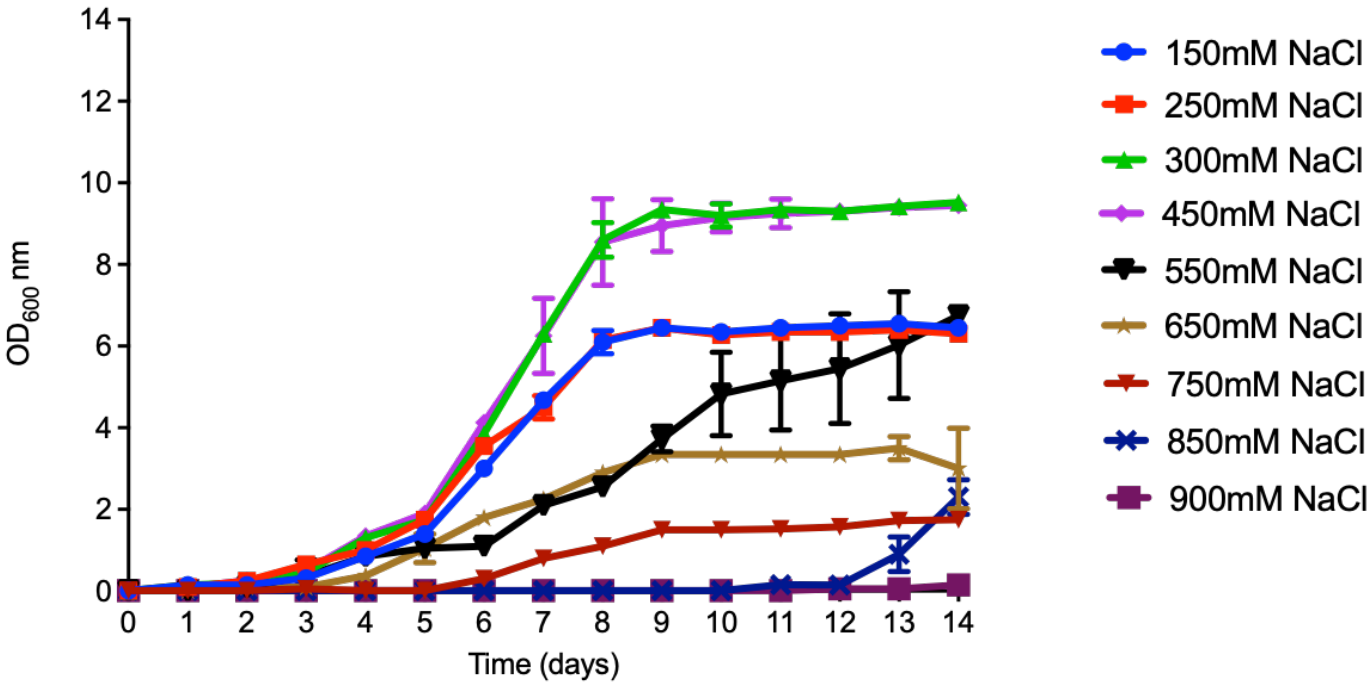

Figure 16: Wild type *M. marinum* growth in supplemented 7H9 medium with addition of different NaCl concentrations. The supplemented medium contains 7H9, 10 % (v/v) ADC and 0.05% Tween 80. 10% ADC contains 150mM salt of NaCl, thus this standard medium was used as positive control indicated by the blue line. The stated NaCl concentrations are reflective of total final NaCl concentration. Daily OD_{600} nm readings were taken in duplicate and averaged over a 14 day period. Data shown as mean mean±SEM (N=6).

Table 7: Growth parameters of WT *M. marinum* growth under elevated NaCl conditions in liquid

NaCl mM	150	250	300	450	550	650	750	850	900
DT± SD	16.47 ±0.01	17.97 ±0.01	23.13± 0.012	16.49± 0.007	49.12± 0.017	43.16 ±0.04	19.22 ±1.49	17. 04±	35.39± 0.011
Max OD	6.25	6.25	9.4	9.5	7.05	3.3	2.60	2.4 5	0.15
DT – doubling time, SD – standard deviation. Description of calculations can be found in methods (section 2.6.7)									

Following these observations, the salt concentration at which WT began to show a growth defect was used as means of comparison for the growth of *rpf* deletion mutants (Figure 17). WT *M. marinum*, Δ*rpfA,* Δ*rpfB.* Δ*rpfE,* Δ*rpfAE* and Δ*rpfAB* were grown in s7H9 with 550mM NaCl. The strains exhibited similar doubling times (17.55-24.21 hrs). There was a slight impairment in growth observed for Δ*rpfAB* on day 1, however, a one-way ANOVA test (multiple comparison) indicated no significant difference in growth between the WT and *rpf* mutants as well as any differences between the *rpf* deleted strains in liquid media with elevated salt ($p>0.05$). Furthermore, the maximum optical densities for WT and *rpf* mutants were also found to be within a similar range (5.97-7.57).

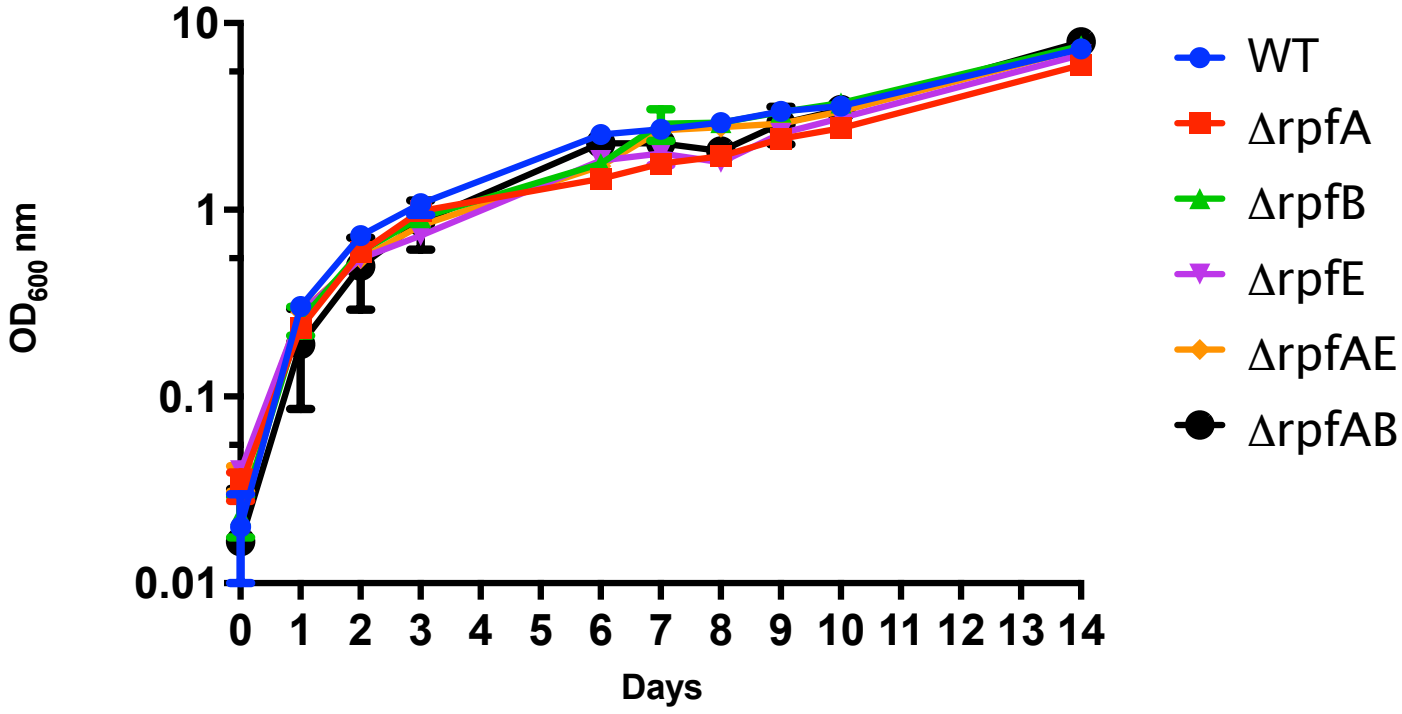

Figure 17: Growth of *M. Marinum Δrpf* mutants at 550mM NaCl in liquid medium. *M. Marinum* WT and *rpf* deletion mutants were grown in s7H9 medium with a final concentration of 550mM NaCl. Daily OD_{600} nm readings were taken over a 14 day period. Error bars represent ± standard deviation of 3 biological replicates, N=9.

Table 8: Growth parameters of *M. marinum* Δ*rpf* mutant growth in s7H9/550mM NaCl

	WT	Δ*rpfA*	Δ*rpfB*	Δ*rpfE*	Δ*rpfAE*	Δ*rpfAB*
Doubling time (hours) (±S.D)	19.10±0.52	17.55±0.02	19.50±0.23	21.97±0.03	24.21±0.02	17.69±0.09
Max O.D	7.27	5.97	7.57	6.77	7.30	7.30
Description of calculations can be found in methods (section 2.6.7)						

4.2.2 Elevated NaCl impairs growth on rpf mutants on solid but not in liquid media

The effects on the growth of *rpf* mutants were investigated using elevated NaCl on 7H10 agar. As mentioned previously none of the deletion mutant had growth defect on standard 7H10 media. However addition of 550mM NaCl resulted in the most pronounced reduction in numbers of colonies for most mutants. The percentage colonies of Δ*rpfA,* Δ*rpfB,* Δ*rpfE,* Δ*rpfAE,* Δ*rpfAB* and Δ*rpfBE* mutants on 7H10 agar containing have been illustrated (Figure 18).

M. marinum strains were grown in s7H9, serially diluted on 7H10 agar (standard) and 7H10 agar with different NaCl concentrations.The solid-coloured bars represent 300mM NaCl 7H10 agar and 500mM NaCl 7H10 agar is represented by chequered bars. The percentage survival of bacteria was calculated by means of Miles and Misra counts (CFU/ml), by subtracting bacteria CFU/ml in NaCl containing 7H10 agar from standard 7H10 bacteria CFU/ml and multiplying by 100.

A percentage decrease compared to WT can be seen for Δ*rpfA,* and this is most pronounced at 550mM NaCl. The double deleted strains Δ*rpfAE,* Δ*rpfAB* and Δ*rpfBE;* exhibit the same pattern of survival on 7H10 with elevated salt, whereas the single deleted strain; Δ*rpfB* survives better at both salt conditions. Δ*rpfE,* on the other hand has a percentage survival of 150% at 300mM NaCl (compared to standard 7H10 media) and does not survive better at 550mM NaCl. A two-way ANOVA test (multiple comparison) indicated that there was no statistical significant difference (95% CI) between WT when individually compared to *ΔrpfA*, *ΔrpfB* and *ΔrpfE* on 7H10 agar with 300 mM NaCl. Interestingly, a significant difference could only be seen in the *Δrpf* double mutants (*ΔrpfAE, ΔrpfAB* and *ΔrpfBE).* However, at the higher NaCl

concentration of 550 mM NaCl, the only *Δrpf* mutant which not display a significant difference when compared to WT or other *Δrpf* mutant strains was *ΔrpfB.*

Whilst the altered survival for Δ*rpfA* may be accounted for by the absence of the *rpfA* gene and thus the absence of the riboswitch which is thought to regulate RpfA in the presence of elevated salt conditions, it does not explain why Δ*rpfE* survives well in both elevated salt conditions on agar. It is possible that the initial bacterial counts for Δ*rpfE* allowed for this improved growth. Furthermore, the impaired survival for all of the Δ*rpf* double strains maybe due to the absence of two of such genes. This coupled with the additional stress of elevated salt, resulted in poor survival of these strains on 7H10 agar.

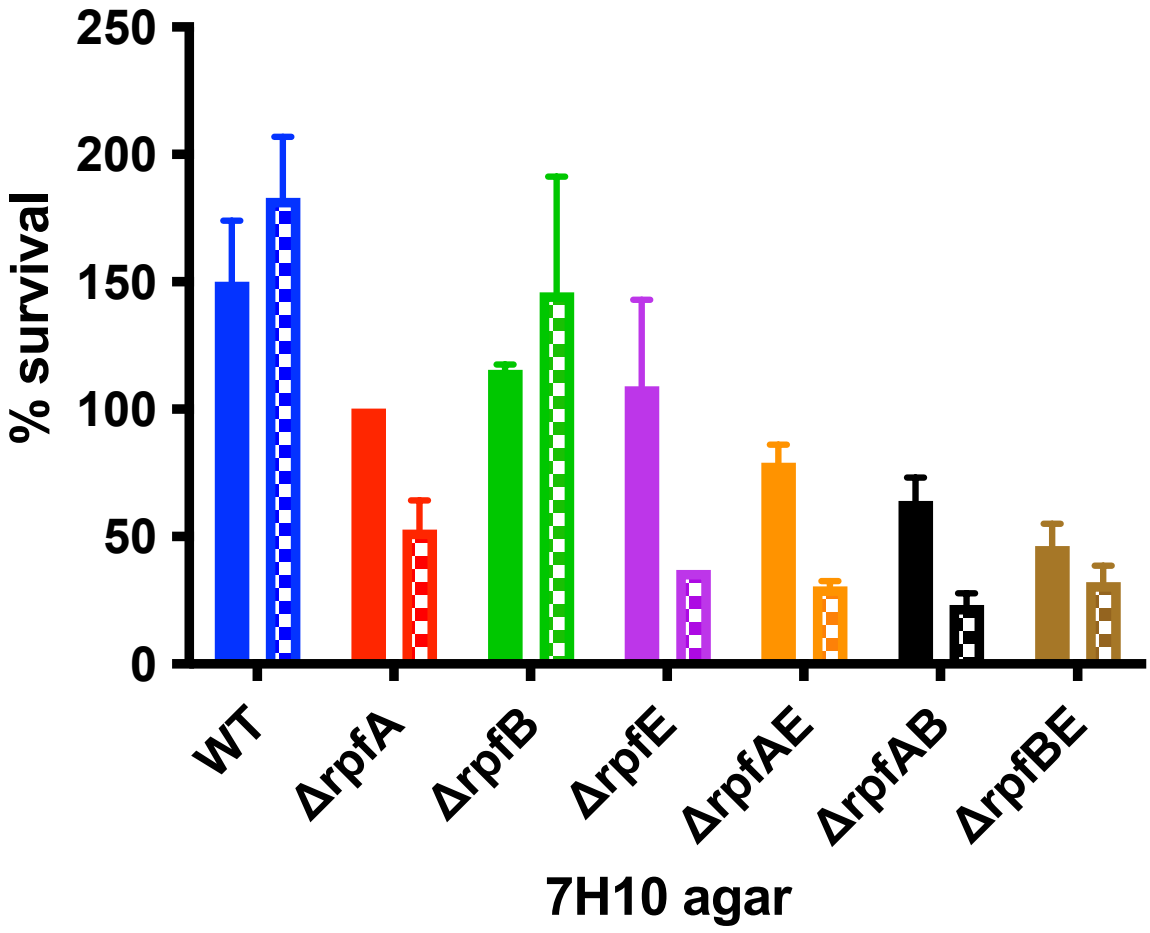

Figure 18: Percentage survival of *M. marinum* WT and Δrpf strains in elevated salt conditions on agar. *M. marinum* strains were grown in 7H9 supplemented medium, serially diluted on 7H10 agar (standard) and 7H10 agar with NaCl. Solid coloured bars represent 300mM NaCl 7H10 agar and chequered bars represent 500mM NaCl 7H10 agar. The percentage survival of bacteria were calculated by means of CFU/ml counts, by subtracting bacteria CFU/ml in NaCl containing 7H10 agar from standard 7H10 bacteria CFU/ml and multiplying by 100. Data presented as means ± standard deviation from 3 individual experiments (N=9)

4.2.3 Δ*rpfA* mutant showed impaired survival during one week storage in 2M NaCl

Previous data gathered in the laboratory indicated that Δ*rpf* mutants can survive in water. However, the data (figure 17) shows the ability of *M. marinum* Δ*rpf* mutants to grow in s7H9 with the addition of 550mM NaCl; suggesting *M. marinum* can also tolerate significant levels of high osmotic environments. It is known that bacteria are subjected to several host stresses during the course of infection. Some of these stresses may include osmotic stress and nutrient depletion (Ehrt & Schnappinger 2011). In order to determine whether the main stress was due to nutrient starvation or merely the presence of high NaCl concentrations, the Δ*rpf* mutants were suspended in 2M NaCl without any nutrients (Figure 19). One-way ANOVA test (Bartlett's test) was performed on *WT*, *ΔrpfA*, *ΔrpfB*, *ΔrpfE* and *ΔrpfAE* indicated a significant difference in 2M NaCl survival (p=0.0441) The results suggest that Δ*rpfE* survives moderately better than the other strains, however, the effects seen were statistically insignificant (p=0.691). Further to this, Δ*rpfA* exhibited some growth defects, which correlates with the slightly reduced Δ*rpfA* growth at 550mM NaCl (Figure 17). The data shows that the deletion of *rpfA* results in impaired survival after 1 week (Figure 19). A further t-test established a significant difference in survival in 2M NaCl between WT and *ΔrpfA* after one week of suspension in the media (p=0.0116). This may indicate a specific role for RpfA in the remodelling of the mycobacterial cell wall during osmotic stress. The data collected suggests that the deletion of *rpfA* leads to impaired growth of mycobacteria at high NaCl concentrations; conversely, the presence of *rpfA* results in better survival and growth in media with high salt concentrations. These findings correlate with *rpfA's* implication in osmotic tolerance and protection as a result of the presence of a putative riboswitch (Block et al., 2010). It does however, appear that

deleting both *rpfA* and *rpfE* also impairs growth in salt as seen in the growth profile of the double *rpf* knockout mutant, Δr*pfAE*, and It may be indicative of a compensatory effect in *rpf's* reminiscent of the "cross talk" between the *rpf's* where the deletion of one leads to the up regulation of another (Downing et al., 2004) . However, this observation might well serve a greater purpose in regards to these proteins' Involvement in stress responses and disease establishment.

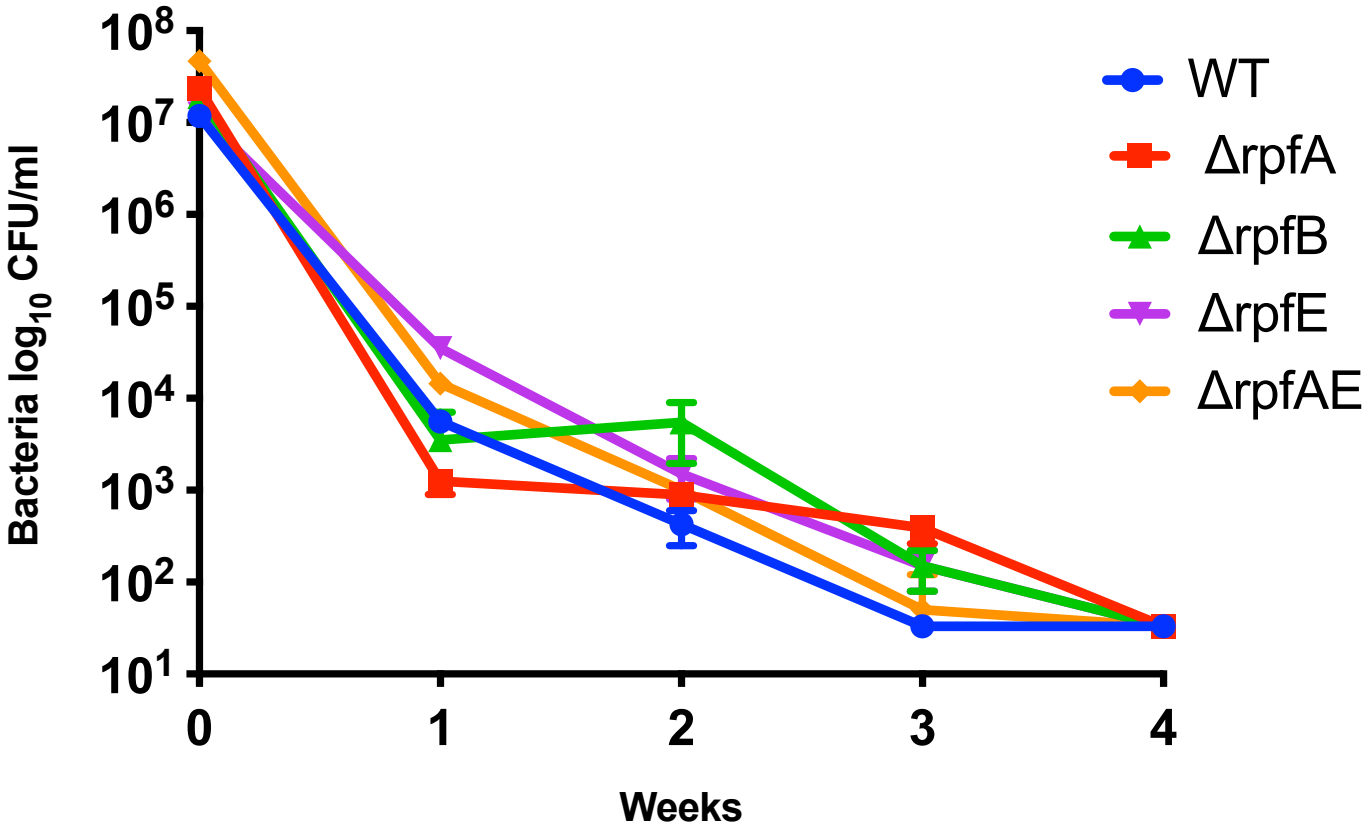

Figure 19: Survival of *M. marinum rpf* mutants in 2M NaCl. *rpf* mutants were incubated at a final NaCl concentration of 2M without nutrients. Weekly CFU/ml counts were taken, with experiments being carried out in duplicate and averaged out over a 4-week period. No survival was seen at 4 weeks for all strains (including week 3 for WT) and values are shown as the limit of detection, 33 CFU/ml. Data presented as mean±SEM (N=6).

4.3 RpfA complementation studies

4.3.1 The *rpfA* riboswitch is required for Mycobacterial osmotic tolerance

The growth of WT *M. marinum, M.marnium ΔrpfA* (deletion of coding region), and five *rpfA* complementation constructs (by Dr.Sarah Glenn) were used to assess the role of the *rpfA* riboswitch in both growth and elevated salt conditions in *M. marinum*. The constructs included, C1; amplified the region from the intragenic promoter to the end of the *rpfA* gene (965486-964315); C2; amplified from the promoter region before the transcriptional start site of *rpfA* (TSS) (965555-964315); C3; amplified from the promoter before the *rpfA* riboswitch (965832-964315); C4; amplified the entire intragenic region of *rpfA* (965985-964315) (see Figure 14). The fifth mutant consisted of a site-directed mutant, which amplified the entire intragenic region of *rpfA* (965985-964315) with a mutation in the ligand-binding site of the *ydaO* motif.

Initially, the growth of the constructs were investigated under standard mycobacterial conditions (Figure 20). The doubling times for WT, *⊿rpfA* and *⊿rpfA* complemented strains in s7H9 were similar (18.82-26.49 hrs, respectively). The lack of difference in growth between the strains was further confirmed by a one-way ANOVA test (multiple comparison), suggesting no statistically significant difference in growth ($p>0.05$).

These findings do not come as a surprise as the *rpfA* mutant has not shown any growth defects in standard medium and the various complemented strains have been hypothesized to be implicated in osmotic tolerance, a stressor which is not present in 7H9 medium.

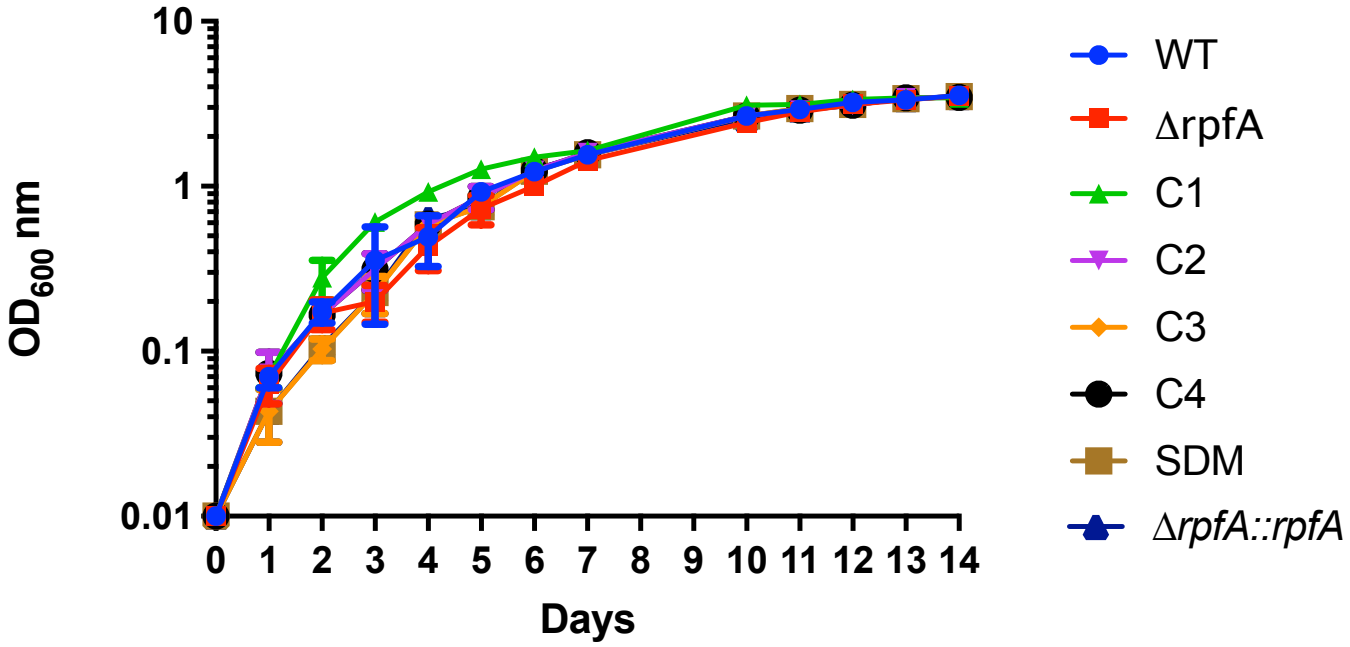

Figure 20: Growth of complemented *ΔrpfA* strains in supplemented 7H9 medium. Daily OD_{600} nm were taken for the strains over a 14 day period.The presented data are mean±SD (N=9).

Table 9: Growth parameters of WT M. marinum, Δ*rpfA* and *rpfA* complemented strains in s7H9 medium

Strain	WT	*ΔrpfA*	C1	C2	C3	C4	SDM	*ΔrpfA rpfA::pMV306*
Doubling time (hours) (±S.D)	20.56±0.06	26.49±0.06	19.30±0.04	21.80±0.04	20.83±0.03	25.27±0.03	18.82±0.03	21.34±0.02
Max OD	3.57	3.53	3.43	3.47	3.50	3.47	3.50	3.50
Description of calculations can be found in methods (section 2.6.7)								

Thus, having established that the complemented *rpfA* strains do not show a difference in growth in standard 7H9 medium. The *rpfA* complemented strains were investigated under elevated salt conditions to establish whether a difference would be present. The growth of WT, *ΔrpfA* and *ΔrpfA* complemented strains on 7H10 agar was investigated on 7H10 agar (figure 21A) using a final salt concentration of 550mM NaCl. This experiment was performed on 7H10 agar as opposed to 7H9 liquid medium as the method would provide a more efficient way to obtain the complementation. The experiment was carried out by growing the strains in 7H9 supplemented medium to ~OD 0.8 and then serially diluting the strains to OD 0.1 and then plating the strains on the 7H10 agar plate with 550mM NaCl.

Δ*rpfA* mutant shows a growth defect compared to WT. The ability of these strains to grow on 7H10 agar with elevated salt was quantified by colony forming units (figure 21B) (Miles and Misra, 1972). As determined by a one-way ANOVA test (Dunnett's multiple comparison), there were statistically significant differences between WT and *ΔrpfA,* C1, C2, C3 and the SDM but not between WT and C4*,* nor between *WT* and *ΔrpfA rpfA::pmv306* (figure 21B).

C1, C2 and Δ*rpfA SDM* strains showed partial complementation, whilst C3, C4 and Δ*rpfA::rpfApmv306* strains grew similarly to WT. The complementation of Δ*rpfA* by *C3, C4, rpfA rpfA::pmv306* (whole *rpfA* gene complementation) versions can accounted for by the inclusion of a number of regulatory components in these strains. It highlights the need for *ydaO* element in *rpfA* regulation and is indicative of this being highly controlled. Notably, the *rpfA* site direct mutant, has a mutation in the pseudoknot of the riboswitch. This means that the riboswitch is unable to bind its ligand and is renders dysfunctional. This finding is of importance as its partial complementation is indicative of the role the ydaO motif plays in *rpfA* gene regulation.

A

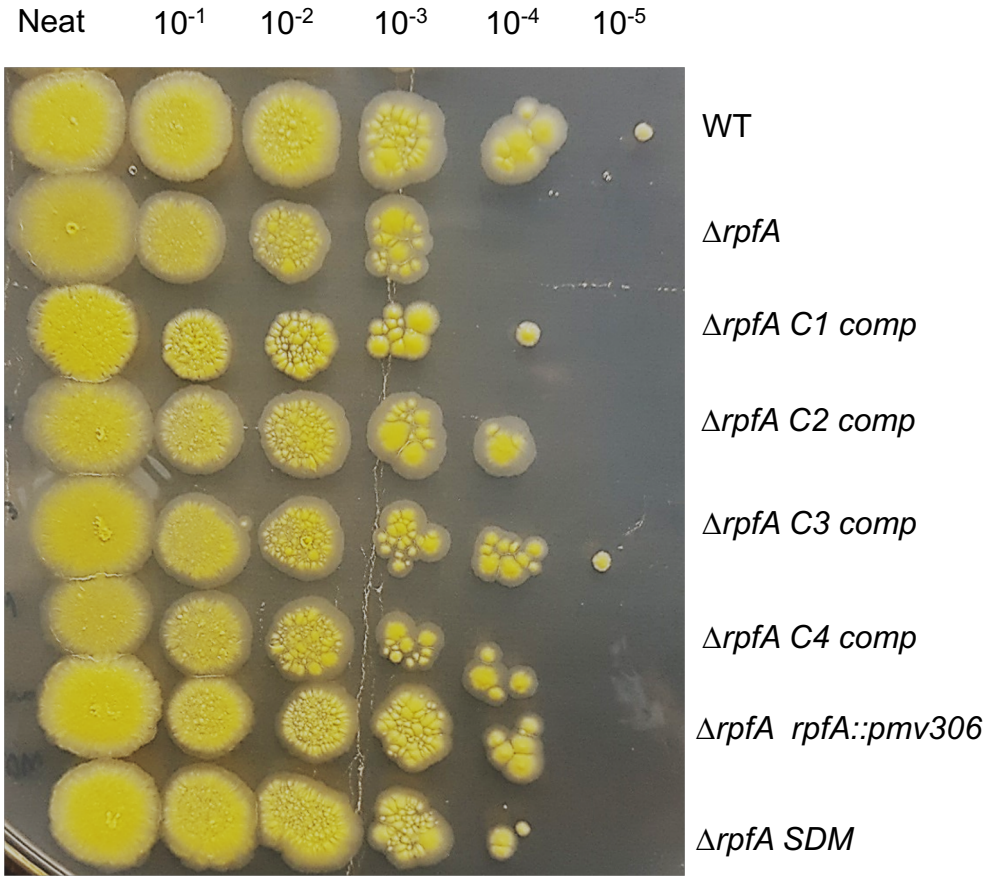

550mM NaCl 7H10 agar

B

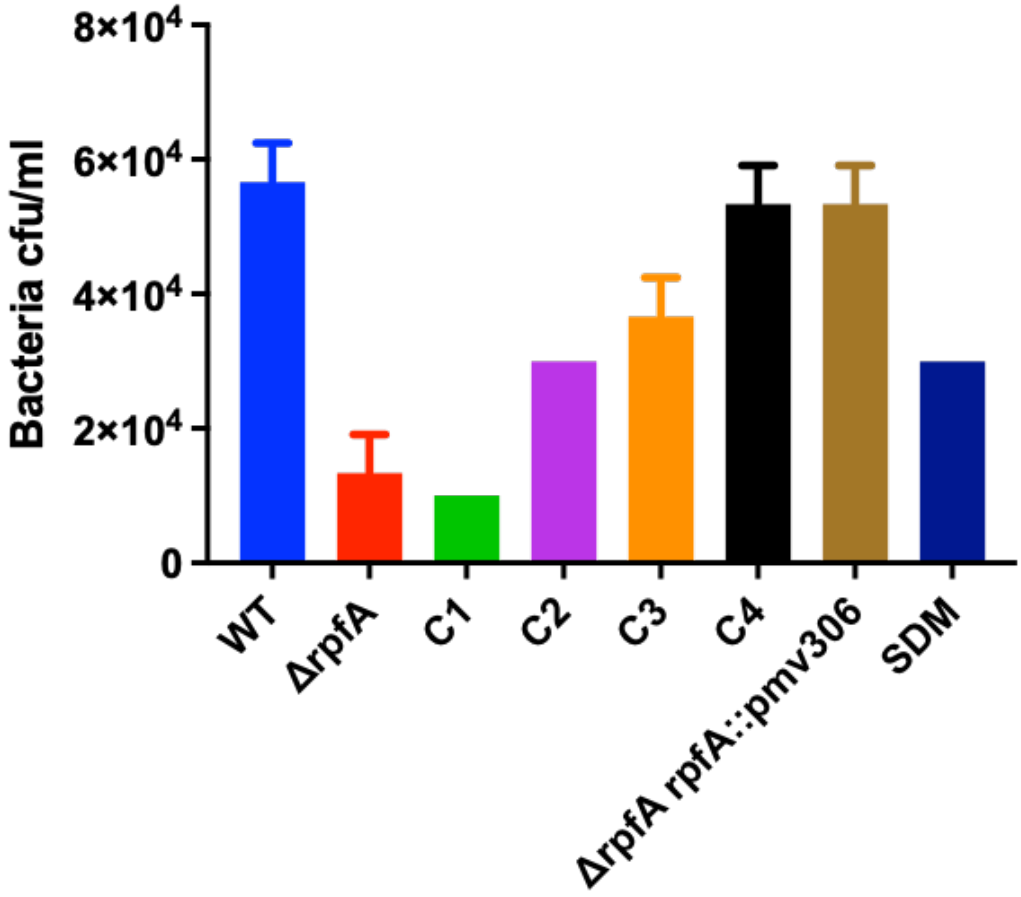

Figure 21: (A) *WT, ΔrpfA* and *rpfA* complemented strains grown on 7H10 agar with 550 mM NaCl; the strains were serially diluted onto 7H10 agar after being grown in 7H9 supplemented medium to OD 0.7 and diluted to OD 0.1. The experiment was performed in triplicate and this is visual representation of one experiment (yellow pigment is due to photochromatogenic pigment present in *M. marinum*) **(B)** Quantification of *WT, ΔrpfA* and *rpfA* complemented strains grown on 7H10 agar with 550 mM NaCl. Data shown as mean with standard deviation (N=9)

4.3.2 Presence of RpfA in the culture supernatant

Literature has previously shown that RpfA is secreted, we show that it can be found in the culture supernatant of growing WT *M. marinum* cultures. The successful generation of the various *rpfA* complemented strains and their viability on different mycobacterial media allowed for further investigations into the way in which *rpfA* is regulated. However, in order to attribute the phenotypes to the presence or absence of the different regulatory components of *rpfA.* it was necessary to identify and confirm the presence of RpfA. As such WT, ∆*rpfA* and ∆*rpfA* complemented strains were grown in 7H9 medium (as described in methods) and the culture supernatant was investigated for the presence of RpfA on a western blot using anti rpf specific antibodies. The predicted size of the RpfA protein is roughly 38 kDa; however, a recombinant RpfA was previously shown to have an anomalous migration in SDS PAGE as much bigger protein (Mukamolova et al., 2002). It was suggested that the proline alanine rich tail present in RpfA caused this anomalous behaviour. Visible ~70 kDa bands were detected in samples from WT, C3, C4, SDM and ∆*rpfA rpfA::pmv306.* As expected, in the *rpfA* deleted strain, no protein is produced (Figure 22). The C1 and C2 complemented strains did not produce secreted versions of RpfA, supporting the lack of complementation observed in the growth experiments (Figure 21). The detection of RpfA in culture supernatants of WT and strains containing the riboswitch was indicative that it might be necessary for RpfA production. It was interesting and important to note that the strains were grown under standard conditions in Sauton's medium and it appeared that the quantities of secreted RpfA in each of the RpfA secreting strains were relatively similar. In order to establish if this notion holds true additional experiments and densitometry studies would be required. It would be interesting to investigate the quantity of RpfA secreted for WT and the complemented

strains when grown under elevated salt conditions in order to establish the extent to which each regulatory component regulates RpfA production.

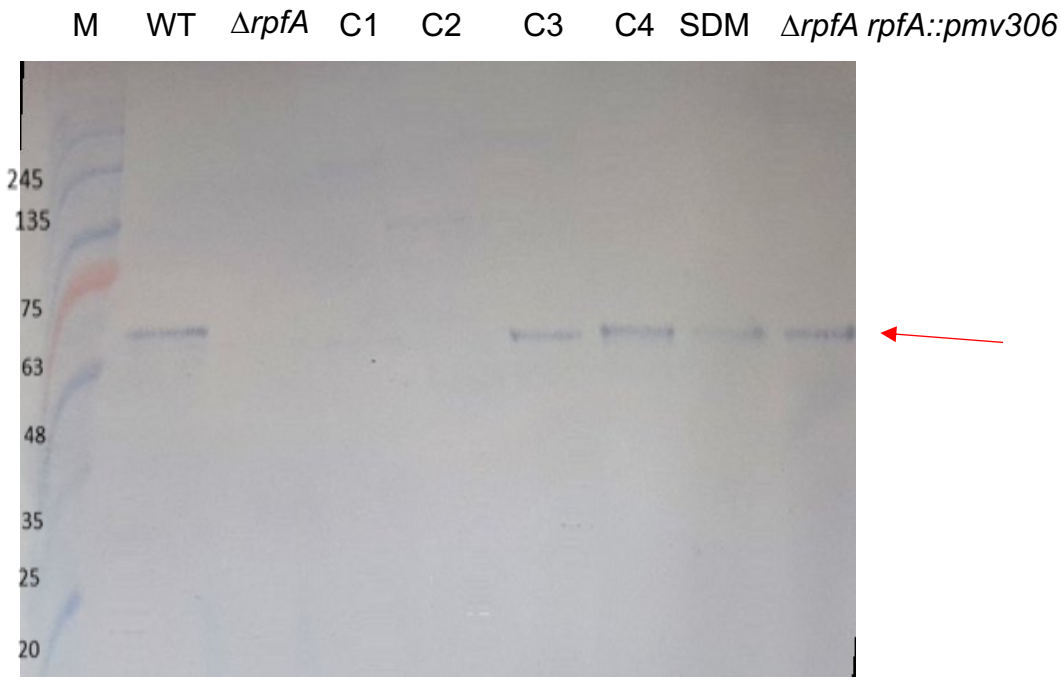

Figure 22: Western blot of *rpfA* complemented strains using anti-Rpf antibodies. The culture supernatant of *rpfA* complemented strains were precipitated using 10% (w/v) TCA and proteins were run on 12% SDS PAGE before transferring onto western blot membrane. Lane 1; marker, lanes 2-8; strains; WT, Δ*rpfA, C1. C2, C3, C4. SDM* and Δ*rpfA::pmv306rpfAcomp*. The predicted size of the full length 38375.6 Da, however it migrates as ~70 kDa protein (red arrow). It can be seen for WT, C3, C4, SDM and Δ*rpfA::pmv306rpfAcomp.* RpfA is absent in Δ*rpfA*; C1 and C2 do not have a secretion signal so RpfA is not secreted or not expressed.

4.4 Discussion

M. marinum is an opportunistic organism of humans and is of zoonotic concern (Jernigan & Farr, 2000). *M. marinum* can readily be found in fresh, brackish and salt water (Aronson, 1926; Tebruegge & Curtis, 2012). Therefore, it was expected that WT *M. marinum* would be able to grow in media with elevated salt concentrations. Studies have shown the presence of other mycobacterial spp, in thermal and glacial environments, identifying 90% and 52% of isolates, respectively (Santos et al., 2015). There have been no previous studies investigating the salt conditions at which *M. marinum* ceases to experience permissible growth. Thus, it has been of interest to not only identify *M. marinum's* ability to grow in both liquid and solid medium with elevated NaCl but to also investigate the regulatory link between mycobacterial survival under osmotic conditions and Rpfs. Rpf's have been of interest in mycobacterial dormancy, latency and indeed TB therapeutics since their discovery in 1998 (Mukamolova et al., 1998a,1998b; Rosser et al., 2017).

The initial experiments using WT *M. marinum* helped establish the conditions at which a decline in optimal growth could be observed (Figure 16). It was not however surprising that WT *M. marinum* was able to grow at higher NaCl concentration of 550mM as it has also previously been seen in both *M. parascrofulaceum* and *M. smegmatis*, which were both capable of growth up to 1882mM NaCl (Santos et al., 2015). However, interestingly these concentrations are considered very high for such non-halophilic organisms, and when compared to other highly stress tolerant bacteria such as *Pseudomonas putida*; an organism which is predominantly incapable of growth in conditions of >1 M NaCl (Santos et al., 2015). These findings promoted a good foundation for further investigations using *M. marinum rpf* mutants. The difference in WT growth observed in liquid medium with the addition of 550mM NaCl,

served as a presmise for which the *rpf* mutants may exhibit more prominant differences in growth.

In s7H9 medium with 550mM NaCl, the *rpf* mutants displayed no difference in growth. Due to the link between RpfA, its associated riboswitch and osmotic tolerance, it was interesting that *ΔrpfA,* did not display any attenuation in growth under these conditions. Given the degree of redundancy within the *rpf* family of proteins, the absence of one of the genes may not be sufficient to adequately demonstrate differences in growth due to a possible compensatory effect by the remaining *rpf* genes. However, the lack of a difference in growth even amongst the double *rpf* mutants, indicated that the strains were still able to grow optimally and similar to WT, in spite of lacking two out of four *rpf* genes when grown in s7H9 with 550mM NaCl. Reasons for this may be due to the difference in growth limitations of bacteria, when multiplying in “suspended” media (s7H9) compared to “surface” media (7H10 agar). Usually during growth in liquid, some cells would adhere to the sides of the containers in which they are grown, but overall, multiplicity of cells results from growth initiated by planktonic cells. Nevertheless, the *M. marinum* strains were incubated in a shaking incubator to alleviate their already clumping prone growth characteristics. Thus, it would also limit the possibility of cells adhering to each other and the growth containers. Ultimately, providing a more favourable growth environment, despite the added osmotic stress created by the presence of NaCl.

In contrast, studies have shown that bacteria on solid food surfaces (Brocklehurst et al., 1997) and agar (Meldrum et al., 2003) display slower growth rates as their growth tends to stem from immobilized cells. Although, the *rpf* mutant experiments in elevated salt conditions were evidently not conducted on food surfaces, it can be

argued that the solid lattice surface can be compared to that of agar. Thus, accounting for the slower growth seen on agar amongst the *rpf* mutants compared to WT.

Additionally, as Rpf's are muralytic enzymes, their absence may lead to a compromised cell wall, which in turn may impact cell-division and growth. Kana and colleagues (2008) showed a more pronounced delayed colony formation in both the quadruple and quintuple *rpf* mutants when grown on 7H11 agar compared to 7H10 agar. The sensitivity of the *rpf* mutants to the higher malachite green concentration in 7H11 (Gillespie et al., 1986) was indicative of cell wall defects in Rpf deficient bacteria. Therefore, bacterial cells with impaired cell walls which may struggle to divide adequately will display a more profound growth defect on agar as colonies formed are only representative of viable cells. However, bacteria grown in liquid media, determined by optical density will not differentiate between dead or living cells. Hence, this may be one of the reasons for only being able to see a notable difference in growth of *rpf* mutants on agar.

Further to this, the difference in growth observed for *rpf* mutants in solid media at 550mM NaCl compared to the same salt concentration in liquid media, may be indicative of the presence of additional stresses unique to immobilised cells growing on solid surfaces. Factors such as oxygen availability, nutrient diffusion, and ability to initiate cell to cell contact, may result in slower growth rates when bacteria are grown on agar (Couvert et al., 2019; Hornung et al., 2018; Morris et al., 2013). Bartek and colleagues (2014) established that Mtb Lsr2 is a global transcriptional regulator needed to control genes involved in adaptation to extremes in oxygen. Mtb *⊿lsr2* is unable to adapt to both high and low levels in oxygen. Additionally, in the absence of *lsr2*, *rpfA* was downregulated (Bartek et al., 2014). However, under elevated salt conditions *rpfA* was upregulated (Hatzios et al., 2013), to possibly serve a role in

osmoregulation and adaptation in mycobacteria. It would be interesting to investigate whether the lsr2 deletion mutant would also display growth and survival defects in high salt media. The exact mechanism of RpfA role in mycobacterial osmotic tolerance remains to be elucidated.

The implication of RpfA in osmotic tolerance would suggest that *M. marinum* strains lacking the entire *rpfA* would display decreased growth in media with elevated NaCl. Notably, the *Δrpf* strains *(ΔrpfA, ΔrpfB, ΔrpfE, ΔrpfAE, ΔrpfAB and Δrpf*BE) all exhibited a decrease in survival at 300mM NaCl 7H10 agar, when compared to WT. However, whilst not all statistically significant; *ΔrpfA, ΔrpfE, ΔrpfAE, ΔrpfAB* and *ΔrpfBE* displayed a more pronounced decrease in growth in agar containing 550mM NaCl, compared to WT (percentage survival derived from survival on standard 7H10 agar). Interestingly, both WT and *ΔrpfB* produced more colonies on agar at 550mM NaCl compared to their respective survival at 300mM NaCl. This may be due to the production of RpfA, and the presence of regulatory genes such as Lsr2 which can influence the control of other genes also required for oxygen adaptation and osmotic tolerance. However, the results for *ΔrpfBE* are surprising as the survival pattern for this strain at both 300mM NaCl and 550mM NaCl mirrors that of *ΔrpfAE* and *ΔrpfAB*, which displays poor survival under elevated salt conditions in these strains. Reasons for this may be more complicated as the *ΔrpfBE* strain has the full upstream region of *rpfA*, including the *rpfA* coding region. Thus, it would seem the presence of RpfA would promote better survival under these conditions as witnessed in other strains with *rpfA* present such as WT and *ΔrpfB.*

The decreased in survival seen in *ΔrpfA* (Figure 18 and Figure 21)*, ΔrpfAE, ΔrpfAB* under elevated salt conditions (Figure 18)*,* may be accounted for by the osmotic stress imposed on the bacteria along with possible limitations in oxygen and nutrients

availability. Although the absence of *rpfA* in these strains, is suggestive of an inability to adequately adapt to osmotic stress as RpfA is not produced.

Further quantitative investigations assessing the combined effects of oxygen and nutrients availability alongside increased osmotic stress may provide more pronounced differences and possibly complementation of these strains.

Studies in *E.coli* and S*almonella spp.* have shown that the lack of availability of essential nutrients leads to a decrease in bacterial energy charge (Chapman & Atkinson, 1971; Walker et al., 1998). Therefore, these reasons may also account for the difference seen in growth of the *rpf* mutants when grown on agar, as these stresses would be less prominent in liquid media. Thus, possibly explaining the lack of difference in growth exhibited by WT, *ΔrpfA* and complemented *ΔrpfA* strains in s7H9. This may be due to the strains being readily able to access nutrients without any additional stresses. This also suggests that the *ydaO* riboswitch is not required for the regulation of *rpfA* gene expression under normal growth conditions, as strains containing the riboswitch and those lacking it grew similarly.

A difference in growth was however, observed when *ΔrpfA* and *ΔrpfA* complemented strains were grown on 7H10 agar with 550mM NaCl. The decrease in colony forming units exhibited by *ΔrpfA, C1, C2,* C3, SDM compared WT and the other *ΔrpfA* complemented strains could be due to the regulatory components included in each of the constructs. The *ΔrpfA* mutant is missing the entire *rpfA* coding region. Thus, even in the presence of the *ydaO* riboswitch ligand (cyclic-di-AMP) and consequent ligand-induced structural changes to the expression platform; the *ydaO* element cannot adequately regulate the expression of *rpfA*, as the lack of *rpfA* coding region, renders its expression unfeasible. This could explain the decrease in growth seen in the *ΔrpfA* mutant. Notably, the *ydaO* element has also been associated with

genes linked to transporters and known osmoprotectants involved in bacterial osmotic shock responses (Nelson et al., 2013). For instance, the expression of *B. subtilis* K^+ transport systems KtrAB and KimA is negatively controlled by the *ydaO* riboswitch, as the binding of two cyclic-di-AMP molecules result in early termination of transcription (Gundlach et al., 2017). Further to which, the direct binding of cyclic-di-AMP to KtrAB and KimA also inhibits potassium uptake (Corrigan et al., 2013; Gundlach et al., 2019). This being the first example of cyclic-di-AMP inhibiting cellular functions directly through protein binding.

Although, there are no studies in mycobacteria which investigate the relationship between the *ydaO* riboswitch and the potential regulation of transport systems implicated in osmotic tolerance. A further explanation for the decrease in growth for *ΔrpfA, C1, C2,* C3 and SDM, is in the possibility that regulation of transporters involved in mycobacterial adaptation to osmotic stress may also be *ydaO* dependent.

Conversely, the C1, C2 and C3 complemented constructs contain the coding region of *rpfA* and are missing the riboswitch, except for SDM, which has a mutation in the pseudoknot of the *ydaO* motif. The initial hypothesis was based on the regulation of *rpfA* gene expression through the *ydaO* riboswitch under mycobacterial osmotic stress. Therefore, it was interesting to see a decrease in growth for these strains. It is possible that in the absence of the *ydaO* element gene expression of *rpfA* cannot be regulated by the riboswitch under osmotic stress conditions, which may result in overexpression of *rpfA*, possibly leading to compromised cell walls resulting in decreased growth on agar. Therefore it may be that specific *rpfA* levels are required for optimal adaptation in osmotic stress. This has been highlighted when an overexpressing RpfA strain in *S. coelicolor* resulted in delayed germination (St-Onge *et al.,* 2015). This could be explored further through timed experiments measuring

mRNA levels and protein quantification to determine the optimal RpfA levels required for osmoadaptation.

Further to which *rpfA* has been shown to be upregulated upon exposure to 140mM NaCl, a lesser concentration than that used in this experiment (Hatzio et al., 2013). It would be interesting to investigate whether the upregulation of *rpfA* is favoured or curtailed by certain NaCl concentrations in mycobacteria. This would ascertain the optimal NaCl concentration for maximum *rpfA* upregulation and permit further investigations into the role of RpfA in mycobacterial osmotic tolerance. Transcriptional profiling of the constructs would help quantify the abundance of *rpfA* transcripts, to determine whether mycobacterial *rpfA* transcription termination is solely ydaO riboswitch dependent under osmotic stress. In addition, SEM/EM studies would also provide insights into the cell wall integrity of these strains.

Unlike many riboswitches, the *ydaO* riboswitch has two ligand binding sites and mutations in either of the sites results in improper binding of cyclic-di-AMP (Ren & Patel, 2014). The SDM construct, has one mutation in the pseudoknot of the motif. The metabolite-sensing domains of riboswitches are highly specific and can differentiate against similar compounds by three orders of magnitude (Nelson et al., 2013). Therefore, the decrease in growth observed for this strain under elevated salt condition on agar was expected, despite the presence of the *rpfA* coding region. This mutation would prevent the cyclic-di-AMP ligand to adhere to the ligand-binding sites. This in turn would prevent the expression platform from reading the ligand-induced structural changes and consequentially *rpfA* gene expression would not be regulated by the *ydaO* riboswitch (Roth & Breaker, 2009). Thus, resulting in a poorer adaptation to osmotic stress presenting itself as the decreased growth seen on selected agar.

Both the *B. subtilis* and *Thermoanaerobacter tengcongenesis ydaO* riboswitches are thought to function through transcription termination mechanisms, whereby the cyclic-di-AMP-RNA complex serves as a genetic 'off' switch (Block et al., 2010; Nelson *et al.,* 2013; Ren & Patel, 2014). Initially, studies in *Streptomycetes* suggested the *ydaO* motif used ribosome binding site occlusion as a mode of regulation; due to a lack of visible transcriptional terminators in hydrolase genes' transcriptional profiles (Haiser et al., 2009). Thus, suggesting *rpfA* and other hydrolase genes in *Streptomycetes* are controlled at the translational level by the *ydaO* element. However, *in* vitro transcription assays in *S. coelicolor* showed a decrease in *rpfA* transcript in response to cyclic-di-AMP and that the *ydaO* riboswitch promoted premature transcription termination. In addition, *rpfA* expression in the streptomycetes is further complicated by the regulation of *rpfA* gene expression via antisense RNAs, something which is yet to be investigated for *rpfA* expression in mycobacteria (St-Onge & Elliot, 2017).

Thus, it is possible that there are similar antisense RNA regulatory mechanisms present for the gene regulation of *rpfA* in mycobacteria. This would seem plausible as Rpfs are cell wall hydrolases and their expression requires tight regulation to preserve cell wall integrity during cell growth and division, which could otherwise have deterimental effects on the cell. Nevertheless, the experimental findings suggest that the *ydaO* riboswitch regulates *rpfA* expression under osmotic stress and that RpfA plays an important role in the adaptation to changes in osmotic conditions in mycobacteria.

While the exact regulatory effect of the mycobacterial *rpfA* riboswitch on *rpfA* expression, remains unclear. The translation of the biological signal by the riboswitch

expression platform following the binding of the ligand may result in a regulatory response controlling transcription elongation, translational initiation, or transcript stability of r*pfA* (Richards & Belasco, 2021; Serganov & Nudler, 2013). Interestingly, recent GFP-based transcriptional fusion constructs using *rpfA* demonstrated that *M. smegatis rpfA* is transcriptionally downregulated in the presence of high levels of cyclic-di-AMP, implicating the *ydaO* riboswitch in *rpfA* regulation (Pal & Ghosh, 2022).

Adaptation to osmotic stress is through cell wall remodelling and producing virulence factors. It is possible that cell wall remodelling is carried out by RpfA during osmotic stress. A proposed way in which the *ydaO* riboswitch regulates *rpfA* under osmotic stress conditions is by transcriptional termination through the binding of cyclic-di-AMP. This mode of regulation seems plausible as *rpfA* is upregulated during elevated salt conditions (Hatzios et al., 2013), to possibly remodel the mycobacterial cell wall during osmoadaptation. Under these conditions, an increase in intracellular cyclic-di-AMP levels is also plausible, as in other actinobacteria, ATP levels have been shown to increase as osmolality increases (Varela et al., 2004). The cyclic-di-AMP can then bind to the aptamer of *ydaO* riboswitch and *rpfA* transcription can be terminated.

To attribute the *rpf* mutants' phenotypes to osmotic stress and rule out previously mentioned stresses such as nutrient availability. The WT and *rpf* mutants were suspended in 2M NaCl. A slight impairment in survival was seen for *ΔrpfA* after week 1 of storage, compared to WT and other *rpf* mutant strains (Figure 19). The survival profiles of *ΔrpfB, ΔrpfE* and *ΔrpfAE,* resulted in slightly higher colony forming units compared to WT. These differences were, however, statistically insignificant. Following 4 weeks of storage no colonies were visible for any of the strains (including week 3 for WT), which may be indicative of bacterial death or possible presence of non-culturable bacteria. The impaired survival of *rpfA* in 2M NaCl, suggests that the

defective phenotype is a result of increased osmotic stress and not nutrient depletion. RpfA is also regulated by CRP and is crucial for virulence (Rickman et al., 2005; Kahramanoglou et al., 2014), suggesting a role in persistence and reactivation of TB (Rickman et al., 2005). However, in *E. coli* CRP functions as an osmoregulator of gene expression (Landis & Johnson., 1999). In Mtb the increase in intracellular cAMP is CRP-dependent and partly PknD dependent (Rebollo-Ramirez et al., 2019). PknD is one of the first sensors of NaCl in Mtb and orchestrates an osmosensory pathway response via phosphorylation of the anti-sigma factor Rv0516c- a substrate highly induced by osmotic stress (Hatzios et al., 2013).

Studies have shown an increase in intracellular cAMP levels upon exposure to 250mM NaCl in Mtb. Unlike Mtb, the classic *E. coli* NaCl model illustrates a correlation in the decrease of intracellular cAMP as NaCl levels increase (Sevin & Sauer., 2014). Yet, in *M. marinum*, the intracellular cAMP levels remained unaltered (Rebollo-Ramirez et al., 2019). This may be due to the lack of expression of adenylate cyclases at 250mM NaCl. Therefore, further to the proposed regulation of *rpfA* via *ydaO* riboswitch; it is possible that *M. marinum rpfA* is also regulated by CRP at NaCl concentrations exceeding 250mM, such as 550mM NaCl used in the elevated salt assays. However, further experiments would need to be conducted.

Next, to determine whether RpfA was secreted, a preliminary western blot using cSN (native protein acquisition) was ran using anti *rpf* specific antibodies. WT, *ΔrpfA* and the *ΔrpfA* complemented strains (C1, C2, C3, C4, SDM and Δ*rpfA rpfA::pmv306*) were investigated for the presence of RpfA. Although the actual size of the RpfA protein is roughly 38kDa in size, a band for RpfA was visible at ~ 70 kda in all strains expect for Δ*rpfA,* C1 *and* C2, where no protein was produced. The increase in size of the protein is due to the rich proline alanine tail present in RpfA. The lack of secreted

RpfA in Δ*rpfA* is because the gene is absent. C1 contains the amplified region from the intragenic promoter to the end of the *rpfA* gene; and C2 has been amplified from the promoter region just before the transcriptional start site, each missing the *ydaO* element. Possible explanations for the lack of RpfA production in C1 and C2 constructs is the absence of the secretion signal, which may have resulted in lack of secretion or expression of RpfA.

Interestingly, strains containing the *ydaO* riboswitch (WT, C4 and Δ*rpfA rpfA::pmv306*) were able to secrete RpfA, signifying a possible regulation of *rpfA* expression via the *ydaO* riboswitch. The bands representing secreted RpfA on the blot for each of the RpfA secreting strains appear similar in size. These were preliminary findings and subjective deductions. Future experiments should include densitometry studies, via chemiluminescence or radiolabelling to quantify the abundance of RpfA in each of the strains. It would also be interesting to investigate the quantity of RpfA secreted for WT and *rpfA* complemented strains when grown under elevated salt conditions to ascertain how RpfA production may be affected by elevated salt conditions and whether riboswitch regulation was affected. Moreover, the detection of ubiquitous marker proteins commonly secreted in culture supernatant would be necessary to ensure the same amount of protein has been loaded onto the SDS page before proceeding with the western blot.

Chapter 5

Probing roles of Rpfs in metal acquisition

5. Introduction

Mtb is a pathogen that lives intracellularly within host macrophages and one of its main traits is its ability to manipulate the metal cation trafficking inside infected macrophages in order to both survive and replicate within the phagosome (Vergne et al., 2004). Once inside the phagosome, Mtb can also escape into the cytosol during later stages of infection (van der Wel et al., 2007; Manzanillo et al., 2012; Welin & Lerm, 2012). One way in which the bacteria are able evade macrophage killing is by arresting phagosome maturation through the manipulation of the host cell endocytic machinery, thus preventing phagosome fusion with late endosome and lysosomes (Rohde et al., 2007). Survival of Mtb also largely stems from its ability to acquire essential micronutrients such as iron and other metals. This aspect is of importance to the data presented in this chapter. Host iron supplies are not readily available to intracellular Mtb as it is sequestered by host proteins such as transferrin and ferritin or through efflux from the phagosome by use of the metal cation transporter NRAMP1 (natural resistance-associated membrane protein) (Forbes & Gros, 2001). Therefore, in order to acquire the host iron supply Mtb has evolved mechanisms to obtain these micronutrients. These include small low molecular weight metal chelators known as siderophores (Andrews et al., 2003; Saha et al., 2016) and specialised systems for their transport.

These can be divided into two categories; mycobactin and carboxymycobactins. Further to this, the use of metals such as zinc and copper by host immune defenses, to kill the intracellular bacteria has also led to Mtb having efficient metal efflux and detoxification systems which prevent metal intoxication and promotes survival of the bacteria.

Iron has been shown to be an essential metal for the survival and growth of bacterial pathogens, including Mtb (Snow, 1970; Ratledge, 2004). This compound can exist in two oxidation states; Fe(II) (ferrous) and Fe (III) (ferric), thus making it a good candidate for the single electron transfer reactions. In the human body Iron exists in the form of haeme, through the binding of porphyrin, an essential component of for oxygen transport, enzymatic reactions and cellular respiration. Whilst iron is highly abundant in the human body it is not easily accessible, with free haeme in the body being sequestered by transport proteins such as transferrin and lactoferrin or stored in ferritin (Morgenthau et al., 2013). In spite of metal being essential for bacterial growth, it can also be toxic, due to the generation of hydroxyl radicals from hydrogen peroxide (Mello Filho et al., 1984). The regulation of iron by Mtb is strict to prevent free circulation of iron in the cell cytoplasm. As many as 155 genes have been shown to be differentially regulated using transcriptional profiling and one third of these genes are regulated by the iron dependent regulator (IdeR) (Rodriguez et al., 2002). Research has shown that IdeR is essential for Mtb survival in mice, highlighting the significance of iron homeostasis for Mtb infection (Schaible et al., 2002). IdeR functions as a transcription repressor and in the presence of iron. Studies in *M. smegmatis* have shown that IdeR binds to the “iron- boxes” at promoters, repressing the expression of genes involved in siderophore synthesis and in turn activates genes encoding iron storage proteins, such as the bacterioferritin assembled from two subunits encoded by *bfrA* and *bfrB* (Rodriguez et al, 2002; Dussurget et al., 1996; Chao et al., 2019).

Siderophores are synthesized by cytoplasmic synthases encoded by two mycobactin operons and it is thought that the synthesis and the transport of siderophores are linked. The membrane proteins responsible for their transportation

are MmpS4 and MmpS5 which are associated with the MmpL4 and MmpL5 superfamily that are apart of type 7 secretion systems. These secretion systems play an important role in the transport of substrates across the mycobacterial cell wall.

Mycobacteria have five chromosomally encoded type 7 secretion systems ESX-1-ESX5 (Figure 23). These systems have evolved due to the complex nature of mycobacterial cell wall, which allows the bacteria to transport a variety of biomolecules across the complex mycobacterial cell wall. Each of these secretion systems preforms distinct roles. Notably, ESX-3 is present in all mycobacterial species and is implicated in metal homeostasis and is regulated by the metals Iron and Zinc in Mtb (Serafini et al., 2013). It has been shown to be involved in siderophore mycobactin based Iron uptake (Tufariello et al., 2016). Research as highlighted prominent advances in siderophore mediated metal acquisition in mycobacteria (Chao et al., 2019). The enhanced understanding of metal acquisition strategies will provide new insights into host-pathogen interactions and improved therapeutic methods for TB.

Hypotheses for this chapter:

1.) The growth defect of *M. marinum ΔrpfAB* and *ΔrpfAEB* mutants is related to an impaired T7SS (Esx-3) and limited capacity to acquire metals
2.) Individual Rpfs play a distinct role in T7SS and are required for the proper assembly of ESX3

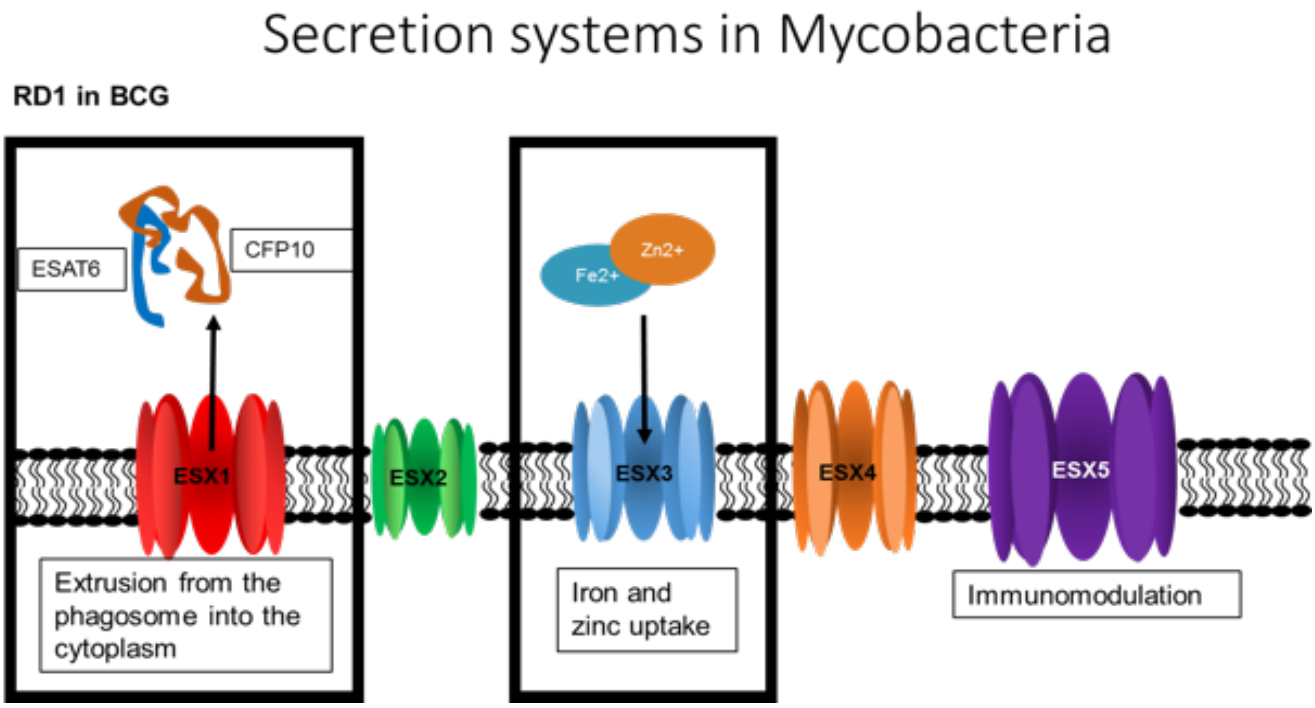

Figure 23: Mycobacterial Type 7 secretion systems Mycobacteria have 5 T7SS and these are illustrated above. ESX1 is important for the secretion of virulence factors such as ESAT6 and CFP10, whilst ESX3 is associated with iron and zinc uptake, ESX5 is involved in immunomodulation and ESX2 and ESX4 are yet to be investigated in depth (adapted from Tufariello et al., 2013).

5.2 Results

5.2.1 Δ*rpfAB had* growth defects which could be genetically and metabolic complemented

As previously illustrated in Chapter 3, Δ*rpfAB* exhibits a growth defect in Sauton's minimal medium, whereby the mutant does not reach as high of an optical density as WT and other single and double *M. marinum rpf* mutants. In order to attribute the phenotype to the deletion of both *rpfA* and *rpfB* each gene was cloned into the pMV306 plasmid that integrates at *attB* site of mycobacterial chromosome and the plasmids electroporated in the Δ*rpfAB* mutant. Growth of the resultant strains, Δ*rpfAB::rpfA* and Δ*rpfAB::rpfB* in Sauton's medium was monitored and the increase in optical density was measured over a 14 day period, by taking daily readings. As per previous findings, in Sauton's medium Δ*rpfAB* exhibits a significantly longer doubling time compared to all other strains, inlcuding WT (43.83 and 15.84 hrs, respectively), in Sauton's medium. The complemented strains; Δ*rpfAB::rpfA* and Δ*rpfAB::rpfB* exhibited a decrease in doubling time (24.84-20.03 hrs, respectively) compared to Δ*rpfAB.* Therefore, it was possible to genetically complement the growth defect phenotype of Δ*rpfAB* in Sauton's medium and restoring it to near WT phenotype (Figure 24). Whilst genetic complementation was achievable and the maximum optical density reached by the mutant was less than that of WT, Δ*rpfAB::rpfA* and Δ*rpfAB::rpfB,* there was no significant difference in doubling times between the strains (Table 10), suggesting that there might be a defect with the cells, such as possible deformations. Interestingly, Δ*rpfAB::rpfB* reaches a slightly higher maximum OD than WT, Δ*rpfAB::rpfA* and Δ*rpfAB.* One-way ANOVA test, showed a statistical difference between the growth of Δ*rpfAB* compared to the other strains ($p<0.05$). The delay in growth for Δ*rpfAB* may

also be due to the reduced nutrients available in Sauton's medium. This is of importance as the notable decrease in iron availability and absence of $ZnSO_4$ maybe the reasons for the poor growth. A key concept, which will be discussed further in this chapter.

The successful complementation using single *rpfA* or *rpfB* genes suggests a level of functional redundancy between *rpfA* and *rpfB*. Thus, when the Δ*rpfAB* mutant is complemented with either *rpfA* or *rpfB* this complementation is able to restore the growth defect seen in the mutant (Figure 24).

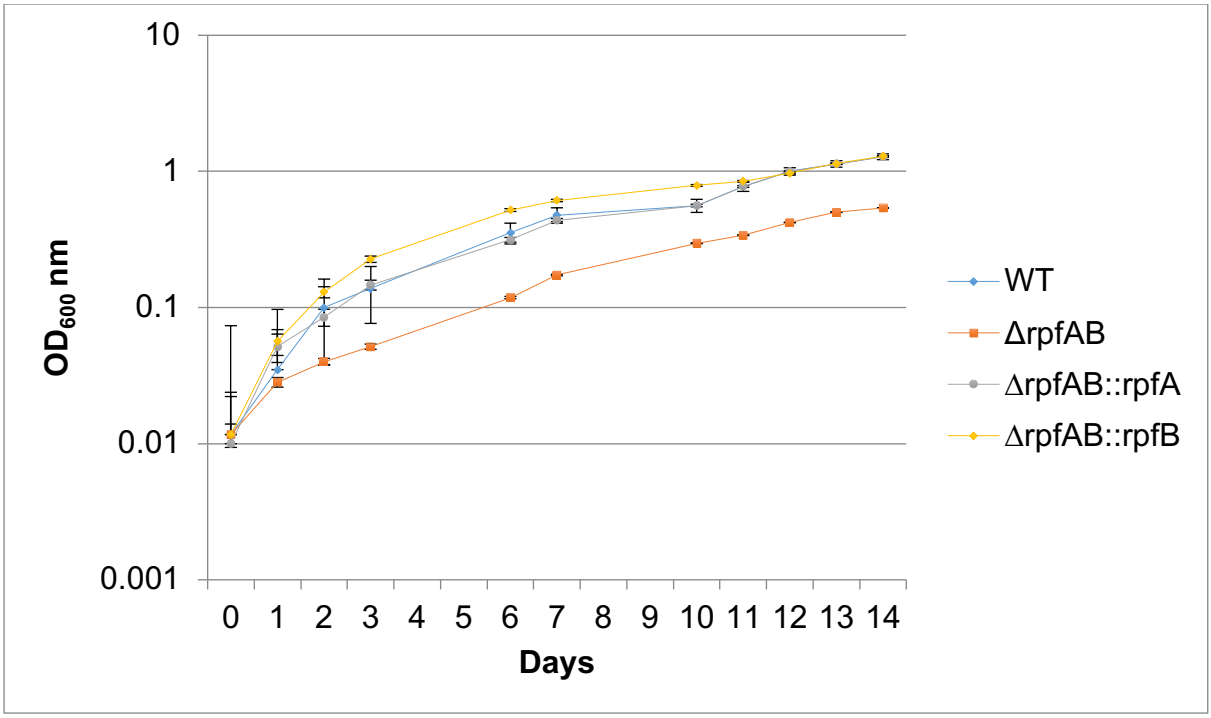

Figure 24: Genetic complementation of Δ*rpfAB* in Sauton's medium; WT, Δ*rpfAB,* Δ*rpfAB::rpfA,* Δ*rpfAB::rpfB* were grown in Sauton's medium + 0.05% (w/v) Tween 80, over 14 days with daily OD600nm readings. The presence of either *rpfA* or *rpfB* in Δ*rpfAB* results in restoration of WT phenotype. The data presented as means ±SEM (N=6)

Table 10: Growth parameters of WT *M. marinum*, Δ*rpfAB* and Δ*rpfAB* complemented strains in Sauton's medium				
Strains	WT	Δ*rpfAB*	Δ*rpfAB::rpfA*	Δ*rpfAB::rpfB*
Doubling time (hours)) (±SD)	15.84 ±0.007	43.83 ±0.178	24.82 ±0.012	20.03 ±0.020

5.2.2 Growth phenotypes of Δ*rpfAB* on solid agar

Depending on the type of mutant generated and the requirements of the mutant, growth defects may not be visible in certain media. Out of all the double *rpf* mutants a growth defect was only seen in Δ*rpfAB* in liquid medium (s7H9). Next, the growth of Δ*rpfAB* was investigated on agar. "Non-culturability" on agar is a common phenotype among mutants of cell wall associated genes and the Δ*rpfAB* mutant also displays this phenotype 7H10 agar (Figure 25). This phenotype comprises of the inability of the bacteria to form visible colonies at higher dilutions once serially diluted onto solid agar (Kana et al., 2008). The bacteria were grown to exponential phase at an optical density between 0.6-0.8, after which the strains were diluted to OD 0.1 and serially diluted from 10^0 to 10^6. The plates were then incubated for a total of 7 days. WT forms colonies at dilutions of 10^5, whereas Δ*rpfAB* only forms colonies until 10^2 (Figure 25). The duration of incubation is of importance as the strain's phenotype has been described has having a "delay" in its growth and this phenotype becomes visible after WT has finished forming visible, countable colonies on 7H10 agar, but the cell wall defects somehow prevent the cell to multiply adequately in order to grow. If however, the Δ*rpfAB* mutant is incubated for approximately 14 days, colonies will form at dilutions of 10^5 (data not shown). This is probably due to the impaired cell wall following the deletion of the *rpf* genes, which may impede division, and subsequent growth of the cells.

The top panel shows the normal growth of WT *M. marinum* and the bottom panel is indicative of the growth defect seen in Δ*rpfAB.* Bacterial colonies are visible at 10^4 dilution for WT whereas Δ*rpfAB* shows the growth of bacteria at 10^2. The notion of delayed colony formation is such that the bacterial colonies will appear after prolonged

incubation compared to that seen for WT bacteria, but the cell wall defects somehow prevent the cell to multiply adequately in order to grow.

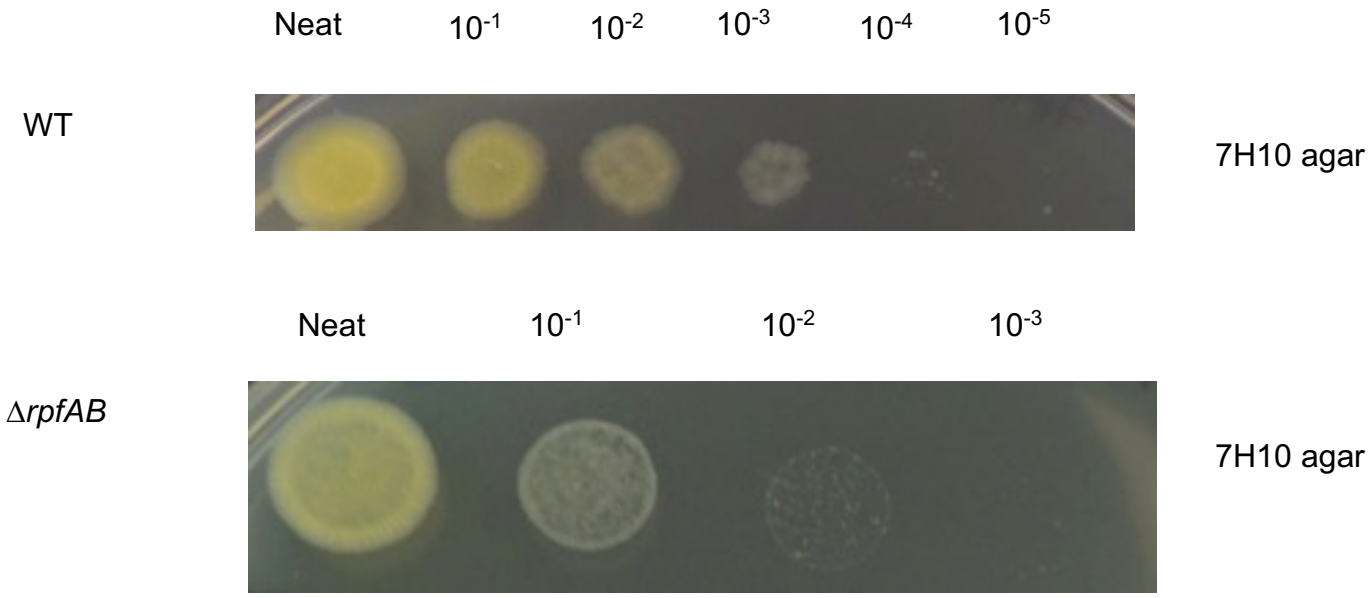

Figure 25: Characterising the growth of WT *M. marinum* and Δ*rpfAB* on 7H10 agar. The Δ*rpfAB* mutant displays delayed colony formation on agar and does not form colonies at higher dilutions compared to WT *M. marinum.* WT *M. marinum* and Δ*rpfAB* were grown in s7H9 and serially diluted onto 7H10 agar. The strains were incubated for 7 days and the images are representatives of 3 biological replicates.

5.2.3 Addition of haemin partially complements growth defect of Δ*rpfAB* in Sauton's medium

The generation of ESX-3 deletion strains has not been possible without the addition of very high iron/zinc concentrations (Serafini et al., 2013). A physiological condition of importance in *M. tuberculosis* infection is the availability of iron as the bacteria use it as a cofactor for enzymes that are involved in redox reactions and other essential functions. Like many other pathogenic bacteria *M. tuberculosis* also fails to grow in the absence of iron.

Tufariello and colleagues (2013) used 100μM haemin to generate ESX-3 mutant in *M. tuberculosis,* as such this concentration was used to investigate if there would be a difference in growth using Δ*rpfAB.* WT, *ΔrpfAB,* Δ*rpfAB::rpfA* and Δ*rpfAB::rpfB*, were grown in Sauton's medium to an OD of 0.7 and diluted to an OD of 0.1, the strains were then added to flasks containing either Sauton's medium and 0.05% tween or Sauton's medium, 0.05% tween and 100μM haemin. Daily samples were taken over a 14 day period, by plating serially diluted bacteria onto 7H10 agar and measuring the increase in growth using the Miles and Misra counts method. Each of the strains were incubated for a period of 7 days before the CFU/ml counts were collected. Surprisingly, the addition of such high concentrations of haemin did not result in attenuated growth in WT and partial "metabolic complementation" of *ΔrpfAB* was achieved (Figure 26B). This was observed as a slight increase in CFU/ml counts in the presence of haemin in Sauton's medium compared to that without haemin (Figure 26A), the growth resulted in a statistically significant difference between *ΔrpfAB,* when compared to WT, Δ*rpfAB::rpfA* and Δ*rpfAB::rpfB,* under both conditions ($p>0.05$). Between the initial plating of *ΔrpfAB* and day 5, there was a 1-log increase in growth (red line), this remained the same until day 8 with a final CFU/ml count of 10^7 over the 14 day

incubation period, in the absence of haemin. However, *ΔrpfAB* growth on 7H10 agar with haemin, results in half a log increase in CFU/ml, at days 3, 5 and 10, with a final CFU/ml of 10^8 . Additionally, the single complemented strains of ∆*rpfAB::rpfA* and ∆*rpfAB::rpfB*, also behaved like WT *M. marinum*, in its colony formation ability, whereby the strains exhibit similar CFU/ml counts at all time points, both in the presence and absence of haemin 7H10 agar plates.

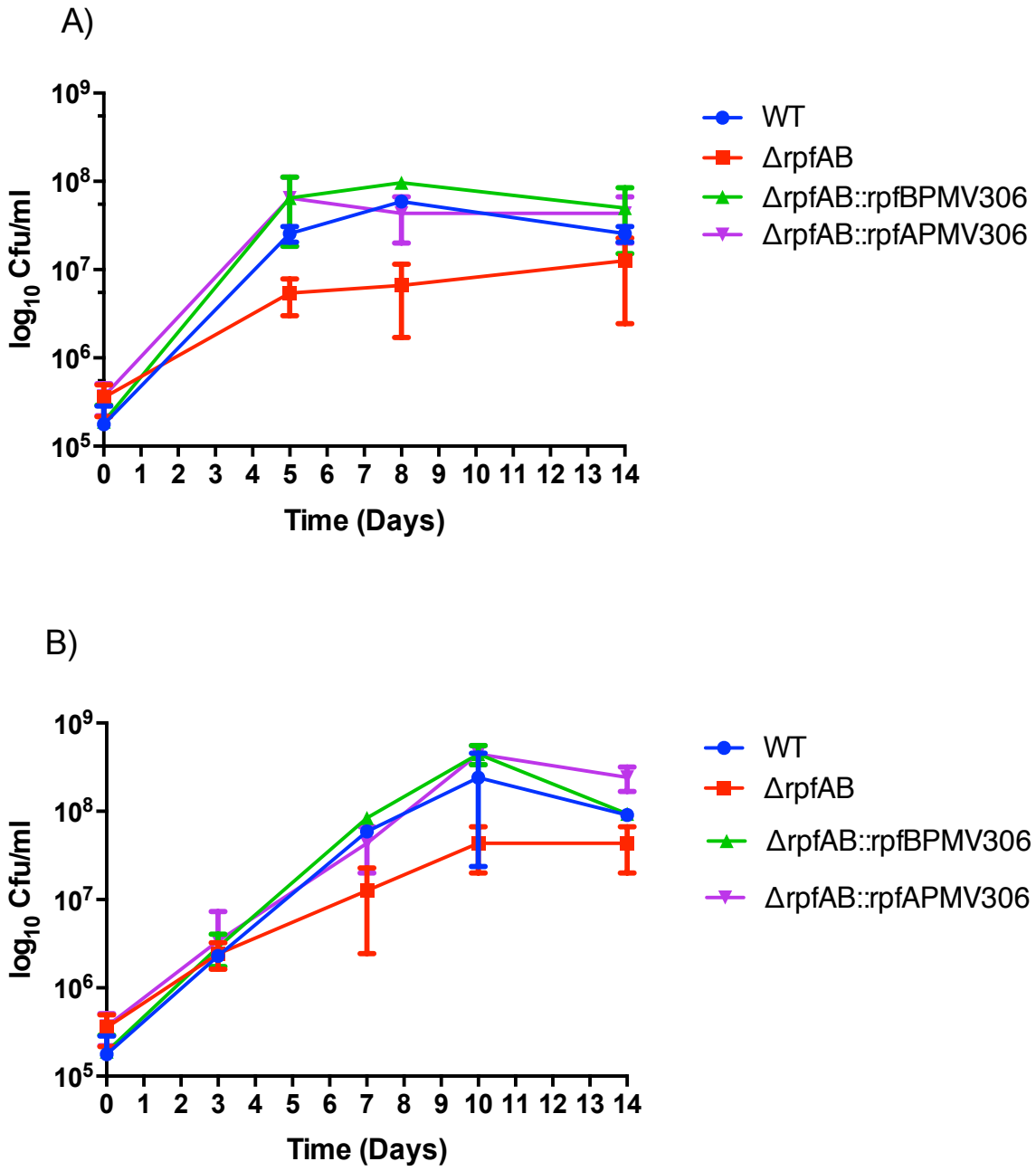

Figure 26: *M. marinum rpf* deletion strains were grown in Sauton's medium + 0.05% Tween 80 and was assessed using CFU/ml counts over a period of 14 days **(A).**
B) WT, *ΔrpfAB* and complemented strains were grown in Sauton's medium+ 0.05% Tween 80 with the addition of 100μM haemin. Data presented as means ±SEM (N=9)

5.2.4 Addition of haemin partially complements growth defect of Δ*rpfAB* on 7H10 agar

Having been able to moderately improve the growth defect of Δ*rpfAB* seen in Sauton's medium through the addition of haemin, the possibility of achieving enhanced growth of Δ*rpfAB* on mycobacterial media was investigated. A pronounced growth defect can be seen on 7H10 agar and is more severe on 7H11 agar. Both WT and Δ*rpfAB* were cultivated for one passage in s7H9 medium for 10 days in a shaking incubator. The cultures were allowed to reach an optical density of 0.6-0.7 before being serially diluted on 7H10 agar (Figure 27; top panels for both strains), The Δ*rpfAB* and indeed other *rpf* mutants have been shown to not reach final optical densities as high as its WT progenitor. The growth of WT *M. marinum* is visible at 10^4 and the addition of haemin at 100μM does not indicate any impairment in WT growth with colonies still growing at 10^{-4} dilution. The Δ*rpfAB* mutant shows one-dilution factor attenuation in growth compared to WT, with colonies growing at 10^3. However the addition of 100 μM haemin, improved the growth of the Δ*rpfAB* mutant and resulted in a similar growth pattern to WT with colonies being produced at 10^4. The yellow appearance of colonies results from the photochromogenic nature or *M. marinum* when colonies are exposed to light.

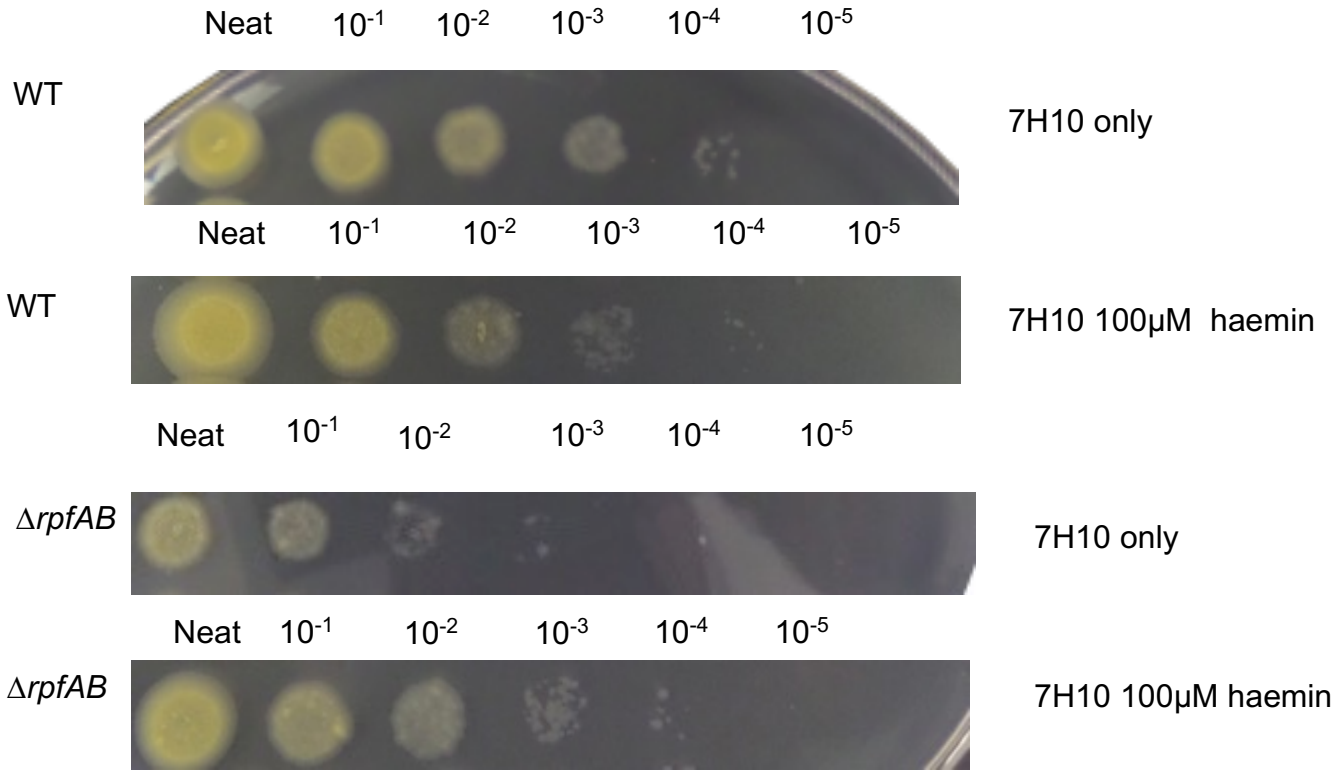

Figure 27: Investigating effects of haemin on Δ*rpfAB* growth on solid medium. WT and *ΔrpfAB* grown in 7H9 liquid medium and serially diluted on 7H10 agar and 7H10 agar containing 100μM haemin (top and bottom rows for each strain, respectively). Representative images from three independent replicates are shown.

5.3 Attempts to generate *M. marinum* triple *rpf* mutants in standard media were unsuccessful

Having achieved partial complementation of Δ*rpfAB* using haemin alone, it appeared that the growth defect of this mutant was due to the inability to acquire certain nutrients/ metabolites either as a direct consequence of a compromised cell wall or indirectly by the essentiality of Rpfs in assembling other components required for the acquisition of these missing elements. Literature, highlighted both iron and zinc as being the two key metals regulated by ESX-3, therefore, *ΔrpfAE* single crossover strain containing a p2NIL plasmid with *rpfE* deletion construct was initially grown in the presence of solely haemin, in attempts to acquire a triple mutant. This, however, resulted in the generation of WT double crossovers. It was therefore attempted to add $ZnSO_4$ to the medium along with haemin. This resulted in better growth as measured by optical density and the subsequent generation of triple *ΔrpfAEB* strain. Many attempts were made to generate a *M. marinum rpf* triple mutant. Various combinations of double *rpf* deletion strains (*ΔrpfAE*, *ΔrpfBE, ΔrpfAB, ΔrpfCE and ΔrpfAC*) were used as background strains in order to delete a further *rpf* gene. This proved impossible on standard 7H10 agar alone. After unsuccessfully screening 3000 colonies, it was only possible to generate the first ever *M. marinum rpf* triple mutant by growing it on specific agar containing haemin and $ZnSO_4$.

The attempts made to generate a triple *rpf* mutant in *M. marinum* using an unmarked in frame-deletion strategy will been described in this chapter. An example of the screening of 16 white sucrose resistant colonies (Δ*rpfAE* background strain, attempting to delete *rpfB*) by PCR is shown in Figure 28. The screen identified all 'WT' double cross overs, which corresponded with *rpfB* gene size of 1.5kb. The successful deletion would generate a PCR product size of ~300bp, similar to the Δ*rpfB* construct

DNA used as a positive control in lane 2. The use of Δ*rpfAE* as a background strain, did not produce a *rpfAEB* deletion strain. Furthermore, it was not possible to generate a triple *rpf* mutant in *M. marinum* using other double deletion background strains such as *rpfB*E, *rpfAC* and *rpfCE*, suggesting that the media requires further supplementation to delete a third *rpf* gene in *M. marinum.*

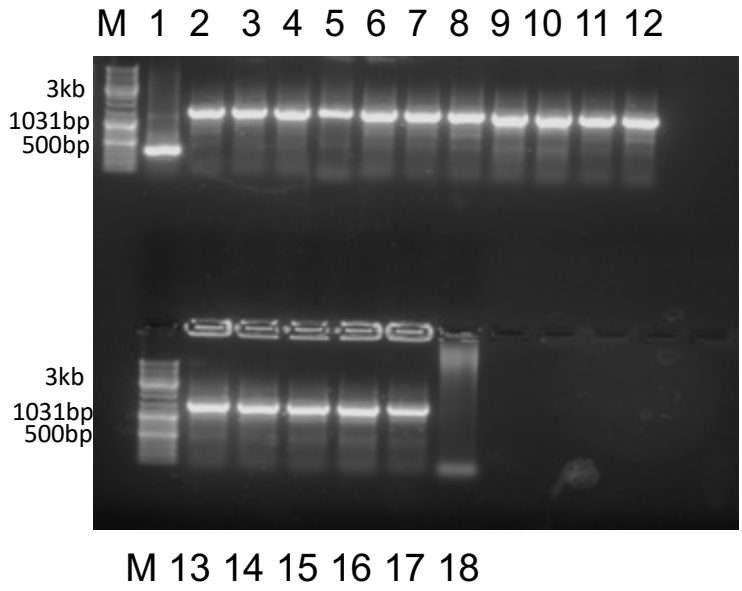

Figure 28: Agarose gel depicting an example of PCR colony screening (Δ*rpfAE* background strain)
M: DNA maker; lane 1, PCR product obtained with *M. marinum* Δ*rpfB* construct (300 bp) (positive control); lanes 2-17; 'WT' DCOs (1300bp)**;** lane 18, negative no template control.

5.3.1 ∆rpfAEB could only be generated in media supplemented with haemin and $ZnSO_4$

The triple *M. marinum rpf* mutant was generated using ∆*rpfAE* strain when mutant candidates were screened in media supplemented with both haemin and $ZnSO_4$. The triple mutant was confirmed by PCR using gene specific deletion primers (Figure 28), as mentioned in chapter 2. A p2NIL plasmid with a PacI cassette containing the upstream and downstream fragments of *rpfB* (Iakobachvili, 2014) was electroporated into *M. marinum* ∆*rpfAB* genetic background strain. The transformants were plated onto 7H10 agar plates containing X-gal and Kanamycin. Blue colonies were picked and grown in standard 7H9 without antibiotics for several generations until the cultures reached the stationary phase to allow for double crossover event to take place. To further confirm the successful deletion of the third *rpf* gene, whole genome sequencing (WGS) was done by Microbes Ng/Birmingham. This section will describe the process of *M. marinum* ∆*rpfAEB* generation and WGS analysis.

Having achieved partial complementation of ∆*rpfAB* using haemin alone, it appeared that the growth defect of this mutant was due to the inability to acquire certain nutrients/ metabolites either as a direct consequence of a compromised cell wall or indirectly by the essentiality of Rpfs in assembling other components required for the acquisition of these missing elements. The *ΔrpfAE* single crossover strain containing a p2NIL plasmid with *rpfB* deletion construct was initially grown in the presence of solely haemin, in attempts to acquire a triple mutant. This, however, resulted in the generation of 100% WT double crossovers. $ZnSO_4$ was added to the medium along with haemin and this resulted in improved growth as measured by optical density and the subsequent generation of triple *ΔrpfAEB* strains.

5.4 PCR confirmation of Δ*rpfAEB* mutant

The resultant colonies were used for PCR screening with *ΔrpfB* specific test primers to identify clones with the deleted *rpfB*. Nonetheless, the screening of 3000 possible double cross-over colonies (white) resulted in WT bacteria. However, by growing the single-cross over colonies (blue colonies) in standard 7H9 media without antibiotics and supplementing the media with haemin and $ZnSO_4$; followed by allowing the bacteria to grow for several generations, it was possible to delete *rpfB* from *M. marinum* Δ*rpfAE* genetic background strain. Ultimately, white sucrose resistant colonies (double-cross overs; possible mutants) were screened by PCR to detect *rpfB* deletion using *ΔrpfB* test primers (figure 29). The sizes of deleted strains correspond to the expected sizes (Table 4) and therefore, show the successful PCR confirmation of the deletion of *rpfB.*

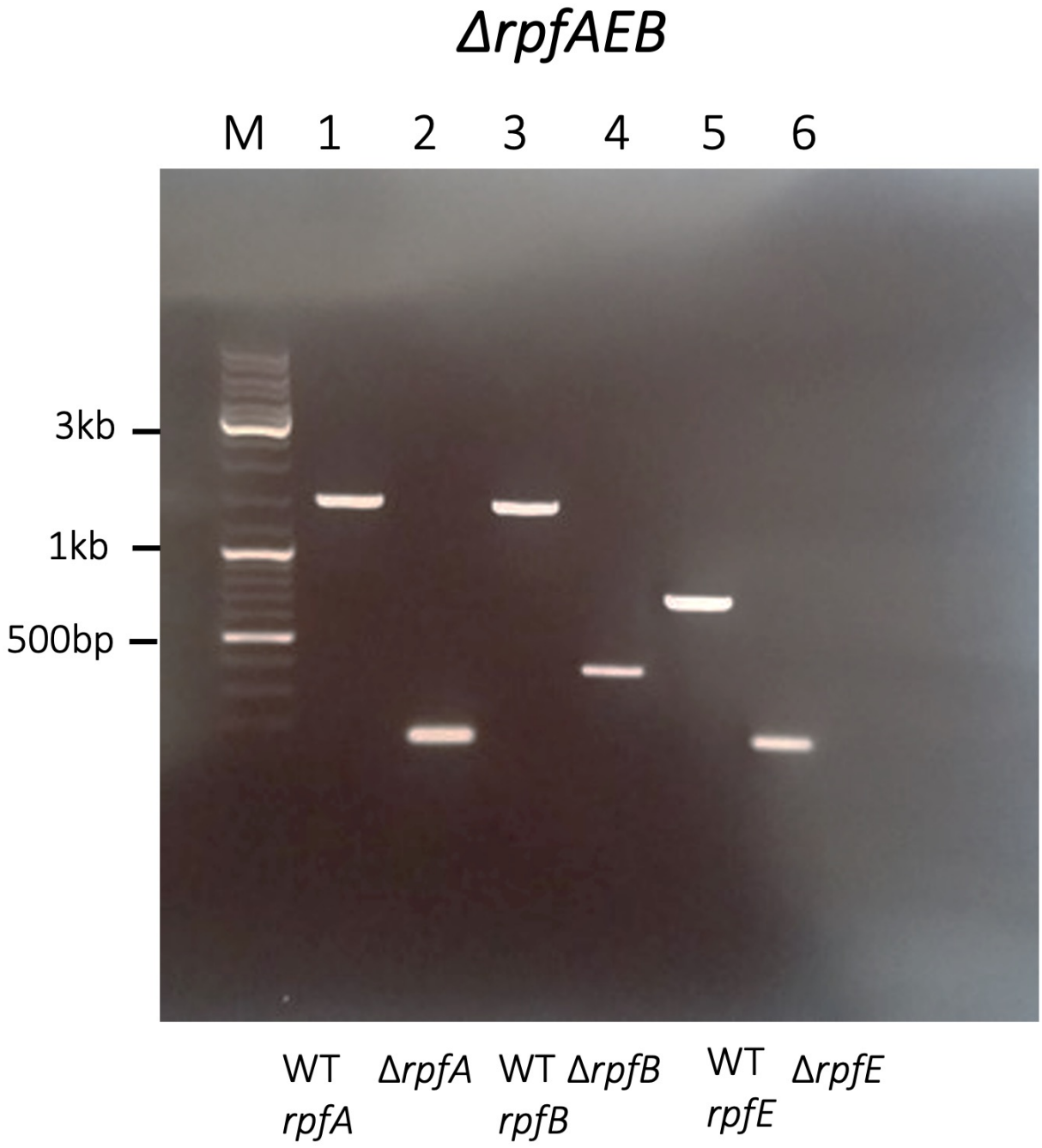

Figure 29: Gene deletion confirmation of *M. marinum* ∆*rpfAEB mutant* using diagnostic PCR. Lanes 1,3 and 5 show the sizes for *rpfA, rpfB* and *rpfE* test products in WT; lanes 2,4 and 6 show the sizes for the deleted strains of *rpfA, rpfB* and *rpfE. M. marinum rpf* deletion strains were confirmed using *rpf* gene specific primers for *rpfA, rpfB* and *rpfE.*

5.4.1 Addition of haemin and $ZnSO_4$ allowed generation of triple *rpf* deletion mutant

The use of haemin and $ZnSO_4$ significantly increased the number *of* Δ*rpfAEB* colonies found on 7H10 agar plates. Initial attempts of screening for a triple *rpf* mutant in *M. marinum* resulted in 90% WT DCO events, with 10% generating SCO's. However, the addition of haemin and $ZnSO_4$ increased the number of mutants generated to 100%. A total of 50 white sucrose resistant colonies were subjected to PCR, using *rpfB* specific test primers and analysed on agarose gel. All of the colonies resulted in mutant phenotypes, with the absence of the already deleted *rpfA* and *rpfE* genes, followed by the implemented deletion of *rpfB.* This is suggestive of a useful method in generating *rpf* related mutant strains.

5.4.2 Genome analysis and confirmation of ∆*rpfAEB* using ∆*rpfAB* as genetic background strain

Whole genome sequencing is a method, which allows for the determination of whole organism's genome. It can comprise of the sequencing of the chromosomal DNA and mitochondrial DNA. Here, the entire genome of the *M. marinum* ∆*rpfAEB* was sequenced and cross referenced against WT *M. Marinum* to identify the missing *rpfs; rpfA, rpfB* and *rpfE,* whose deletion had already been confirmed via PCR using gene specific primers. The triple mutant showed a total number of contigs in the assembly as 241, with an assembled genome size of 6430760bp (Figure 30).

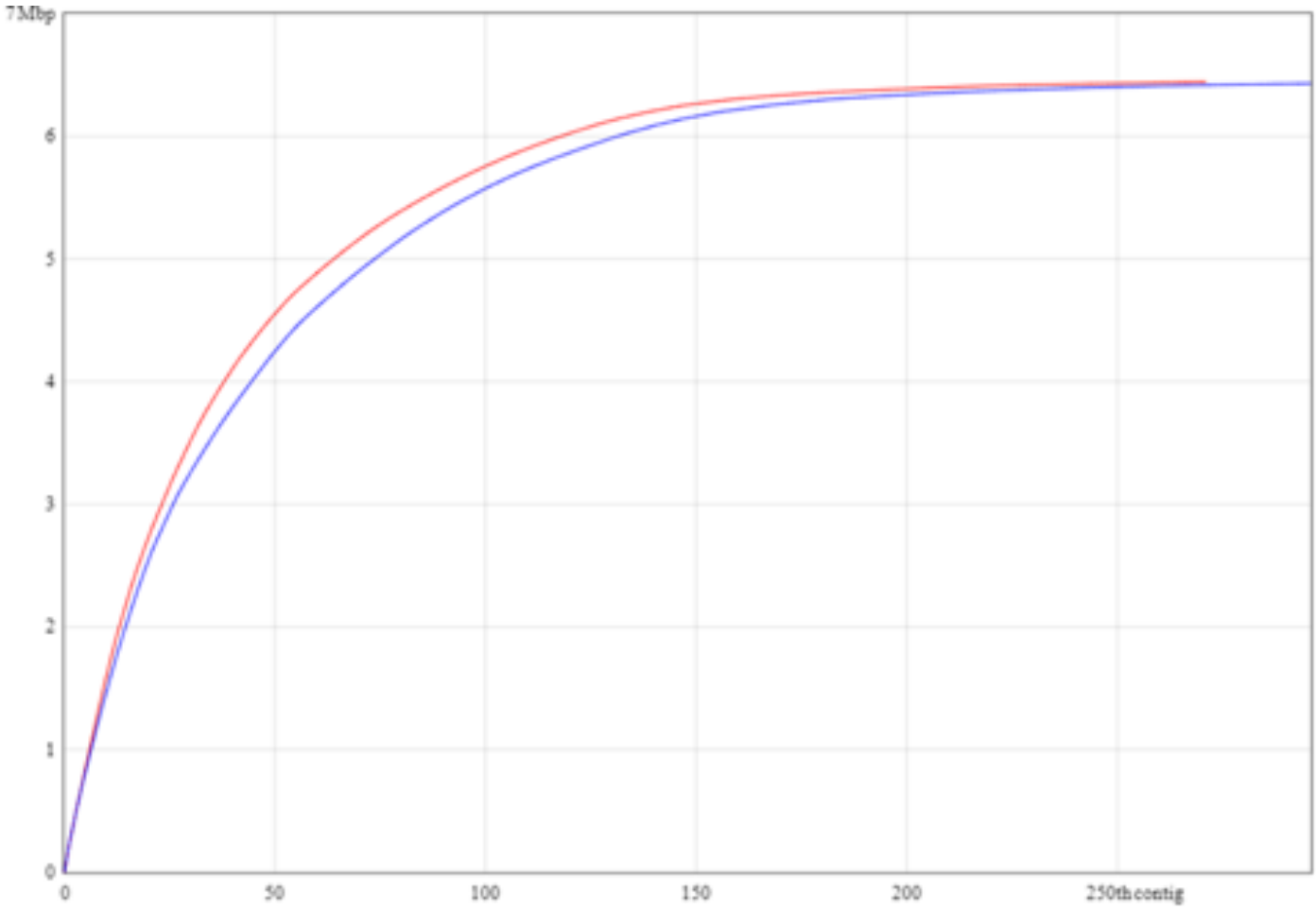

Figure 30: The total number of contigs and bases in the assembly of Δ*rpfAEB*.

Following genome assembly, the sequence was analysed using BLAST, to confirm the deletion of all three *rpf* genes in *M. marinum*. The results indicated the absence of the following genomic coordinates for each gene; *rpfA (5717800-5719000)*, *rpfB (5501100-5502000)* and *rpfE (4656900-4657800)*, confirming the successful deletion of all three genes as the missing genomic coordinates coincide with those of the *rpfs* (Figure 31).

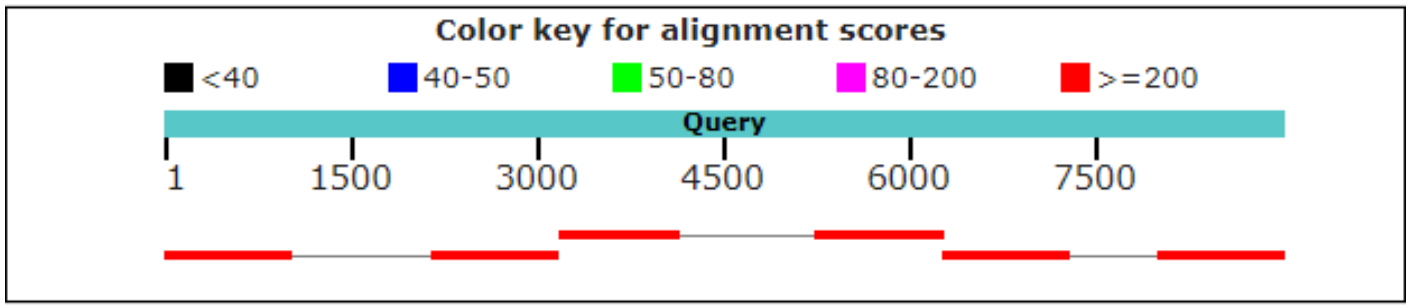

Alignments Download Graphics Distance tree of results

Description	Max score	Total score	Query cover	E value	Ident	Accession
NODE_67_length_28849_cov_36.7413	1916	3708	22%	0.0	99%	Query_39394
NODE_29_length_59122_cov_39.6694	1881	3747	22%	0.0	100%	Query_39356
NODE_8_length_131310_cov_36.2178	1877	3743	22%	0.0	100%	Query_39335

Figure 31: BLAST of whole genome sequencing of *M. marinum* Δ*rpfAEB* strain. The Δ*rpfAEB* strain was sent for whole genome sequencing and analysed to identify the missing *rpf* genes. The blast confirms the deletion of *rpfA, rpfB* and *rpfE* in *M. marinum* as can be seen in the above BLAST analysis.

5.4.3 Identification of single nucleotide polymorphisms (SNP) within Δ*rpfAEB* mutant

Following the whole genome sequencing of Δ*rpfAEB* and having confirmed the absence of the 3 deleted *rpf* genes. Genome analysis comparing the genome of the mutant strain to the reference genome of WT *M. marinum* identified 12 SNP's that were present in the genome of the mutant. Only one SNP resulted in a frameshift mutation (Table 11). This encoded a conserved hypothetical secreted protein with an unknown function in *M. marinum* (*MMAR_1927*). Three out of the five identified intergenic region mutations, were found in *MMAR_1593*; a gene encoding for a PE-PGRS family protein. Three other SNPs were found in a PE-PGRS family protein encoding region (*MMAR_1594).* Interestingly, a missense variant mutant was found in the genetic region encoding for a molybdenum cofactor biosynthesis protein A2 (MoaA2) (*MMAR_4663*). Mtb, *Rv0869c;* is an orthologue of this gene. Moreover, the intergenic region mutation detected in position 4657909, was an unannotated region and no identified gene could be found. The presence of SNPs can alter the phenotype of the deletion mutant, in such a way that the phenotype might in fact be attributed to the SNPs present and not the deletion of the genes. Therefore, merely using PCR as means of confirming gene deletion will not assist in identifying the presence of SNPs, thus, making whole genome sequencing a very useful tool in ascertaining the generation of true mutants. As a whole, whole genome sequencing of Δ*rpfAEB*, provided further confirmation of the deletion of *rpf* genes in *M. marinum.*

Table 11: SNP's identified in *M. marinum* Δ*rpfAEB* mutant compared to reference genome *M. marinum M*

Gene region in M. marinum	**WT nucleotide**	**Mutation**	**Type of gene mutation**	**Impact**	**Amino acid**
MMAR_0457	TG	T	intergenic region	MODIFIER	
MMAR_1593	CG	C	Intergenic region	MODIFIER	
MMAR_1593	A	C	intergenic region	MODERATE	
MMAR_1593	G	T	intergenic region	MODERATE	
MMAR_1594	C	T	Synonymous variant	LOW	Pro3608 Pro
MMAR_1594	C	A	Missense variant	MODERATE	Trp1357 Leu
MMAR_1594	A	C	Missense variant	MODERATE	Trp1357 Gly
MMAR_1927	C	CG	Frameshift variant	HIGH	Gly177fs
4657909 (non-identified region)	A	G	intergenic region	MODERATE	
MMAR_3778	T	C	Synonymous variant	LOW	Ala195Ala
MMAR_4613	C	T	Missense variant	MODERATE	Ser274Leu
MMAR_4663	T	C	Missense variant	MODERATE	Val186Ala

5.4.4 Detection of Rpfs in WT and Δ*rpfAEB* using western blot

Literature has previously illustrated the presence of Rpf's in the culture supernatant, which coincides with the presence of RpfA and RpfB from our mass spectrometry data of WT Mtb. Given that the culture supernatant obtained from WT *M. marinum* improves the growth of Δ*rpfAEB* mutant, the location of Rpfs in *M. marinum* was investigated. Culture supernatant analysis, using spent media (OD 0.7) in which *WT M. marinum* was grown, indicated that RpfA could be found in culture supernatant of WT *M. marinum* at a size above 50 kDa. This protein band was absent in the *rpfA* mutant. Preliminary, western blots of the culture supernatant using anti sheep, anti-Rpf antibodies, also indicated a single band correspondent with that of RpfA. Further to this, other preliminary western blots of both RpfC and RpfB could be found in the cell membrane fractions of WT *M. marinum,* whilst being absent in the Δ*rpfAEB* mutant (Figure 32).

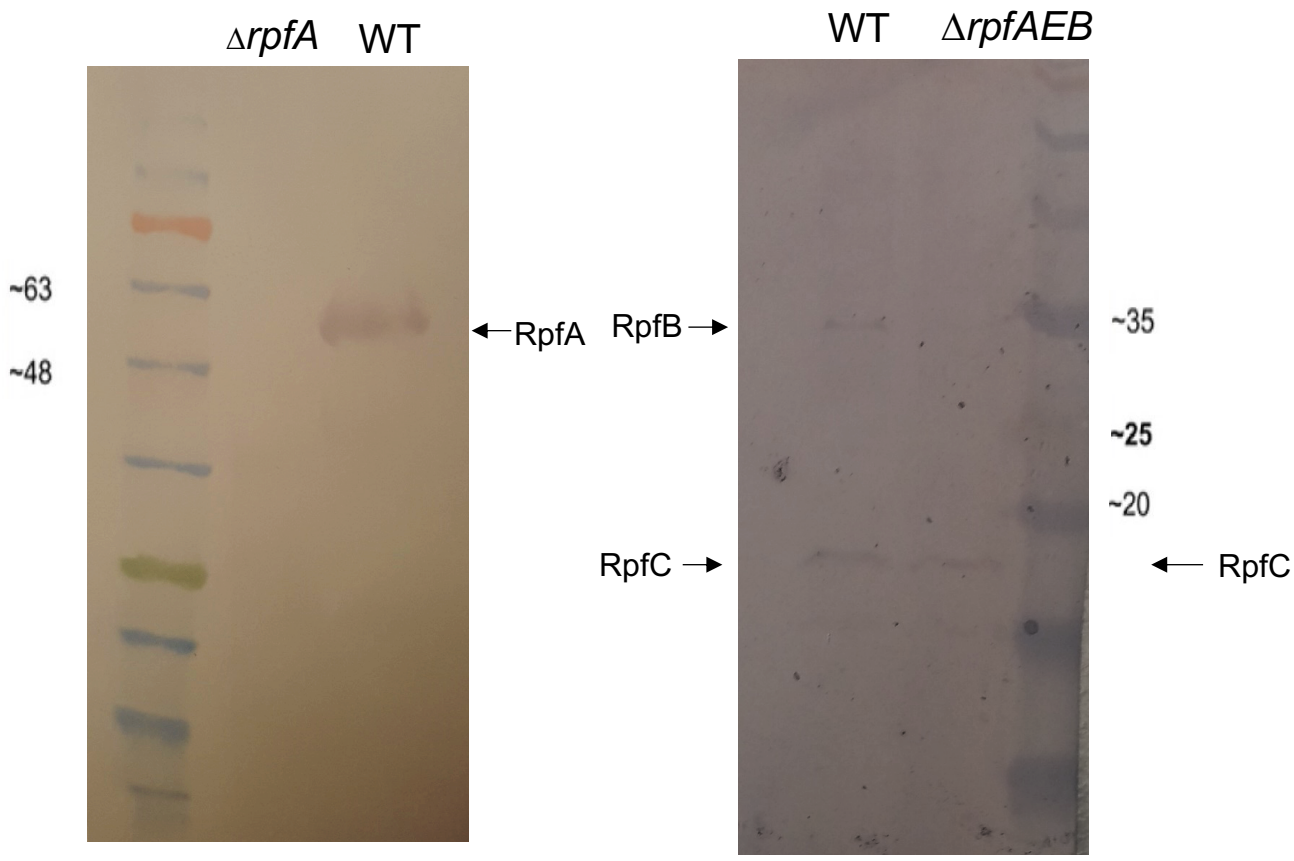

Figure 32: Rpf location in *M. marinum*; Culture supernatant and membrane fractions from WT, Δ*rpfA* and Δ*rpfAEB* were analysed by western blotting using anti-sheep, anti-Rpf antibodies, RpfA was found in culture supernatant (left image), RpfB and RpfC were present in cell membrane fraction (right image).

5.5 *M. marinum rpf* triple mutants have distinct phenotypic features

5.5.1 Growth in liquid

The growth of both WT *M. marinum* and Δ*rpfAEB* was investigated in s7H9 medium and Sauton's minimal medium, in order to establish any differences in growth between the two strains. The experiment was conducted by growing the strains to an OD of 0.8 in s7H9 medium and diluting to an OD of 0.1, after which the bacteria was inoculated in sealed tubes and daily OD measurements were taken over a period of 14 days.

Having established a reproducible and reliable growth defect phenotype for Δ*rpfAEB,* a series of complementation experiments were set up using: WT cSN grown, heated WT cSN, Δ*rpfA* cSN and heated Δ*rpfA* cSN, all initially grown in Sauton's medium. The addition of culture supernatant from spent WT *M. marinum* grown in Sauton's improved the growth of Δ*rpfAEB,* allowing for the mutant to exhibit a growth pattern similar into WT (figure 34C). An apparent growth defect can be seen for Δ*rpfAEB* growth defect in standard 7H9 medium, compared to WT (Figure 33A). The data indicated a significant difference in doubling time between WT and Δ*rpfAEB* when grown in the two media. Δ*rpfAEB* exhibited an even greater growth defect as determined by doubling time in Sauton's medium (16.47±0.115 and 423.27±0.003 hrs, respectively) , compared that seen in s7H9 medium (19.67±0.013 and 73.63±0.019 hrs, respectively), including a longer lag phase, compared to WT *M. marinum* (Figure 33B). It was possible to complement the phenotype through the addition of culture supernatant collected from spent media in which WT *M. marinum* was grown. The ability to improve growth through the addition of culture supernatant suggests that there are secreted substrates, which aid the growth of the mutant.

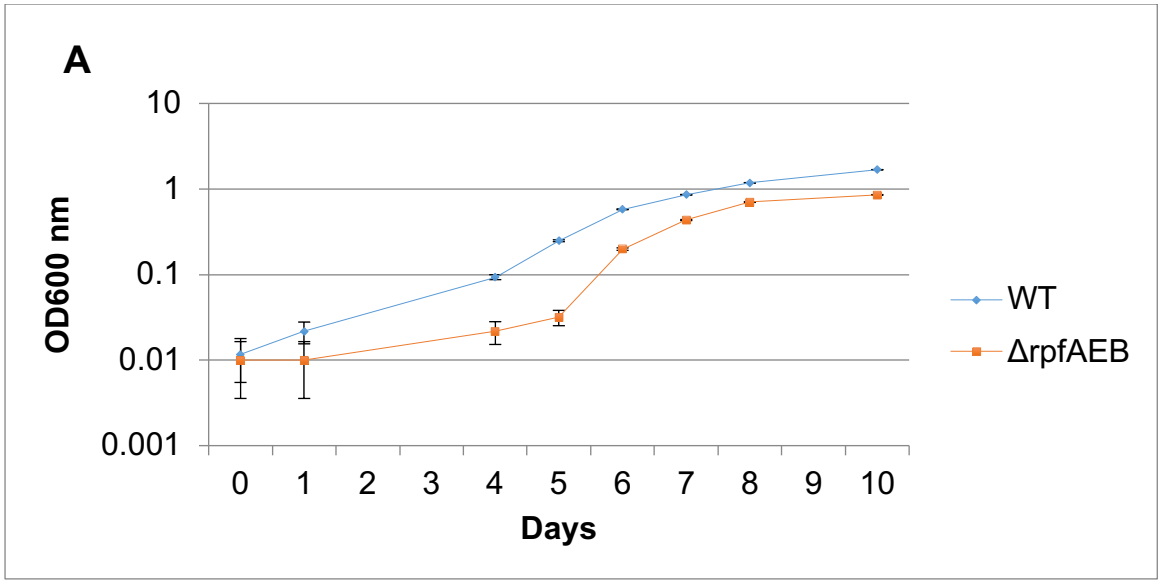

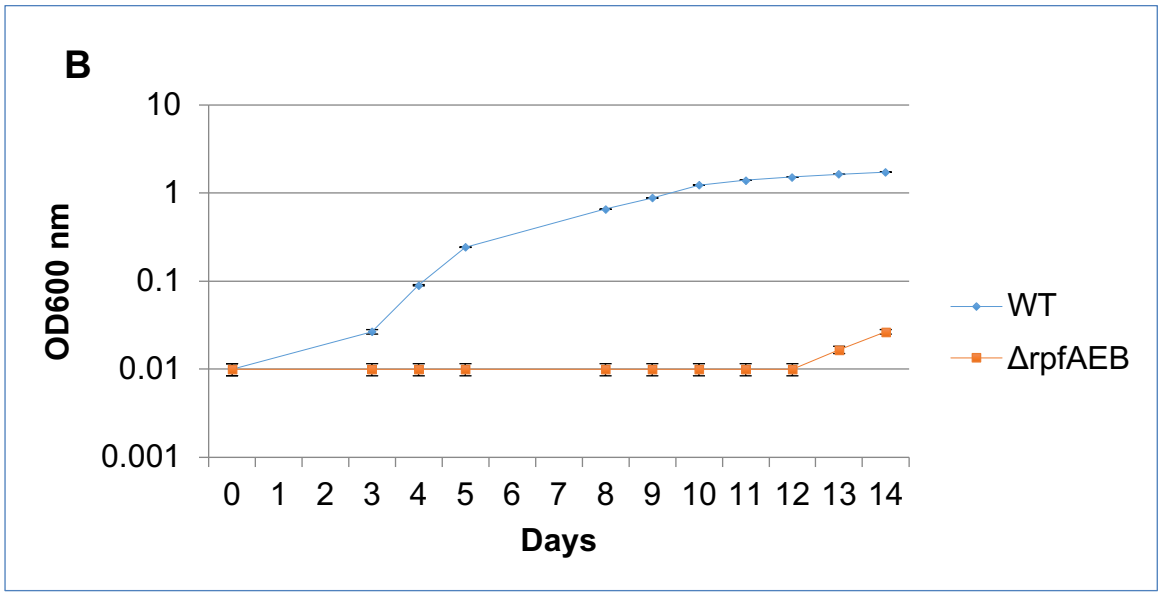

Figure 33i: Characterisation of Δ*rpfAEB* in liquid medium; (A) growth of WT and Δ*rpfAEB* in s7H9 medium **(B)** growth of WT and Δ*rpfAEB* in Sauton's medium. The data is a representative of 2 biological experiments was repeated 2 times and error bars are presented as mean±SEM, N=6

Table 12: Growth parameters of WT *M. marinum* and *ΔrpfAEB* in liquid media				
Strains	WT		*ΔrpfAEB*	
Culture media	s7H9	Sauton's	s7H9	Sauton's
Doubling time (hours)(±S.D)	19.67±0.013	16.47±0.115	73.63±0.019	423.27±0.003

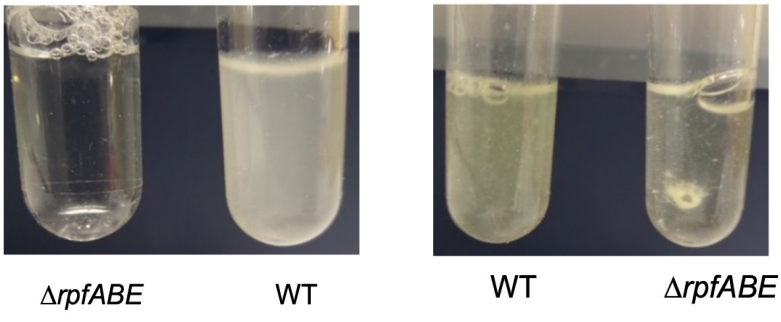

Figure 33: Depiction of WT and *ΔrpfAEB* growth in Sauton's medium/0.05% Tween 80 (left) and Sauton's medium + cSN (right).

Given that the impaired growth of Δ*rpfAEB* mutant could be rescued using culture supernatant from WT *M. marinum* and having confirmed the presence RpfA in the culture supernatant. The properties of the culture supernatant was investigated by growing Δ*rpfAEB* in culture supernatant from Δ*rpfA* mutant to see if the improved growth was solely due to the presence of RpfA or if other factors may have contributing to the improved growth of the mutant. Figure 32A illustrates the growth of WT, Δ*rpfAEB,* Δ*rpfAEB::rpfB* in culture supernatant derived from Δ*rpfA* grown in Sauton's medium/ 0.05% Tween 80/ 50% . The Δ*rpfA* strain was grown to OD 0.7, filtered and freeze dried. This was diluted in Sauton's to produce a 50% culture supernatant medium. It was possible to improve the growth of Δ*rpfAEB,* by shortening the long lag phase, in spite of the absence of RpfA in the culture supernatant. The doubling times for WT, Δ*rpfAEB* and Δ*rpfAEB::rpfB* resulted in similar results (30.91±0.025,32.39±0.01 and 38.02±0.031, respectively). Notably, the addition of

Δ*rpfA* derived cSN to Sauton's medium, reduced the long lag phase and decreased the doubling time for Δ*rpfAEB*. Furthermore, a similar growth pattern to WT was also observed for Δ*rpfAEB::rpfB* in this growth medium. However, whilst Δ*rpfAEB* did not reach as high of an optical density as WT or Δ*rpfAEB::rpfB* at all growth stages, there was a significant improvement in growth compared to the growth of Δ*rpfAEB* in Sauton's, as the doubling time was significantly reduced (from 423.27±0.003 to 32.39±0.017). The addition of Δ*rpfA* cSN to Sauton' mediums did not impair the growth of WT growth and the same growth pattern was observed for WT as that without cSN in Sauton's medium for this strain.

Next, the effects of both heated WT and heated Δ*rpfA* culture supernatant was assessed against the growth of WT, Δ*rpfAEB* and Δ*rpfAEB::rpfB* (Figure 34C and 34B, respectively). cSN from both strains were harvested, heated for 10mins, filtered and added to growing culture of WT, Δ*rpfAEB,* Δ*rpfAEB::rpfB .* The results produced similar growth for all strains when compared to that of their growth in standard Sauton's medium. In both heated WT cSN and heated Δ*rpfA* cSN the Δ*rpfAEB* mutant exhibited a growth defect with a longer lag phase than WT, whilst the complemented strain, Δ*rpfAEB::rpfB* grew like WT, and reached a similar final OD as the WT strain. Although the doubling time for Δ*rpfAEB* was decreased to 137.41±0.003 in the presence of heated Δ*rpfA* cSN, a further decrease was observed in the presence of Δ*rpfA* cSN (32.39±0.017), with the biggest decrease in doubling time observed upon the addition of heated WT cSN (17.49±0.009).

As the experiments were carried out in loosely sealed tubes, in a shaking incubator and reading were taken over 10 days. It is possible that the long lag phase can be attributed do to a limitation of oxygen. These inferences can be made as the growth comparison of the triple mutant to WT when grown in larger flasks, still show a defect

in triple mutant growth, however a difference in lag phase is much less noticeable under these experimental conditions (data not shown).

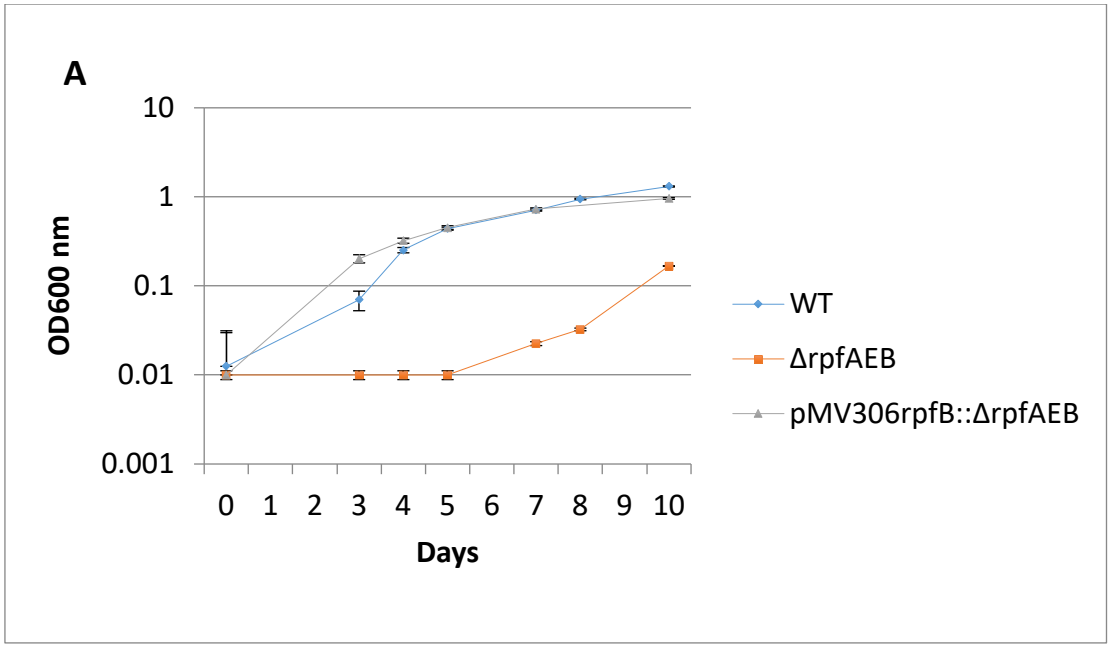
A
OD600 nm
10
1
0.1
0.01
0.001
0 1 2 3 4 5 6 7 8 9 10
Days
WT
ΔrpfAEB
pMV306rpfB::ΔrpfAEB

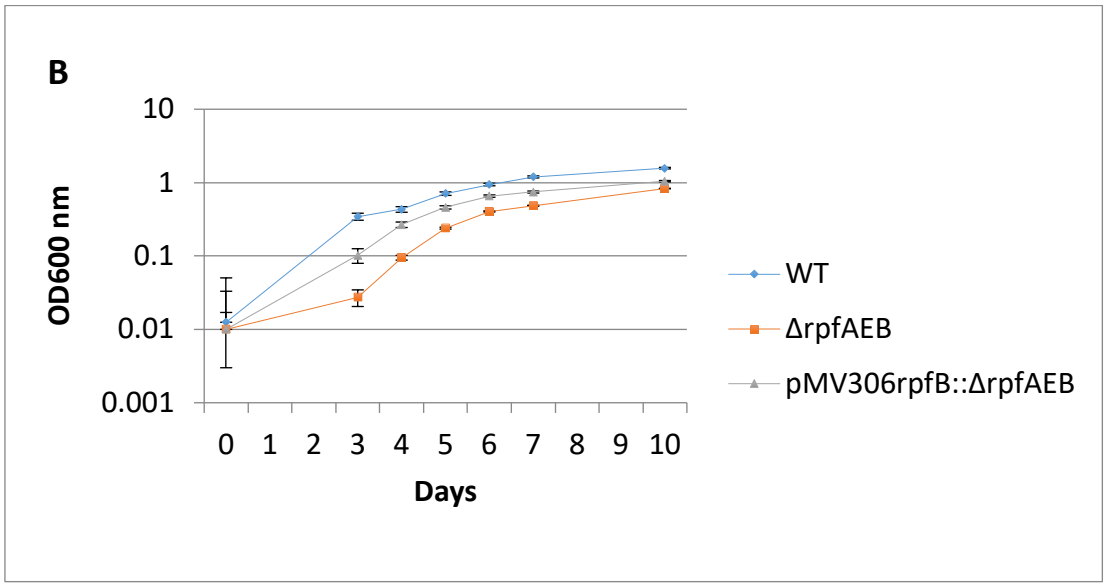
B
OD600 nm
10
1
0.1
0.01
0.001
0 1 2 3 4 5 6 7 8 9 10
Days
WT
ΔrpfAEB
pMV306rpfB::ΔrpfAEB

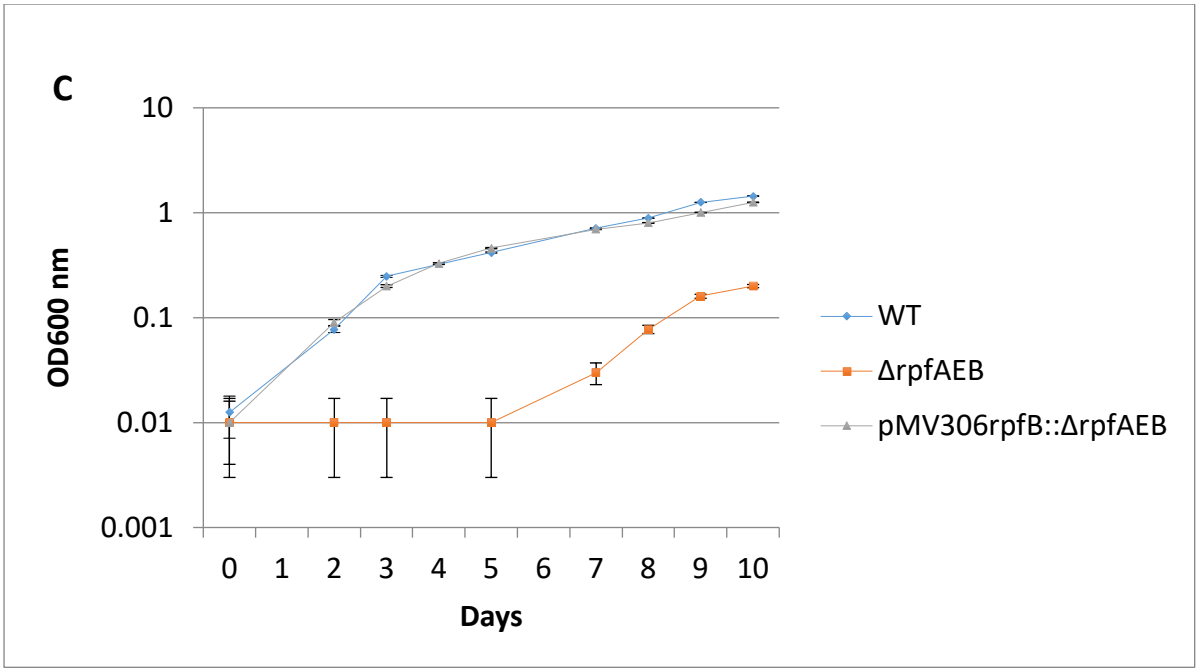

Figure 34: Complementation studies of *ΔrpfAEB* using cSN (**A)** The effects of heated WT cSN (Sauton's medium/0.05% Tween 80 / 50% cSN) **B)** The effects of 50% *ΔrpfA* cSN (derived from Δ*rpfA* grown in Sauton's medium/ 0.05% Tween 80) **C)** The effects of heated 50% *ΔrpfA* cSN (derived from Sauton's medium/ 0.05% Tween 80), on the growth of WT (blue line), *ΔrpfAEB* (orange line), *pMV306rpfB::ΔrpfAEB* (silver line) The experiment is representative of 2 biological replicates. The data is represented as mean±SEM (N=6)

Table 13: Growth parameters of WT *M. marinum*, *ΔrpfAEB*, *pMV306rpfB::ΔrpfAEB* in cSN									
Strains	WT			*ΔrpfAEB*			pMV306*rpfB::ΔrpfAEB*		
Culture media	Heated WT cSN	ΔrpfA cSN	Heated Δ*rpfA* cSN	Heated WT cSN	Δ*rpfA* cSN	Heated Δ*rpfA* cSN	Heated WT cSN	Δ*rpfA* cSN	Heated Δ*rpfA* cSN
Doubling time (hours) (±S.D)	28.33± 0.020	30.91± 0.025	31.74± 0.027	17.49±0 .009	32.39 ±0.01 7	137.41 ±0.003	42.51± 0.016	38.02±0 .031	21.09± 0.019

5.5.2 Addition of cSN to agar moderately improves Δ*rpfAEB* growth on agar

Having established the improved growth of Δ*rpfAEB* through the addition of culture supernatant to both s7H9 and Sauton's media. The effects of adding freeze dried culture supernatant to 7H11 agar was investigated. This is because 7H11 agar has been shown to produce a greater growth defect of mycobacteria than that of 7H10 agar. The experiment was conducted in order to comparatively identify further improvements in growth for Δ*rpfAEB*. The work featured in this section was conducted by Oliver Sampson as part of his undergraduate dissertation.

cSN from WT *M. marinum* grown to OD 0.7 was harvested, filtered and freeze dried. The freeze dried cSN was diluted in distilled water and 10% was added to 7H11 agar. WT and Δ*rpfAEB* strains were serially diluted and grown on standard 7H11 and 7H11 agar supplemented with 10% cSN. Preliminary findings indicated an improved growth of Δ*rpfAEB* on 7H11 agar supplemented with 10% cSN, compared to s7H11 (Figure 35). The WT strain produced colonies at a dilution of 10^{-4} on both types of agar, whereas Δ*rpfAEB* produced visible growth in the neat fraction on s7H11 agar, with the addition of cSN enabling Δ*rpfAEB* to produce visible colonies at 10^{-3}.

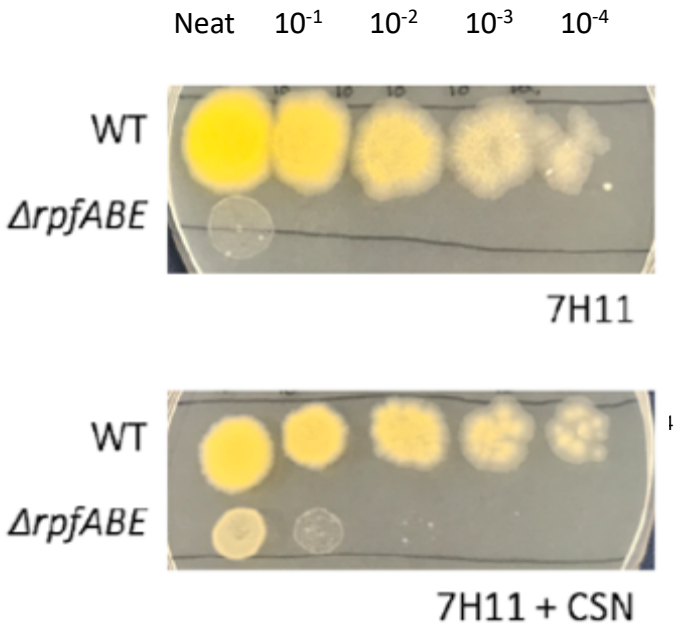

Figure 35: Investigating the effects of cSN on *M. marinum* Δ*rpfAEB* in7H11. The Δ*rpfAEB* growth defect is more pronounced on 7H11 (top panel). Bottom image depicts addition of 10% v/v cSN in 7H11. cSN slightly improves the growth defect of Δ*rpfAEB* in 7H11. 10 µl of mid log phase cultures OD 0.5 were serially diluted on to the plates and incubated at 32 ˚C for 7 days. Image represents 1 of 3 biological replicates.

5.5.3 Δ*rpfAEB* 's growth defect is most pronounced on 7H11 agar plates with reduced glycerol

Preliminary investigations of the effects of reduced glycerol on agar of *M. marinum* WT and *rpf* deletion strains indicated differences in growth on both 7H10 and 7H11 agar (Figure 36). The experiment was carried out by growing the bacterial strains to exponential phase (OD 0.6-0.8), the strains where then diluted to an OD 0.1 before being serially diluted onto 7H10 agar without glycerol and 7H11 agar without glycerol. All strains were incubated for duration of 7 days at 32°C. The strains were serially diluted from neat to 10^{-5} and the experiments display colony-forming units of dilutions of up to 10^{-4}. On 7H10 agar without glycerol WT, Δ*rpfAE,* Δ*rpfCE,* Δ*rpfBE* all show visible colonies at 10^{-4}, whereas Δ*rpfAB* and Δ*rpfAEB* exhibit growth defects on 7H10 agar without glycerol. Δ*rpfAB* shows colonies at 10^{-3} and Δ*rpfAEB* only has colonies visible in the neat dilution. Moreover, Δ*rpfC* also appears to have a reduction in colony forming units by forming colonies at 10^{-3}, it is possible that this gene is required for growth and that the deletion of this gene results in a very slight defect in growth compared to WT.

In comparison, when the strains were grown in the absence of glycerol on 7H11 agar, there was an overall reduction in colony forming units for all strains. WT, Δ*rpfC,* Δ*rpfAE,* Δ*rpfBE* all formed colonies at dilutions of 10^{-3}. The phenotypes for both Δ*rpfAB* and Δ*rpfAEB,* were a more pronounced defect of that which was seen on 7H10 agar without glycerol. Δ*rpfAB* forms faintly visible colonies at 10^{-1} and Δ*rpfAEB* barely forms colonies in the neat dilution. Interestingly, Δ*rpfCE* appears to grow the better than WT, Δ*rpfC,* Δ*rpfAE,* Δ*rpfCE,* Δ*rpfBE,* Δ*rpfAB* and Δ*rpfAEB* on 7H11 agar without glycerol. This may be due to the sole presence of *rpfA* and *rpfB,* these two *rpfs* maybe the more

important *rpfs* in regards to growth as their combined deletion was the only mutant to warrant a distinct phenotype in minimal medium and solid agar.

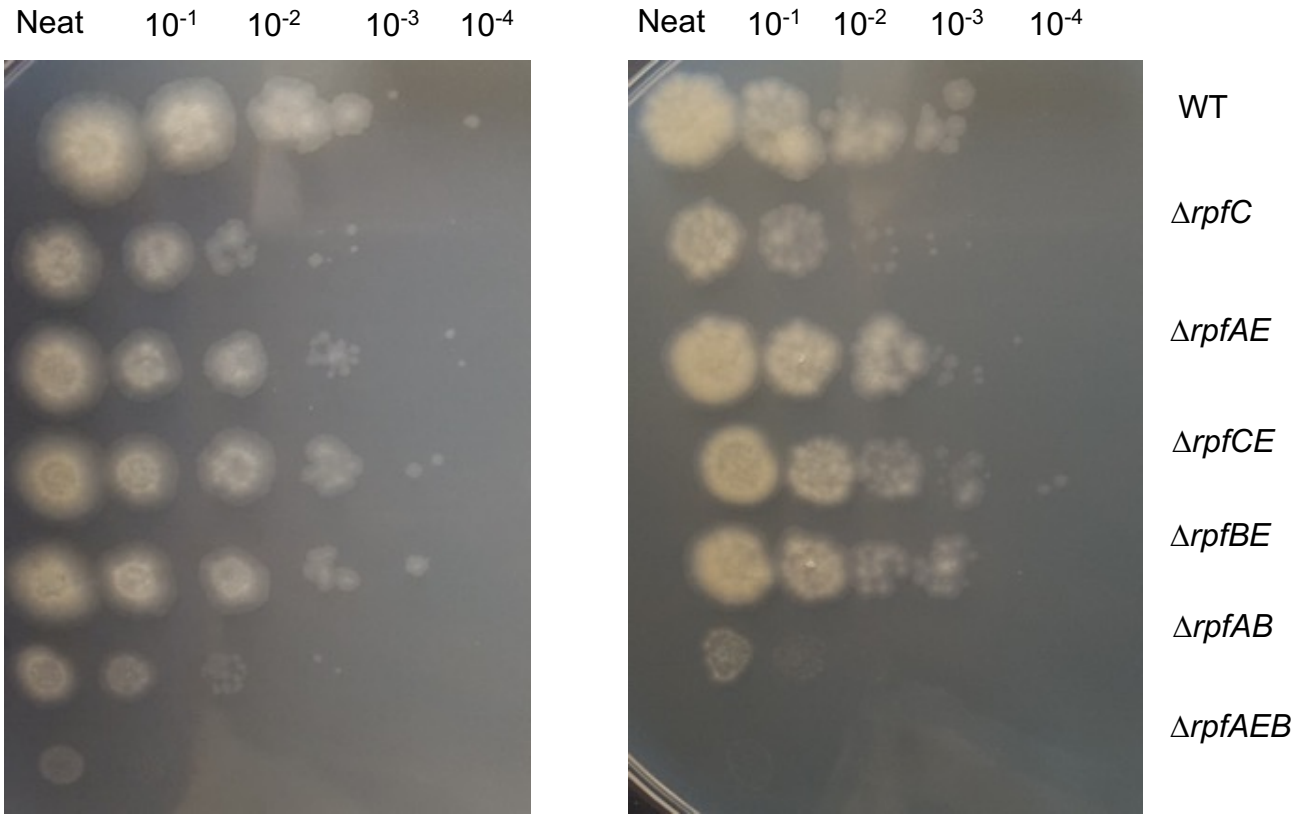

Figure 36: Characterisation of WT and *Δrpf* mutants on 7H11 agar with reduced glycerol. Serial dilution of *M. marinum* Δ*rpf* strains on mycobacterial agar; 7H10 and 7H11 agar. Strains were grown to exponential phase and diluted to OD 0.1 before being serially diluted on agar plates. Experiments are representative of three biologically independent experiments. Δ*rpfC* , Δ*rpfAB* and Δ*rpfAEB* exhibit "delayed colony formation" on agar, whereby the strains do not form visible colonies at higher dilutions compared to WT strain. The delayed colony formation defect can be seen at it most extreme in Δ*rpfAEB* mutant on 7H11 agar. Image represents one of 3 biological replicates.

5.5.4 Potential loss of cording factor and aggregation in Δ*rpfAEB*

Mycobacteria spp. cells aggregate as they grow, and clumping or "cording" is a common feature of this bacteria. This has been linked to biofilm formation in *M. marinum* (Hall-Stoodley et al., 2006). In the first instance, any improper division of cells or changes in "cording" may be visualised using phase microscopy. To assess this WT *M. marinum* and Δ*rpfAEB* were grown in Sauton's medium containing 0.05% glycerol. The strains were diluted to an OD of 0.3, mounted on microscopy slides and visualised under phase microscopy (Figure 37). *Mycobacteria spp* possess a unique feature known as cord like factor, this is a protein which is present on the surface of the cells, this in turn allows for bacteria to aggregate. It was initially thought that only tuberculosis causing strains were able to form serpentine cords. Non -tuberculosis strains such as *M. kansasii, M. avium* and *M. marinum* form what is known as pseudocords (McCarter et al., 1998; Yagupsky et al., 1990).

The phase microscopy of WT *M. marinum* showed evident clumping, along with the distinct serpentine like feature (Figures 35A and 35B). The triple mutant Δ*rpfAEB,* appears scattered and is surrounded by a slime like structure, which may be a result of lysed cells or perhaps a secreted substance to enhance the survival of the mutant (Figure 37D). Notably, Δ*rpfAEB,* forms bulging structures as it grows (Figure 37C), where it appears that the cell swells into leaf like forms. The abnormal growth seen for Δ*rpfAEB* could be attributed to the absence of Rpfs as this phenotype was not detected in WT.

Sauton's medium + 0.05% Glycerol

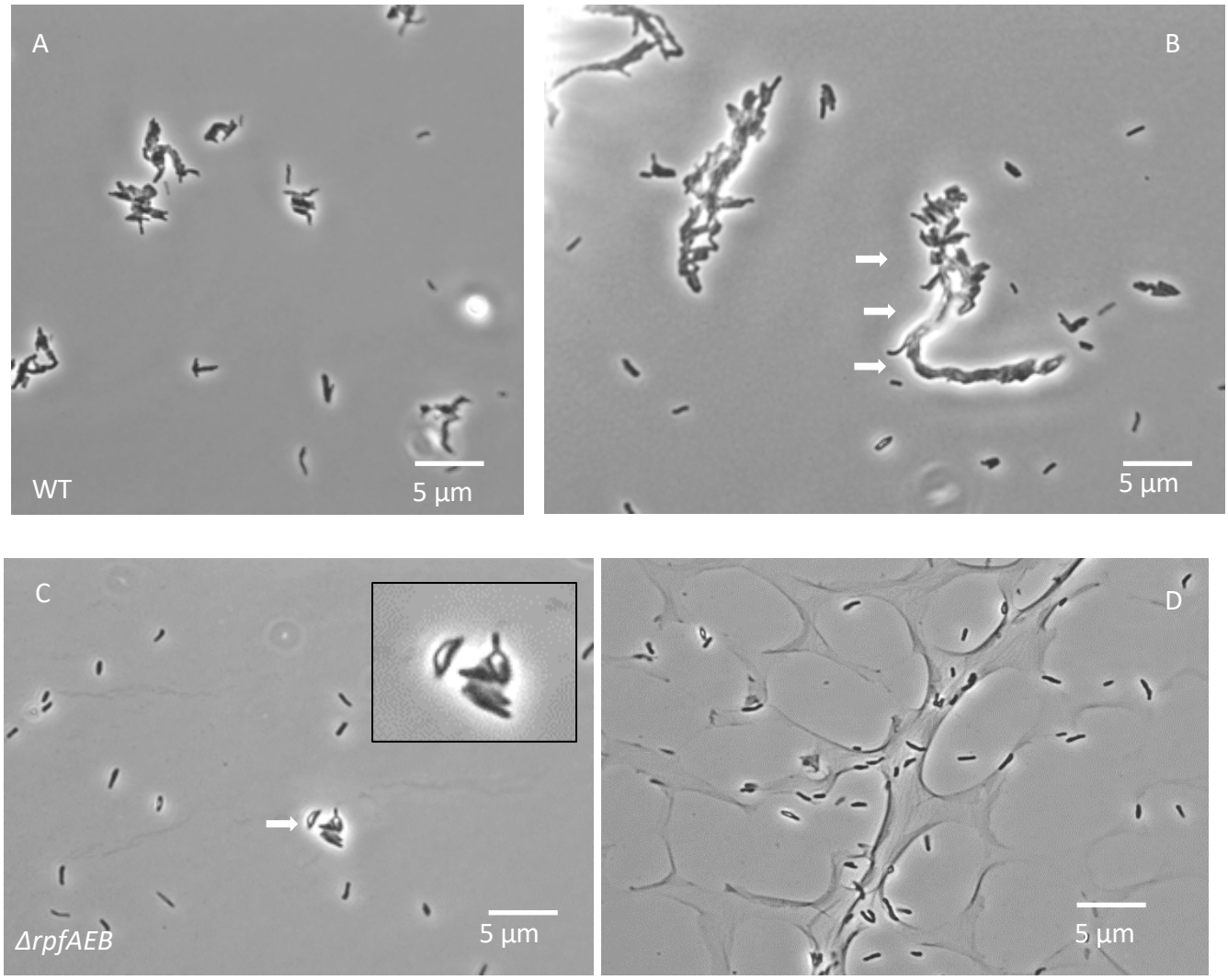

Figure 37: Phase contrast microscopy of WT and Δ*rpfAEB* grown in Sauton's /0.05% Tween 80/0.05% glycerol. **(A)** and **(B)** show WT *M. marinum* in typical cord like formation of cells as a result of cell aggregation (white arrows). The deletion of *rpfAEB* **(C, D**) Morphological differences show scattered cells that do not form cord like structures **(D)** and leaf-like bulging structures (inset and white arrow) **(C)**.

5.5.5 Effect of $ZnSO_4$, haemin and culture supernatant on Δ*rpfAEB* growth on agar

The growth of Δ*rpfAEB* on 7H10 agar was investigated in order to assess any growth defects. Similar to the Δ*rpfAB* mutant the Δ*rpfAEB* mutant also has delayed colony formation on solid agar (Figure 38). A common feature of *rpf* mutants, which has previously been noted in literature (Kana et al., 2008). It is not precisely known what causes the delayed in growth seen in agar. We may however, attribute the difference seen in growth to the absence of the Rpf proteins. This is due to Rpfs being cell wall hydrolyzing enzymes that allow mycobacteria to come out of their dormant state and grow. Based on the data gathered from the Mtb *rpf* null strain we discovered that the strain had various T7SS components completely missing. Supplementing the agar with $ZnSO_4$ and haemin can complement this growth defect.

As the addition of $ZnSO_4$ further improved the growth of the single crossover strain used to generate *ΔrpfAEB,* the effects of $ZnSO_4$ and haemin on the growth of *ΔrpfAEB,* was investigated. Very little is known about Zinc uptake systems in Mycobacteria. *M. tuberculosis Zur* null mutant has shown upregulation of genes encoding a putative ABC-Zinc transporter system (Rv2059-Rv2060) and a zinc low-affinity transporter (Rv0106), suggesting their role in the uptake of this metal, however their functionality and effective role in Zinc uptake remains to be defined (Maciag et al., 2007).

M. marinum WT and *ΔrpfAEB* strain were grown in 7H9 supplemented medium and serially diluted on 7H10 agar containing 0.1 mM $ZnSO_4$ and haemin. We have been able to chemically complement *ΔrpfAEB* strain using $ZnSO_4$ and haemin, suggesting that the *ΔrpfAEB* strain is deficient in both iron and zinc possibly due to the absence or impaired assembly of ESX-3.

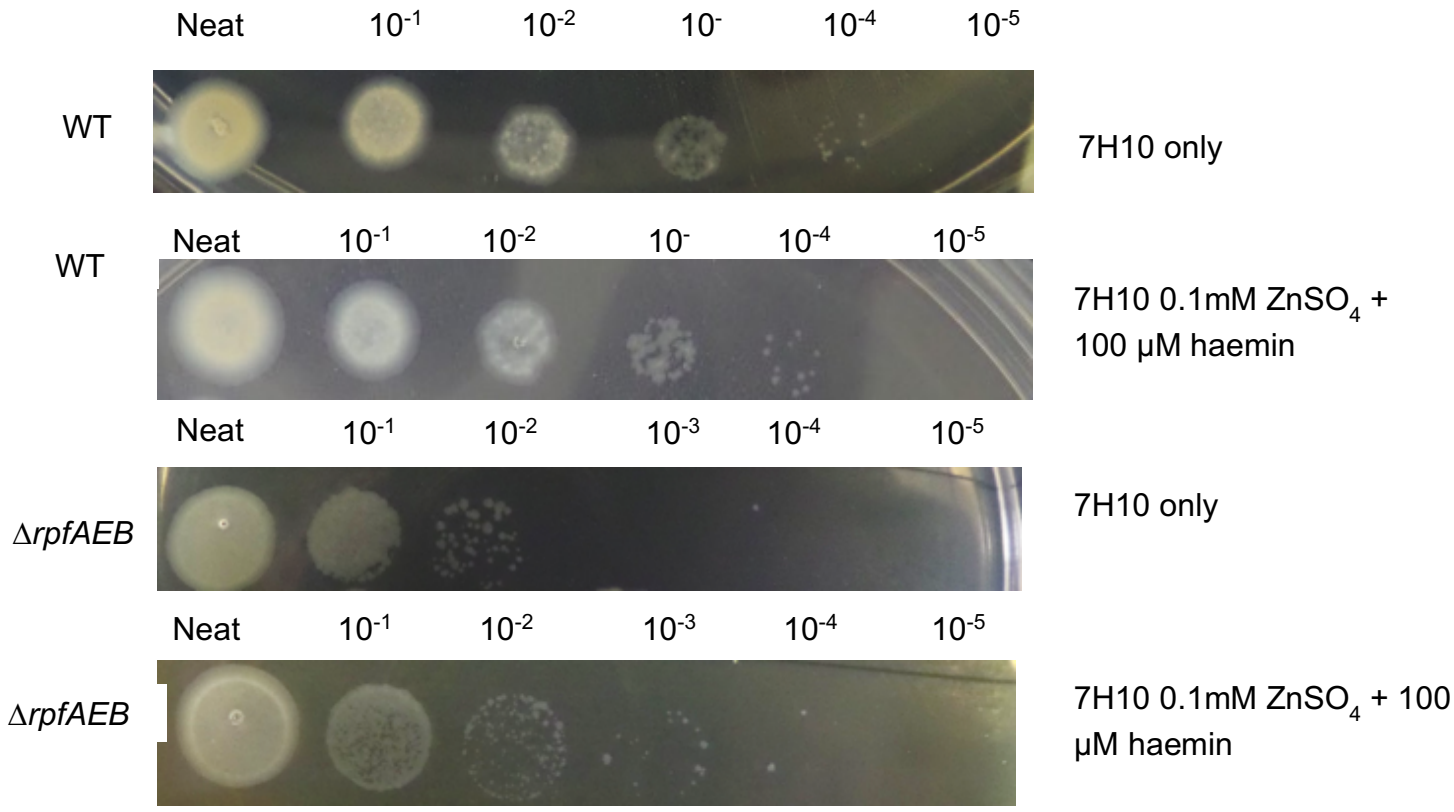

Figure 38: Investigating the effects of $ZnSO_4$ and haemin on Δ*rpfAEB* growth using solid agar (7H10); top panel indicates the growth of WT on 7H10 agar alone and 7H10 agar + $ZnSO_4$/haemin, bottom panels indicate the growth of Δ*rpfAEB* on 7H10 agar alone and growth on 7H10 agar + $ZnSO_4$/haemin. The images are a representation of experiments carried out as 3 biological replicates, N=9.

5.6 Purification of recombinant *M. marinum* RpfA

Having established that RpfA can be found in the culture supernatant via both mass spectrometry and western blot techniques and that the presence of *rpfA* in the culture supernatant aids the improvement of Δ*rpfAEB* growth, we tried to investigate the effects of adding recombinant RpfA to growing *M. marinum* WT, Δ*rpfAEB,* Δ*rpfAEB*::rpfB and Δ*rpfAEB*::rpfB complemented strains. Recombinant RpfA was purified from E.coli following a 16 hour induction. The gel filtration products were collected and ran on a 12% SDS-PAGE in order to visualize the protein and to ensure that the expected size of the protein match that found on the gel. The RpfA protein was then confirmed using anti-sheep, anti-rpf specific antibodies on a western blot (Figure 39).

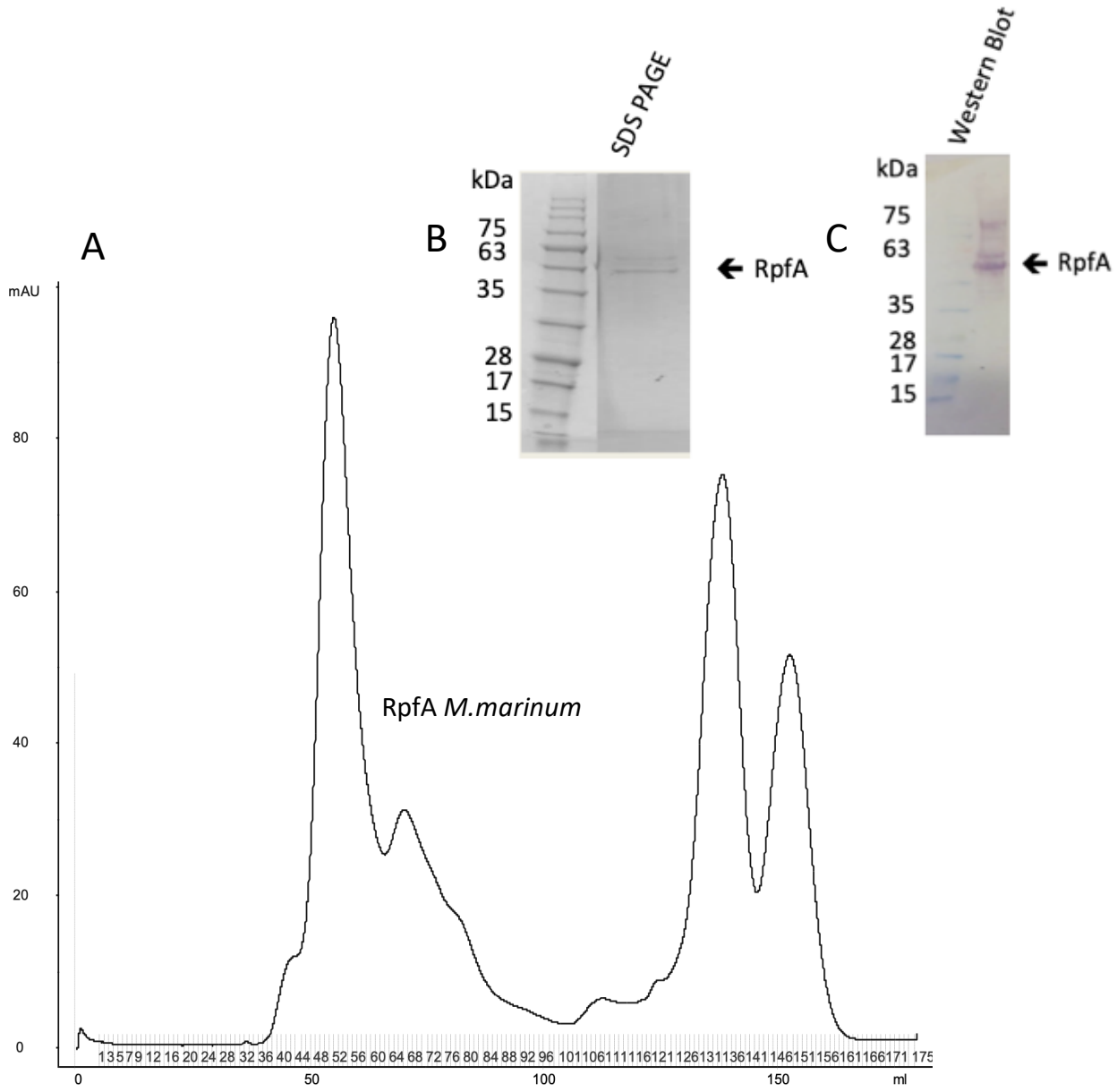

Figure 39: Protein purification and visualisation on blots of RpfA. (A) Chromatogram of the purification of recombinant RpfA. The protein was expressed for 16 hours, then purified using IMAC and size exclusion chromatography on Superdex 75, a peak at 108 mins. **(B)** 12% SDS-PAGE of purified RpfA , lane 2-5 represents pooled fractions. **(C)** Western blot of SDS page using anti Rpf specific antibodies, raised in sheep

5.6.2 Recombinant RpfA does not improve the growth of Δ*rpfAEB*

Rpfs are required for the resuscitation of dormant, 'non‐culturable' cells of *M. luteus* (Mukamolova et al., 1998) and can reduce the lag phase of *M. luteus* at low cell density in minimal media, as well as reduce the apparent lag phase of *M. smegmatis.* Purified RpfA, showed maximal activity at subpicomolar concentrations (Mukamolova et al., 2002).

Preliminary experiments included the addition of recombinant *M. marinum* RpfA to growing WT, Δ*rpfAEB* and *rpfAEB::*rpfB in Sauton's medium, in order to investigate whether recombinant RpfA acquired in its native form could improve the delayed growth exhibited by Δ*rpfAEB* in minimal media. RpfA was serially diluted 10-fold in Sauton's and added to growing cultures of the different strains. The findings did not indicate any significant improvements in growth of Δ*rpfAEB* compared to Δ*rpfAEB* growth in the absence of recombinant RpfA ($p>0.05$). Similarly, both WT and *rpfAEB::*rpfB strains grew in the same manner as they did without the addition of recombinant RpfA to Sauton's medium.

6. Discussion

The scientific investigations of the data presented in this chapter were conducted in order to characterise the first ever *M. marinum ΔrpfAEB* mutant and to better understand why this mutant required the supplementation of haemin and $ZnSo_4$ to s7H9 for it to be generated. *M. marinum* is a closely related organism of Mtb and is a widely used model organism to study mycobacterial pathogenesis (Stinear et al., 2008). Rpfs have been shown to play an important role in the resuscitation and growth of dormant Mtb (Gupta et al., 2010; Kana et al., 2008). These proteins were the first example of mycobacterial proteins playing an important role in reactivation of chronic infection, however, the precise modes or reactivation remain unknown (Tufariello et al., 2006; Rosser et al., 2017). Given that TB accounts for an estimated 9 million new cases and 2 million deaths globally, insights into how reactivation of dormant Mtb occurs would provide therapeutic advances in this field. Literature pertaining to the investigation of Rpf proteins has been numerous over the years. The first instance of Rpf activity was shown in *Mi. luteus* and signified the muralytic activity of the protein (Mukamolova et al., 2002). Kana and colleagues (2008), showed the collective deletion of all 5 *rpfs* in Mtb still permitted growth of the organism *In vitro*, but interestingly, noted a marked plating phenotype, consisting of a delay in colony formation on agar upon the deletion of 3 or more rpfs. The proteins were also shown to be dispensable for growth *In vivo,* highlighting some functional redundancy (Downing et al., 2004; 2005; Tufariello et al., 2004). Further *rpf* studies were also conducted in other organisms, which exhibit dormant cell stages, such as; *Streptomyces*, *Bacillus*, *Clostridum* and *Myxococcus,* highlighting the wide-spread homologs of *rpfs,* their role in cell wall modification and germination.

Therefore, the work in this chapter, focuses on characterising the growth of *ΔrpfAB* using haemin and $ZnSO_4$; characterising the growth of *ΔrpfAEB* in *M. marinum* and investigating the novel potential relationship between mycobacterial metal acquisition and Rpfs. Initial attempts to generate a *M. marinum ΔrpfAEB* mutant using the previously described unmarked in-frame deletion strategy by Parish and Stoker (2000), proved unsuccessful. The *M. marinum* organism is a slow-growing bacterium and requires 14-21 days to grow. Whilst various double deletion background strains were used in attempts to generate a triple *rpf* mutant using s7H9 medium, this was also not possible, in spite of nearly screening 3000 colonies via PCR. The delayed reactivation phenotype witnessed in the Mtb deleted *rpfB* strain (Tufariello at al., 2004; 2006), initially prompted for the use of the M. marinum *ΔrpfB* strain as a background strain in attempts to generate the *M. marinum rpf* triple mutant. The single deletion of *M. marinum rpfB* highlighted a small but significant delay in growth (data not shown), which suggested that the use of this strain might be easier to generate further deletions. It was possible to generate many double deletion strains in *M. marinum* without much difficulty, however, only *ΔrpfAB,* displayed attenuated growth in Sauton's medium. This may be due to *rpfA* and *rpfB* having a similar muralytic role, and thus resulting in visible growth changes when both are deleted. Based on this attenuated phenotype, *ΔrpfAB* appeared to be a suitable strain for the deletion of a third *rpf*. Therefore, the deletion of *rpfE* was attempted in *ΔrpfAB*, however, this also proved unsuccessful. This may have been due to the nature of the *rpfE* construct as the *rpfE* gene is smaller than that of *rpfA* and *rpfB*, which may have rendered the recombination event more difficult. The *ΔrpfAE* strain was then used as a background strain in attempt to delete *rpfB*, and whilst the double-crossover events were successful and

produced WT strains, there was no successful generation of *rpf* triple mutants in *M. marinum* at this stage.

Preliminary proteomics studies carried out using a Mtb rpf null strain and WT Mtb, highlighted the absence of many ESX3 proteins of the type 7 secretion system (T7SS) in the mutant strain compared WT (data not shown). Some of the absent proteins in Mtb rpf null strain included; EsxG/EsxH, PE5, MmpS5/MmpL5, EspC, EsxW and MycP1. These are components of ESX-3 system and it is associated with mycobactin-mediated iron acquisition. Tufariello and colleagues (2016), were able to rescue Δesx-3, ΔesxG, ΔesxH, and Δpe5–ppe4 strain using media supplemented with haemin and mycobactin. Taking this into consideration along with the proteomics data from the Mtb rpf-null strain, and the growth defect displayed by *ΔrpfAB* in minimal medium, we hypothesised that the addition of haemin to the growth media of the *ΔrpfAB* mutant might improve growth. The addition of 100μM haemin (Tufariello et al., 2016) to *ΔrpfAB* improved both the growth in Sauton's medium and agar and did not attenuate the growth of WT. This further suggested a possible link between ESX-3 related proteins and Rpfs. Therefore; 100μM haemin was added to the medium containing *ΔrpfAE* as a background strain with the *ΔrpfB* constructed electroporated into it, in attempts to generate a *ΔrpfAEB* strain. Interestingly, this did not result in the successful generation of a *Δ*rpfAEB strain in *M. marinum*. Thus, further literature investigations into the metal uptake by ESX-3 proteins, highlighted $ZnSO_4$ as the other metal possibly required for the successful generation of a triple *rpf* mutant in *M. marinum*. This prompted us to incorporate both haemin and $ZnSO_4$ into the medium when screening for the triple mutant. This proved to be the only way to successfully generate a triple *rpf* mutant in *M. marinum*.

The growth of *ΔrpfAB* in s7H9 did not result in a growth phenotype, whoever, *ΔrpfAB* exhibits a growth defect in Sauton's medium compared to WT and other *rpf M. marinum* deletion strains and displays "delayed colony formation" on 7H10 agar, with a more pronounced defect on 7H11 agar. This delayed colony formation is consistent with previous *rpf* deletion data in Mtb (Kana et al., 2008) and is the *rpf* double deletion strain with the most profound defect displayed in delayed reactivation kinetics in mice following immune suppression (Russell-Goldman et al., 2008). In Sauton's medium, *ΔrpfAB* does not reach optical densities as high as that of WT and other *M. marinum rpf* deletion strains. The exact mechanisms surrounding this remain yet to be elucidated. Sauton's medium is a minimal mycobacterial medium, containing fewer nutrients compared to s7H9, which includes less haemin and $ZnSO_4$. It takes longer for cells to biosynthesise macromolecules during the initial growth stages; therefore, the presence of minor discrepancies in growth during the lag phase may be less obvious in nutrient rich media such as s7H9 and becomes more pronounced in the minimal medium. This can be seen in the growth of both *ΔrpfAB* and *ΔrpfAEB* when grown in Sauton's medium. Possible explanations for the *ΔrpfAB's* growth defect in Sauton's medium may be due to inabilities of the bacteria to divide properly as a result of missing both *rpfA* and *rpfB*. Given RpfB's ability to form complexes with other proteins involved in cell division and cell wall remodelling, it may suggest an additional, compensatory role for rpfA, as there is some degree of redundancy within the *rpf* genes (Hett et al., 2007). We suggest that, rpfA and rpfB carry out similar function in regards to cell wall cleavage and can compensate in the absence of one of the genes. Notably, *ΔrpfAB* growth defect in Sauton's could be successfully complemented both genetically and "metabolically". The restoration of either *rpfA* or *rpfB* in pMV306 plasmid, allowed for *ΔrpfAB* to grow like WT in minimal medium. Moreover, *ΔrpfAB*

growth defect phenotype could be complemented through the addition of 100μM haemin to Sauton's medium, as measured by an increase in colony forming units on 7H10 agar, resembling WT growth. Further, suggestive of a potentially novel link between metal acquisition, assembly of protein/ siderophore transportation and *rpf* role in mycobacteria.

The delayed colony formation of *ΔrpfAB* on both 7H10 and 7H11 agar, highlights an inability to form colonies as aptly as WT and indeed other *rpf* mutants on this medium. The difference between 7H11 and 7H10 media is that 7H11 has a fourfold higher concentration of malachite green and that cell wall defects are highlighted by malachite green sensitivities (Gillespie et al., 1986), which *ΔrpfAB* exhibits. This impaired culturability of *ΔrpfAB* cells on agar was not only suggestive of defects in division, it also highlighted the possible inability for the cells to uptake certain nutrients within the medium, resulting in delayed growth. The delayed colony formation on agar could be complemented with both haemin and $ZnSO_4$, indicating that *ΔrpfAB* required additional haemin and $ZnSO_4$ in the growth medium in order to grow optimally.

Having successfully improved the growth of *ΔrpfAB* using haemin and $ZnSO_4$ in liquid and agar media and generated *ΔrpfAEB* in *M. marinum* with the same metals, we sought to characterise the phenotypes of *ΔrpfAEB* using WT and complemented *ΔrpfAEB* strains. Although there have been triple rpf mutants generated in Mtb, no *ΔrpfAEB* strain has previously been generated in *M. marinum* (Kana et al., 2008). Firstly, the growth of *ΔrpfAEB* and WT *M. marinum* was investigated in s7H9 and Sauton's medium. *ΔrpfAEB* displayed a growth defect in s7H9, which is more pronounced in Sauton's medium compared to WT and other *M. marinum rpf* deletion strains. Although, *ΔrpfAEB* grows in a similar way to WT in s7H9, the triple mutant never reaches optical densities as high as WT during all stages of growth. In minimal

medium, *ΔrpfAEB* experiences a 10 day long lag phase before it begins to grow, suggestive of difficulties in division and biosynthesis of cell wall components allowing for growth of cells. In order to attribute this distinct phenotype to the absence of *rpf* genes, complemented strains were generated in *ΔrpfAEB* using the pMV306 containing *rpfA* and *rpfB*, separately. Notably, this growth defect phenotype could be complemented both genetically and "metabolically", as seen in *M. marinum ΔrpfAB*. The genetic complementation of this strain is consistent with previous results of complementation studies in Mtb triple mutants*, ΔrpfACB* and *ΔrpfACD*; whereby the growth defect could be restored genetically and through the addition of culture filtrate from WT Mtb strain (Kana et al., 2008). The exact reasons for the growth defects are not exactly know to date, however, a functional hierarchy has been suggested amongst the Rpf's, based on their studies in Mtb. It was postulated that RpfB and RpfE outrank RpfD and RpfC (Kana et al., 2008). RpfB and RpfE are also the two Rpfs that have bee shown to interact with RipA- a partnering peptidoglycan hydrolase (Hett et al., 2007). As such, the deletion of both these genes in the generated triple mutant, suggest an increased inability for the strain to adequately interact with other cell wall hydrolases and subsequent cell division. However, interesting insights into the potential role of *rpf's* have been provided through both the ability to successfully generate *ΔrpfAEB* using haemin and $ZnSO_4$ and later "metabolically' complementing *ΔrpfAEB* using these metals. The growth defect seen in Sauton's medium can be significantly improved through the addition of these metals. Although the growth defect is not entirely restored to WT growth, the lag phase is shortened in *M. marinum ΔrpfAEB.* This is suggestive of a link between the ability of *rpf* lacking strains in mycobacteria in acquiring nutrients in media, to grow optimally.

The nutritional requirement and uptake mechanisms have been intensively studied in Mtb; including the transport of carbohydrates, lipids, phosphorus and sulfur-containing solutes. Recently, more focus has been given into the transport, immunological and pathological involvement of inorganic cations such as the metals; Fe^{2+} / Fe^{3+} and Zn^{2+} (Chao et al., 2019; Gao et al., 2018; Goethe et al., 2020). Mycobacteria have a unique cell-envelope structure. The hydrophobic and thick barrier of this structure makes the exchange of metabolites difficult (Brennan & Nikaido, 1995). In regard to mycobacterial iron and zinc uptake, the ESX-3/Type VII secretion system is present in all Mycobacterial species and mediates the secretion of specific sets of effector proteins essential for iron sequestration in Mtb and *M. bovis* and is involved in the regulation of both iron and zinc in *M. smegmatis* (Serafini et al., 2009). There is no research to date, which has investigated this role in *M. marinum*. Furthermore, The correct assembly and stability of ESX-3 protomers has been shown to be critical for the functioning of the ESX-3 secretion system (Famelis et al., 2019). Some Rpfs have structural similarities to LTGs. In other bacteria, LTGs play a role in the assembly of secretion systems such as Type II (T2SS), T3SS and T4SS, as well as surface organelles, including Type 4 Pili (T4P) and flagella (Koraimann, 2003; Zahrl et al., 2005; Scheurwater & Burrows, 2011; Herlihey & Clarke, 2016). Therefore, the proposed additional role for Rpfs, involves generating spaces through cell wall cleavage of the cell wall to allow for the efficient assembly and anchoring of T7SS in the cell envelope in mycobacteria. Upon the deletion of *eccD3*, the main transmembrane protein of ESX-3 system, its absence resulted in a distinct morphology of *M. smegmatis*, which highlighted a possible change to the cell wall architecture. Conversely, from an *rpf* involved perspective, it is possible that the absence of Rpfs prevent the efficient assembly of some of the proteins of the ESX system. This theory

coincides with the deletion of the ESX3 locus in *M. smegmatis* resulting in both the inability of the cells to use bound iron and poor growth of the Mycobacteria (Siegrist et al., 2009).

The growth of bacteria on agar compared to liquid media, allows for the isolation of colonies and renders it impermissible for damaged or dead cells to be included in the quantification of growth. Therefore, the delayed colony formation phenotype observed by both *ΔrpfAB, ΔrpfAEB* on 7H10 and 7H11 agar, is indicative of the cells impaired ability to adequately cleave the peptidoglycan and promote the addition of PG precursors promoting both division and growth of the cells. This is also reflected in the extended lag phase seen in *ΔrpfAEB* when grown in Sauton's medium. However, given that the *ΔrpfAEB* strain was initially grown to an OD similar to WT in s7H9 before being plated onto the agar plates, it may also signify the presence of dead or severally damaged cells incapable of forming colonies on the agar. Initial experiments managed to improve the growth of *ΔrpfAB* on 7H10 using haemin, to a growth similar to that of WT. Similarly; growth of *ΔrpfAEB* could also be improved using haemin and $ZnSO_4$ on 7H10. The exact molecular mechanisms surrounding the reasons for improved growth are not yet known. It can be speculated that the concentration of available iron for *ΔrpfAEB* and *ΔrpfAB* is insufficient for its efficient uptake or that the ESX-3 system, responsible for iron and zinc uptake is potentially disassembled as a result of absent Rpfs. Thus, rendering the strain incapable of secreting the iron-chelating protein EsxG-EsxH complex required for mycobacterial growth under low iron conditions (Serafini et al., 2009; Siegrist, 2009; Serafini et al., 2013). Therefore, the presence of excess amounts of iron, in the form of haemin, may allow for alternative iron-acquiring systems other than ESX-3 to be used by *ΔrpfAEB.* This could be through the diffusion of haemin via the already compromised cell wall in

ΔrpfAEB. As literature has indicated that it is possible for ESX-3 deletion mutants to survive, provided that there is an abundance of iron in the growth medium.

The addition of culture supernatants (cSN) from growing mycobacterial cultures has been extensively used to resuscitate non-culturable mycobacterial cells, from sputum samples and to improve the growth of *rpf*-deleted strains. Using preliminary data, the presence of RpfA was located in the cSN and RpfB and RpfC in the cell membrane fractions of *M. marinum*. Next, we sought to investigate whether the improved growth of *ΔrpfAEB* was solely due to the presence of Rpfs in cSN or if it could be attributed to other secreted proteins and nutrients present in the cSN. Interestingly, the *ΔrpfAEB* growth defect in liquid medium could be improved through the addition of; cSN from spent WT medium, heated WT cSN and heated cSN from *M. marinum ΔrpfA* strain. The effects of heated cSN from both strains suggested that the improved growth was not only due to the presence of Rpfs, as heating the cSN would denature the Rpfs, and could be due to the presence of siderophores. The heat stability of siderophores has been shown in the soil dwelling *Streptomyces* bacteria, by autoclaving cell-free filtrate, which resulted in 93.4 % of the initial sidrophore contents being retained (Schütze et al., 2015). The lack of possible heat-induced attenuation of siderophores or indeed other compounds that could be responsible for the improved growth in *ΔrpfAEB* growth in Sauton's medium, could be unique to *M. marinum* as it is both an environmental and pathogenic mycobacteria.

Given the confirmation of native RpfA in cSN using western blotting, we sought to investigate the effects of purified recombinant RpfA on *ΔrpfAEB* growth in liquid media. Although, the recombinant form of the protein was attained and visualised on a western blot, it was not possible to improve the growth of *ΔrpfAEB* growth using

recombinant RpfA. This could be due to the protein not being in its native form, or that the RpfA protein was not stable for long, and resulted in its denaturation.

M. marinum WT and *ΔrpfAEB* were subjected to phase contrast microscopy, following growth in Sauton's medium. The *ΔrpfAEB* cells appeared scattered and 'leaf-like' in structure, compared to WT, which displayed the typical cord formation seen in Mycobacteria. Cord formation is a virulence factor in both Mtb complex and *M. marinum*. It has been linked to trehalose dimycolate (TDM), but can be affected by mutations in genes not directly involved in TDM biosynthesis. Trehalose monomycolates are transported by Mycobacterial membrane protein Large 3 (MmpL3), an essential gene and it is thought to be responsible for the coordination of cell wall deposition during cell septation and elongation. The MmpL3 is a possible target for mycobacterial drug development and multiple compounds have been identified for genetic therapy (Grzegorzewicz et al., 2012; La Rosa et al., 2012; Foss et al., 2016; Tahlan et al., 2012). There is evidence indicating that the disruption of MmpL proteins in Mycobacteria results in significant attenuated growth. A possible theory for the lack of cording seen in *ΔrpfAEB* under phase microscopy maybe as a result of the cell being unable to transport lipids effectively, perhaps due to missing MmpL proteins.

Under laboratory conditions glycerol is the favoured carbon source of Mtb. MmpL3, ideR, embA, have previously been shown to be essential for the growth of Mtb on media containing both glucose and glycerol (Rodriguez et al., 2002; Domenech et al., 2005). RpfE has been shown to interact with an endopeptidase and probably has a role in peptidoglycan hydrolysis during cell division, a process that is likely to be involved in the switch from slow to fast growth rate. WT M. marinum and rpf deletion strains; *ΔrpfC, ΔrpfAE, ΔrpfCE, ΔrpfBE, ΔrpfAB* and *ΔrpfAEB* investigated on 7H10

and 7H11 agar with reduced glycerol, illustrated delayed colony formation for both *ΔrpfAB* and *ΔrpfAEB,* with a more pronounced delay in colony formation when grown on 7H11. *ΔrpfAE, ΔrpfCE* and *ΔrpfBE* double deletion strains have *rpfE* missing, in spite of which, both rpfAE and rpfCE formed colonies at 10^4 and grow slightly better than WT and the other rpf deletion strains on 7H11 agar with reduced glycerol. However, on 7H10 agar with reduced glycerol *ΔrpfCE* and *ΔrpfBE* displayed a similar growth pattern to WT. Collectively, this suggests, that having the presence of either RpfB or RpfA, is more favourable for growth on agar with reduced glycerol, as the absence of both rpfA and rpfAB, results in a delayed colony formation phenotype. Notably, the results for exacerbated poor growth on 7H11 compared to 7H10 with reduced glycerol was expected as 7H11 is a minimal mycobacterial agar. Therefore, it is possible that the enhanced slow growth seen on 7H10 agar, in the form of "delayed colony formation", is exacerbated as a result of three missing rpf's in M. marinum and not as a direct result of the specific removal of *rpfE*. This is because there is no attenuation on growth in the double rpf mutants with *rpfE* missing and that the presence of *rpfA* and *rpfB*, which may compensate for the absence of *rpfE.*

7. Final remarks and conclusion

Tuberculosis infection is unfortunately not a thing of the past and it still remains a major global health issue. Resuscitation-promoting factors are responsible for reactivating latent TB, which in turn accounts for 5-10% of the active TB cases. It is therefore of grave importance to understand the molecular mechanisms which underpins the reactivation, to better aid therapeutic efforts. Whilst a lot of focus has been around proteins and their involvement in the reactivation of dormant bacteria, the exact mechanisms by which Rpfs activity leads to reactivation remains unknown and indeed the regulations of *rpf* gene expression are not yet understood. Mycobacteria, such as *M. marinum* produce multiple Rpfs and Mtb possesses five *rpf*-like genes, with sequence homology to the first Rpf found in *Mi. luteus* (Mukamolova et al., 1998a;1998b).

Previous literature signified an apparent functional redundancy of Rpfs (A-E) for *in vitro* and *in vivo* growth of Mtb, as their absence still allowed for the growth of the bacteria (Downing et al., 2004; 2005; Tufariello et al., 2004). In spite of studies confirming *rpfA–E* as being collectively dispensable for Mtb growth, the sequential deletion of *rpfs* has suggested a functional hierarchy when grown under different conditions (Kana et al., 2008). The deletion of individual *rpfA–E* genes has been shown to be accompanied by upregulation of some or all of the remaining *rpf*-like genes (Downing et al., 2004). However, the loss of one *rpf* gene does lead to the compensatory transcriptional upregulation of another, but instead suggested that Rpf's are regulated by distinct mechanisms (Downing et al., 2005; Kana et al., 2008).

Mtb expression data analysis of *rpfs* has shown the differential expression of these genes under different growth stages and stress conditions, highlighting specific roles for Rpfs during growth stages and stress conditions. For instance, *rpfD* and *rpfE* have

been implicated in playing a role during acidic stress; *rpfE* and *rpfC* are important for hypoxia, whereas all *rpfs* may play a role during early phases of nutrient starvation, with standalone significant decreased in *rpfA*, *rpfB* and *rpfE* expression following further incubation up to 96 h (Gupta et al., 2010). All of which is more suggestive of some degree of functional specialisation due to their differentially regulated expression, which may in turn suggest a specific link between different Rpf proteins and different environmental stress factors. Thus, we have been able to propose potential specific roles for Rpf proteins, supported by the data presented within this thesis (Figure 40). Our data indicate that all Rpfs may be involved in the remodelling of the mycobacterial cell wall and the proper assembly of the T7SS components. Although peptidoglycan remodelling and the direct role of Rpfs in the assembly of T7SS were not investigated in this project striking growth phenotypes of Rpf mutants suggest that they have impaired ability to acquire nutrients and specifically iron and zinc. Findings of this project and previously published results demonstrated that Rpf have specific roles in mycobacterial stress response. RpfA plays a role in osmotic tolerance as shown in chapter 4; RpfB may play a role in hypoxia (Kesavan *et al.,* 2008) and has been shown to be co-transcribed with the downstream gene; *ksgA,* involved in ribosome maturation, suggesting an involvement of RpfB in ribosome maturation via an RNA switch (Schwenk et al., 2018).

RpfC, appears to be implicated in growth and both RpfD andRpfE could be important for adaptation to acidic stress (Gupta et al., 2010). Furthermore, RpfE has also been postulated to be involved in nutrient starvation, by promoting mycobacterial resuscitation (Uhía et al., 2018).

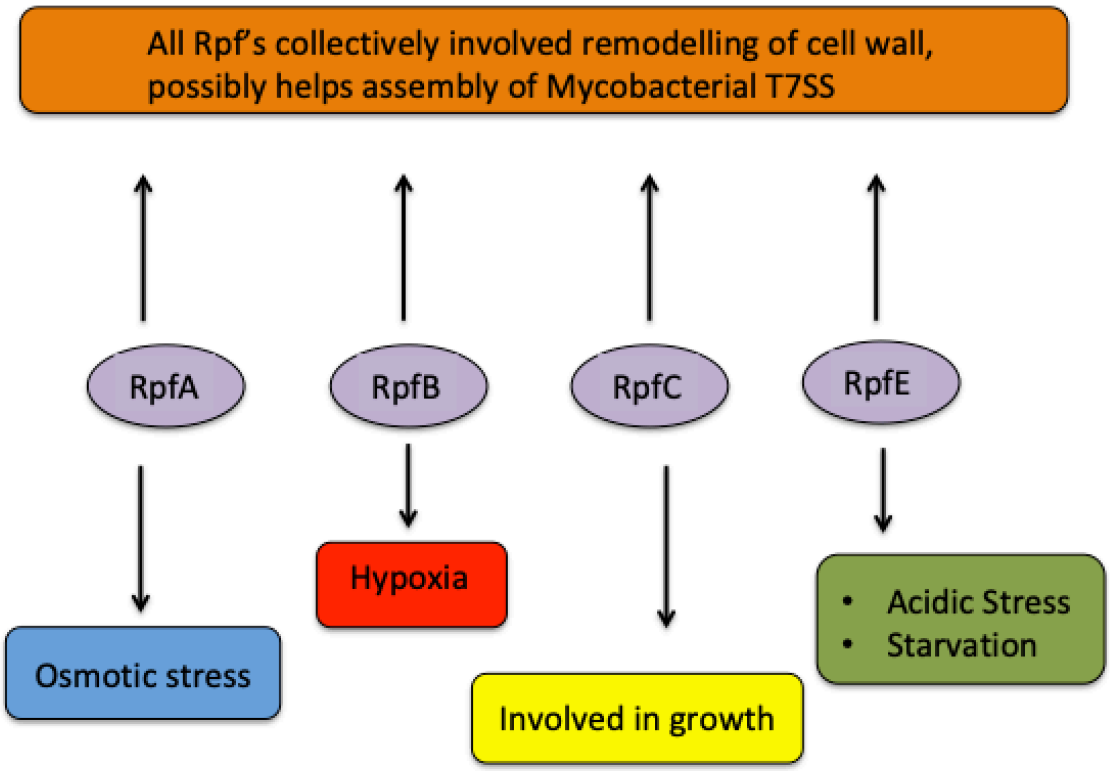

Figure 40: The proposed roles of specific Mycobacterial Rpf in stress response and possible T7SS involvement

Thus, the fundamental aim of the work presented has been to determine the role of RpfA in osmotic stress and Rpf possible involvement in the assembly of T7SS. This work, highlights for the first time that Rpf may have specific roles in mycobacterial stress response.

In agreeance with previous literature *M. marinum* Rpfs are dispensable for growth in both standard and minimal mycobacterial media; we have also investigated the roles of *rpf's* under elevated salt conditions, with a particular focus on the implication of *rpfA*

in relation to osmotic tolerance, aided by the presence of the *ydaO* element. The *ydaO* riboswitch has only been studied in *B. subtilis*, whereby where it prematurely terminates transcription in response to high levels of cyclic di-AMP (c-di-AMP) (Nelson et al., 2013). However, similar to *rpfA* in mycobacteria, the *rpfA* in streptomycetes has a long 5'UTR with both structural and sequence similarity to the sensor domain of the *B. subtilis ydaO* riboswitch (Haiser et al., 2009; Block et al., 2010; Nelson et al., 2013). St-Onge and colleagues (2015) showed that the *S. coelicolor rpfA* riboswitch controls *rpfA* transcription during growth, and their in-line probing experiments, indicated that the *S. coelicolor rpfA* 5′ UTR sequence effectively bound c-di-AMP. Thus, regulating *rpfA* transcription in the same way as the ydaO element in *B. subtilis.*

The initial investigation of the single and double *rpf* mutants under standard mycobacterial conditions such as 7H9 liquid media and 7H10 agar, indicated no difference in growth between the mutant strains and WT following 14-day incubation, except for in the case of Δ*rpfAB* which has shown to not reach as high of an optical density compared to the other *rpf* mutants *when* grown in Sauton's medium, along with delayed colony formation on 7H10. This has shown that the *rpf* genes are not actually required for growth in *M. marinum.* This is not to say that the *rpf* genes' function has been resolved. The impaired growth of Δ*rpfAB* under minimal liquid growth conditions*,* illustrates this notion very well, as the phenotype can be complemented by the addition of specific nutrients which the bacteria appear to be unable to attain from the growth culture. Thus, it is possible to link the deletion of *rpfA and rpfB* to a defect in the cell wall which perhaps affects the cell's capacity to acquire certain metals.

This work has demonstrated the ability of *rpfA* to survive better under elevated salt conditions, and a reduction in colony forming units was observed with the use of

550mM NaCl on 7H10 agar. This pronounced reduction in survival was only seen on solid medium and not in liquid. That may be accounted for by the difference in experimental methods, in that liquid media provides better aeration as the flasks are shaking and the availability of nutrients from the broth is more likely to be available to the bacteria due to the environment in which the bacteria are suspended. Whereas, the plating of bacteria on solid agar not only requires the plates to be sealed and limits oxygen availability, it also does not promote the bacteria to grow outside of the confines where it is plated, thus this limits the bacteria into only being able to utilise the nutrients where it is plated

In order to elucidate the specific role that each of the *rpf's* may have, it is necessary to deciphered the complex regulatory components which they possess. The crucial role of PG, requires the strict control of its cleavage and the proteins, such as Rpfs, which are responsible for some of the hydrolysis of the cell wall (Haiser et al., 2009). Mtb *ΔrpfB* strain exhibits delayed reactivation from chronic TB (Russell-Goldman et al., 2008; Tufariello et al., 2006) and controls outer membrane integrity and are associated with β-lactam tolerance (Wivagg & Hung, 2012). Both RpfB and RpfE have been shown to form complexes with RipA, an endopeptidase. However, RipA does not bind to RpfC, RpfD or RpfA (Cohen-Gonsaud et al., 2005).

In the case of *rpfA,* it is regulated by a number of components such as Lsr2, CRP-binding site and most notably to this work the presence of a riboswitch, known as the *ydaO* element. The *ydaO* element is known to bind ci-di-AMP, a very abundant substance in the body and the environment. The biding of this ligand to the riboswitch, allows for the transcription of *rpfA.* We had hypothesized that the alteration to the binding site of the *ydaO* element would allow for the bacteria to survive worse as it would prevent the adequate transcription and subsequent translation of RpfA, which

in turn would prevent osmotic tolerance. Interestingly, we managed to prove the hypothesis right by illustrating that in the absence of *rpfA,* and the entire upstream region, including all the transcriptional regulators had a worse survival compared to WT. however, this did not provide insight into which regulatory component was the most important in regard to osmotic tolerance.

The generation of *rpfA* complemented strains of various constructs containing different sections of the upstream regions of this gene, allowed for a better understanding of *rpfA* gene regulation and its role in osmotic stress. It is possible to complement the reduced survival of the ∆*rpfA* mutant with C3, C4 and by restoring *rpfA* into ∆*rpfA.* Both the C3, and C4 constructs contain a large section of the upstream regions of *rpfA* and both include the *ydaO* element. The fact that the site-directed mutant which had the ligand binding site of the riboswitch mutated also showed a reduced survival on agar with elevated NaCl, and behaved like the ∆*rpfA* mutant is not only suggestive of the transcriptional and translational regulation of *rpfA* being complicated but it also provides strong evidence that the main regulatory component responsible for *rpfA's* role in osmotic tolerance is the *ydaO* element.

The interest into investigations of putative riboswitches and our understanding of their ability to regulate genes at both the transcriptional and translational levels has increased over recent years. *rpfA* is not the only *rpf* gene to be associated with the presence of a riboswitch as both *rpfB* and *rpfE* are thought to contain putative riboswitches (Schwenk et al., 2018). However, unlike *rpfA;* the riboswitches of *rpfB and rpfE's* remain to be classified. Although, the work featured in this thesis does not contain data using RT-qPCR, this experimental method would be useful In order to better understand the transcriptional regulation of *rpfA* and thus, future work should be centred around experimentally investigating the transcriptional levels of *rpfA,* in WT

M. marinum, ∆*rpfA* and the complemented ∆*rpfA* strains under both standard conditions and under elevated salt conditions.

In order to do this, one could investigate the mRNA levels of the strains and analyse the differences at transcriptional levels, this coupled with the use of SDS pages and western blots would allow for the quantification of the proteins for each strain along with the direct visualisation of amount of protein present.

One very interesting notion that remains unknown is whether the riboswitches are unique to the *rpf* gene that they are associated with or whether or not they carry out the exact same role in each of the riboswitch containing *rpfs* in regards to transcriptional regulation. It therefore poses the question as to whether the riboswitch of rpfB or *rpfE* could be transformed into *rpfA* and allow for *rpfA* to provide the bacteria with osmotic tolerance.

Lastly, and rather notably, great efforts were made in attempt to generate a *rpf* triple mutant in *M. marinum,* in order to further investigate the specific roles of these genes in mycobacterial stress response, as that remains to be elucidated. The most noteworthy of experimental findings within this thesis would be the discovery that *M. marinum ΔrpfAEB* could only be achieved through the addition of and zinc has opened new avenues for *rpf* research by hypothesising a new and novel association between Rpfs and the assembly of type 7 secretion systems. The very obvious phenotype of the triple mutant in liquid but particularly on agar, allows for the further investigation into the potential link of *rpfs*, type 7 secretion systems and metal acquisition in mycobacteria. The notion of targeting the bacteria's ability to acquire host metals for survival is one which has been intriguing over more recent years. If *rpfs* are responsible for the involvement of the assembly of mycobacterial type 7 secretions systems and particularly the ESX-3 systems, it may lead to very interesting advances

in mycobacterial drug therapy. Thus, it would be interesting to explore the susceptibility of *rpf* mutants to metal chelating agents and investigate the survival.

By possibly finding differences in susceptibility to the metal chelating agents, we might be able to better appoint each *rpf* to a particular function and possible ESX-3 component assembly. It is also of great importance to investigate the proteomic and secretomic profiles of the *rpf* triple mutant in order to solidify the notion of rpfs being involved in ESX-3 assembly.

As a whole, the results explained in this thesis, have described a convincing role for rpfA in osmotic tolerance, with the scope for investigating the levels of transcription and translation of this protein under elevated salt conditions. We've also illustrated a collective possible role for *rpfs*, in the potential involvement of the ESX-3 system assembly. This may in turn have a significant clinical implication, as there can be therapeutic means of targeting the metal acquisition of bacteria.

Based on the experimental findings presented in this thesis we have postulated some roles for *rpfs* in relation to stress response and reactivation from dormancy.

As a whole, this thesis has shown the generation of several *M. marinum rpf* mutants and has attempted to elucidate their role in stress response, and a novel and possible link to the assembly of T7SS using a number of approaches. Whilst *rpf* mutants have previously been generated in both *Mtb* and M. smegmatis, the generation of *rpf* mutants in *M. marinum* is a novel one and the experiments shown here have given a greater insight into the way in which *rpfs* work at a molecular and physiological level.

8. References

Aitken R. (1937). Lupus Vulgaris. British medical journal, 1(3968), 160–163. https://doi.org/10.1136/bmj.1.3968.160

Akif, M., Akhter, Y., Hasnain, S. E., & Mande, S. C. (2006). Crystallization and preliminary X-ray crystallographic studies of *Mycobacterium tuberculosis* CRP/FNR family transcription regulator. Acta crystallographica. Section F, Structural biology and crystallization communications, 62 (Pt9), 873–875. https://doi.org/10.1107/S1744309106027977

Andrews, S. C., Robinson, A. K., & Rodríguez-Quiñones, F. (2003). Bacterial iron homeostasis. FEMS microbiology reviews, 27(2-3), 215-237.

Ang, P., Rattana-Apiromyakij, N., & Goh, C. L. (2000). Retrospective study of *Mycobacterium marinum* skin infections. International journal of dermatology, 39(5), 343-347.

Anthony P, Moran OH, Brennan PJ. (2009). Microbial glycobiology: structures, relevance and applications. Elsevier, Oxford, United Kingdom

Altendorf, K., Booth, I. R., Gralla, J. A. Y., Greie, J. C., Rosenthal, A. Z., & Wood, J. M. (2009). Osmotic stress. EcoSal Plus, 3(2).

Al Qaseer, K., Turapov, O., Barthe, P., Jagatia, H., De Visch, A., Roumestand, C., ... & Mukamolova, G. V. (2019). Protein kinase B controls Mycobacterium tuberculosis growth via phosphorylation of the transcriptional regulator Lsr2 at threonine 112. *Molecular microbiology*, *112*(6), 1847-1862.

Al Zayer M., Stankowska D., Dziedzic R., Sarva K., Madiraju M. V., Rajagopalan M. (2011). *Mycobacterium tuberculosis mtrA* merodiploid strains with point mutations in the signal-receiving domain of MtrA exhibit growth defects in nutrient broth. *Plasmid* 65 210–218.

Anantharaman, V., & Aravind, L. (2003). Evolutionary history, structural features and biochemical diversity of the NlpC/P60 superfamily of enzymes. Genome biology, 4(2), R11. https://doi.org/10.1186/gb-2003-4-2-r11

Atrih, A., & Foster, S. J. (1999). The role of peptidoglycan structure and structural dynamics during endospore dormancy and germination. Antonie Van Leeuwenhoek, 75(4), 299-307.

Aronson, J. D. (1926). Spontaneous tuberculosis in salt water fish. The journal of infectious diseases, 315-320.

ArunMohan, M. V., Tejaswi, H. J., & Ranganath, T. S. (2016). Socio-demographic profile of TB-HIV co-infected adults and it's association with tuberculosis treatment outcome, in a South Indian city. International Journal Of Community Medicine And Public Health, 3, 3498-3503.

Bai, G., McCue, L. A., & McDonough, K. A. (2005). Characterization of *Mycobacterium tuberculosis* Rv3676 (CRPMt), a cyclic AMP receptor protein-like DNA binding protein. Journal of bacteriology, 187(22), 7795–7804. https://doi.org/10.1128/JB.187.22.7795-7804.2005

Bai, G., Schaak, D. D., & McDonough, K. A. (2009). cAMP levels within *Mycobacterium tuberculosis* and *Mycobacterium bovis* BCG increase upon infection of macrophages. FEMS Immunology & Medical Microbiology, 55(1), 68-73.

Balsalobre, C., Johansson, J., & Uhlin, B. E. (2006). Cyclic AMP-dependent osmoregulation of crp gene expression in *Escherichia coli*. Journal of bacteriology, 188(16), 5935-5944.

Balloux, F., & van Dorp, L. (2017). Q&A: What are pathogens, and what have they done to and for us?. *BMC biology*, *15*(1), 1-6.

Barnard, A. M., Green, J., & Busby, S. J. (2003). Transcription regulation by tandem-bound FNR at Escherichia coli promoters. *Journal of bacteriology*, *185*(20), 5993-6004.

Barry, C. E., Boshoff, H. I., Dartois, V., Dick, T., Ehrt, S., Flynn, J., ... & Young, D. (2009). The spectrum of latent tuberculosis: rethinking the biology and intervention strategies. *Nature Reviews Microbiology*, *7*(12), 845-855.

Barrick, J. E., Corbino, K. A., Winkler, W. C., Nahvi, A., Mandal, M., Collins, J., ... & Breaker, R. R. (2004). New RNA motifs suggest an expanded scope for riboswitches in bacterial genetic control. Proceedings of the National Academy of Sciences, 101(17), 6421-6426.

Bartek, I. L., Woolhiser, L. K., Baughn, A. D., Basaraba, R. J., Jacobs Jr, W. R., Lenaerts, A. J., & Voskuil, M. I. (2014). *Mycobacterium tuberculosis* Lsr2 is a global transcriptional regulator required for adaptation to changing oxygen levels and virulence. MBio, 5(3), e01106-14.

Bell, L. C., & Noursadeghi, M. (2018). Pathogenesis of HIV-1 and *Mycobacterium tuberculosis* co-infection. Nature Reviews Microbiology, 16(2), 80-90.

Behr, M. A., & Waters, W. R. (2014). Is tuberculosis a lymphatic disease with a pulmonary portal?. The Lancet. Infectious diseases, 14(3), 250–255. https://doi.org/10.1016/S1473-3099(13)70253-6

Berg, O. G., & von Hippel, P. H. (1988). Selection of DNA binding sites by regulatory proteins. II. The binding specificity of cyclic AMP receptor protein to recognition sites. Journal of molecular biology, 200(4), 709–723. https://doi.org/10.1016/0022-2836(88)90482-2

Block, K. F., Hammond, M. C., & Breaker, R. R. (2010). Evidence for widespread gene control function by the *ydaO* riboswitch candidate. Journal of bacteriology, 192(15), 3983-3989.

Buist, G., Steen, A., Kok, J., & Kuipers, O. P. (2008). LysM, a widely distributed protein motif for binding to (peptido) glycans. Molecular microbiology, 68(4), 838-847.

Boon, C., Li, R., Qi, R., & Dick, T. (2001). Proteins of *Mycobacterium bovis* BCG induced in the Wayne dormancy model. Journal of bacteriology, 183(8), 2672-2676.

Boutte, C. C., Baer, C. E., Papavinasasundaram, K., Liu, W., Chase, M. R., Meniche, X., Fortune, S. M., Sassetti, C. M., Ioerger, T. R., & Rubin, E. J. (2016). A cytoplasmic peptidoglycan amidase homologue controls mycobacterial cell wall synthesis. eLife, 5, e14590. https://doi.org/10.7554/eLife.14590

Bradley, J. A., Amend, J. P., & LaRowe, D. E. (2019). Survival of the fewest: Microbial dormancy and maintenance in marine sediments through deep time. Geobiology, 17(1), 43-59.

Bramwell J. P. (1851). On the Use of Cod-Liver Oil in Pulmonary Consumption. Monthly Journal of Medical Science, 3(14), 131–136.

Brennan, P. J., & Nikaido, H. (1995). The envelope of mycobacteria. *Annual review of biochemistry*, *64*(1), 29-63.

Brennan, P. J. (2003). Structure, function, and biogenesis of the cell wall of Mycobacterium tuberculosis. Tuberculosis, 83(1-3), 91-97.

Bretl, D. J., Demetriadou, C., & Zahrt, T. C. (2011). Adaptation to environmental stimuli within the host: two-component signal transduction systems of *Mycobacterium tuberculosis*. Microbiology and molecular biology reviews : MMBR, 75(4), 566–582. https://doi.org/10.1128/MMBR.05004-11

Brocklehurst, T. F., Mitchell, G. A., & Smith, A. C. (1997). A model experimental gel-surface for the growth of bacteria on foods. Food Microbiology, 14(4), 303-311.

Brooks MN, Rajaram MV, Azad AK, Amer AO, Valdivia-Arenas MA, Park JH, Núñez G, Schlesinger LS. (2011). NOD2 controls the nature of the inflammatory response and subsequent fate of *Mycobacterium tuberculosis* and *M. bovis* BCG in human macrophages. Cell Microbiol. 13(3):402-18. doi: 10.1111/j.1462-5822.2010.01544.x.

Bunyan, J. (2021). *Life and Death of Mr. Badman*. Litres.

Chao, M. C., & Rubin, E. J. (2010). Letting sleeping dos lie: does dormancy play a role in tuberculosis?. Annual review of microbiology, 64, 293-311.

Chao, A., Sieminski, P. J., Owens, C. P., & Goulding, C. W. (2019). Iron Acquisition in Mycobacterium tuberculosis. *Chemical reviews*, *119*(2), 1193–1220. https://doi.org/10.1021/acs.chemrev.8b00285

Chapman, A. G., Fall, L., & Atkinson, D. E. (1971). Adenylate energy charge in Escherichia coli during growth and starvation. Journal of bacteriology, 108(3), 1072-1086.

Chatterjee, A., Sharma, A. K., Mahatha, A. C., Banerjee, S. K., Kumar, M., Saha, S., ... & Kundu, M. (2018). Global mapping of MtrA-binding sites links MtrA to regulation of its targets in Mycobacterium tuberculosis. Microbiology, 164(1), 99-110.

Chengalroyen, M. D., Beukes, G. M., Gordhan, B. G., Streicher, E. M., Churchyard, G., Hafner, R., ... & Kana, B. D. (2016). Detection and quantification of differentially culturable tubercle bacteria in sputum from patients with tuberculosis. American journal of respiratory and critical care medicine, 194(12), 1532-1540.

Cho, Y. H., Lee, E. J., Ahn, B. E., & Roe, J. H. (2001). SigB, an RNA polymerase sigma factor required for osmoprotection and proper differentiation of *Streptomyces coelicolor*. Molecular Microbiology, 42(1), 205-214.

Cohen-Gonsaud, M., Barthe, P., Bagnéris, C., Henderson, B., Ward, J., Roumestand, C., & Keep, N. H. (2005). The structure of a resuscitation-promoting factor domain from *Mycobacterium tuberculosis* shows homology to lysozymes. Nature structural & molecular biology, 12(3), 270-273.

Colangeli, R., Helb, D., Vilchèze, C., Hazbón, M. H., Lee, C. G., Safi, H., ... & Alland, D. (2007). Transcriptional regulation of multi-drug tolerance and antibiotic-induced responses by the histone-like protein Lsr2 in *M. tuberculosis*. PLoS pathogens, 3(6), e87.

Colangeli, R., Haq, A., Arcus, V.L., Summers, E., Magliozzo, R.S., McBride, A., Mitra, A.K., Radjainia, M., Khajo, A., Jacobs WR, Salgame P, & Alland D. (2009). The multifunctional histone-like protein Lsr2 protects mycobacteria against reactive oxygen intermediates. *Proc. Natl. Acad. Sci. U. S. A.* 106: 4414–4418.

Cole, S., Brosch, R., Parkhill, J., Garnier, T., Churcher, C., Harris, D., ... & Barrell, B. G. (1998). Deciphering the biology of *Mycobacterium tuberculosis* from the complete genome sequence. Nature, 396(6707), 190-190.

Corrigan, R. M., Campeotto, I., Jeganathan, T., Roelofs, K. G., Lee, V. T., & Gründling, A. (2013). Systematic identification of conserved bacterial c-di-AMP receptor proteins. Proceedings of the National Academy of Sciences of the United States of America, 110(22), 9084–9089. https://doi.org/10.1073/pnas.1300595110

Costanzo, V., Robertson, K., Ying, C. Y., Kim, E., Avvedimento, E., Gottesman, M., ... & Gautier, J. (2000). Reconstitution of an ATM-dependent checkpoint that inhibits chromosomal DNA replication following DNA damage. *Molecular cell*, *6*(3), 649-659.

Commichau, F.M., Halbedel, S. (2013). The resuscitation promotion concept extends to firmicutes. Microbiology (Reading). 159(Pt 7):1298-1300. doi: 10.1099/mic.0.069484-0.

Couvert, O., Divanac'h, M. L., Lochardet, A., Thuault, D., & Huchet, V. (2019). Modelling the effect of oxygen concentration on bacterial growth rates. Food microbiology, 77, 21–25. https://doi.org/10.1016/j.fm.2018.08.005

Crubézy, E., Ludes, B., Poveda, J. D., Clayton, J., Crouau-Roy, B., & Montagnon, D. (1998). Identification of Mycobacterium DNA in an Egyptian Pott's disease of 5,400 years old. Comptes rendus de l'Academie des sciences. Serie III, Sciences de la vie, 321(11), 941–951. https://doi.org/10.1016/s0764-4469(99)80009-2

Daniel T. M. (2000). The origins and precolonial epidemiology of tuberculosis in the Americas: can we figure them out?. The international journal of tuberculosis and lung disease : the official journal of the International Union against Tuberculosis and Lung Disease, 4(5), 395–400.

Daniel, J., Deb, C., Dubey, V. S., Sirakova, T. D., Abomoelak, B., Morbidoni, H. R., & Kolattukudy, P. E. (2004). Induction of a novel class of diacylglycerol acyltransferases and triacylglycerol accumulation in *Mycobacterium tuberculosis* as it goes into a dormancy-like state in culture. Journal of bacteriology, 186(15), 5017-5030.

Dalton, T., Cegielski, P., Akksilp, S., Asencios, L., Caoili, J. C., Cho, S. N., ... & Kang, H. (2012). Prevalence of and risk factors for resistance to second-line drugs in people with multidrug-resistant tuberculosis in eight countries: a prospective cohort study. The Lancet, 380(9851), 1406-1417.

Davis, J. M., Clay, H., Lewis, J. L., Ghori, N., Herbomel, P., & Ramakrishnan, L. (2002). Real-time visualization of mycobacterium-macrophage interactions leading to initiation of granuloma formation in zebrafish embryos. Immunity, 17(6), 693-702.

De Chiara C., Homšak M., Prosser G. A., Douglas H. L., Garza-Garcia A., Kelly G., et al., (2020). D-Cycloserine destruction by alanine racemase and the limit of irreversible inhibition. Nat. Chem. Biol. 16, 686–694. 10.1038/s41589-020-0498-9

Deb, C., Lee, C. M., Dubey, V. S., Daniel, J., Abomoelak, B., Sirakova, T. D., ... & Kolattukudy, P. E. (2009). A novel in vitro multiple-stress dormancy model for *Mycobacterium tuberculosis* generates a lipid-loaded, drug-tolerant, dormant pathogen. PloS one, 4(6), e6077.

Dharmadhikari, A. S., & Nardell, E. A. (2008). What animal models teach humans about tuberculosis. *American journal of respiratory cell and molecular biology*, *39*(5), 503-508.

Dhillon, J., Fourie, P. B., & Mitchison, D. A. (2014). Persister populations of Mycobacterium tuberculosis in sputum that grow in liquid but not on solid culture media. *Journal of Antimicrobial Chemotherapy*, *69*(2), 437-440.

Dorman, C. J. (2004). H-NS: a universal regulator for a dynamic genome. Nature Reviews Microbiology, 2(5), 391-400.

Dorman C. J. (2007). H-NS, the genome sentinel. Nature reviews microbiology, 5(2), 157–161. https://doi.org/10.1038/nrmicro1598

Domenech P, Reed MB, Barry CE III (2005) Contribution of the *Mycobacterium tuberculosis* MmpL Protein Family to Virulence and Drug Resistance. Infect Immun 73: 3492–3501.

Dubos, R. and Dubos, J. (1952) The White Plague: Tuberculosis, Man, and Society. 3rd Edition, Little, Brown and Company, Boston.

Dusthackeer, A., Balasubramanian, M., Shanmugam, G., Priya, S., Nirmal, C. R., Sam Ebenezer, R., ... & Subbian, S. (2019). Differential culturability of Mycobacterium tuberculosis in culture-negative sputum of patients with pulmonary tuberculosis and in a simulated model of dormancy. *Frontiers in microbiology*, *10*, 2381.

Dziadek, B., Brzostek, A., Grzybowski, M., Fol, M., Krupa, A., Kryczka, J., ... & Dziadek, J. (2016). Mycobacterium tuberculosis AtsG (Rv0296c), GlmU (Rv1018c) and SahH (Rv3248c) proteins function as the human IL-8-binding effectors and contribute to pathogen entry into human neutrophils. *PLoS One*, *11*(2), e0148030.

Dutta, N. K., & Karakousis, P. C. (2014). Latent tuberculosis infection: myths, models, and molecular mechanisms. *Microbiology and Molecular Biology Reviews*, *78*(3), 343-371.

Dussurget, O., Rodriguez, M., & Smith, I. (1996). An ideR mutant of *Mycobacterium smegmatis* has derepressed siderophore production and an altered oxidative-stress response. Molecular microbiology, 22(3), 535-544.

Dziusmikeyeva, M., and Gorenok, D. (2012). Tuberculosis in immunocompromised hosts: Pathogenetic and pathologic peculiarities.

Ealand, C., Rimal, B., Chang, J., Mashigo, L., Chengalroyen, M., Mapela, L., ... & Kana, B. (2018). Resuscitation-promoting factors are required for *Mycobacterium smegmatis* biofilm formation. Applied and environmental microbiology, 84(17), e00687-18.

Ehrt, S., & Schnappinger, D. (2009). Mycobacterial survival strategies in the phagosome: defence against host stresses. *Cellular microbiology*, *11*(8), 1170-1178.

Elliot, M. A., & Flärdh, K. (2012). Streptomycete spores. eLS.

Esmail H, Barry CE, 3rd, Young DB, Wilkinson RJ. (2014). The ongoing challenge of latent tuberculosis. Phil Trans R Soc Lond B Biol Sci 369:20130437.

Essers, L., & Schoop, H. J. (1978). Evidence for the incorporation of molecular oxygen, a pathway in biosynthesis of N-glycolylmuramic acid in Mycobacterium phlei. *Biochimica et Biophysica Acta (BBA)-General Subjects*, *544*(1), 180-184.

Ezeamama, A. E., Mupere, E., Oloya, J., Martinez, L., Kakaire, R., Yin, X., ... & Whalen, C. C. (2015). Age, sex, and nutritional status modify the CD4+ T-cell recovery rate in HIV–tuberculosis co-infected patients on combination antiretroviral therapy. International Journal of Infectious Diseases, 35, 73-79.

Famelis, N., Rivera-Calzada, A., Degliesposti, G., Wingender, M., Mietrach, N., Skehel, J. M., ... & Geibel, S. (2019). Architecture of the mycobacterial type VII secretion system. *Nature*, *576*(7786), 321-325.

Faraj, A., Clewe, O., Svensson, R. J., Mukamolova, G. V., Barer, M. R., & Simonsson, U. S. (2020). Difference in persistent tuberculosis bacteria between in vitro and sputum from patients: implications for translational predictions. *Scientific Reports*, *10*(1), 1-10.

Firth, J. (2014). History of tuberculosis. *History*, *22*, 30-31.

Flynn, J. L., Capuano, S. V., Croix, D., Pawar, S., Myers, A., Zinovik, A., & Klein, E. (2003). Non-human primates: a model for tuberculosis research. Tuberculosis, 83(1-3), 116-118.

Foss, M. H., Pou, S., Davidson, P. M., Dunaj, J. L., Winter, R. W., Pou, S., ... & Purdy, G. E. (2016). Diphenylether-modified 1, 2-diamines with improved drug properties for development against Mycobacterium tuberculosis. *ACS infectious diseases*, *2*(7), 500-508.

Forbes, J. R., & Gros, P. (2001). Divalent-metal transport by NRAMP proteins at the interface of host–pathogen interactions. Trends in microbiology, 9(8), 397-403.

Fol, M., Chauhan, A., Nair, N. K., Maloney, E., Moomey, M., Jagannath, C., ... & Rajagopalan, M. (2006). Modulation of *Mycobacterium tuberculosis* proliferation by MtrA, an essential two-component response regulator. Molecular microbiology, 60(3), 643-657.

Frith, J.A. (2014). History of tuberculosis. Part 1 - phthisis, consumption and the white plague. Journal of Military and Veterans' Health, 22, 29-35.

Fränzel, B., Trötschel, C., Rückert, C., Kalinowski, J., Poetsch, A., & Wolters, D. A. (2010). Adaptation of Corynebacterium glutamicum to salt-stress conditions. *Proteomics*, *10*(3), 445-457.

Gao, H., Dai, W., Zhao, L., Min, J., & Wang, F. (2018). The role of zinc and zinc homeostasis in macrophage function. *Journal of immunology research*, *2018*.

Gardner, P. P., Daub, J., Tate, J. G., Nawrocki, E. P., Kolbe, D. L., Lindgreen, S., ... & Bateman, A. (2009). Rfam: updates to the RNA families database. *Nucleic acids research*, *37*(suppl_1), D136-D140.

Geiman, D. E., Kaushal, D., Ko, C., Tyagi, S., Manabe, Y. C., Schroeder, B. G., ... & Bishai, W. R. (2004). Attenuation of Late-Stage Disease in Mice Infected bythe *Mycobacterium tuberculosis* mutant lacking the SigF alternate sigma factor and identification of SigF-dependent genes by microarray analysis. Infection and immunity, 72(3), 1733-1745.

Gillespie, J., Barton, L. L., & Rypka, E. W. (1986). Phenotypic changes in mycobacteria grown in oxygen-limited conditions. Journal of medical microbiology, 21(3), 251-255.

Girardin, S. E., Travassos, L. H., Hervé, M., Blanot, D., Boneca, I. G., Philpott, D. J., ... & Mengin-Lecreulx, D. (2003). Peptidoglycan molecular requirements allowing detection by Nod1 and Nod2. Journal of Biological Chemistry, 278(43), 41702-41708.

Glenn, S. M., Gap-Gaupool, B., Waddell, S. J., Bacon, J., Crosatti, M., Hincks, J., ... & Mukamolova, G. V. (2021). Exposure to nitric oxide drives transition to resuscitation-promoting factor-dependency in mycobacteria. bioRxiv.

Glickman, M. S., Cox, J. S., & Jacobs Jr, W. R. (2000). A novel mycolic acid cyclopropane synthetase is required for cording, persistence, and virulence of Mycobacterium tuberculosis. *Molecular cell*, *5*(4), 717-727.

Goethe, E., Laarmann, K., Lührs, J., Jarek, M., Meens, J., Lewin, A., & Goethe, R. (2020). Critical role of Zur and SmtB in zinc homeostasis of Mycobacterium smegmatis. *MSystems*, *5*(2), e00880-19.

Gordhan, B. G., Peters, J. S., McIvor, A., Machowski, E. E., Ealand, C., Waja, Z., ... & Kana, B. D. (2021). Detection of differentially culturable tubercle bacteria in sputum using mycobacterial culture filtrates. *Scientific reports*, *11*(1), 1-11.

Gordon, B. R., Li, Y., Wang, L., Sintsova, A., Van Bakel, H., Tian, S., ... & Liu, J. (2010). Lsr2 is a nucleoid-associated protein that targets AT-rich sequences and virulence genes in Mycobacterium tuberculosis. Proceedings of the National Academy of Sciences, 107(11), 5154-5159.

Gorla, P., Plocinska, R., Sarva, K., Satsangi, A. T., Pandeeti, E., Donnelly, R., ... & Madiraju, M. V. (2018). MtrA response regulator controls cell division and cell wall metabolism and affects susceptibility of mycobacteria to the first line antituberculosis drugs. Frontiers in microbiology, 9, 2839.

Gosset, G., Zhang, Z., Nayyar, S., Cuevas, W. A., & Saier Jr, M. H. (2004). Transcriptome analysis of Crp-dependent catabolite control of gene expression in *Escherichia coli*. Journal of bacteriology, 186(11), 3516-3524.

Gundlach, J., Herzberg, C., Kaever, V., Gunka, K., Hoffmann, T., Weiß, M., Gibhardt, J., Thürmer, A., Hertel, D., Daniel, R., Bremer, E., Commichau, F. M., & Stülke, J. (2017). Control of potassium homeostasis is an essential function of the second messenger cyclic di-AMP in *Bacillus subtilis*. Science signaling, 10(475), eaal3011. https://doi.org/10.1126/scisignal.aal3011

Gundlach, J., Krüger, L., Herzberg, C., Turdiev, A., Poehlein, A., Tascón, I., ... & Stülke, J. (2019). Sustained sensing in potassium homeostasis: Cyclic di-AMP controls potassium uptake by KimA at the levels of expression and activity. Journal of Biological Chemistry, 294(24), 9605-9614.

Gupta, R. K., Srivastava, B. S., & Srivastava, R. (2010). Comparative expression analysis of rpf-like genes of *Mycobacterium tuberculosis* H37Rv under different physiological stress and growth conditions. Microbiology, 156(9), 2714-2722.

Green, J., Scott, C., & Guest, J. R. (2001). Functional versatility in the CRP-FNR superfamily of transcription factors: FNR and FLP.

Grigg, E. R. N. (1958). The Arcana of Tuberculosis. With a Brief Epidemiologic History of the Disease in the USA: Parts I and II. American Review of Tuberculosis and Pulmonary Diseases, 78(2), 151-172.

Grosset, J. (2003). *Mycobacterium tuberculosis* in the extracellular compartment: an underestimated adversary. Antimicrobial agents and chemotherapy, 47(3), 833-836.

Haiser, H. J., Yousef, M. R., & Elliot, M. A. (2009). Cell wall hydrolases affect germination, vegetative growth, and sporulation in *Streptomyces coelicolor*. Journal of bacteriology, 191(21), 6501–6512. https://doi.org/10.1128/JB.00767-09

Hall-Stoodley, L., Brun, O. S., Polshyna, G., & Barker, L. P. (2006). Mycobacterium marinum biofilm formation reveals cording morphology. *FEMS microbiology letters*, *257*(1), 43-49.

Hayman J. (1984). *Mycobacterium ulcerans*: an infection from Jurassic time?. Lancet (London, England), 2(8410), 1015–1016. https://doi.org/10.1016/s0140-6736(84)91110-3

Hatzios, S. K., Baer, C. E., Rustad, T. R., Siegrist, M. S., Pang, J. M., Ortega, C., ... & Bertozzi, C. R. (2013). Osmosensory signaling in *Mycobacterium tuberculosis* mediated by a eukaryotic-like Ser/Thr protein kinase. Proceedings of the National Academy of Sciences, 110(52), E5069-E5077.

Harper, J., Skerry, C., Davis, S. L., Tasneen, R., Weir, M., Kramnik, I., ... & Jain, S. K. (2012). Mouse model of necrotic tuberculosis granulomas develops hypoxic lesions. Journal of Infectious Diseases, 205(4), 595-602.

Harriff, M. J., Cansler, M. E., Toren, K. G., Canfield, E. T., Kwak, S., Gold, M. C., & Lewinsohn, D. M. (2014). Human lung epithelial cells contain *Mycobacterium tuberculosis* in a late endosomal vacuole and are efficiently recognized by CD8+ T cells. PloS one, 9(5), e97515.

Hartmann, M., Barsch, A., Niehaus, K., Pühler, A., Tauch, A., & Kalinowski, J. (2004). The glycosylated cell surface protein Rpf2, containing a resuscitation-promoting factor motif, is involved in intercellular communication of *Corynebacterium glutamicum*. Archives of microbiology, 182(4), 299-312.

Herlihey, F. A., & Clarke, A. J. (2016). Controlling autolysis during flagella insertion in Gram-negative bacteria. *Protein Reviews*, 41-56.

Hernandez-Pando, R., Jeyanathan, M., Mengistu, G., Aguilar, D., Orozco, H., Harboe, M., ... & Bjune, G. (2000). Persistence of DNA from *Mycobacterium tuberculosis* in superficially normal lung tissue during latent infection. The Lancet, 356(9248), 2133-2138.

Hett, E. C., Chao, M. C., Steyn, A. J., Fortune, S. M., Deng, L. L., & Rubin, E. J. (2007). A partner for the resuscitation-promoting factors of Mycobacterium tuberculosis. *Molecular microbiology*, *66*(3), 658-668.

Houben, R. M., & Dodd, P. J. (2016). The global burden of latent tuberculosis infection: a re-estimation using mathematical modelling. PLoS medicine, 13(10), e1002152.

Honeyborne, I., McHugh, T. D., Kuittinen, I., Cichonska, A., Evangelopoulos, D., Ronacher, K., ... & Waddell, S. J. (2016). Profiling persistent tubercule bacilli from patient sputa during therapy predicts early drug efficacy. BMC medicine, 14(1), 1-13.

Honaker, R. W., Leistikow, R. L., Bartek, I. L., & Voskuil, M. I. (2009). Unique roles of DosT and DosS in DosR regulon induction and *Mycobacterium tuberculosis* dormancy. Infection and immunity, 77(8), 3258-3263.

Hoffmann T., Bremer E. (2016). “Management of osmotic stress by *Bacillus subtilis*: genetics and physiology,” in *Stress and Environmental Regulation of Gene Expression and Adaptation in Bacteria*, ed. de Bruijn F. J. (Hoboken, NJ: Wiley-Blackwell Publishers;), 657–676.

Hoffmann, T., & Bremer, E. (2017). Guardians in a stressful world: the Opu family of compatible solute transporters from Bacillus subtilis. *Biological chemistry*, *398*(2), 193-214.

Hornung, R., Grünberger, A., Westerwalbesloh, C., Kohlheyer, D., Gompper, G., & Elgeti, J. (2018). Quantitative modelling of nutrient-limited growth of bacterial colonies in microfluidic cultivation. *Journal of the Royal Society Interface*, *15*(139), 20170713.

Hoshino, Y., Nakata, K., Hoshino, S., Honda, Y., Tse, D. B., Shioda, T., ... & Weiden, M. (2002). Maximal HIV-1 replication in alveolar macrophages during tuberculosis requires both lymphocyte contact and cytokines. *The Journal of experimental medicine*, *195*(4), 495-505.

Hoshino, Y., Hoshino, S., Gold, J. A., Raju, B., Prabhakar, S., Pine, R., ... & Weiden, M. (2007). Mechanisms of Polymorphonuclear Neutrophil—Mediated Induction of HIV-1 Replication in Macrophages during Pulmonary Tuberculosis. *The Journal of infectious diseases*, *195*(9), 1303-1310.

Hofer, A. M., & Lefkimmiatis, K. (2007). Extracellular calcium and cAMP: second messengers as “third messengers”?. *Physiology*, *22*(5), 320-327.

Huang, W., Qi, Y., Diao, Y., Yang, F., Zha, X., Ren, C., ... & Shen, J. (2014). Use of resuscitation-promoting factor proteins improves the sensitivity of culture-based tuberculosis testing in special samples. American journal of respiratory and critical care medicine, 189(5), 612-614.

Imboden, P., & Schoolnik, G. K. (1998). Construction and characterization of a partial Mycobacterium tuberculosis cDNA library of genes expressed at reduced oxygen tension. Gene, 213(1-2), 107-117.

Indrigo, J., Hunter, R. L., & Actor, J. K. (2003). Cord factor trehalose 6,6'-dimycolate (TDM) mediates trafficking events during mycobacterial infection of murine macrophages. *Microbiology (Reading, England)*, *149*(Pt 8), 2049–2059. https://doi.org/10.1099/mic.0.26226-0

Ishizuka, H., Hanamura, A., Kunimura, T., & Aiba, H. (1993). A lowered concentration of cAMP receptor protein caused by glucose is an important determinant for catabolite repression in Escherichia coli. *Molecular microbiology*, *10*(2), 341-350.

Jankute, M., Cox, J. A., Harrison, J., & Besra, G. S. (2015). Assembly of the mycobacterial cell wall. *Annual review of microbiology*, *69*, 405-423.

Jernigan, J. A., & Farr, B. M. (2000). Incubation period and sources of exposure for cutaneous Mycobacterium marinum infection: case report and review of the literature. *Clinical infectious diseases*, *31*(2), 439-443.

Jesse, H. E., Roberts, I. S., & Cavet, J. S. (2014). Metal ion homeostasis in Listeria monocytogenes and importance in host–pathogen interactions. *Advances in microbial physiology*, *65*, 83-123.
Hansen, J. M., Golchin, S. A., Veyrier, F. J., Domenech, P., Boneca, I. G., Azad, A. K., ... & Behr, M. A. (2014). N-glycolylated peptidoglycan contributes to the immunogenicity but not pathogenicity of Mycobacterium tuberculosis. *The Journal of infectious diseases*, *209*(7), 1045-1054.

Johnson, J. W., Fisher, J. F., & Mobashery, S. (2013). Bacterial cell-wall recycling. *Annals of the New York Academy of Sciences*, *1277*(1), 54-75.

Kahramanoglou, C., Cortes, T., Matange, N., Hunt, D. M., Visweswariah, S. S., Young, D. B., & Buxton, R. S. (2014). Genomic mapping of cAMP receptor protein (CRPMt) in Mycobacterium tuberculosis: relation to transcriptional start sites and the role of CRPMt as a transcription factor. *Nucleic acids research*, *42*(13), 8320-8329.

Kai, M., Haustein, M., Molina, F., Petri, A., Scholz, B., & Piechulla, B. (2009). Bacterial volatiles and their action potential. *Applied microbiology and biotechnology*, *81*(6), 1001-1012.

Kalivoda, E. J., Brothers, K. M., Stella, N. A., Schmitt, M. J., & Shanks, R. M. (2013). Bacterial cyclic AMP-phosphodiesterase activity coordinates biofilm formation. *PLoS One*, *8*(7), e71267.

Kana, B. D., Gordhan, B. G., Downing, K. J., Sung, N., Vostroktunova, G., Machowski, E. E., ... & Mizrahi, V. (2008). The resuscitation-promoting factors of Mycobacterium tuberculosis are required for virulence and resuscitation from dormancy but are collectively dispensable for growth in vitro. *Molecular microbiology*, *67*(3), 672-684.

Kana, B. D., & Mizrahi, V. (2010). Resuscitation-promoting factors as lytic enzymes for bacterial growth and signaling. *FEMS Immunology & Medical Microbiology*, *58*(1), 39-50.

Kang, C. M., Abbott, D. W., Park, S. T., Dascher, C. C., Cantley, L. C., & Husson, R. N. (2005). The *Mycobacterium tuberculosis* serine/threonine kinases PknA and PknB: substrate identification and regulation of cell shape. Genes & development, 19(14), 1692-1704.

Kaprelyants, A. S., Gottschal, J. C., & Kell, D. B. (1993). Dormancy in non-sporulating bacteria. *FEMS microbiology letters*, *104*(3-4), 271-285.

Katayama, T., Kato, T., Tanaka, M., Douglas, T. A., Brouchkov, A., Abe, A., ... & Asano, K. (2010). Tomitella biformata gen. nov., sp. nov., a new member of the suborder Corynebacterineae isolated from a permafrost ice wedge. *International journal of systematic and evolutionary microbiology*, *60*(12), 2803-2807.

Kell, D. B., & Young, M. (2000). Bacterial dormancy and culturability: the role of autocrine growth factors. Current opinion in microbiology, 3(3), 238-243.

Keep, N. H., Ward, J. M., Cohen-Gonsaud, M., & Henderson, B. (2006). Wake up! Peptidoglycan lysis and bacterial non-growth states. Trends in microbiology, 14(6), 271-276.

Kesavan, A. K., Brooks, M., Tufariello, J., Chan, J., & Manabe, Y. C. (2009). Tuberculosis genes expressed during persistence and reactivation in the resistant rabbit model. *Tuberculosis*, *89*(1), 17-21.

Kim M. G., Strych U., Krause K., Benedik M., Kohn H. (2003). N (2)-substituted D, L-cycloserine derivatives. J. Antibiot. 56, 160–168. 10.7164/antibiotics.56.160

Kondratieva, T., Rubakova, E., Kana, B. D., Biketov, S., Potapov, V., Kaprelyants, A., & Apt, A. (2011). Mycobacterium tuberculosis attenuated by multiple deletions of rpf genes effectively protects mice against TB infection. Tuberculosis, 91(3), 219-223.

Koraimann, G. (2003). Lytic transglycosylases in macromolecular transport systems of Gram-negative bacteria. *Cellular and Molecular Life Sciences CMLS*, *60*(11), 2371-2388.

Kouidmi, I., Levesque, R. C., & Paradis-Bleau, C. (2014). The biology of Mur ligases as an antibacterial target. *Molecular microbiology*, *94*(2), 242-253.

Kotani, S., Yanagida, I., Kato, K., & Matsuda, T. (1970). Studies on peptides, glycopeptides and antigenic polysaccharide-glycopeptide complexes isolated from an L-11 enzyme lysate of the cell walls of Mycobacterium tuberculosis strain H37Rv. *Biken journal: journal of Research Institute for Microbial Diseases*, *13*(4), 249-275.

Kumawat, K., Pathak, S. K., Spetz, A. L., Kundu, M., & Basu, J. (2010). Exogenous Nef is an inhibitor of Mycobacterium tuberculosis-induced tumor necrosis factor-α production and macrophage apoptosis. *Journal of Biological Chemistry*, *285*(17), 12629-12637.

Krause, A. K. (1928). Tuberculosis and public health. American Review of Tuberculosis, 18(3), 271-322.

Krämer, R. (2010). Bacterial stimulus perception and signal transduction: response to osmotic stress. The Chemical Record, 10(4), 217-229.

Körner, H., Sofia, H. J., & Zumft, W. G. (2003). Phylogeny of the bacterial superfamily of Crp-Fnr transcription regulators: exploiting the metabolic spectrum by controlling alternative gene programs. FEMS microbiology reviews, 27(5), 559-592.

Larrouy-Maumus, G., Marino, L. B., Madduri, A. V., Ragan, T. J., Hunt, D. M., Bassano, L., ... & De Carvalho, L. P. S. (2016). Cell-envelope remodeling as a determinant of phenotypic antibacterial tolerance in Mycobacterium tuberculosis. *ACS infectious diseases*, *2*(5), 352-360.

La Rosa, V., Poce, G., Canseco, J. O., Buroni, S., Pasca, M. R., Biava, M., ... & De Rossi, E. (2012). MmpL3 is the cellular target of the antitubercular pyrrole derivative BM212. *Antimicrobial agents and chemotherapy*, *56*(1), 324-331.

Landis, L., Xu, J., & Johnson, R. C. (1999). The cAMP receptor protein CRP can function as an osmoregulator of transcription in Escherichia coli. Genes & development, 13(23), 3081–3091. https://doi.org/10.1101/gad.13.23.3081

Lee, J. J., Lee, S. K., Song, N., Nathan, T. O., Swarts, B. M., Eum, S. Y., ... & Eoh, H. (2019). Transient drug-tolerance and permanent drug-resistance rely on the trehalose-catalytic shift in Mycobacterium tuberculosis. Nature communications, 10(1), 1-12.

Leistikow, R. L., Morton, R. A., Bartek, I. L., Frimpong, I., Wagner, K., & Voskuil, M. I. (2010). The Mycobacterium tuberculosis DosR regulon assists in metabolic homeostasis and enables rapid recovery from nonrespiring dormancy. Journal of bacteriology, 192(6), 1662-1670.

Lin, C. T., Chen, Y. C., Jinn, T. R., Wu, C. C., Hong, Y. M., & Wu, W. H. (2013). Role of the cAMP-dependent carbon catabolite repression in capsular polysaccharide biosynthesis in Klebsiella pneumoniae. *PLoS One*, *8*(2), e54430.

Loebel, R. O., Shorr, E., & Richardson, H. B. (1933a). The influence of foodstuffs upon the respiratory metabolism and growth of human tubercle bacilli. *Journal of bacteriology*, *26*(2), 139-166.

Loebel, R. O., Shorr, E., & Richardson, H. B. (1933b). The influence of adverse conditions upon the respiratory metabolism and growth of human tubercle bacilli. *Journal of bacteriology*, *26*(2), 167-200.

Loraine J, Pu F, Turapov O, Mukamolova GV. (2016). Development of an *in vitro* assay for detection of drug-induced resuscitation-promoting-factor-dependent mycobacteria. Antimicrob Agents Chemother. 60(10):6227-33.

Lurie, M. B., Abramson, S., & Heppleston, A. G. (1952). On the response of genetically resistant and susceptible rabbits to the quantitative inhalation of human type tubercle

bacilli and the nature of resistance to tuberculosis. The Journal of Experimental Medicine, 95(2), 119.

Machowski, E. E., Senzani, S., Ealand, C., & Kana, B. D. (2014). Comparative genomics for mycobacterial peptidoglycan remodelling enzymes reveals extensive genetic multiplicity. *BMC microbiology*, *14*(1), 1-12.

Mahapatra, S., Crick, D. C., McNeil, M. R., & Brennan, P. J. (2008). Unique structural features of the peptidoglycan of Mycobacterium leprae. *Journal of bacteriology*, *190*(2), 655-661.

Mandal, M., & Breaker, R. R. (2004). Gene regulation by riboswitches. Nature reviews Molecular cell biology, 5(6), 451-463.

Manzanillo, P. S., Shiloh, M. U., Portnoy, D. A., & Cox, J. S. (2012). Mycobacterium tuberculosis activates the DNA-dependent cytosolic surveillance pathway within macrophages. Cell host & microbe, 11(5), 469-480.

Manina, G., Dhar, N., & McKinney, J. D. (2015). Stress and host immunity amplify Mycobacterium tuberculosis phenotypic heterogeneity and induce nongrowing metabolically active forms. Cell host & microbe, 17(1), 32-46.

Major, R. H. (1932). Diseases of the circulatory system. *Classic Descriptions of Disease*, 417.

Major, R. H. (1945). *Classic descriptions of disease: with biographical sketches of the authors*. Charles C Thomas Pub Limited.

Mattow, J., Jungblut, P. R., Schaible, U. E., Mollenkopf, H. J., Lamer, S., Zimny-Arndt, U., ... & Kaufmann, S. H. (2001). Identification of proteins from Mycobacterium tuberculosis missing in attenuated Mycobacterium bovis BCG strains. Electrophoresis, 22(14), 2936-2946.

Maulitz, R. C., & Maulitz, S. R. (1973). The king's evil in Oxfordshire. *Medical history*, *17*(1), 87-89.

McCarter, Y. S., I. N. Ratkiewicz, and A. Robinson. (1998). Cord formation in BACTEC medium is a reliable, rapid method for presumptive identification of *Mycobacterium tuberculosis* complex. J. Clin. Microbiol. **36**2769-2771

McCUNE Jr, R. M., Tompsett, R., & McDermott, W. (1956). The fate of Mycobacterium tuberculosis in mouse tissues as determined by the microbial enumeration technique: II. The conversion of tuberculous infection to the latent state by the administration of pyrazinamide and a companion drug. The Journal of experimental medicine, 104(5), 763-802.

McCUNE, R. M., Feldmann, F. M., Lambert, H. P., & McDermott, W. (1966). Microbial persistence: I. The capacity of tubercle bacilli to survive sterilization in mouse tissues. *The Journal of experimental medicine*, *123*(3), 445-468.

Meachen, G. N. (1936). A Short History of Tuberculosis. *A Short History of Tuberculosis.*

Meldrum, R. J., Brocklehurst, T. F., Wilson, D. R., & Wilson, P. D. G. (2003). The effects of cell immobilization, pH and sucrose on the growth of Listeria monocytogenes Scott A at 10 C. Food Microbiology, 20(1), 97-103.

Mello Filho, A. C., Hoffmann, M. E., & Meneghini, R. (1984). Cell killing and DNA damage by hydrogen peroxide are mediated by intracellular iron. Biochemical Journal, 218(1), 273.

Miles, A. A., Misra, S. S., & Irwin, J. O. (1938). The estimation of the bactericidal power of the blood. *Epidemiology & Infection*, *38*(6), 732-749.

Misra, R., Menon, D., Arora, G., Virmani, R., Gaur, M., Naz, S., ... & Singh, Y. (2019). Tuning the Mycobacterium tuberculosis alternative sigma factor sigf through the multidomain regulator Rv1364c and osmosensory kinase protein Kinase D. *Journal of bacteriology*, *201*(7), e00725-18.

Morgenthau, A., Pogoutse, A., Adamiak, P., Moraes, T. F., & Schryvers, A. B. (2013). Bacterial receptors for host transferrin and lactoferrin: molecular mechanisms and role in host–microbe interactions. Future Microbiology, 8(12), 1575-1585.

Morris, B. E., Henneberger, R., Huber, H., & Moissl-Eichinger, C. (2013). Microbial syntrophy: interaction for the common good. FEMS microbiology reviews, 37(3), 384–406. https://doi.org/10.1111/1574-6976.12019

Mukamolova, G. V., Kaprelyants, A. S., Young, D. I., Young, M., & Kell, D. B. (1998a). A bacterial cytokine. Proceedings of the National Academy of Sciences of the United States of America, 95(15), 8916–8921. https://doi.org/10.1073/pnas.95.15.8916

Mukamolova, G. V., Yanopolskaya, N. D., Kell, D. B., & Kaprelyants, A. S. (1998b). On resuscitation from the dormant state of Micrococcus luteus. Antonie Van Leeuwenhoek, 73(3), 237-243.

Mukamolova, G. V., Kormer, S. S., Kell, D. B., & Kaprelyants, A. S. (1999). Stimulation of the multiplication of Micrococcus luteus by an autocrine growth factor. Archives of microbiology, 172(1), 9-14.

Mukamolova, G. V., Turapov, O. A., Young, D. I., Kaprelyants, A. S., Kell, D. B., & Young, M. (2002). A family of autocrine growth factors in Mycobacterium tuberculosis. Molecular microbiology, 46(3), 623-635.

Mukamolova, G. V., Kaprelyants, A. S., Kell, D. B., & Young, M. (2003). Adoption of the transiently non-culturable state--a bacterial survival strategy?. Advances in microbial physiology, 47, 65–129. https://doi.org/10.1016/s0065-2911(03)47002-1

Mukamolova, G. V., Murzin, A. G., Salina, E. G., Demina, G. R., Kell, D. B., Kaprelyants, A. S., & Young, M. (2006). Muralytic activity of Micrococcus luteus Rpf and its relationship to physiological activity in promoting bacterial growth and resuscitation. Molecular microbiology, 59(1), 84-98.

Mukamolova, G. V., Turapov, O., Malkin, J., Woltmann, G., & Barer, M. R. (2010). Resuscitation-promoting factors reveal an occult population of tubercle bacilli in sputum. American journal of respiratory and critical care medicine, 181(2), 174-180.

Muttucumaru, D. N., Roberts, G., Hinds, J., Stabler, R. A., & Parish, T. (2004). Gene expression profile of Mycobacterium tuberculosis in a non-replicating state. Tuberculosis, 84(3-4), 239-246.

Morse, D., Brothwell, D. R., & Ucko, P. J. (1964). Tuberculosis in ancient Egypt. *American Review of Respiratory Disease*, *90*(4), 524-541.

Nelson, J. W., Sudarsan, N., Furukawa, K., Weinberg, Z., Wang, J. X., & Breaker, R. R. (2013). Riboswitches in eubacteria sense the second messenger c-di-AMP. Nature chemical biology, 9(12), 834-839.

Neyrolles, O., Hernández-Pando, R., Pietri-Rouxel, F., Fornès, P., Tailleux, L., Payán, J. A. B., ... & Gicquel, B. (2006). Is adipose tissue a place for Mycobacterium tuberculosis persistence?. PloS one, 1(1), e43.

Nerlich, A. G., Haas, C. J., Zink, A., Szeimies, U., & Hagedorn, H. G. (1997). Molecular evidence for tuberculosis in an ancient Egyptian mummy. *The Lancet*, *350*(9088), 1404.

Nikitushkin, V. D., Demina, G. R., Shleeva, M. O., & Kaprelyants, A. S. (2013). Peptidoglycan fragments stimulate resuscitation of “non-culturable” mycobacteria. *Antonie Van Leeuwenhoek*, *103*(1), 37-46.

Pavlova, N., & Penchovsky, R. (2019). Genome-wide bioinformatics analysis of FMN, SAM-I, glmS, TPP, lysine, purine, cobalamin, and SAH riboswitches for their applications as allosteric antibacterial drug targets in human pathogenic bacteria. *Expert opinion on therapeutic targets*, *23*(7), 631-643.

Nicolas, P., Mäder, U., Dervyn, E., Rochat, T., Leduc, A., Pigeonneau, N., ... & Noirot, P. (2012). Condition-dependent transcriptome reveals high-level regulatory architecture in Bacillus subtilis. *Science*, *335*(6072), 1103-1106.

Nguyen, H. T., Wolff, K. A., Cartabuke, R. H., Ogwang, S., & Nguyen, L. (2010). A lipoprotein modulates activity of the MtrAB two-component system to provide intrinsic multidrug resistance, cytokinetic control and cell wall homeostasis in Mycobacterium. Molecular microbiology, 76(2), 348-364.

Ordas, A., Raterink, R. J., Cunningham, F., Jansen, H. J., Wiweger, M. I., Jong-Raadsen, S., ... & Spaink, H. P. (2015). Testing tuberculosis drug efficacy in a zebrafish high-throughput translational medicine screen. Antimicrobial agents and chemotherapy, 59(2), 753-762.

Pal, A. K., & Ghosh, A. (2022). c-di-AMP signaling plays important role in determining antibiotic tolerance phenotypes of *Mycobacterium smegmatis*. Scientific reports, 12(1), 13127. https://doi.org/10.1038/s41598-022-17051-z

Pinto, D., Sao-Jose, C., Santos, M. A., & Chambel, L. (2013). Characterization of two resuscitation promoting factors of Listeria monocytogenes. *Microbiology*, *159*(Pt_7), 1390-1401.

Patel, N. R., Zhu, J., Tachado, S. D., Zhang, J., Wan, Z., Saukkonen, J., & Koziel, H. (2007). HIV impairs TNF-α mediated macrophage apoptotic response to Mycobacterium tuberculosis. *The Journal of Immunology*, *179*(10), 6973-6980.

Patel, H. M., Palkar, M., & Karpoormath, R. (2020). Exploring MDR-TB Inhibitory Potential of 4-Aminoquinazolines as Mycobacterium tuberculosis N-Acetylglucosamine-1-Phosphate Uridyltransferase (GlmUMTB) Inhibitors. *Chemistry & Biodiversity*, *17*(8), e2000237.

Pastan, I., & Perlman, R. (1970). Cyclic Adenosine Monophosphate in Bacteria: In many bacteria the synthesis of inducible enzymes requires this cyclic nucleotide. *Science*, *169*(3943), 339-344.

Plocinska R., Purushotham G., Sarva K., Vadrevu I. S., Pandeeti E. V., Arora N., et al., (2012). Septal localization of the *Mycobacterium tuberculosis* MtrB sensor kinase promotes MtrA regulon expression. *J. Biol. Chem.* 287 23887–23899.

Provvedi, R., Boldrin, F., Falciani, F., Palu, G., & Manganelli, R. (2009). Global transcriptional response to vancomycin in Mycobacterium tuberculosis. *Microbiology*, *155*(4), 1093-1102

Rath, H., Reder, A., Hoffmann, T., Hammer, E., Seubert, A., Bremer, E., Völker, U., & Mäder, U. (2020). Management of Osmoprotectant Uptake Hierarchy in *Bacillus subtilis* via a SigB-Dependent Antisense RNA. *Frontiers in microbiology*, *11*, 622. https://doi.org/10.3389/fmicb.2020.00622

Raymond, J. B., Mahapatra, S., Crick, D. C., & Pavelka, M. S. (2005). Identification of the namH gene, encoding the hydroxylase responsible for the N-glycolylation of the mycobacterial peptidoglycan. *Journal of Biological Chemistry*, *280*(1), 326-333.

Reith, J., & Mayer, C. (2011). Peptidoglycan turnover and recycling in Gram-positive bacteria. *Applied microbiology and biotechnology*, *92*(1), 1-11.

Parikka, M., Hammaren, M. M., Harjula, S. K. E., Halfpenny, N. J., Oksanen, K. E., Lahtinen, M. J., ... & Rämet, M. (2012). *Mycobacterium marinum* causes a latent infection that can be reactivated by gamma irradiation in adult zebrafish.

Parish, T., & Stoker, N. G. (2000). Use of a flexible cassette method to generate a double unmarked *Mycobacterium tuberculosis tlyA plcABC* mutant by gene replacement. Microbiology, 146(8), 1969-1975.

Parish, T., Smith, D. A., Kendall, S., Casali, N., Bancroft, G. J., & Stoker, N. G. (2003). Deletion of two-component regulatory systems increases the virulence of *Mycobacterium tuberculosis*. Infection and immunity, 71(3), 1134-1140.

Parrish, N. M., Dick, J. D., & Bishai, W. R. (1998). Mechanisms of latency in Mycobacterium tuberculosis. Trends in microbiology, 6(3), 107-112.

Pawlowski, A., Jansson, M., Sköld, M., Rottenberg, M. E., & Källenius, G. (2012). Tuberculosis and HIV co-infection. PLoS pathogens, 8(2), e1002464.

Price, C. T., Bukka, A., Cynamon, M., & Graham, J. E. (2008). Glycine betaine uptake by the ProXVWZ ABC transporter contributes to the ability of *Mycobacterium tuberculosis* to initiate growth in human macrophages. Journal of bacteriology, 190(11), 3955-3961.

Rohde, K. H., Abramovitch, R. B., & Russell, D. G. (2007). Mycobacterium tuberculosis invasion of macrophages: linking bacterial gene expression to environmental cues. Cell host & microbe, 2(5), 352-364.

Prouty, M. G., Correa, N. E., Barker, L. P., Jagadeeswaran, P., & Klose, K. E. (2003). Zebrafish-*Mycobacterium marinum* model for mycobacterial pathogenesis. FEMS Microbiology Letters, 225(2), 177-182.

Rajagopalan, M., Dziedzic, R., Al Zayer, M., Stankowska, D., Ouimet, M. C., Bastedo, D. P., ... & Madiraju, M. V. (2010). *Mycobacterium tuberculosis* origin of replication and the promoter for immunodominant secreted antigen 85B are the targets of MtrA, the essential response regulator. Journal of Biological Chemistry, 285(21), 15816-15827.

Pang, X., Vu, P., Byrd, T. F., Ghanny, S., Soteropoulos, P., Mukamolova, G. V., ... & Howard, S. T. (2007). Evidence for complex interactions of stress-associated regulons in an mprAB deletion mutant of Mycobacterium tuberculosis. *Microbiology*, *153*(4), 1229-1242.

Ratledge, C. (2004). Iron, mycobacteria and tuberculosis. Tuberculosis, 84(1-2), 110-130.

Ravagnani, A., Finan, C. L., & Young, M. (2005). A novel firmicute protein family related to the actinobacterial resuscitation-promoting factors by non-orthologous domain displacement. BMC genomics, 6(1), 1-14.

Rebollo-Ramirez, S., & Larrouy-Maumus, G. (2019). NaCl triggers the CRP-dependent increase of cAMP in Mycobacterium tuberculosis. Tuberculosis, 116, 8-16.

Ren, A., & Patel, D. J. (2014). c-di-AMP binds the *ydaO* riboswitch in two pseudo-symmetry-related pockets. Nature chemical biology, 10(9), 780–786. https://doi.org/10.1038/nchembio.1606

Richards, J., & Belasco, J. G. (2021). Riboswitch control of bacterial RNA stability. Molecular microbiology, 116(2), 361–365. https://doi.org/10.1111/mmi.14723

Rickman, L., Scott, C., Hunt, D. M., Hutchinson, T., Menéndez, M. C., Whalan, R., ... & Buxton, R. S. (2005). A member of the cAMP receptor protein family of transcription regulators in *Mycobacterium tuberculosis* is required for virulence in mice and controls

transcription of the rpfA gene coding for a resuscitation promoting factor. Molecular microbiology, 56(5), 1274-1286.

Rodriguez, G. M., Voskuil, M. I., Gold, B., Schoolnik, G. K., & Smith, I. (2002). ideR, an essential gene in *Mycobacterium tuberculosis*: role of IdeR in iron-dependent gene expression, iron metabolism, and oxidative stress response. Infection and immunity, 70(7), 3371-3381.

Rogers HJ, Perkins HR & Ward JB (1980) Microbial Cell Walls and Membranes, Chapman and Hall, London.

Rosser, A., Stover, C., Pareek, M., & Mukamolova, G. V. (2017). Resuscitation-promoting factors are important determinants of the pathophysiology in *Mycobacterium tuberculosis* infection. Critical reviews in microbiology, 43(5), 621-630.

Roth, A., & Breaker, R. R. (2009). The structural and functional diversity of metabolite-binding riboswitches. Annual review of biochemistry, 78, 305–334. https://doi.org/10.1146/annurev.biochem.78.070507.135656

Roychowdhury, A., Wolfert, M. A., & Boons, G. J. (2005). Synthesis and proinflammatory properties of muramyl tripeptides containing lysine and diaminopimelic acid moieties. ChemBioChem, 6(11), 2088-2097.

Provvedi, R., Boldrin, F., Falciani, F., Palu, G., & Manganelli, R. (2009). Global transcriptional response to vancomycin in *Mycobacterium tuberculosis*. Microbiology, 155(4), 1093-1102.

Ruggiero, A., Tizzano, B., Pedone, E., Pedone, C., Wilmanns, M., & Berisio, R. (2009). Crystal structure of the resuscitation-promoting factor ΔDUFRpfB from *M. tuberculosis.* Journal of molecular biology, 385(1), 153-162.

Russell, D. G. (2003). Phagosomes, fatty acids and tuberculosis. Nature cell biology, 5(9), 776-778.

Russell-Goldman, E., Xu, J., Wang, X., Chan, J., & Tufariello, J. M. (2008). A Mycobacterium tuberculosis Rpf double-knockout strain exhibits profound defects in reactivation from chronic tuberculosis and innate immunity phenotypes. *Infection and immunity*, *76*(9), 4269-4281.

Rustad, T. R., Harrell, M. I., Liao, R., & Sherman, D. R. (2008). The enduring hypoxic response of *Mycobacterium tuberculosis.* PloS one, 3(1), e1502.

Saha, M., Sarkar, S., Sarkar, B., Sharma, B. K., Bhattacharjee, S., & Tribedi, P. (2016). Microbial siderophores and their potential applications: a review. Environmental Science and Pollution Research, 23(5), 3984-3999.

Salo, W. L., Aufderheide, A. C., Buikstra, J., & Holcomb, T. A. (1994). Identification of Mycobacterium tuberculosis DNA in a pre-Columbian Peruvian mummy. Proceedings of the National Academy of Sciences of the United States of America, 91(6), 2091–2094. https://doi.org/10.1073/pnas.91.6.2091

Salina, E. G., Grigorov, A. S., Bychenko, O. S., Skvortsova, Y. V., Mamedov, I. Z., Azhikina, T. L., & Kaprelyants, A. S. (2019). Resuscitation of dormant “non-culturable” *Mycobacterium tuberculosis* is characterized by immediate transcriptional burst. Frontiers in cellular and infection microbiology, 9, 272.

Salgame, P., Geadas, C., Collins, L., Jones-López, E., & Ellner, J. J. (2015). Latent tuberculosis infection–revisiting and revising concepts. Tuberculosis, 95(4), 373-384.

Santos, R., de Carvalho, C. C., Stevenson, A., Grant, I. R., & Hallsworth, J. E. (2015). Extraordinary solute-stress tolerance contributes to the environmental tenacity of mycobacteria. Environmental microbiology reports, 7(5), 746-764.

Sato, K., Tomioka, H., Shimizu, T., Gonda, T., Ota, F., & Sano, C. (2002). Type II alveolar cells play roles in macrophage-mediated host innate resistance to pulmonary mycobacterial infections by producing proinflammatory cytokines. The Journal of infectious diseases, 185(8), 1139-1147.

Seidi, K., & Jahanban-Esfahlan, R. (2013). A novel approach to eradicate latent TB: based on resuscitation promoting factors. Journal of Medical Hypotheses and Ideas, 7(2), 69-74.

Serafini, A., Pisu, D., Palù, G., Rodriguez, G. M., & Manganelli, R. (2013). The ESX-3 secretion system is necessary for iron and zinc homeostasis in *Mycobacterium tuberculosis*. PloS one, 8(10), e78351.

Serganov, A., & Nudler, E. (2013). A decade of riboswitches. Cell, 152(1-2), 17–24. https://doi.org/10.1016/j.cell.2012.12.024

Sévin, D. C., & Sauer, U. (2014). Ubiquinone accumulation improves osmotic-stress tolerance in *Escherichia coli*. Nature chemical biology, 10(4), 266-272.

Sexton, D. L., St-Onge, R. J., Haiser, H. J., Yousef, M. R., Brady, L., Gao, C., Leonard, J., & Elliot, M. A. (2015). Resuscitation-promoting factors are cell wall-lytic enzymes with important roles in the germination and growth of *Streptomyces coelicolor*. *Journal of bacteriology*, *197*(5), 848–860. https://doi.org/10.1128/JB.02464-14

Schaible, U. E., Collins, H. L., Priem, F., & Kaufmann, S. H. (2002). Correction of the iron overload defect in β-2-microglobulin knockout mice by lactoferrin abolishes their increased susceptibility to tuberculosis. The Journal of experimental medicine, 196(11), 1507-1513.

Schleifer, K. H., & Kandler, O. (1972). Peptidoglycan types of bacterial cell walls and their taxonomic implications. *Bacteriological reviews*, *36*(4), 407-477.

Schönlein, J. L. (1839). *Allgemeine und specielle Pathologie und Therapie*. Verlags-Comptoir.

Schütze, E., Ahmed, E., Voit, A., Klose, M., Greyer, M., Svatoš, A., ... & Kothe, E. (2015). Siderophore production by streptomycetes—stability and alteration of

ferrihydroxamates in heavy metal-contaminated soil. *Environmental Science and Pollution Research*, *22*(24), 19376-19383.

Scheurwater, E. M., & Burrows, L. L. (2011). Maintaining network security: how macromolecular structures cross the peptidoglycan layer. *FEMS microbiology letters*, *318*(1), 1-9.

Schleifer, K. H., & Kandler, O. (1972). Peptidoglycan types of bacterial cell walls and their taxonomic implications. Bacteriological reviews, 36(4), 407-477.

Schultz, J. E., & Matin, A. (1991). Molecular and functional characterization of a carbon starvation gene of Escherichia coli. Journal of molecular biology, 218(1), 129-140.

Schwenk S, Moores A, Nobeli I, McHugh TD, Arnvig KB. (2018). Cell-wall synthesis and ribosome maturation are co-regulated by an RNA switch in *Mycobacterium tuberculosis.* Nucleic Acids Res. 46(11):5837-5849.

Scriba, T. J., Penn-Nicholson, A., Shankar, S., Hraha, T., Thompson, E. G., Sterling, D., ... & ACS Cohort Study Team. (2017). Sequential inflammatory processes define human progression from *M. tuberculosis* infection to tuberculosis disease. PLoS pathogens, 13(11), e1006687.

Shah, I. M., Laaberki, M. H., Popham, D. L., & Dworkin, J. (2008). A eukaryotic-like Ser/Thr kinase signals bacteria to exit dormancy in response to peptidoglycan fragments. *Cell*, *135*(3), 486-496.

Shah, I. M., & Dworkin, J. (2010). Induction and regulation of a secreted peptidoglycan hydrolase by a membrane Ser/Thr kinase that detects muropeptides. *Molecular microbiology*, *75*(5), 1232-1243.

Sharma, A. K., Chatterjee, A., Gupta, S., Banerjee, R., Mandal, S., Mukhopadhyay, J., ... & Kundu, M. (2015). MtrA, an essential response regulator of the MtrAB two-component system, regulates the transcription of resuscitation-promoting factor B of *Mycobacterium tuberculosis*. Microbiology, 161(6), 1271-1281.

Shleeva, M. O., Mukamolova, G. V., Telkov, M. V., Berezinskaia, T. L., Syroeshkin, A. V., Biketov, S. F., & Kaprel'iants, A. S. (2003). Formation of nonculturable *Mycobacterium tuberculosis* and their regeneration. Mikrobiologiia, 72(1), 76-83.

Shleeva, M. O., Kudykina, Y. K., Vostroknutova, G. N., Suzina, N. E., Mulyukin, A. L., & Kaprelyants, A. S. (2011). Dormant ovoid cells of *Mycobacterium tuberculosis* are formed in response to gradual external acidification. Tuberculosis, 91(2), 146-154.

Shleeva, M., Goncharenko, A., Kudykina, Y., Young, D., Young, M., & Kaprelyants, A. (2013). Cyclic AMP-dependent resuscitation of dormant Mycobacteria by exogenous free fatty acids. PLoS One, 8(12), e82914.

Shockman, G. D., & Höltje, J. V. (1994). Microbial peptidoglycan (murein) hydrolases. In *New comprehensive biochemistry* (Vol. 27, pp. 131-166). Elsevier.

Siegrist, M. S., Unnikrishnan, M., McConnell, M. J., Borowsky, M., Cheng, T. Y., Siddiqi, N., ... & Rubin, E. J. (2009). Mycobacterial Esx-3 is required for mycobactin-mediated iron acquisition. *Proceedings of the National Academy of Sciences*, *106*(44), 18792-18797.

Singh, K. K., Zhang, X., Patibandla, A. S., Chien Jr, P., & Laal, S. (2001). Antigens of *Mycobacterium tuberculosis* expressed during preclinical tuberculosis: serological immunodominance of proteins with repetitive amino acid sequences. Infection and immunity, 69(6), 4185-4191.

Singh, K. K., Athira, P. J., Bhardwaj, N., Singh, D. P., Watson, U., & Saini, D. K. (2021). Acetylation of response regulator protein MtrA in *M. tuberculosis* regulates its repressor activity. Frontiers in microbiology, 11, 516315.

Smith, T. (1934). *Parasitism and disease* (pp. 1-196). Princeton.

Som, N. F., Heine, D., Holmes, N. A., Munnoch, J. T., Chandra, G., Seipke, R. F., ... & Hutchings, M. I. (2017). The conserved actinobacterial two-component system MtrAB coordinates chloramphenicol production with sporulation in *Streptomyces venezuelae* NRRL B-65442. Frontiers in microbiology, 8, 1145.

Snow, G. (1970). Mycobactins: iron-chelating growth factors from mycobacteria. Bacteriological reviews, 34(2), 99-125.

Spreadbury, C. L., Pallen, M. J., Overton, T., Behr, M. A., Mostowy, S., Spiro, S., ... & Cole, J. A. (2005). Point mutations in the DNA-and cNMP-binding domains of the homologue of the cAMP receptor protein (CRP) in Mycobacterium bovis BCG: implications for the inactivation of a global regulator and strain attenuation. *Microbiology*, *151*(2), 547-556.

St-Onge, R. J., Haiser, H. J., Yousef, M. R., Sherwood, E., Tschowri, N., Al-Bassam, M., & Elliot, M. A. (2015). Nucleotide second messenger-mediated regulation of a muralytic enzyme in Streptomyces. *Molecular microbiology*, *96*(4), 779-795.

St-Onge, R. J., & Elliot, M. A. (2017). Regulation of a muralytic enzyme-encoding gene by two non-coding RNAs. *RNA biology*, *14*(11), 1592-1605.

Stewart, G. R., Robertson, B. D., & Young, D. B. (2003). Tuberculosis: a problem with persistence. Nature Reviews Microbiology, 1(2), 97-105.

Stinear, T. P., Seemann, T., Harrison, P. F., Jenkin, G. A., Davies, J. K., Johnson, P. D., ... & Cole, S. T. (2008). Insights from the complete genome sequence of Mycobacterium marinum on the evolution of Mycobacterium tuberculosis. *Genome research*, *18*(5), 729-741.

Swaim, L. E., Connolly, L. E., Volkman, H. E., Humbert, O., Born, D. E., & Ramakrishnan, L. (2006). *Mycobacterium marinum* infection of adult zebrafish causes caseating granulomatous tuberculosis and is moderated by adaptive immunity. Infection and immunity, 74(11), 6108-6117.

Tahlan K, Wilson R, Kastrinsky DB, Arora K, Nair V, Fischer E, Barnes SW, Walker JR, Alland D, Barry CE, Boshoff HI. (2012). SQ109 targets MmpL3, a membrane transporter of trehalose monomycolate involved in mycolic acid donation to the cell wall core of *Mycobacterium tuberculosis*. Antimicrob Agents Chemother 56(4): 1797–1809.

Tan, S., Sukumar, N., Abramovitch, R. B., Parish, T., & Russell, D. G. (2013). Mycobacterium tuberculosis responds to chloride and pH as synergistic cues to the immune status of its host cell. *PLoS pathogens*, *9*(4), e1003282.

Tebruegge, M., & Curtis, N. (2012). *Mycobacterium marinum* infection. Hot Topics in Infection and Immunity in Children VIII, 201-210.

Telkov, M. V., Demina, G. R., Voloshin, S. A., Salina, E. G., Dudik, T. V., Stekhanova, T. N., ... & Kaprelyants, A. S. (2006). Proteins of the Rpf (resuscitation promoting factor) family are peptidoglycan hydrolases. Biochemistry (Moscow), 71(4), 414-422.

Thunnissen, A. M. W., Rozeboom, H. J., Kalk, K. H., & Dijkstra, B. W. (1995). Structure of the 70-kDa soluble lytic transglycosylase complexed with bulgecin A. Implications for the enzymic mechanism. Biochemistry, 34(39), 12729-12737.

Tufariello, J. M., Jacobs Jr, W. R., & Chan, J. (2004). Individual *Mycobacterium tuberculosis* resuscitation-promoting factor homologues are dispensable for growth in vitro and in vivo. Infection and immunity, 72(1), 515-526.

Turapov, O., Glenn, S., Kana, B., Makarov, V., Andrew, P. W., & Mukamolova, G. V. (2014). The *in vivo* environment accelerates generation of Resuscitation-promoting factor–dependent mycobacteria. American journal of respiratory and critical care medicine, 190(12), 1455-1457.

Turapov, O., O'Connor, B. D., Sarybaeva, A. A., Williams, C., Patel, H., Kadyrov, A. S., ... & Mukamolova, G. V. (2016). Phenotypically adapted *Mycobacterium tuberculosis* populations from sputum are tolerant to first-line drugs. Antimicrobial agents and chemotherapy, 60(4), 2476-2483.

Tsai, M. C., Chakravarty, S., Zhu, G., Xu, J., Tanaka, K., Koch, C., ... & Chan, J. (2006). Characterization of the tuberculous granuloma in murine and human lungs: cellular composition and relative tissue oxygen tension. Cellular microbiology, 8(2), 218-232.

Uhía, I., Krishnan, N., & Robertson, B. D. (2018). Characterising resuscitation promoting factor fluorescent-fusions in mycobacteria. *BMC microbiology*, *18*(1), 1-9.

Varela, C. A., Baez, M. E., & Agosin, E. (2004). Osmotic stress response: quantification of cell maintenance and metabolic fluxes in a lysine-overproducing strain of Corynebacterium glutamicum. *Applied and environmental microbiology*, *70*(7), 4222-4229.

Van der Wel, N., Hava, D., Houben, D., Fluitsma, D., van Zon, M., Pierson, J., ... & Peters, P. J. (2007). *M. tuberculosis* and *M. leprae* translocate from the phagolysosome to the cytosol in myeloid cells. Cell, 129(7), 1287-1298.

Van Heijenoort, J. (2011). Peptidoglycan hydrolases of Escherichia coli. Microbiology and Molecular Biology Reviews, 75(4), 636-663.

Vergne, I., Chua, J., Singh, S. B., & Deretic, V. (2004). Cell biology of *Mycobacterium tuberculosis* phagosome. Annual review of cell and developmental biology, 20, 367.

Via, L. E., Curcic, R., Mudd, M. H., Dhandayuthapani, S., Ulmer, R. J., & Deretic, V. (1996). Elements of signal transduction in Mycobacterium tuberculosis: in vitro phosphorylation and in vivo expression of the response regulator MtrA. *Journal of Bacteriology*, *178*(11), 3314-3321.

Virchow, R. (1863). *Die krankhaften Geschwülste: Dreißig Vorlesungen* (Vol. 1). Hirschwald.

Vollmer, W., Blanot, D., and de Pedro, M.A. (2008) Peptidoglycan structure and architecture. FEMS Microbiol Rev 32: 149–167.

Voloshin, S. A., & Kaprelyants, A. S. (2005). Cell aggregation in cultures of Micrococcus luteus, studied by dynamic light scattering. *Applied Biochemistry and Microbiology*, *41*(6), 570-573.

Voskuil, M. I., Schnappinger, D., Visconti, K. C., Harrell, M. I., Dolganov, G. M., Sherman, D. R., & Schoolnik, G. K. (2003). Inhibition of respiration by nitric oxide induces a *Mycobacterium tuberculosis* dormancy program. The Journal of experimental medicine, 198(5), 705-713.

Walker, S. L., Brocklehurst, T. F., & Wimpenny, J. W. T. (1998). Adenylates and adenylate-energy charge in submerged and planktonic cultures of *Salmonella enteritidis* and *Salmonella typhimurium.* International journal of food microbiology, 44(1-2), 107-113.

Warmbold, B., Ronzheimer, S., Freibert, S. A., Seubert, A., Hoffmann, T., & Bremer, E. (2020). Two MarR-type repressors balance precursor uptake and glycine betaine synthesis in *Bacillus subtilis* to provide cytoprotection against sustained osmotic stress. Frontiers in microbiology, 11, 1700.

Watson, P. Y., & Fedor, M. J. (2012). The ydaO motif is an ATP-sensing riboswitch in Bacillus subtilis. Nature chemical biology, 8(12), 963-965.

Wayne, L. G., & Lin, K. Y. (1982). Glyoxylate metabolism and adaptation of *Mycobacterium tuberculosis* to survival under anaerobic conditions. Infection and immunity, 37(3), 1042-1049.

Wayne, L. G., & Sohaskey, C. D. (2001). Nonreplicating persistence of Mycobacterium tuberculosis. Annual review of microbiology, 55, 139.

Wayne, L. G., & Hayes, L. G. (1996). An in vitro model for sequential study of shiftdown of Mycobacterium tuberculosis through two stages of nonreplicating persistence. *Infection and immunity*, *64*(6), 2062–2069. https://doi.org/10.1128/iai.64.6.2062-2069.1996
Welin, A., & Lerm, M. (2012). Inside or outside the phagosome? The controversy of the intracellular localization of *Mycobacterium tuberculosis.* Tuberculosis, 92(2), 113-120.

Weidel, W., & Pelzer, H. (1964). BAGSHAPED MACROMOLECULES--A NEW OUTLOOK ON BACTERIAL CELL WALLS. *Adv Enzymol Relat Areas Mol Biol*, *26*, 193-232.

Witte, C. E., Whiteley, A. T., Burke, T. P., Sauer, J. D., Portnoy, D. A., & Woodward, J. J. (2013). Cyclic di-AMP is critical for Listeria monocytogenes growth, cell wall homeostasis, and establishment of infection. *MBio*, *4*(3), e00282-13.

Wivagg, C. N., & Hung, D. T. (2012). Resuscitation-promoting factors are required for β-lactam tolerance and the permeability barrier in *Mycobacterium tuberculosis*. Antimicrobial agents and chemotherapy, 56(3), 1591-1594.

Whalen, C., Horsburgh, C. R., Hom, D., Lahart, C., Simberkoff, M., & Ellner, J. (1995). Accelerated course of human immunodeficiency virus infection after tuberculosis. *American journal of respiratory and critical care medicine*, *151*(1), 129-135.

Whitehorn, J., Ayles, H., & Godfrey-Faussett, P. (2010). Extra-pulmonary and smear-negative forms of tuberculosis are associated with treatment delay and hospitalisation. *The international journal of tuberculosis and lung disease*, *14*(6), 741-744.

World Health Organization (2015) A guide to monitoring and evaluation for collaborative TB/HIV activities.

World Health Organization. (2019). Global tuberculosis report 2019. World Health Organization.

World Health Organization. (2020). *Global tuberculosis report 2020*. World Health Organization.

World Health Organization. (2021). *Global tuberculosis report 2022*. World Health Organization.

Wu, K. J., Boutte, C. C., Ioerger, T. R., & Rubin, E. J. (2019). Mycobacterium smegmatis HtrA blocks the toxic activity of a putative cell wall amidase. *Cell reports*, *27*(8), 2468-2479.

Yagupsky, P. V., Kaminski, D. A., Palmer, K. M., & Nolte, F. S. (1990). Cord formation in BACTEC 7H12 medium for rapid, presumptive identification of Mycobacterium tuberculosis complex. *Journal of Clinical Microbiology*, *28*(6), 1451-1453.

Ye, Z., Li, H., Jia, Y., Fan, J., Wan, J., Guo, L., ... & Shen, C. (2020). Supplementing resuscitation-promoting factor (Rpf) enhanced biodegradation of polychlorinated biphenyls (PCBs) by Rhodococcus biphenylivorans strain TG9T. *Environmental Pollution*, *263*, 114488.

Young, D. B., Gideon, H. P., & Wilkinson, R. J. (2009). Eliminating latent tuberculosis. *Trends in microbiology*, *17*(5), 183-188.

Zahrl, D., Wagner, M., Bischof, K., Bayer, M., Zavecz, B., Beranek, A., ... & Koraimann, G. (2005). Peptidoglycan degradation by specialized lytic transglycosylases associated with type III and type IV secretion systems. *Microbiology*, *151*(11), 3455-3467.

Zahrt, T. C., & Deretic, V. (2000). An essential two-component signal transduction system in Mycobacterium tuberculosis. *Journal of bacteriology*, *182*(13), 3832-3838.

Zhang, Y., Yang, Y., Woods, A., Cotter, R. J., & Sun, Z. (2001). Resuscitation of dormant Mycobacterium tuberculosis by phospholipids or specific peptides. *Biochemical and biophysical research communications*, *284*(2), 542-547.